Journal Information

Maejo International Journal of Science and Technology (ISSN 1905-7873 © 2012), the international journal for preliminary communications in Science and Technology is the first peerrefereed scientific journal of Maejo University (www.mju.ac.th). Intended as a medium for communication, discussion, and rapid dissemination of important issues in Science and Technology, articles are initially published online in an open access format, which thereby gives authors the chance to communicate with a wide range of readers in an international community.

Publication Information

MIJST is published triannually. Articles are available online and can be accessed free of charge at http://www.mijst.mju.ac.th. Printed and bound copies of each volume are produced and distributed to authors and selected groups or individuals.

Abstracting/Indexing Information

MIJST is covered and cited by Science Citation Index Expanded, SCOPUS, Journal Citation Reports/Science Edition, Zoological Record, Chemical Abstracts Service (CAS), SciFinder Scholar, Directory of Open Access Journals (DOAJ), CAB Abstracts, ProQuest, and Google Scholar.

Contact Information

Editorial office: Maejo International Journal of Science and Technology (MIJST), 1st floor, Orchid Building, Maejo University, San Sai, Chiang Mai 50290, Thailand

Tel: +66-53-87-3880
E-mails: duang@mju.ac.th

MAEJO INTERNATIONAL JOURNAL OF SCIENCE AND TECHNOLOGY

MAEJO INTERNATIONAL JOURNAL OF SCIENCE AND TECHNOLOGY

The International Journal for the Publication of Preliminary Communications in Science and Technology

http://www.mijst.mju.ac.th
ISSN 1905-7873

MAEJO INTERNATIONAL JOURNAL OF SCIENCE AND TECHNOLOGY

Volume 6, Issue 1 (January - April 2012)

CONTENTS

http://www.mijst.mju.ac.th
ISSN 1905-7873

MAEJO INTERNATIONAL JOURNAL OF SCIENCE AND TECHNOLOGY

Volume 6, Issue 1 (January - April 2012)

Author Index

Instructions for Authors

A proper introductory e-mail page containing the title of the submitted article and certifying its originality should be sent to the editor (Duang Buddhasukh, e-mail : duang@mju.ac.th). The manuscript proper together with a list of suggested referees should be attached in separate files. The list should contain at least 5 referees with appropriate expertise. Three referees should be non-native from 3 different countries. Each referee's academic/professional position, scientific expertise, affiliation and e-mail address must be given. The referees should not be affiliated to the same university/institution as any of the authors, nor should any two referees come from the same university/institution. The editorial team, however, retain the sole right to decide whether or not the suggested referees are approached.

Failure to conform to the above instructions will result in non-consideration of the submission.

Please also ensure that English and style is properly edited before submission. UK style of spelling should be used. Authors who would like to consult a professional service can visit www.proof-reading-service.com, www.editage.com, www.enago.com, www.bioedit.co.uk (bioscience and medical papers), www.bioscienceeditingsolutions.com, www.scribendi.com, www.letpub.com, www.papersconsulting.com or www.sticklerediting.com.

Important : Manuscript with substandard English and style will not be considered.

Warning : Plagiarism (including self-plagiarism) may be checked for at *the last* stage of processing and, if detected, will result in a rejection and blacklisting.

Manuscript Preparation

Manuscripts must be prepared in English using a word processor. MS Word for Macintosh or Windows, and .doc or .rtf files are preferred. Manuscripts may be prepared with other software provided that the full document (with figures, schemes and tables inserted into the text) is exported to a MS Word format for submission. Times or Times New Roman font is preferred. The font size should be 12 pt and the line spacing 'at least 17 pt'. A4 paper size is used and margins must be 1.5 cm on top, 2.0 cm at the bottom and 2.0 cm on both left and right sides of the paper. Although our final output is in .pdf format, authors are asked NOT to send manuscripts in this format as editing them is much more complicated. Under the above settings, a manuscript submitted should not be longer than **15 pages** for a full paper or **20 pages** for a review paper.

A template file may be downloaded from the *Maejo Int. J. Sci. Technol.* homepage. (DOWNLOAD HERE)

Authors' full mailing addresses, homepage addresses, phone and fax numbers, and e-mail addresses homepages can be included in the title page and these will be published in the manuscripts and the Table of Contents. The corresponding author should be clearly identified. It is the corresponding author's responsibility to ensure that all co-authors are aware of and approve of the contents of a submitted manuscript.

A brief (200 word maximum) Abstract should be provided. The use in the Abstract of numbers to identify compounds should be avoided unless these compounds are also identified by names.

A list of three to five keywords must be given and placed after the Abstract. Keywords may be single words or very short phrases.

Although variations in accord with contents of a manuscript are permissible, in general all papers should have the following sections: Introduction, Materials and Methods, Results and Discussion, Conclusions, Acknowledgments (if applicable) and References.
Authors are encouraged to prepare Figures and Schemes in colour. Full colour graphics will be published free of charge.

Tables and Figures should be inserted into the main text, and numbers and titles supplied for all Tables and Figures. All table columns should have an explanatory heading. To facilitate layout of large tables, smaller fonts may be used, but in no case should these be less than 10 pt in size. Authors should use the Table option of MS Word to create tables, rather than tabs, as tab-delimited columns are often difficult to format in .pdf for final output.
Figures, tables and schemes should also be placed in numerical order in the appropriate place within the main text. Numbers, titles and legends should be provided for all tables, schemes and figures. Chemical structures and reaction schemes should be drawn using an appropriate software package designed for this purpose. As a guideline, these should be drawn to a scale such that all the details and text are clearly legible when placed in the manuscript (i.e. text should be no smaller than 8-9 pt).

For bibliographic citations, the reference numbers should be placed in square brackets, i.e. [ ], and placed before the punctuation, for example [4] or [1-3], and all the references should be listed separately and as the last section at the end of the manuscript.

Format for References

Journal :

1. D. Buddhasukh, J. R. Cannon, B. W. Metcalf and A. J. Power, "Synthesis of 5-n-alkylresorcinol dimethyl ethers and related compounds *via* substituted thiophens", *Aust. J. Chem.*, **1971**, *24*, 2655-2664.

Text :

2. A. I. Vogel, "A Textbook of Practical Organic Chemistry", 3rd Edn., Longmans, London, **1956,** pp. 130-132.

Chapter in an edited text :

3. W. Leistritz, "Methods of bacterial reduction in spices", in "Spices: Flavor Chemistry and Antioxidant Porperties" (Ed. S. J. Risch and C-T. Ito), American Chemical Society, Washington, DC, **1997**, Ch. 2.

Thesis / Dissertation :

4. W. phutdhawong, "Isolation of glycosides by electrolytic decolourisation and synthesis of pentinomycin", *PhD. Thesis*, **2002**, Chiang Mai University, Thailand.

Patent :

5. K. Miwa, S. Maeda and Y. Murata, "Purification of stevioside by electrolysis", *Jpn. Kokai Tokkyo Koho 79 89,066* (**1979**).

Proceedings :

6. P. M. Sears, J. Peele, M. Lassauzet and P. Blackburn, "Use of antimicrobial proteins in the treatment of bovine mastitis", Proceedings of the 3rd International Mastitis Seminars, **1995**, Tel-Aviv, Israel, pp. 17-18.

(Download Submission Checklist)

Manuscript Revision Time

Authors who are instructed to revise their manuscript should do so within **45** days. Otherwise the revised manuscript will be regarded as a new submission.

Maejo International Journal of Science and Technology

ISSN 1905-7873
Available online at www.mijst.mju.ac.th

Editor's Note

The upkeep of the standard of a journal is a major and time-consuming job. At Maejo, however, we are willing to go to the extremes to do that kind of job. In trying to maintain the standards of an international journal, we subject every submitted article to a series of screening that may sometimes be inconvenient or plain unpleasant to a fair number of authors, to whom we sincerely apologise. As a matter of fact, some of their complaints have had a role in shaping several of our journal's policies which will better serve future contributors. In so far as the language and academic standards of an article are not compromised, we thank them for their candid comments and always welcome more contributions from them.

Duang Buddhasukh
Editor-in-Chief

Maejo Int. J. Sci. Technol. **2012**, *6*(01), 1-11

Maejo International Journal of Science and Technology

ISSN 1905-7873

Available online at www.mijst.mju.ac.th

Communication

Enhancement of carotenoid and chlorophyll content of an edible freshwater alga (Kai: *Cladophora* sp.) by supplementary inorganic phosphate and investigation of its biomass production

Taweesak Khuantrairong and Siripen Traichaiyaporn*

Algae and Water Quality Research Unit, Department of Biology, Faculty of Science, Chiang Mai University, Chiang Mai, 50200 Thailand

* Corresponding author, e-mail: tsiripen@yahoo.com; tel +66 (0)53 943 346; fax +66 (0)53 852 259

Received: 10 March 2011 / Accepted: 1 January 2012 / Published: 12 January 2012

Abstract: Enhancement of the carotenoid and chlorophyll content of an edible freshwater alga (Kai: *Cladophora* sp.) by supplementary inorganic phosphate in canteen wastewater was investigated. The mass cultivation of the alga was conducted at ambient temperature and light intensity in diluted canteen wastewater enhanced with dipotassium hydrogen phosphate at 5-20 mg L^{-1}. An increase in total carotenoid and chlorophyll was observed. However, it had no effect on biomass production. As a result of the algal cultivation, there was a dramatic improvement in the quality of canteen wastewater.

Keywords: freshwater alga, *Cladophora*, Kai

INTRODUCTION

Algae are a significant source of human food, especially in Asia. In Thailand an edible freshwater alga, *Cladophora* (known locally as Kai), consists of two species, namely *C. glomerata* and a to-be-identified *Cladophora* sp. [1]. Kai is abundant in Nan and Mekong Rivers in the northern part of Thailand. The local people around these rivers collect it for domestic consumption and it is sold in the local markets. Many reports on the nutritional value of *Cladophora* spp. show that they contain a significant amount of carotenoids that are nutritionally essential for humans and animals [1-5]. Carotenoids and chlorophylls, which are found in plants and algae, are extremely important in photosynthesis and growth [6-8]. They are also powerful antioxidants that are beneficial to human

health and are now used for supplementary food and animal feed. Previous studies have suggested that they can prevent or delay cancer and degenerative diseases in humans and animals by contributing to antioxidative defenses against metabolic oxidative by-products [9-11].

Mass cultivation of algae in canteen wastewater for use as feed for Mekong giant catfish [2] and *Tuptim tilapia* [12] had been done. It was found that the algal biomass production strongly correlated with water quality and environmental factors, e.g. temperature, light intensity and nutrient concentration, results which were similarly obtained elsewhere [13-15]. However, several researches have indicated that phosphorus is a main factor related to growth and production of *Cladophora* [13-24]. Other researches have also shown that phosphorus is effective for algal carotenoid and chlorophyll production [25-30]. In contrast, stimulation of carotenoid and chlorophyll production with phosphorus starvation has been reported [31-35].

Culturing of algae in wastewater can also improve the water quality by decreaseing BOD, COD and nutrients of the wastewater [2,12,36]. In this research, mass cultivation of *Cladophora* sp. (Kai) in canteen wastewater with different phosphate concentrations was carried out to investigate the effects of supplementary phosphorus on carotenoid and chlorophyll content of this alga, its biomass production and physico-chemical characteristics of the culture water.

MATERIALS AND METHODS

Culture Media Preparation

One thousand litres of canteen wastewater were collected from the canteen wastewater clarifier of Maejo University and left to settle in an open cement pond for 3 weeks to allow microorganisms to break down solid organic waste. The wastewater was then filtered through an 80-μm plankton net filter [36]. The filtrate was diluted to 10% and analysed for pH, dissolved oxygen (DO), biochemical oxygen demand (BOD), total hardness, ammonia-nitrogen (NH_3-N), nitrate-nitrogen (NO_3^--N), nitrite-nitrogen (NO_2^--N), total Kjeldal nitrogen (TKN) and orthophosphate-phosphorus (PO_4^{3-}-P) by following the methods of APHA et al [37].

Culture Condition

Cladophora sp. (Kai) was obtained from the Algae and Water Quality Research Unit, Chiang Mai University. The alga was cultured for 12 weeks at ambient air temperature (21-28^oC) and light intensity (12,333-39,267 lux) by attachment on plastic nets (60 g m^{-2}) in cement raceway ponds (size 1.2×2.3×0.5 m) each containing diluted canteen wastewater 20 cm deep (552 L per experiment) with continuous pump-driven circulation of 0.15 m s^{-1} [2,4]. A complete randomised design (CRD) was carried out with addition of dipotassium hydrogen orthophosphate (K_2HPO_4) at concentrations of 5, 10, 15 and 20 mg L^{-1} (treatment 1, 2, 3 and 4 respectively) with diluted canteen wastewater without K_2HPO_4 as control. The experiment was done in triplicate.

Carotenoid and Chlorophyll Analysis

The alga at 12 weeks of culturing was harvested, washed with tap water, air dried and freeze-dried. The total carotenoid content was determined according to the method of Britton [38]. The freeze-dried sample (0.4 g) was homogenised with 20 mL of 95% ethanol in an extraction tube. Two

mL of 5% KOH were then added, air was driven out of the tube with nitrogen gas and the tube was stored in the dark for at least 2 hours. Ether (3×5 ml) was added to extract the carotenoid portion. The ether supernatant was separated and its absorbance was read at 400-700 nm with a spectrophotometer. The total amount of carotenoid was calculated according to the following equation: total carotenoid = [(A_{max}/0.25)×ether supernatant volume]/sample weight, where A_{max} = maximum absorbance.

Extraction of carotenoid components and chlorophylls was performed by a modified method of Yoshii et al. [3] and Dere et al. [39] as follows: the freeze-dried sample (0.5 g) was mixed with ice-cooled acetone (25 mL) in the dark, the mixture stored in the dark at -20°C for 18 hours and the supernatant filtered. Carotene, xanthophyll and chlorophylls a and b (μg g^{-1}) were determined spectrophotometrically at 470, 645 and 662 nm respectively by means of equations proposed by Lichtenthaler and Wellburn [40]:

Chlorophyll a = $11.75A_{662} - 2.35A_{645}$

Chlorophyll b = $18.61A_{645} - 3.960A_{662}$

Carotene = $(1000A_{470} - 2.270C_a - 81.4\ C_b) / 227$ (C_a = chlorophyll a, C_b = chlorophyll b)

Xanthophyll = total carotenoid – carotene

Biomass Production

The growth in terms of biomass (g m^{-2} wet weight) and specific growth rate (SGR) (% d^{-1}) were measured every week following the method of Premila and Rao [41]. The SGR was calculated as SGR (% d^{-1}) = $\{[\ln(m_1/m_0)]/t\}\times100$, where m_0 = initial weight, m_1 = final weight, and t = time of culture in days.

Water Quality Analysis

Water samples from all the experimental ponds were collected once a week and analysed [37] for the physico-chemical properties, viz. temperature, pH, DO, BOD, total hardness, NH_3-N, NO_3^--N, NO_2^--N, TKN and PO_4^{3-}-P.

Statistical Analysis

The data were presented as mean value ± standard deviation. Comparison of mean values was made by one-way analysis of variance (ANOVA), followed by Duncan's multiple range test (DMRT) at a significance level of $p<0.05$.

RESULTS AND DISCUSSION

Carotenoid and Chlorophyll Content

Table 1 lists the carotenoid and chlorophyll content of *Cladophora* sp. (Kai) culture at different phosphate concentrations. The highest values of these pigments were observed in treatment 4 with K_2HPO_4 at 20 mg L^{-1} added to the culture medium, whereas the lowest values were observed in the control group with no addition of K_2HPO_4.

Table 1. Carotenoid and chlorophyll content of *Cladophora* sp. (Kai) cultured at different phosphate concentrations

Pigment	Amount of pigments (μg g^{-1} dry weight)				
	Control	Treatment 1	Treatment 2	Treatment 3	Treatment 4
	$K_2HPO_4(mgL^{-1})$= 0	$K_2HPO_4(mgL^{-1})$= 5	$K_2HPO_4(mgL^{-1})$= 10	$K_2HPO_4(mgL^{-1})$= 15	$K_2HPO_4(mgL^{-1})$= 20
Total carotenoid	889±157 [a]	1,084±253 [a]	1,130±147 [a]	1,151±151 [a]	1,729±212 [b]
Carotene	44±4[a]	86±9[b]	87±6[b]	96±7[bc]	103±9[c]
Xanthophyll	779±42[a]	997±254[a]	1043±145[a]	1055±154[a]	1626±220[b]
Chlorophyll a	148±13[a]	270±30[b]	309±20[bc]	305±52[bc]	348±17[c]
Chlorophyll b	56±31[a]	173±11[b]	245±15[bc]	200±49[c]	249±16[c]

Note: Each value is mean ± SD
Data in the same row with different superscripts are significantly different ($p<0.05$).

Carotenoids in green algae are produced in two different compartments and by two different pathways, i.e. the acetate-mevalonate pathway and the phosphoglyceraldehyde-pyruvate pathway, and they are further synthesised from isopentenyl diphosphate and its isomers [42-43]. In the present study it was observed that phosphate increased carotenoid and chlorophyll production in the alga, which agrees with the findings by Khuantrairong and Traichaiyaporn [4-5] that total carotenoid, β-carotene, lutein and zeaxanthin in *Cladophora* sp. positively correlate with phosphate level. Celekli et al. [29] reported that the phosphate supply increased biomass and carotenoid production in a blue-green alga (*Spirulina platensis*) while Latasa and Berdalet [25] deserved that the synthesis of pigments in a dinoflagellate *Heterocapsa* sp. stopped upon phosphorus limitation. In contrast, Buapet et al. [30] suggested that phosphorus enrichment had no significant effect on chlorophyll a production by *Ulva reticulate* seaweed. Subudhi and Singh [35] reported that a high concentration of phosphate-phosphorus reduced the chlorophyll content of *Azolla pinnata* blue-green alga. Enhancement of astaxanthin in a green alga (*Haematococcus pluvialis*) [31,34] and that of β-carotene, zeaxanthin and violaxanthin in a marine microalga (*Nannochloropsis gaditana*) [33] were observed upon phosphorus limitation. Leonardos and Geider [32] stated that the nitrate-to-phosphate supply ratio was related to carotenoid and chlorophyll-a production in the cryptophyte *Rhinomonas reticulata*.

Biomass Production

For 12-week cultures, the biomass production was similar among the treatments and ranged between 3,406-3,464 g m^{-2} (wet weight) (Figure 1). The highest value, 4,167 g m^{-2}, was observed in treatment 3 after culturing for 10 weeks. However, statistical analysis indicated that *Cladophora* sp. (Kai) cultured at different phosphorus concentrations showed no significant difference in growth ($p>0.05$).

The specific growth rate (SGR) was similar among treatments and ranged between -2.7–38.9% d^{-1}. After one week of cultivation, the alga began to grow quickly and the highest SGR values

were observed (Figure 2). Statistical analysis showed that the biomass production rate was not significantly different among the treatments ($p>0.05$).

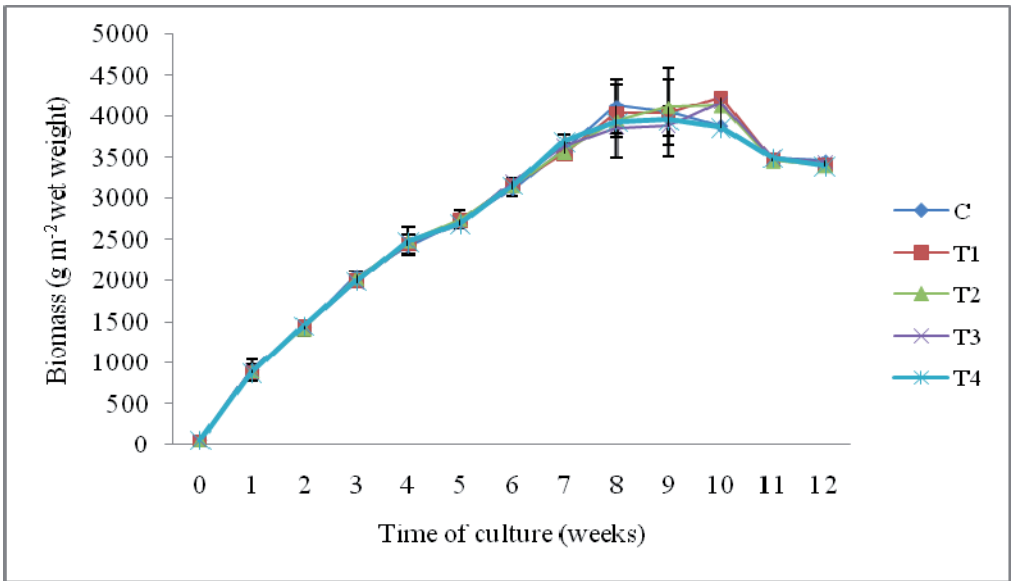

Figure 1. Biomass production of *Cladophora* sp. (Kai) cultured at different phosphorus concentrations (C = control group, T1 = treatment 1 (+5 mg L^{-1} K_2HPO_4), T2 = treatment 2 (+10 mg L^{-1} K_2HPO_4), T3 = treatment 3 (+15 mg L^{-1} K_2HPO_4), and T4 = treatment 4 (+20 mg L^{-1} K_2HPO_4))

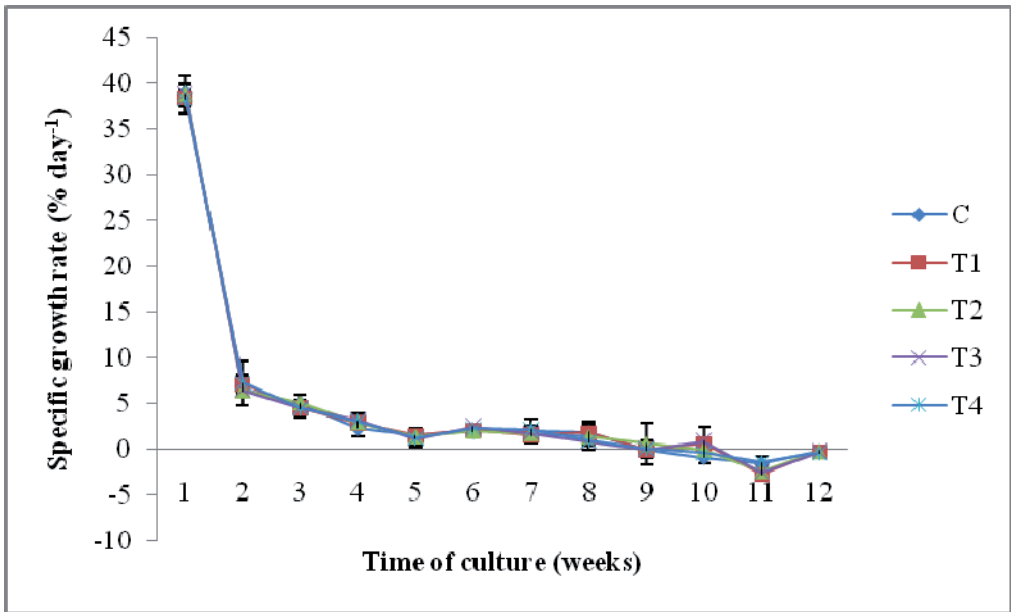

Figure 2. Specific growth rate (SGR) of *Cladophora* sp. (Kai) cultured at different phosphorus concentrations (C = control group, T1 = treatment 1 (+5 mg L^{-1} K_2HPO_4), T2 = treatment 2 (+10 mg L^{-1} K_2HPO_4), T3 = treatment 3 (+15 mg L^{-1} K_2HPO_4), and T4 = treatment 4 (+20 mg L^{-1} K_2HPO_4))

Thus, the biomass production and SGR of the alga cultured at different phosphorus concentrations showed no difference among all the treatments, indicating that the added phosphate had no effect on biomass production. Phosphorus is one of the main factors related to growth and production of freshwater *Cladophora* [13-24]. However, although Auer and Canale [24] observed that high dissolved phosphorus values in water induced an increase in stored phosphorus and growth rate of *Cladophora*, our results agreed with the findings that when phosphorus is above a certain concentration (0.01 mg L^{-1}), it has no effect on the growth and biomass production of *Cladophora* [13,18,44]. The biomass production of *Cladophora* also strongly depends on environmental conditions, especially temperature and light intensity. High biomass production was observed in winter season and under high light intensity [2, 5, 21].

Water Quality

For 12-week cultures, the physico-chemical properties of water of all treatments ranged as follows: temperature 19-28^{o}C, pH 8.3-8.9, DO 8.47-11.75 mg L^{-1}, BOD 1.00-10.27 mg L^{-1}, total hardness 38.91-68.21 mg L^{-1} (as $CaCO_3$), NH_3-N 0.07-1.07 mg L^{-1}, NO_3^--N 0.19-1.58 mg L^{-1}, NO_2^--N 0.002-0.012 mg L^{-1}, TKN 0.19-4.16 mg L^{-1} and PO_4^{3-}-P 0.004-14.780 mg L^{-1} (Figure 3). It was noted that the PO_4^{3-}-P levels in all treatments were higher than the critical phosphorus level of 0.01 mg L^{-1} for *Cladophora* growth in the natural ecosystem [20].

High DO values occurred in all experiments as a result of aeration by the air pump. Algae cultivation in canteen wastewater with high nutrients has been observed to dramatically reduce nitrogen and phosphorous levels and at the same time produce a useful product for animal feed [36]. In this work, it was noted that culturing of *Cladophora* sp. (Kai) showed similar improvement in water quality with decreasing BOD and nutrient levels (NH_3-N, NO_3^--N, TKN and PO_4^{3-}-P).

CONCLUSIONS

This study demonstrates that phosphate added to the culture of *Cladophora* sp. (Kai) enhances production of carotenoids and chlorophylls but has no effect on biomass production. In addition, cultivation of the alga in canteen wastewater improves the water quality by decreasing BOD and nutrients levels.

ACKNOWLEDGEMENTS

Financial support from Thailand Research Fund (TRF) through the Royal Golden Jubilee Ph.D. Program (Grant No. PHD/0130/2548) is acknowledged.

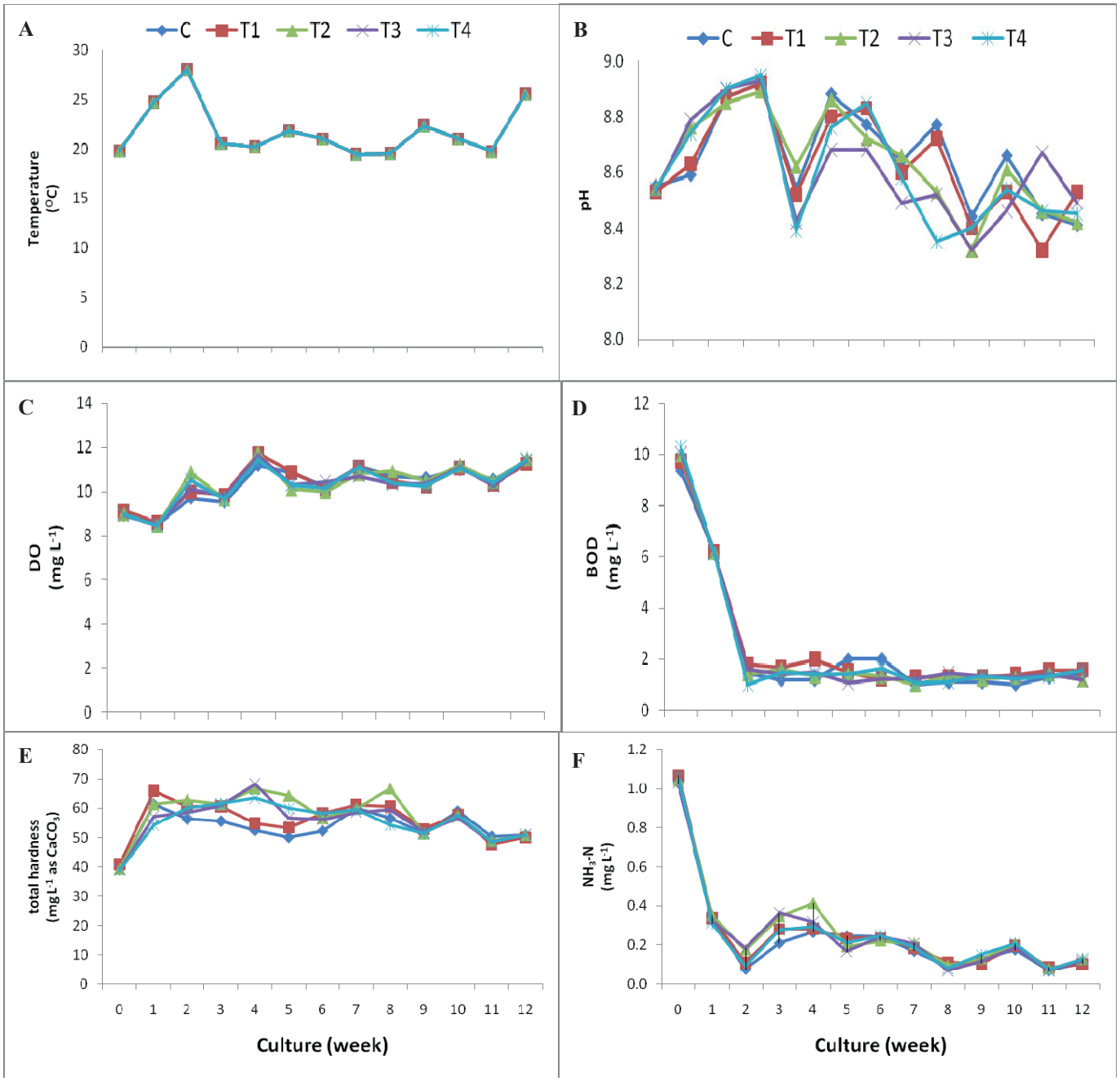

Figure 3. Water quality of *Cladophora* sp. (Kai) culture: water temperature (A), pH (B), DO (C), BOD (D), total hardness (E), and NH_3-N (F) (C = control group, T1 = treatment 1, T2 = treatment 2, T3 = treatment 3, and T4 = treatment 4)

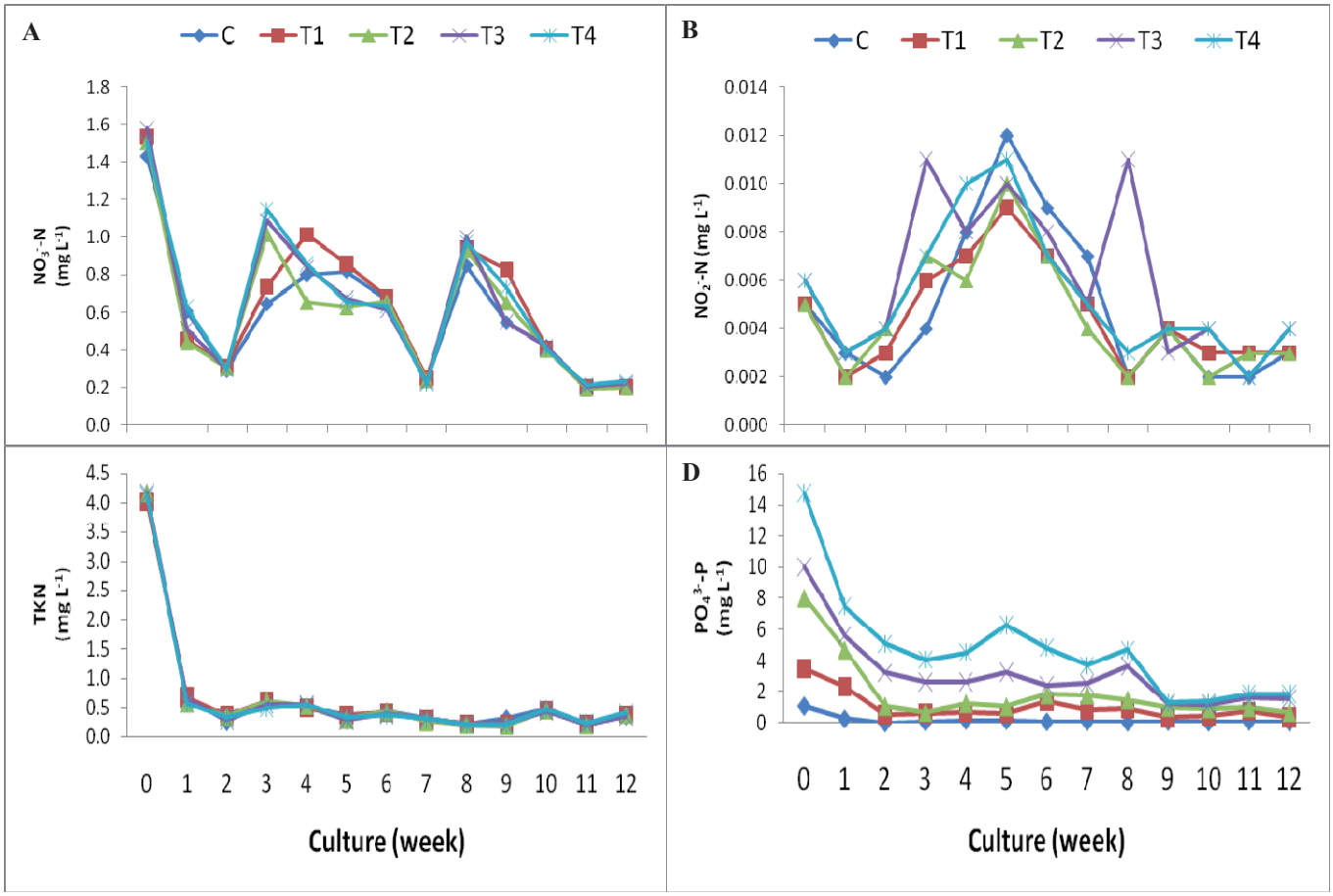

Figure 3 (Continued). Water quality of *Cladophora* sp. (Kai) culture: NO_3^--N (A), NO_2^--N (B), TKN (C), and PO^{3-}-P (D) (C = control group, T1 = treatment 1, T2 = treatment 2, T3 = treatment 3, and T4 = treatment 4)

REFERENCES

1. Y. Peerapornpisal, D. Amornlertpison, C. Rujjanawate, K. Ruangrit and D. Kanjanapothi, "Two endemic species of macroalgae in Nan river, northern Thailand, as therapeutic agents", *ScienceAsia,* **2006**, *32* (supplement 1), 71-76.
2. S. Traichaiyaporn, B. Waraegsiri and J. Promya, "Culture of a green alga genus *Cladophora* (Kai) as feed for the Mekong giant catfish (*Pangasianodon gigas*, Chevey)", Final Report of The Thailand Research Fund, Bangkok, Thailand, **2011**.
3. Y. Yoshii, T. Hanyuda, I. Wakana, K. Miyaji, S. Arai, K. Ueda and I. Inouye, "Carotenoid compositions of *Cladophora* balls (*Aegagropila linnaei*) and some members of the Cladophorales (Ulvophyceae, Chlorophyta): Their taxonomic and evolutionary implication", *J. Phycol.*, **2004**, *40*, 1170-1177.
4. T. Khuantrairong and S. Traichaiyaporn, "Production of biomass, carotenoid and nutritional values of *Cladophora* sp. (Kai) by cultivation in mass culture", *Phycologia*, **2009**, *48* (supplement), 60-66.

5. T. Khuantrairong and S. Traichaiyaporn, "The nutritional value of edible freshwater alga *Cladophora* sp. (Chlorophyta) grown under different phosphorus concentrations", *Int. J. Agric. Biol.,* **2011**, *13*, 297-300.
6. T. W. Goodwin, "The Biochemistry of the Carotenoids", 2nd Edn., Chapman and Hall, New York, **1980**, pp.207-256.
7. A. F. H. Marker, "The use of acetone and methanol in the estimation of chlorophyll in the presence of phaeophytin", *Freshwat. Biol.*, **1972**, *2*, 361-385.
8. R. B. Woodward, "The total synthesis of chlorophyll", Harvard University (no date), http://www.iupac.org/publications/pac/1961/pdf/0203x0383.pdf (Accessed: 29 Dec. 2011).
9. P. Burtin, "Nutritional value of seaweeds", *Electron. J. Environ. Agric. Food Chem.*, **2003**, *2*, 498-503.
10. G. S. Omenn, G. E. Goodman, M. D. Thornquist, J. Balmes, M. R. Cullen, A. Glass, J. P. Keogh, F. L. Meyskens, B. Valanis, J. H. Williams, S. Barnhart and S. Hammar, "Effects of a combination of beta carotene and vitamin A on lung cancer and cardiovascular disease", *New Engl. J. Med.*, **1996**, *334*, 1150-1155.
11. H. Tapiero, D. M. Townsend and K. D. Tew, "The role of carotenoids in the prevention of human pathologies", *Biomed. Pharmacother.*, **2004**, *58*, 100-110.
12. J. Promya, "Assessment of immunity stimulating capacity and meat, egg qualities of hybrid Tumtim tilapia ND56 (*Oreochromis* sp.) fed on raw *Spirulina*", *PhD Thesis*, **2008**, Chiang Mai University, Thailand.
13. B. A. Whitton, "Studies on the growth of riverain *Cladophora* in culture", *Arch. Microbiol.*, **1967**, *58*, 21-29.
14. C. E. R. Pitcairn and H. A. Hawkes, "The role of phosphorus in the growth of *Cladophora*", *Water Res.*, **1973**, *7*, 159-162.
15. S. L. Wong and B. Clark, "Field determination of the critical nutrient concentrations for *Cladophora* in streams", *J. Fish. Res. Board Can.*, **1976**, *33*, 85-92.
16. P. B. Birch, D. M. Gordon and A. J. McComb, "Nitrogen and phosphorus nutrition of *Cladophora* in the Peel-Hervey estuarine system of Western Australia", *Bot. Mar.*, **1981**, *24*, 381-387.
17. J. M. Graham, M. T. Auer, R. P. Canale and J. P., Hoffmann, "Ecological studies and mathematical modeling of *Cladophora* in Lake Huron: 4. Photosynthesis and respiration as functions of light and temperature", *J. Great Lakes Res.*, **1982**, *8*, 100-111.
18. J. P. Hoffmann and L. E. Graham, "Effects of selected physicochemical factors on growth and zoosporogenesis of *Cladophora glomerata* (Chlorophyta)", *J. Phycol.*, **1984**, *20*, 1-7.
19. J. R. Wharfe, K. S. Taylor and H. A. C. Montgomery, "The growth of *Cladophora glomerata* in a river receiving sewage effluent", *Water Res.*, **1984**, *18*, 971-979.
20. D. S. Painter and G. Kamaitis, "Reduction of *Cladophora* biomass and tissue phosphorus in Lake Ontario, 1972-83", *Can. J. Fish. Aquat. Sci.*, **1987**, *44*, 2212-2215.
21. W. K. Dodds and D. A. Gudder, "The ecology of *Cladophora*", *J. Phycol.*, **1992**, *28*, 415-427.

22. S. N. Higgins, R. E. Hecky and S. J. Guildford, "Environmental controls of *Cladophora* growth dynamics in eastern Lake Erie: Application of the *Cladophora* growth model (CGM)", *J. Great Lakes Res.*, **2006**, *32*, 629-644.
23. S. N. Higgins, S. Y. Malkin, E. T. Howell, S. J. Guildford, L. Campbell, V. Hiriart-Baer and R. E. Hecky, "An ecological review of *Cladophora glomerata* (Chlorophyta) in the Laurentian Great Lakes", *J. Phycol.*, **2008**, *44*, 839-854.
24. M. T. Auer and R. P. Canale, "Ecological studies and mathematical modeling of *Cladophora* in Lake Huron: 3. The dependence of growth rates on internal phosphorus pool size", *J. Great Lakes Res.*, **1982,** *8*, 93-99.
25. M. Latasa and E. Berdalet, "Effect of nitrogen or phosphorus starvation on pigment composition of cultured *Heterocapsa* sp.", *J. Plankton Res.*, **1994**, *16*, 83-94.
26. N. Leonardos and I. A. N. Lucas, "The nutritional values of algae grown under different culture conditions for *Mytilus edulis* L. larvae", *Aquaculture,* **2000**, *182*, 301-315.
27. M. Menéndez, J. Herrera and F. A. Comin, "Effect of nitrogen and phosphorus supply on growth, chlorophyll content and tissue composition of the macroalga *Chaetomorpha linum* (O.F. Müll.) Kütz, in a Mediterranean coastal lagoon", *Sci. Mar.*, **2002**, *66*, 355-364.
28. M. Orosa, D. Franqueira, A. Cid and J. Abalde, "Analysis and enhancement of astaxanthin accumulation in *Haematococcus pluvialis*", *Bioresour. Technol.*, **2005**, *96*, 373-378.
29. A. Celekli, M. Yavuzatmaca and H. Bozkurt, "Modeling of biomass production by *Spirulina platensis* as function of phosphate concentrations and pH regimes", *Bioresour. Technol.*, **2009**, *100*, 3625-3629.
30. P. Buapet, R. Hiranpan, R. J. Ritchie and A. Prathep, "Effect of nutrient inputs on growth, chlorophyll, and tissue nutrient concentration of *Ulva reticulata* from a tropical habitat", *ScienceAsia*, **2008**, *34*, 245-252.
31. B. R. Brinda, R. Sarada, B. S. Kamath and G. A. Ravishankar, "Accumulation of astaxanthin in flagellated cells of *Haematococcus pluvialis* - cultural and regulatory aspects", *Curr. Sci.*, **2004**, *87*, 1290-1295.
32. N. Leonardos and R. J. Geider, "Elemental and biochemical composition of *Rhinomonas reticulata* (Cryptophyta) in relation to light and nitrate-to-phosphate supply ratios", *J. Phycol.*, **2005**, *41*, 567-576.
33. E. Forján, I. Garbayo, C. Casal and C. Vílchez, "Enhancement of carotenoid production in *Nannochloropsis* by phosphate and sulphur limitation", in "Communicating Current Research and Educational Topics and Trends in Applied Microbiology" (Ed. A. Méndez-Vilas), Formatex Research Center, Badajoz (Spain), **2007**, pp.356-364.
34. P. He, J. Duncan and J. Barber, "Astaxanthin accumulation in the green alga *Haematococcus pluvialis*: Effects of cultivation parameters", *J. Intgr. Plant Biol.*, **2007**, *49*, 447-451.
35. B. P. R. Subudhi and P. K. Singh, "Effect of phosphorus and nitrogen on growth, chlorophyll, amino nitrogen, soluble sugar contents and algal heterocysts of water fern *Azolla pinnata*", *Biol. Plantarum*, **1979**, *21*, 401-406.

36. J. Promya, S. Traichaiyaporn and R. Deming, "Phytoremediation of kitchen wastewater by *Spirulina platensis* (Nordstedt) Geiteler: Pigment content, production variable cost and nutritional value", *Maejo Int. J. Sci. Technol.*, **2008**, *2*, 159-171.
37. APHA, AWW and WPCF, "Standard Method for Examination of Water and Waste Water", 16th Edn., American Public Health Association, Washington DC, **1985.**
38. G. Britton, "Workshop on carotenoid: The qualitative and quantitative analysis", Prince of Songkla University, Thailand, **2005**, pp.9-16.
39. S. Dere, T. Günes and R. Sivaci, "Spectrophotometric determination of chlorophyll-a, b and total carotenoid contents of some algae species using different solvents", *Turk. J. Bot.*, **1998**, *22*, 13-17.
40. H. K. Lichtenthaler and A. R. Wellburn, "Determination of total carotenoids and chlorophyll a and b of leaf extract in different solvents", *Biochem. Soc. Trans.*, **1983**, *11*, 591-592.
41. V. E. Premila and M. U. Rao, "Effect of crude oil on the growth and reproduction of some benthic marine algae of Visakhapatnam coastline", *Indian J. Mar. Sci.*, **1997**, *26*, 195-200.
42. F. X. Cunningham, "Regulation of carotenoid synthesis and accumulation in plants", *Pure Appl. Chem.*, **2002**, *74*, 1409-1417.
43. V. G. Ladygin, "Biosynthesis of carotenoids in the chloroplasts of algae and higher plants", *Russ. J. Plant Physiol.*, **2000**, *47*, 904-923.
44. V. J. Bellis and D. A. McLarty, "Ecology of *Cladophora glomerata* (L.) Kütz. in Southern Ontario", *J. Phycol.*, **1967**, *3*, 57-63.

Maejo Int. J. Sci. Technol. **2012**, *6*(01), 12-27

Maejo International Journal of Science and Technology

ISSN 1905-7873
Available online at www.mijst.mju.ac.th

Full Paper

Performance of self-excited induction generator with cost-effective static compensator

Yogesh K. Chauhan [1,*], Sanjay K. Jain [2] and Bhim Singh [3]

[1] Department of Electrical Engineering, School of Engineering, Gautam Buddha University, G.B. Nagar-201310, India
[2] Electrical and Instrumentation Engineering Department, Thapar University, Patiala-147004, India
[3] Department of Electrical Engineering, Indian Institute of Technology, New Delhi-110016, India

* Corresponding author, e-mail: chauhanyk@yahoo.com

Received: 6 June 2010 / Accepted: 8 January 2012 / Published: 13 January 2012

Abstract: The performance of a system consisting of a three-phase self-excited induction generator (SEIG) with static compensator (STATCOM) for feeding static resistive-inductive (R-L) and dynamic induction motor (IM) loads was investigated. The cost-effective STATCOM providing stable operation was designed by connecting additional shunt capacitance with the load. The STATCOM-controlled algorithm was realised by controlling the source current using two control loops with proportional-integral (PI) controller: one for controlling the SEIG terminal voltage and the other for maintaining the DC bus voltage. The SEIG-STATCOM performance was studied for two designs of STATCOM, namely cost-effective STATCOM and full-rating STATCOM. The cost-effective SEIG-STATCOM system with the proposed control scheme exhibited improved performance with respect to starting time, voltage dip, generator current and total harmonic distortion under various transient conditions.

Keywords: self-excited induction generator (SEIG), static compensator (STATCOM), voltage regulation, renewable energy source

INTRODUCTION

The fast rate of fossil fuel depletion is drawing attention to explore the alternative energy sources, e.g. small hydropower, wind and tidal power [1, 2]. The induction generator [3, 4] which operates in grid or self-excited mode is a strong candidate to harness electrical energy from these

sources. An isolated electric supply using a self-excited induction generator (SEIG) is an economical option for such small-capacity applications as lighting and small motor loads in remote locations.

The SEIG consists of a cage induction machine excited through an externally connected capacitor bank. The primary advantages of the SEIG in small capacity are the simple, brush-less and rugged construction, lower maintenance cost, small size and improved transient performance. The terminal voltage of SEIG is governed by parameters such as capacitance, prime mover speed and speed-torque characteristic and load. A poor voltage regulation results when the SEIG is loaded [5, 6] due to the increasing difference between the volt-ampere reactive (VAR) supplied by the capacitor bank and that demanded by the generator and load. The series capacitors [7-9] have been used with the SEIG for improved voltage regulation. The application of a thyristor as a static switch has resulted in such schemes as saturable core reactors and switching shunt capacitors for achieving improved voltage regulation of SEIG [10-12].

The modern power electronic converters are characterised by fast response, improved switching features and low cost. These converters are being applied as flexible alternating current transmission systems (FACTS) for various control and regulating purposes. The performance and cost of the shunt capacitor, static VAR compensator (SVC) and STATCOM were compared [13]. The STATCOM is normally a current controlled–voltage source inverter (CC-VSI) and has wide applications in the power system for improving power quality, harmonic elimination, reactive power compensation and load balancing [14,15]. The installation issue and capability of STATCOM have been demonstrated for the voltage limited feeder and industrial facility [16,17]. The concepts of static compensation for SEIG have been described for static loads [18,19]; the steps in designing a STATCOM for SEIG system have been summarised [20]. However, most of these attempts have been made to feed three-phase static loads and very little efforts are made for SEIG feeding the dynamic (motor) loads.

In this paper, the performance of SEIG with STATCOM on feeding a static R-L load and induction motor is investigated. The dynamic model of the system is developed and a methodology to decide the ratings of STATCOM components such as the DC bus capacitor, AC side filter and insulated gate bipolar transistors (IGBT) is presented. The system performance is also studied for cost-effective STATCOM and full-rating STATCOM designs.

SYSTEM DESCRIPTION AND CONTROL SCHEME

The schematic description of the SEIG-STATCOM system is shown in Figure 1. A suitable capacitor bank is needed to obtain the rated voltage at no load. The STATCOM consists of an IGBT-based 3-ϕ CC-VSI, an AC side-filter inductor, and a capacitor on the self-supporting DC bus. The scheme to control the STATCOM is depicted in Figure 2. In this scheme, two control loops are employed: one for controlling the terminal voltage of SEIG and other for maintaining the DC bus voltage. The proportional-integral (PI) controller is used with both control loops, which possess the advantage of being simple, effective and easy to tune.

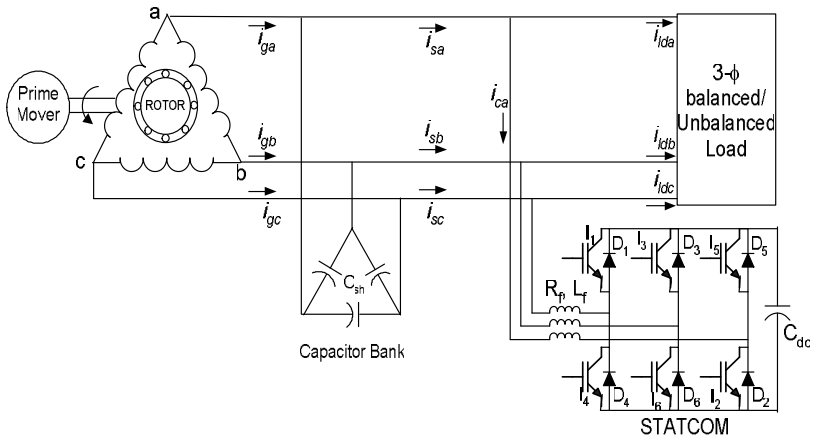

Figure 1. SEIG-STATCOM system supplying the load

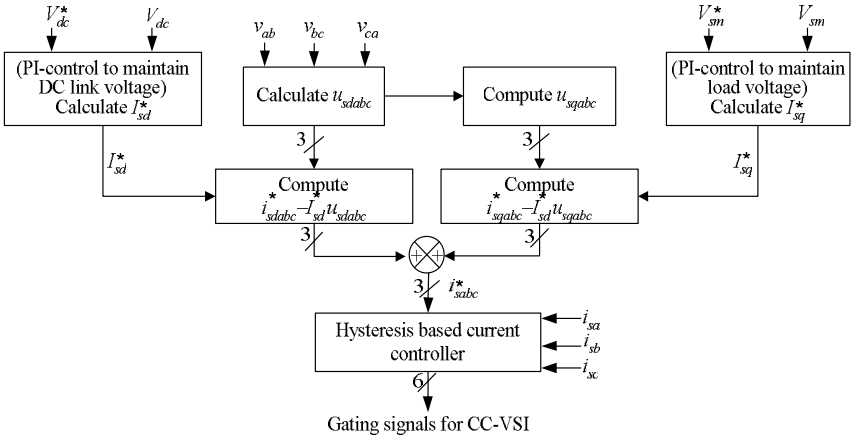

Figure 2. Control scheme for STATCOM

The control scheme is based on direct control of the source current, which consists of in-phase I^*_{sd} and quadrature I^*_{sq} components. I^*_{sd} is the current drawn from SEIG to maintain the DC bus voltage by charging (or discharging) the DC bus capacitor. I^*_{sq} is the reactive current required to maintain the SEIG terminal voltage. To regulate the DC bus voltage, the error signal for the PI controller is obtained from the sensed DC bus voltage V_{dc} and its reference value V^*_{dc}. The output of this PI controller is taken as I^*_{sd}. The 3-ϕ reference in-phase current i^*_{sdabc} is obtained by multiplying I^*_{sd} with the sinusoidal in-phase unit voltage template u_{sdabc}. To regulate the SEIG terminal voltage, the error signal for PI controller is obtained from the amplitude of SEIG voltage V_{sm} and its reference value V^*_{sm}. The output of this PI controller is taken as I^*_{sq}. The 3-ϕ reference quadrature current i^*_{sqabc} is obtained by multiplying I^*_{sq} with the sinusoidal quadrature unit voltage template u_{sqabc}. The total reference source current i^*_{sabc} is taken as the sum of i^*_{sdabc} and i^*_{sqabc}. The sensed and reference source currents are processed in a rule based carrier less hysteresis band current controller to generate gating signals (S_a, S_b, S_c) for IGBT of CC-VSI of STATCOM.

DESIGN METHODOLOGY

The STATCOM is designed considering that the VAR rating of STATCOM is fixed, the source voltage is completely sinusoidal and the pulse width modulation (PWM) inverter operates in linear mode. The VAR rating of STATCOM, $(VAR)_{\text{STATCOM}}$, is estimated using the capacitance needed for providing the rated voltage at no load (C_{NL}) and that needed for a stable operation of the induction motor while being loaded to its rated capacity (C_{FL}). These capacitances are computed using sequential unconstrained minimisation technique (SUMT) in conjunction with Rosenbroack's direct search method [23]. The problem formulation is briefed in Appendix I. The $(VAR)_{\text{STATCOM}}$ is computed as

$$(VAR)_{\text{STATCOM}} = 3V_{ab}^2\left[\frac{1}{X_{C_{FL}}} - \frac{1}{X_{C_{NL}}}\right] \tag{1}$$

and STATCOM line current I_{st} is calculated as

$$I_{st} = \frac{(VAR)_{STATCOM}}{\sqrt{3}V_{ab}} \tag{2}$$

The reference DC bus voltage V_{dcr} of the voltage source converter of STATCOM depends upon the AC voltage. The STATCOM does not provide adequate compensation during the transient condition of low V_{dcr}, whereas high V_{dcr} may stress the devices. The V_{dcr} is calculated using the peak supply line voltage V_m [15] as

$$V_{dcr} = (1.2\text{-}2.0)V_m,\ V_{dcr} > V_m \tag{3}$$

The DC bus capacitor C_{dc} stores energy and maintains the DC bus voltage with small ripple. The C_{dc} is calculated using an energy balanced equation characterised by appropriate response time t and actual DC bus voltage V_{dca}:

$$C_{dc} = \frac{\sqrt{3}V_{ab}I_{st}t}{\left\{V_{dcr}^2 - V_{dca}^2\right\}} \tag{4}$$

The AC filter inductance L_f is decided by the allowable ripple in the compensation current [20]. L_f is calculated by assuming a linear mode operation (modulation index m=1) and a switching frequency f_s of 10 kHz:

$$L_f = \frac{\left(\frac{\sqrt{3}}{2}\right)V_{dc}}{6af_sK_{rp}} \tag{5}$$

where the range of factor a (transient current) =1.2-2.0 and K_{rp} (peak-to-peak ripple) =0.05-0.1.

The ratings of IGBT suitable for medium rating and high frequency operation are decided as follows:

$$\begin{aligned} V_{dev} &= (1 + K_L + K_t)V_m \\ I_{dev} &= \sqrt{2}K_s(K_{rp} + 1)I_{st} \end{aligned} \tag{6}$$

where the ranges of K_L (factor for filter inductor drop), K_t (factor for transient voltage) and K_s (factor of safety) are taken as 0.05-0.1, 0.1-0.2 and 1.25-1.50 respectively.

SYSTEM MODEL

The complete system as shown in Figure 1 consists of SEIG, STATCOM with associated control, and loads. The dynamic model of each component is presented herewith.

SEIG Model

The induction generator model is developed in a stationary q-d reference frame considering the effect of both main and cross flux saturation [21, 22]. The model, i.e. the q-d axis stator and rotor currents and the rotor speed (ω_r), in state space form is expressed using equations (7) and (8) respectively:

$$p[i] = [L]^{-1}([v] - [r][i] - [G][i]) \tag{7}$$

$$p\omega_r = \frac{P}{2J}(T_P - T_{em}) \tag{8}$$

where $T_{em} = \frac{3P}{4} L_m \left(i_{qs} i_{dr} - i_{ds} i_{qr}\right)$, and $[v]$, $[i]$, $[r]$, $[L]$, $[G]$ and T_P are defined in Appendix-II.

Shunt Capacitor Model

The q-d axis stator currents i_{qs} and i_{ds} are converted into 3-ϕ stator currents i_{ga} , i_{gb} and i_{gc} using 2-ϕ to 3-ϕ transformation [22]. Kirchhoff's current law (KCL) [22] is applied to obtain the capacitor equations governing the SEIG voltage as

$$\begin{aligned} pv_{ab} &= \frac{\left\{\left(i_{ga} - i_{lda} - i_{ca}\right) - \left(i_{gb} - i_{ldb} - i_{cb}\right)\right\}}{3C_{sh}} \\ pv_{bc} &= \frac{\left\{\left(i_{ga} - i_{lda} - i_{ca}\right) + 2\left(i_{gb} - i_{ldb} - i_{cb}\right)\right\}}{3C_{sh}} \end{aligned} \tag{9}$$

and $$v_{ab} + v_{bc} + v_{ca} = 0 \tag{10}$$

where i_{ga}, i_{lda} and i_{ca} are line 'a' currents for the generator, load and STATCOM respectively.

STATCOM Model

The charging (or discharging) of the DC bus capacitor C_{dc} using hysteresis current controller switching functions (S_a, S_b, S_c) is expressed as

$$pV_{dc} = \frac{\left(i_{ca} S_a + i_{cb} S_b + i_{cc} S_c\right)}{C_{dc}} \tag{11}$$

The DC bus voltage V_{dc} is reflected as voltages e_a, e_b and e_c on the AC side of the PWM inverter as

$$\begin{bmatrix} e_a \\ e_b \\ e_c \end{bmatrix} = \frac{V_{dc}}{3} \begin{bmatrix} 2 & -1 & -1 \\ -1 & 2 & -1 \\ -1 & -1 & 2 \end{bmatrix} \begin{bmatrix} S_a \\ S_b \\ S_c \end{bmatrix} \tag{12}$$

The AC side filter equations in state space form are expressed as

$$pi_{ca} = \frac{\{(v_{bc} + 2v_{ab}) - (e_{bc} + 2e_{ab}) - 3R_f i_{ca}\}}{3L_f}$$
$$pi_{cb} = \frac{\{(v_{bc} - v_{ab}) - (e_{bc} - e_{ab}) - 3R_f i_{cb}\}}{3L_f} \quad (13)$$

where $e_{ab} = e_a - e_b$ and $e_{bc} = e_b - e_c$.

Static R-L Load

The static load is considered as delta-connected. The phase currents for static R-L load (i_{prla}, i_{prlb} and i_{prlc}) are expressed as

$$pi_{prla} = (v_{ab} - R_a i_{prla})/L_a$$
$$pi_{prlb} = (v_{bc} - R_b i_{prlb})/L_b \quad (14)$$
$$pi_{prlc} = (v_{ca} - R_c i_{prlc})/L_c$$

Correspondingly, the line currents (i_{rla}, i_{rlb} and i_{rlc}) can be obtained as follows:

$$i_{rla} = (i_{prla} - i_{prlc})$$
$$i_{rlb} = (i_{prlb} - i_{prla}) \quad (15)$$
$$i_{rlc} = (i_{prlc} - i_{prlb})$$

Induction Motor Load

The values for v_{qs} and v_{ds} are obtained from SEIG voltages (v_{ab}, v_{bc}, v_{ca}) using 3-ϕ to 2-ϕ transformation [22]. The state space model of an induction motor dynamic load is similar to the induction generator model. It is expressed using motor parameters as

$$p[i_m] = [L_m]^{-1}([v_m] - [r_m][i_m] - [G_m][i_m]) \quad (16)$$

$$p\omega_{rm} = \frac{P_m}{2J_m}(T_{emm} - T_L) \quad (17)$$

The equations (7–17) represent the model of the complete system. These equations are solved by fourth-order Runge-Kutta integration method [22] in MATLAB.

RESULTS AND DISCUSSION

An investigation was carried out on a 3.7-kW induction machine operated as SEIG, which was loaded with a static R-L load of 0.8 pf and a 1.5-kW induction motor load. The parameters of this machine are given in Appendix III. The capacitances C_{NL} and C_{FL} were calculated as 16.1 μF and 26.5 μF respectively for the rated SEIG voltage at no load and at the rated motor load under steady state.

It was observed that the motor was unable to start even with C_{FL} and resulted in a voltage collapse because the capacitor bank was unable to meet the excessive VAR requirements of SEIG and the motor load during starting. The starting of the motor was successful with a capacitance of 36μF. The performance during voltage buildup, the starting of motor at 2.0 sec., and the subsequent loading on motor at 4.0 sec. are shown in Figure 3. During starting, the terminal voltage dropped to 0.25 p.u. and the induction motor took 0.7 sec. to stabilise the start-up transients. The excessive dip in voltage level and the longer duration for start-up were of serious quality concern. In addition, the SEIG exhibited poor voltage regulation even for the static load.

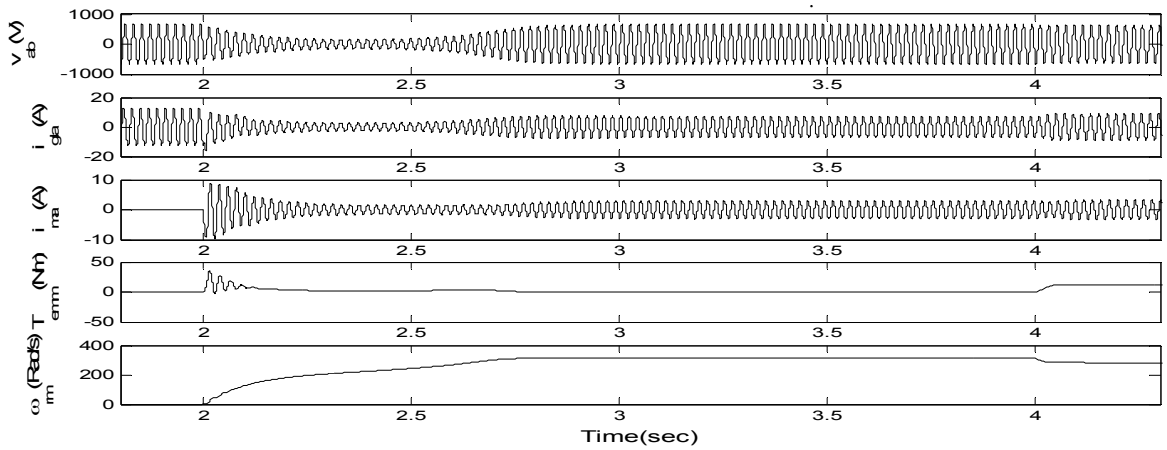

Figure 3. SEIG feeding motor load with successful starting and consequent loading (Load conditions: 1.5-kW induction motor load at 2.0 sec. with C_{sh} = 36 µF)

The application of STATCOM was investigated for effective control and improved performance. The STATCOM was designed to give a cost-effective operation by selecting the C_{dc} after considering the VAR requirement carefully. For a cost-effective STATCOM, the required VAR rating of STATCOM was calculated using the limiting capacitance of C_{NL} and $(C_{FL}+C_{NL})/2$ while an additional $(C_{FL}-C_{NL})/2$ shunt capacitance was switched on with the load. For a full-rating STATCOM, the VAR rating of STATCOM was calculated with limiting capacitances C_{NL} and C_{FL}. For both the cost-effective and full-rating STATCOM designs, the shunt capacitance C_{NL} needed to achieve the rated SEIG voltage at no load was taken as 16.1μF. The different values of C_{FL} were obtained for the static and motor loads.

The capacitance needed for successful starting of the induction motor, which was 36 μF, was taken as C_{FL} for the motor load. C_{FL} for the static load was considered as the capacitance needed to obtain the rated voltage at steady state, which was 30.4μF. The STATCOM parameters are summarised in Table 1 for both cost-effective and full-rating STATCOM designs. The IGBT of reduced current ratings were needed for a cost-effective STATCOM, which reduced the cost, and therefore the operation should be cost-effective.

Table 1. STATCOM design parameters

Parameter	Cost-effective STATCOM		Full-rating STATCOM	
	2.2kW static load (0.8 pf)	1.5 kW IM load	2.2kW static load (0.8 pf)	1.5 kW IM load
STATCOM rating	1.21 kVAR	1.615 kVAR	2.42 kVAR	3.23 kVAR
Current supplied by STATCOM	1.68 A	2.25 A	3.37 A	4.5 A
Ref. DC bus voltage	700 V	700 V	700 V	700 V
DC bus capacitance	86.3 µF	118.1 µF	172.6 µF	236.3 μF
AC filter inductance	11.16 mH	8.16 mH	5.58 mH	4.08 mH
Device selection	IGBT	IGBT	IGBT	IGBT
Device voltage rating	1094 V	1094 V	1094 V	1094 V
Device current rating	5.5 A	7.5 A	11.0 A	15.0 A

On the basis of STATCOM design parameters, a comparison between the cost-effective and full rating STATCOM is summarised in Table 2.

Table 2. Comparison of performance parameters for cost-effective and full-rating STATCOM

Performance parameter	Cost-effective STATCOM	Full-rating STATCOM
Performance (voltage regulation, starting time, THD, etc.)	Reasonably good	Good
Energy consumption (mainly in IGBT, DC bus capacitor and filter inductor loss)	Low (lower IGBT current rating, lower DC bus capacitance and higher filter inductor)	High (higher IGBT current rating, higher DC bus capacitance and lower filter inductor)
Overall cost (IGBT, DC bus capacitor, filter inductor)	Low	High

Performance with Balanced Static R-L Load

The performance characteristics of the systems with cost-effective and full-rating STATCOM are shown in Figure 4 and Figure 5 respectively for feeding balanced 0.8-pf static R-L load. A load of 2.2 kW was applied at 2.5 sec., which was changed to 3.0 kW at 3.0 sec. and 2.2 kW at 3.5 sec.

With cost-effective STATCOM (Figure 4), the visible transients lasting for about 0.2 sec were observed in v_{ab}, i_{ga} and V_{dc} due to the application of 2.2-kW load. The V_{dc} momentarily decreased to 480V and varied between 480-800V before returning to the reference value. With full-rating STATCOM (Figure 5), the transients settled down after 5-6 cycles and the DC bus voltage decreased to 500V momentarily with the application of 2.2-kW load. The increase in static load to 3.0 kW at 3.0 sec. did not result in any appreciable transients due to the choice of C_{dc} corresponding to the motor load. In both cost-effective and full-rating STATCOM, V_{dc} dropped momentarily to 630V and gradually returned to the reference value with the PI controller action. When the load was reduced to 2.2 kW at 3.5 sec., the dynamics of the system changed accordingly. V_{dc} momentarily rised to 760V before returning to the reference mark. A steady state was achieved within 0.12 sec. and 0.25 sec. with the full-rating and cost-effective STATCOM respectively.

Performance with Unbalanced Static R-L Load

The system performance with the cost-effective STATCOM was studied for an unbalanced R-L load and the corresponding characteristics for three-phase generator voltage v_{abc}, generator current i_{gabc}, load current i_{rlabc}, compensation current i_{cabc}, and DC bus voltage V_{dc} are shown in Figure 6. Initially, the 2.2-kW, 3.0-kW and 1.0-kW loads of 0.8 pf were applied on 'a', 'b' and 'c' phases respectively at 3.0 sec. Further, an acute unbalance was made by unloading of 'c' phase at 3.5 sec. The STATCOM responded satisfactory during the unbalanced load condition and maintained the balanced condition at SEIG terminals.

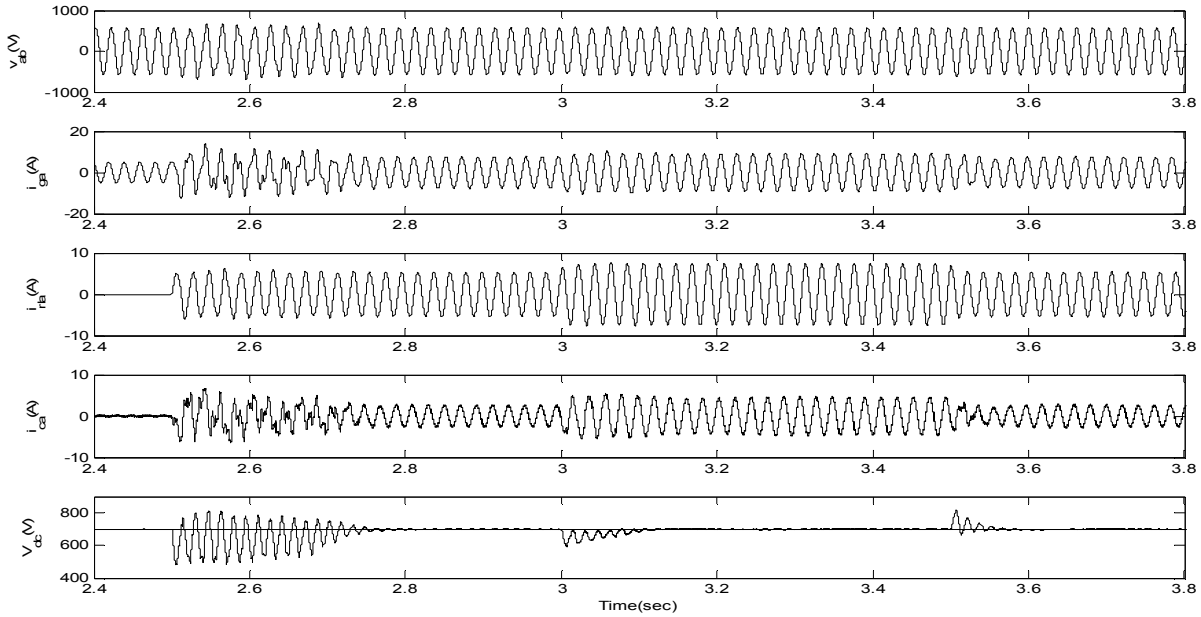

Figure 4. Performance characteristics of SEIG-STATCOM (cost-effective) system with 0.8-pf static R-L load (Load conditions : 2.2 kW at 2.5 sec., 3.0 kW at 3.0 sec. and 2.2 kW at 3.5 sec.)

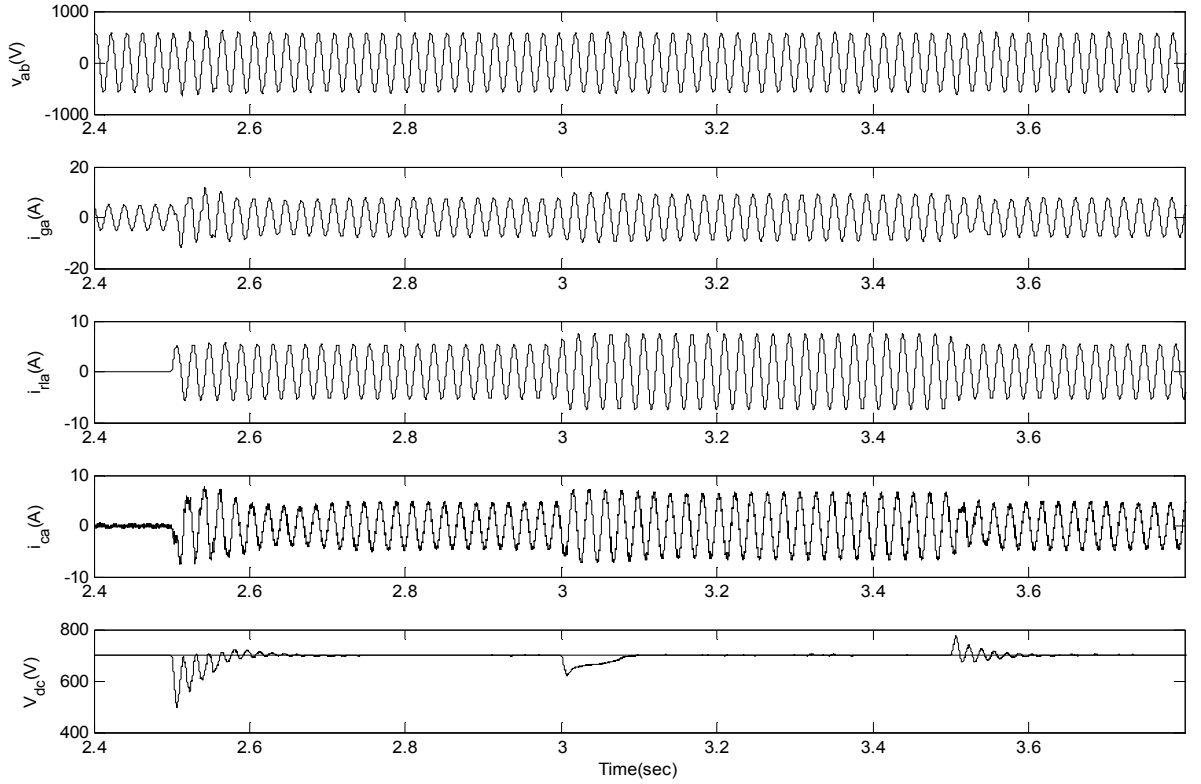

Figure 5. Performance characteristics of SEIG-STATCOM (full rating) with 0.8-pf static R-L load (Load conditions: 2.2 kW at 2.5 sec., 3.0 kW at 3.0 sec., and 2.2 kW at 3.5 sec.)

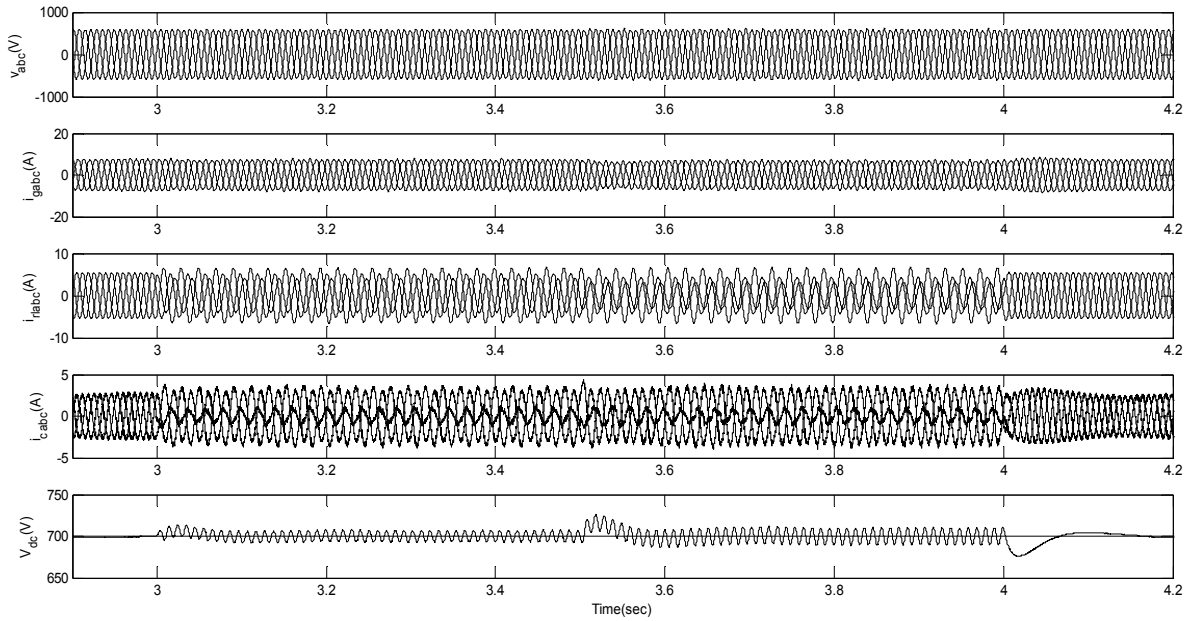

Figure 6. Performance characteristics of SEIG-STATCOM (cost-effective) with unbalanced 0.8-pf R-L load (Load conditions: 3-φ load (2.2 kW, 3.0 kW, 1.0 kW) at 3.0 sec.; load (2.0 kW, 3.0 kW, unloading on 'c' phase) at 3.5 sec; and balanced 3-φ loading of 2.2.0 kW at 4.0 sec.)

Performance with Motor Load

The performance characteristics of the system during the starting and sudden loading of an induction motor are shown in Figures 7 and 8 for cost-effective and full-rating STATCOM respectively. The motor at no load was switched on at 3.0 sec. and was loaded at 4.0 sec. During the starting of the motor, excessive reactive VAR were drawn and therefore the V_{dc} dropped to 300V level with both STATCOM. The V_{dc} quickly rose above the reference 700V before returning to reference level after replenishing the charge on DC bus capacitor. At starting, the transients in v_{ab}, i_{ga}, i_{ma}, T_{emm} and V_{dc} were more visible with cost-effective STATCOM due to its lower rating and the uncharged capacitor connection across the motor load terminals. Because of a lower compensation level, the i_{ca} under steady state was lower compared to the corresponding value with full-rating STATCOM. With cost-effective STATCOM, the SEIG voltage decreased by 10% and the transients were settled in 0.5 sec., whereas these values were 6% and 0.4 sec. respectively for full-rating STATCOM. Without STATCOM, as shown in Figure 3, the decrease in SEIG voltage was 30%. The motor was loaded with rated load torque at 4.0 sec. After small transients, the system response changed accordingly. The increase in i_{ga}, i_{ma}, and T_{emm} and the decrease in ω_{rm} were observed. The V_{dc} decreased to 670V before returning to steady-state reference value of 700V.

The performance of SEIG-IM configuration was compared in the presence and absence of STATCOM and the key parameter indices of the system are summarised in Table 3. The total harmonic distortion (THD) was obtained through fast Fourier transform (FFT) using discrete Fourier transform (DFT) algorithm of MATLAB. The generator-side THD values were within a permissible level, which demonstrated a satisfactory overall system performance.

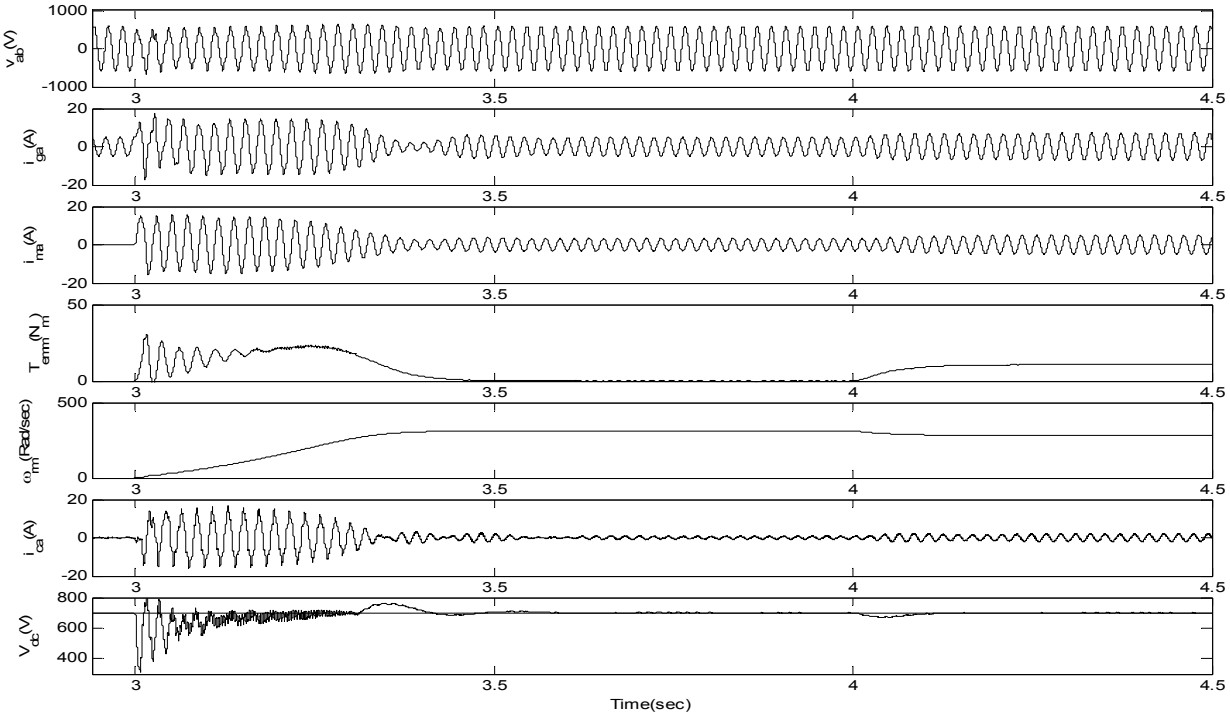

Figure 7. Performance characteristics of SEIG-STATCOM (cost-effective) with induction motor load (Load conditions: T_L= 0 at 3.0 sec. and T_L= rated torque at 4.0 sec.)

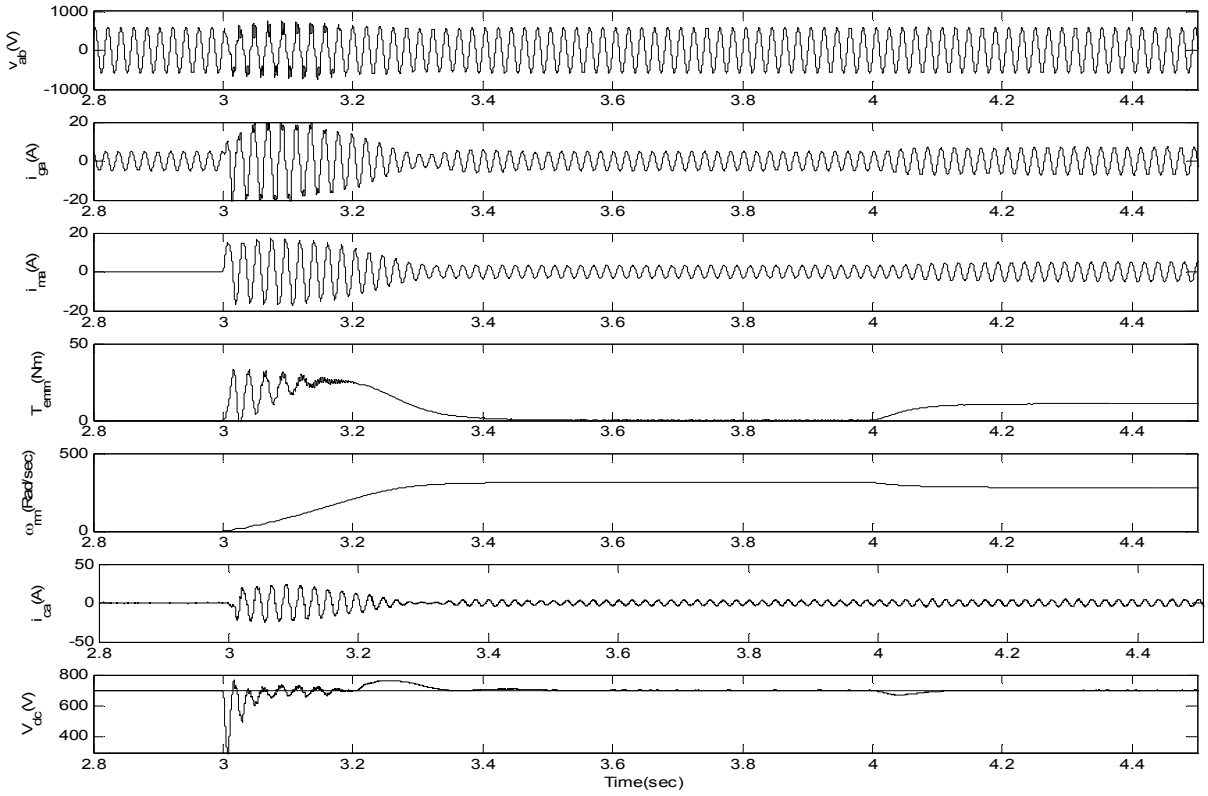

Figure 8. Performance characteristics of SEIG-STATCOM (full-rating) with induction motor load (Load conditions : T_L= 0 at 3.0 sec. and T_L= rated torque at 4.0 sec.)

Table 3. Comparison of performance indices of the system with and without STATCOM

Performance index	Without STATCOM	With STATCOM	
		Cost-effective design	Full-rating design
Supply voltage dip at start-up	75%	10.0%	6.1%
Start-up time	0.7 sec	0.18	0.16 sec
Supply current THD at full motor load	NA	1.4%	1.3%
Rise/drop in DC bus voltage of STATCOM at the time of sudden IM loading	NA	840V/300V	790V/330V
Drop in DC bus voltage with full torque loading of IM	NA	625V	650V

CONCLUSIONS

The investigations on SEIG-STATCOM system have been presented for feeding static R-L and induction motor loads. The dynamic model of the system has been developed in state space form. The STATCOM parameters have been calculated for two design cases, namely the cost-effective and full-rating designs using the proposed design procedure. The cost-effective STATCOM was designed to provide a stable operation by connecting additional shunt capacitance with the load. The system performance has been presented for both the cost-effective and full-rating STATCOM. With a controlling algorithm, the system exhibited improved performance in terms of parameters such as starting time, voltage dip, generator current and total harmonic distortion in the supply current under various transient conditions. The full-rating STATCOM could be considered for critical applications having stringent performance consideration while the cost-effective STATCOM should be for remote applications where the cost is important.

Appendix I

The per phase equivalent circuit of SEIG feeding induction motor load at steady state is shown in Figure 9. In the equivalent circuit, the SEIG parameters R_s and X_{ls} are stator resistance and leakage reactance respectively, R_r and X_{lr} are rotor resistance and leakage reactance respectively, and X_m is the magnetising reactance. The corresponding parameters are presented with subscript m for motor load. X_{csh} is the reactance offered by the capacitor bank, and F and v are per unit frequency and prime-mover speed respectively.

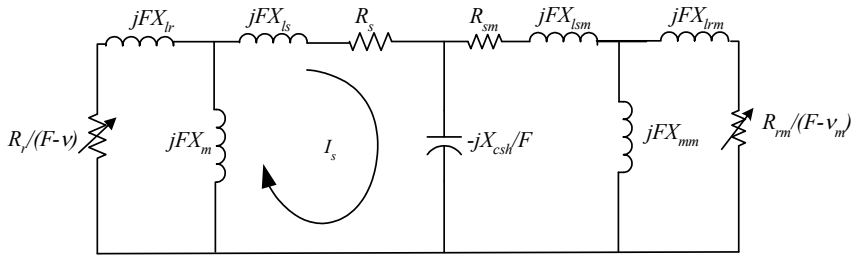

Figure 9. Per phase equivalent of SEIG feeding motor load

Applying KVL on stator side loop of induction generator results in

$$Z_{\text{loop}}\,\mathrm{I_s} = 0$$

Under steady state condition, I_s cannot be zero and therefore Z_{loop} should be zero. An optimisation problem has been formulated to obtain the unknown variables X_{csh} and F. The objective function F_n is expressed as

$$F_n(X_{csh}, F) = abs(Z_{loop})$$

The values of X_{csh} and F should lie between the respective minimum and maximum limits:

$$\left(F_{\text{mn}} \le F \le F_{\text{mx}}\right), \left(X_{cmn} \le X_{csh} \le X_{cmx}\right)$$

The above optimisation problem is solved through SUMT in conjunction with the Rosenbroack method of direct search technique [23]. After the convergence, the capacitance is computed.

Appendix II

The induction machine model is developed in a stationary reference frame while incorporating the effects of both the main flux and cross-flux saturation. The forms of $[v], [i], [r], [L]$ and $[G]$ are given as

$$[v] = \begin{bmatrix} v_{qs} & v_{ds} & v_{qr} & v_{dr} \end{bmatrix}^T ; \quad [i] = \begin{bmatrix} i_{qs} & i_{ds} & i_{qr} & i_{dr} \end{bmatrix}^T ; \; [r] = diag\begin{bmatrix} r_s & r_s & r_r & r_r \end{bmatrix}$$

$$[L] = \begin{bmatrix} L_{sq} & L_{dq} & L_{mq} & L_{dq} \\ L_{dq} & L_{sq} & L_{dq} & L_{md} \\ L_{mq} & L_{dq} & L_{rq} & L_{dq} \\ L_{dq} & L_{md} & L_{dq} & L_{rd} \end{bmatrix} \quad [G] = \begin{bmatrix} 0 & 0 & 0 & 0 \\ 0 & 0 & 0 & 0 \\ 0 & -\omega_r L_m & 0 & L_r \\ -\omega_r L_m & 0 & L_r & 0 \end{bmatrix}$$

The air gap voltage of SEIG does not remain constant during loading. Therefore, the magnetising inductance is calculated by calculating the magnetising current as

$$i_m = \sqrt{\left(i_{qs} + i_{qr}\right)^2 + \left(i_{ds} + i_{dr}\right)^2}$$

The inductances in $[L]$ are evaluated [21] as

$$L_m = \lambda_m / i_m,\ L = d\lambda_m / di_m, \cos\mu = i_{dm} / i_m,\ \sin\mu = i_{qm} / i_m$$

$$L_{dq} = (L - L_m)\cos\mu\sin\mu$$

$$L_{mq} = L\cos^2\mu + L_m\sin^2\mu,\ L_{md} = L\sin^2\mu + L_m\cos^2\mu$$

$$L_{sq} = L_{ls} + L_{mq},\ L_{sd} = L_{ls} + L_{md}, L_{rq} = L_{lr} + L_{mq},\ L_{rd} = L_{lr} + L_{md}$$

The prime mover torque driving the induction machine is expressed as

$$T_P = 6200 - 20\omega_r$$

Appendix III

Generator parameters

3.7 kW, 415 V, Δ-connected, 7.6 A (line), 50 Hz, 4 pole, J=0.0842 kg-m^2 cage induction machine. R_s=0.0585 pu, R_r=0.06196 pu, X_{ls}=X_{lr}=0.1015 pu, $X_{m(unsat)}$=2.858 pu.

Magnetisation characteristic of SEIG

$L_m = K_1 i_m^2 + K_2 i_m + K_3$

where $K_1 = -0.0091$, $K_2 = 2.0024$, $K_3 = 348.35$.

Motor parameters

1.5 kW, 415 V, Δ-connected, 3.2 A (line), 50 Hz, 4 pole, J=0.0205 kg-m^2 cage induction machine. R_{sm}=0.0832 pu, R_{rm}=0.0853 pu, X_{lsm}=X_{lrm}=0.1101 pu, $X_{mm(unsat)}$=1.83 pu.

Magnetisation characteristic of motor

$L_{mm} = K_{m1} i_{mm}^5 + K_{m2} i_{mm}^4 + K_{m3} i_{mm}^3 + K_{m4} i_{mm}^2 + K_{m5} i_{mm} + K_{m6}$

where $K_{m1} = 0.0072$, $K_{m2} = -0.0849$, $K_{m3} = 0.4298$, $K_{m4} = 0.9924$, $K_{m5} = 0.6847$, $K_{m6} = 1.171$.

REFERENCES

1. S. Major, T. Commins, and A. Noppharatana, "Potential of wind power for Thailand: An assessment", *Maejo Int. J. Sci. Technol.* **2008**, *2*, 255-266.
2. F. F. Li, J. Kueck, T. Rizy and T. King, "A preliminary analysis of the economics of using distributed energy as a source of reactive power supply", Report for the U.S. Department of Energy, **2006**, www.localpower.org/documents/reporto_doe_reactivepowerandde.pdf**.**
3. E. D. Bassett and F. M. Potter, "Capacitive excitation for induction generators", *AIEE Trans. (Elect. Eng.)*, **1935**, *54*, 540-545.
4. J. M. Elder, J. T. Boys and J. L. Woodward, "Self-excited induction machine as a small low-cost generator", *IEE Proc. Gener. Transm. Distrib.*, **1984**, *131*, 33-41.
5. S. S. Murthy, O. P. Malik and A. K. Tandon, "Analysis of self excited induction generators", *IEE Proc. Gener. Transm. Distrib.*, **1982**, *129,* 260-265.
6. L. Shridhar, B. Singh, C. S. Jha and B. P. Singh, "Analysis of self excited induction generator feeding induction motor", *IEEE Trans. Ener. Convers*., **1994**, *9,* 390-396.
7. E. Bim, J. Szajner and Y. Burian, "Voltage compensation of an induction generator with long-shunt connection", *IEEE Trans. Ener. Convers*., **1989**, *4*, 526-530.
8. M. H. Haque, "Selection of capacitors to regulate voltage of a short-shunt induction generator", *IET Gener. Transm. Distrib.*, **2009**, *3*, 257–265.
9. L. Wang and J. Y. Su "Effects of long-shunt and short-shunt connections on voltage variations of a self-excited induction generator", *IEEE Trans. Ener. Convers*., **1997**, *12,* 368-374.
10. S. M. Alghuwainem, "Steady-state analysis of an induction generator self excited by a capacitor in parallel with saturable reactor", *Electr. Mach. Power Syst.*, **1998**, *26*, 617-625.
11. S. C. Kuo and L. Wang, "Analysis of isolated self-excited induction generator feeding a rectifier load", *IEE Proc. Gener. Transm. Distrib.*, **2002**, *149,* 90-97.
12. T. L. Maguire and A. M. Gole, "Apparatus for supplying an isolated DC load from a variable-speed self-excited induction generator", *IEEE Trans. Ener. Convers*., **1993**, *8,* 468-475.
13. A. S. Yome and N. Mithulananthan, "Comparison of shunt capacitor, SVC and STATCOM in static voltage stability margin enhancement", *Int. J. Electr. Eng. Edu.*, **2004,** *41*, 158-171.
14. B. Singh, K. Al-Haddad and A. Chandra, "Harmonic elimination, reactive power compensation and load balancing in three-phase, four-wire electric distribution systems supplying non-linear loads", *Electr. Power Syst. Res.*, **1998**, *44*, 93-100.
15. S. K. Jain, P. Agarwal and H. O. Gupta, "Fuzzy logic controlled shunt active power filter for power quality improvement", *IEE Proc. Electr. Power Appl.*, **2002**, *149*, 317-328.

16. S. M. Ramsay, P. E. Cronin, R. J. Nelson, J. Bian and F. E. Menendez, "Using distribution static compensators (D-STATCOMs) to extend the capability of voltage-limited distribution feeders", Proceedings of IEEE Rural Electric Power Conference, **1996**, Fort Worth, TX, USA, pp. A4:1-A4:7.
17. K. N. Choma and M. Etezadi-Amoli, "The application of a DSTATCOM to an industrial facility", Proceedings of IEEE Power Engineering Society Winter Meeting, **2002**, New York, USA, Vol. 2, pp. 725-728.
18. B. Singh and L. B. Shilpakar, "Analysis of a novel solid state voltage regulator for a self-excited induction generator", *IEE Proc. Gener. Transm. Distrib.*, **1998**, *145,* 647-655.
19. S. C. Kuo and L. Wang, "Analysis of voltage control for a self-excited induction generator using a current-controlled voltage source inverter (CC-VSI)", *IEE Proc. Gener. Transm. Distrib.*, **2001**, *148,* 431-438.
20. B. Singh, S. S. Murthy and S. Gupta, "Analysis and design of STATCOM-based voltage regulator for self-excited induction generators", *IEEE Trans. Ener. Convers.*, **2004**, *19*, 783-790.
21. E. Levi, "Applications of the current state space model in analyses of saturated induction machines", *Electr. Power Syst. Res.*, **1994**, *31*, 203-216.
22. P. C. Krause, "Analysis of electrical machinery", McGraw Hill, New York, **1986**.
23. S. S. Rao, "Engineering optimization, theory and practice", New Age International, New Delhi, **1998**.

Maejo Int. J. Sci. Technol. **2012**, *6*(01), 28-46

Maejo International Journal of Science and Technology

ISSN 1905-7873
Available online at www.mijst.mju.ac.th

Full Paper

Benthic diatoms of Mekong River and its tributaries in northern and north-eastern Thailand and their application to water quality monitoring

Sutthawan Suphan [1,*], Yuwadee Peerapornpisal [1] and Graham J. C. Underwood [2]

[1] Department of Biology, Faculty of Science, Chiang Mai University, 50200, Thailand
[2] Department of Biological Sciences, University of Essex, Colchester, Essex, United Kingdom CO4 3SQ

* Corresponding author, e-mail: suttawan@hotmail.com

Received: 7 February 2011 / Accepted: 6 May 2011 / Published: 26 January 2012

Abstract: Biomonitoring of benthic diatoms was performed to assess the water quality of Mekong River and its tributaries in northern and north-eastern Thailand. Fourteen sampling sites along the river and its tributaries were investigated. Two hundred and fifty-two species in 53 genera of diatoms were recorded. Each sampling site had distinct water chemistry and other physical variables. Cluster analysis identified 11 groups at 80% similarity. The relationship between diatom community composition and water quality variables was determined by statistical techniques. A number of diatom species were found to be useful as indicators of some physico-chemical properties of water.

Keywords: benthic diatoms, water quality, biomonitoring, Mekong River

INTRODUCTION

One of the most important natural resources for human life is water resource. Human use including household, industrial, agricultural and recreational activities affects water quality. There is an urgent need to develop a more sustainable practice for the management and efficient use of water resources as well as the need to protect the ecosystems where these resources are located. Therefore, it is important to monitor the quality of our limited water supplies. Presently, there are several methods to monitor water quality. One of the methods that is successfully used for monitoring aquatic environments around the world is biological assessment of water quality. It is considered an essential part in the assessment of the ecological quality of running waters apart from

the data obtained from other sources such as hydrology, eco-morphology, physico-chemical water analysis and eco-toxicological analysis [1].

In rivers and streams, benthic diatoms, the most common and diverse primary producers [2], are regarded as bioindicators due to their sensitivity and strong response to many physical, chemical and biological changes [3]. Diatoms are successfully used for monitoring aquatic environments around the world, especially in Europe, USA and Japan [4-5].

In Thailand, Mekong River flows through Chiang Rai province in the north. As it continues along its path in Laos, it once again flows back into Loei, Nong Khai, Nakhon Panom, Mukdaharn, Amnaj Charoen and Ubon Ratchadhani provinces in the north-east of Thailand. There are many smaller rivers which are tributaries that may affect the Mekong River. Thus, the water quality in the Mekong River and its tributaries should be monitored continuously.

There have been few studies of diatoms in the Mekong River in the past [6-8]. In this study, the diversity and distribution of benthic diatoms in the Mekong River and its tributaries in northern and north-eastern Thailand was investigated. In addition the relationship between diatoms species and some water physico-chemical properties was studied. The basic ecological data that could be applied to develop sustainable water resources were also obtained. Furthermore, the study should provide more information on diatoms in the South-east Asian region where very few reports on benthic diatoms were documented.

MATERIALS AND METHODS

Study Area

Fourteen sampling sites along the Mekong River and its tributaries in northern and north-eastern Thailand were selected based on the distance and environmental impact. Nine sites were located along Mekong River and five sites along its tributaries. The detail of each sampling site is shown in Figure 1. Diatom samples and physico-chemical water quality were determined 3 times per year in each season during July 2005 – April 2007.

Benthic Diatom Collection and Identification

Ten replicates of benthic diatoms were collected at each sampling site. Diatoms were taken from stone surfaces using a toothbrush and a 10-cm^2 plastic sheet. The samples were put in plastic boxes and fixed with Lugol's solution on site. Diatom samples were then taken to the laboratory and cleaned by concentrated acid digestion method [9]. Briefly, each sample was centrifuged at 3,500 rpm for 15 minutes. The diatom cells were placed in an 18-cm core tube, added with concentrated nitric acid, heated in a boiler (70-80^oC) for 30-45 minutes, and rinsed 4-5 times with deionised water.

Each cleaned diatom sample was mounted on a microscope slide with Naphrax®, a mountant with a high refractive index [9-10]. Up to 300 diatom valves were counted and identified with an Olympus CH30 microscope at ×1000 magnification. Taxonomy and nomenclature was determined according to the relevant references [8, 11-17].

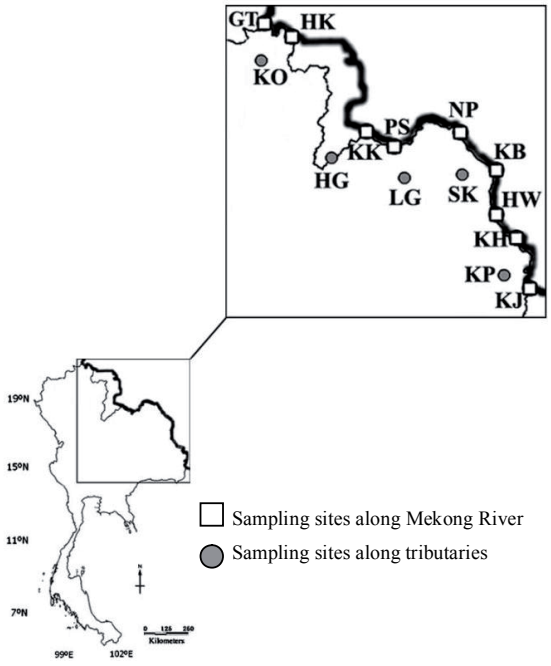

Site 1 Golden Triangle, Chiang Rai province (GT)
Site 2 Kok River, Chiang Rai province (KO)
Site 3 Ban Had Krai, Chiang Rai province (HK)
Site 4 Hueng River, Loei province (HG)
Site 5 Kaeng Khood Khoo, Loei province (KK)
Site 6 Ponpisai, Nong Khai province (PS)
Site 7 Laung River, Nong Khai province (LG)
Site 8 Mueng, Nakhon Phanom province (NP)
Site 9 Songkram River, Sakonnakron province (SK)
Site 10 Kaeng Ka Bao, Nakhon Phanom province (KB)
Site 11 Had Hin Win Chai, Amnat Charoen province (HW)
Site 12 Kaeng Hin Kan, Mukdahan province (KH)
Site 13 Kaeng Sapue, Ubon Ratchathani province (KP)
Site 14 Khong Jium, Ubon Ratchathani province (KJ)

Figure 1. Map of Thailand showing the location of 14 sampling sites along Mekong River and its tributaries

Physico-Chemical Data

Water samples were collected in triplicate at each sampling site. The samples were put in polyethylene bottles and kept in a cool box at 5-7 ^{o}C. Water chemical and physical properties were determined by established methods [18]; soluble reactive phosphorus (SRP) was determined by ascorbic acid method, nitrate nitrogen (NO_3^--N) by cadmium reduction method, ammonia nitrogen (NH_4^+-N) by Nesslerisation method, alkalinity (as mg/L $CaCO_3$) by phenolpthalein methyl orange indicator method, dissolved oxygen (DO) by azide modification of the Winkler method, and biochemical oxygen demand (BOD) by 5-day incubation and azide modification of the Winkler method. The pH was measured with a pH meter, conductivity with a conductivity meter, turbidity with a turbidity meter, water temperature with a thermometer, and water velocity with a velocity meter (Aquaflow Probe - Model 6900, Ricky Hydrological Company).

Data Analysis

ANOVA single factor was performed on water quality and data sets on benthic diatoms assemblage to determine any significant differences between groups. Pearson's correlation was also calculated for certain variables. Water quality data and diatom species were analysed with canonical correspondence analysis (CCA), a multivariate direct gradient analysis method widely used in ecology, to determine the relationship between physico-chemical water quality and diatom species using multivariate statistical package (MVSP) software. Cluster analysis was performed on the log of transformed water quality data using MVSP software with unweighted pair-group method of arithmetic averages (UPGMA) cluster method to show similarity percentage between samples.

Environmental variables of the clusters were then tested for significance between groups with ANOVA single factor. The number of benthic diatoms in each group was calculated by Minitab program to find significant differences and correlations between groups.

RESULTS AND DISCUSSION

Diatom Diversity and Distribution

A total of 135,859 benthic diatom cells were counted. Two hundred and fifty-two species of benthic diatoms were found and classified into 3 classes, 6 subclasses, 14 orders, 27 families and 53 genera. The majority (88.5%) was in Bacillariophyceae class with the remaining 6.0% in Fragilariophyceae class and 5.5% in Coscinodiscineae class. *Nitzschia* was the genus with the highest number of species (30 species) followed by *Navicula* (25 species), *Gomphonema* (16 species), *Eunotia* (14 species), *Luticola* (12 species) and *Pinnularia* (8 species). The number of diatom species recorded was similar to that reported for other river systems of comparable size. Holmes and Whitton [19] listed 230 diatom species collected from Tees River in northern England while Archibald [20] recorded 310 diatom species from Sundays and Great Fish Rivers in South Africa. Similarly, 267 species of diatoms found in La Trobe River and tributaries in Australia was reported [21]. The distribution of the diatoms is shown in Figure 2. The lowest number of diatoms was recorded at HK in Chiang Rai, northern Thailand, during the fourth sampling in July 2006 (rainy season).

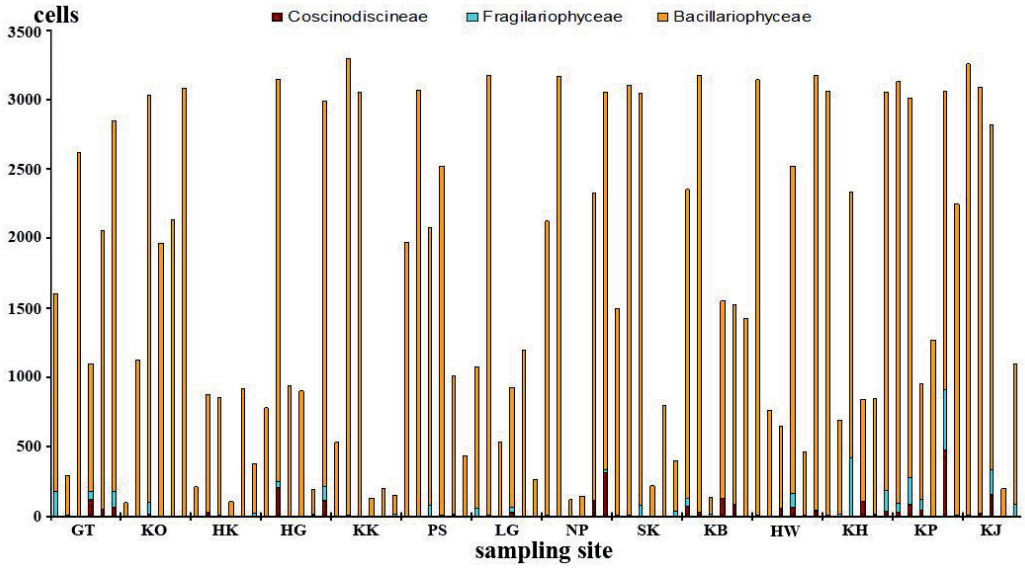

Figure 2. Number of benthic diatoms in Mekong River and its tributaries between July 2005 –April 2007

Among the 252 species, 29 were common species as shown in Table 1 and Figures 3. *Nitzschia palea* showed the highest percentage (36.0%) followed by *Mayamaea atomus* (35.4%), *Eolimna minima* (25.3%), *Navicula cryptotenelloides* (24.9%), *Cymbella* sp.1 (21.3%) and *Achnanthidium minutissimum* (20.5%).

Table 1. Twenty nine common species of benthic diatoms in Mekong River and its tributaries. The percentage of relative abundance is shown in bracket.

Taxa	
Nitzschia palea (Kützing) Smith (36.0%)	*Planothidium frequentissimum* (Lange-Bertalot) Round & Bukhtiyarova(11.9%)
Mayamaea atomus (Kützing) Lange-Bertalot (35.4%)	*Cymbella sumatrensis* Hustedt (11.7%)
Navicula symmetrica Patrick (33.4%)	*Nitzschia filiformis* (Smith) Hustedt (11.4%)
Eolimna minima (Grunow) Lange-Bertalot (25.3%)	*Ulnaria ulna* (Nitzsch) Compère (10.8%)
Navicula cryptotenelloides Lange-Bertalot (24.9%)	*Eolimna subminuscula* (Manguin) Gerd Moser (9.8%)
Gomphonema lagenula Kützing (24.6%)	*Fragilaria bidens* Heiberg (9.0%)
Cymbella sp.1 (21.3%)	*Melosira varians* Agardh (9.0%)
Achnanthidium minutissimum (Kützing) Czarnecki (20.5%)	*Navicula menisculus* Schumann (6.9%)
Navicula cryptotenella Lange-Bertalot (19.9%)	*Nitzschia dissipata* (Kützing) Grunow (6.6%)
Nitzschia inconspicua Grunow (19.2%)	*Geissleria decussis* (Østrup) Lange-Bertalot&Metzeltin (5.9%)
Nitzschia supralitorea Lange-Bertalot (17.2%)	*Achnanthidium convergens* (Kobayasi) Kobayasi (5.9%)
Navicula rostellata Kützing (14.5%)	*Frustulia undosa* Metzeltin & Lange-Bertalot (4.7%)
Encyonema sp.1 (14.3%)	*Sellaphora pupula* (Kützing) Mereschkovsky (3.1%)
Luticola goeppertiana (Bleisch) Mann in Round, Crawford & Mann (13.7%)	*Nitzschia microcephala* Grunow (2.9%)
Nitzschia clausii Hantzsch (13.1%)	

According to Jüttner et al. [22], *M. atomus*, *A. minutissimum* and *N. palea* were common species in streams in agricultural catchments of Kathmandu valley, Nepal. Duong et al.[23] reported the impact of urban pollution in Hanoi area on benthic communities collected from Red, Nhue and Tolich Rivers in Vietnam. They also reported that the diatom assemblage at the Tolich site consisted mainly of *Nitzschia umbonata*, *N. palea* and *Eolimma minima*. Some of these diatoms were reported to have preference for tropical regions without being restricted to these latitudes [23-24]. *Cymbella turgidula* was recorded in many tropical countries such as Sri Lanka [25] and Río Savegre River in the central and southern parts of Costa Rica [26]. *Cymbella tumida* was also reported to be widespread but very often found in the tropics [11]. Patrick and Reimer [27] reported this species from New England. *Diploneis subovalis* was found in Iceland and Finland, but with higher frequency in tropical rivers [11]. *Gomphonema parvulum* var. *lagenula* was regarded as a tropical species [26].

Common species, especially *Cymbella turgidula*, *C. tumida* and *Gomphonema parvulum* var. *lagenula* (currently regarded as a synonym of *Gomphonema lagenula*) were found in many streams and rivers in Thailand [8, 28-38].

Water Physico-Chemical Properties

The water physico-chemical properties of Mekong River and its tributaries between July 2005 - April 2007 are shown in Table 2. Broad differences were apparent between sampling sites. The water temperature ranged between 25-32^{o}C, the temperatures at GT, KO and HK in the north being lower than those in the north-eastern areas. The water velocity was highest (8.30 m/s) at KB in the Mekong River. All sampling sites showed neutral pH with the highest (7.67) at GT and the lowest (6.75) at SK. Average alkalinity ranged between 23.3-67.8 mg/L. The highest value of conductivity was recorded at SK in the north-eastern area. The highest DO and BOD values were observed at KO in the north-eastern area, as were the highest NO_3^--N (1.57 mg/L) and SRP (0.24 mg/L). The highest NH_4^+-N (0.53 mg/L) was recorded at KP and the lowest (0.21 mg/L) at GT.

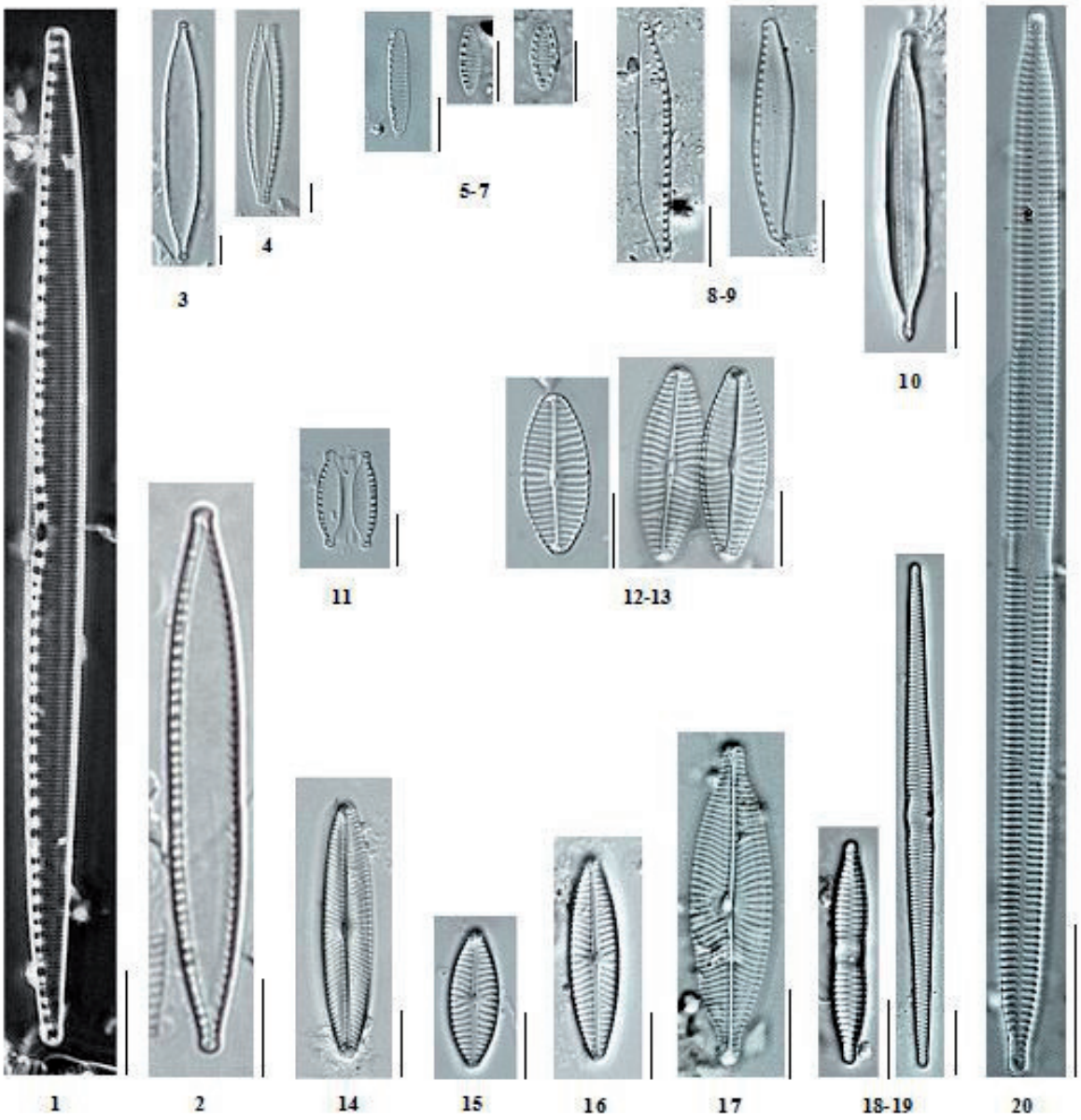

Figure 3. Common species of benthic diatoms in Mekong River and its tributaries (scale bar = 10 μm)

(1) *Nitzschia filiformis* (W. Smith) Hustedt, (2) *Nitzschia palea* (Kützing) W. Smith, (3-4) *Nitzschia inconspicua* Grunow, (5-7) *Nitzschia supralitorea* Lange-Bertalot, (8-9) *Nitzschia clausii* Hantzsch, (10) *Nitzschia dissipata* (Kützing) Grunow, (11) *Nitzschia microcephala* Grunow, (12-13) *Navicula menisculus* Schumann, (14) *Navicula symmetrica* R.M. Patrick, (15) *Navicula cryptotenelloides* Lange-Bertalot, (16) *Navicula cryptotenella* Lange-Bertalot, (17) *Navicula rostellata* Kützing, (18-19) *Fragilaria bidens* Heiberg, (20) *Ulnaria ulna* (Nitzsch) P. Compère

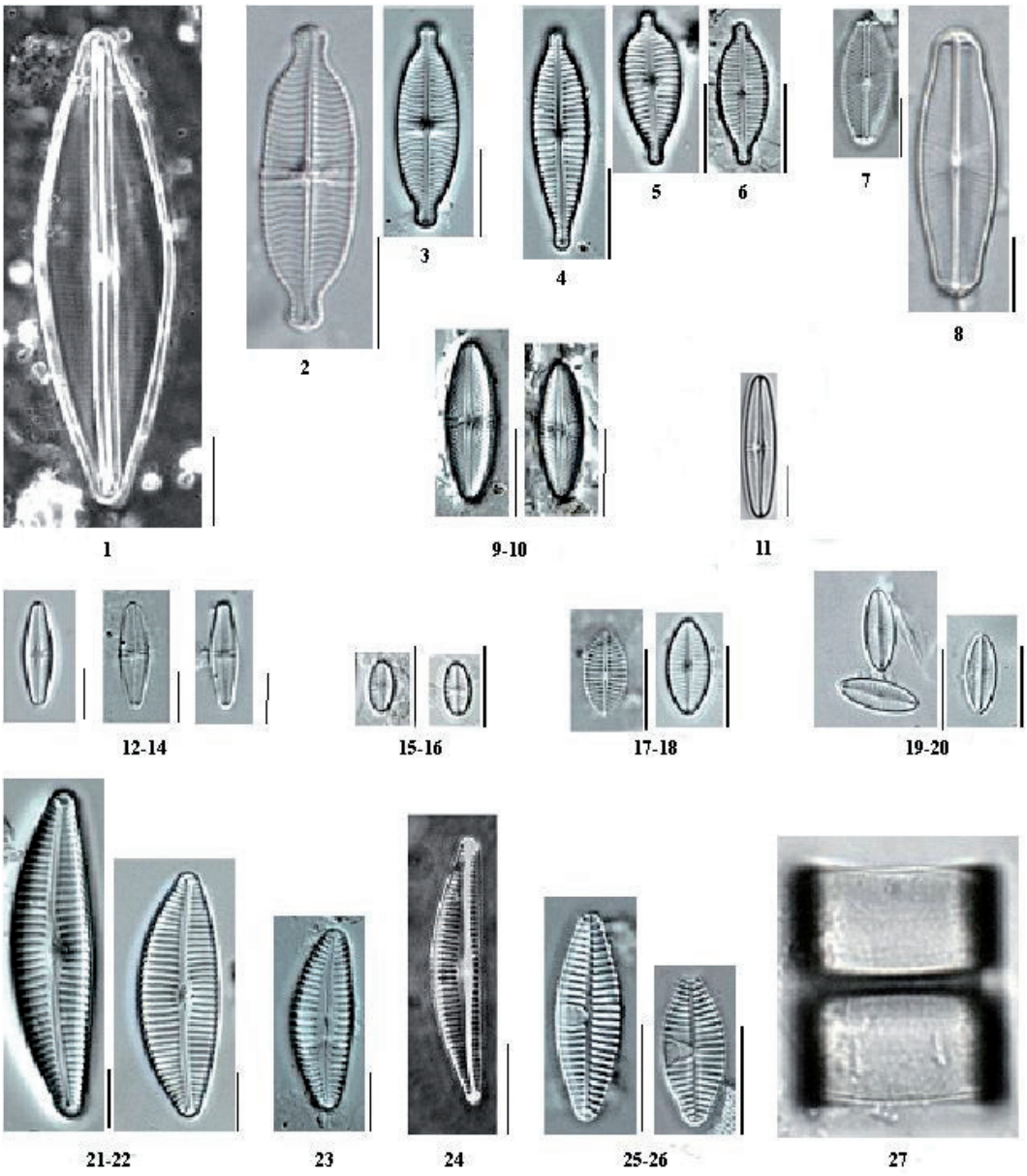

Figure 3 (continued). Common species of benthic diatoms in Mekong River and its tributaries (scale bar = 10 μm)

(1) *Frustulia undosa* D. Metzeltin & H. Lange-Bertalot , (2-3) *Geissleria decussis* (Østrup) Lange-Bertalot&Metzeltin, (4-6) *Gomphonema lagenula* Kützing, (7-8) *Sellaphora pupula* (Kützing) Mereschkovsky, (9-10) *Luticola goeppertiana* (Bleisch) D.G.Mann in Round,Crawford&Mann, (11) *Achnanthidium convergens* (H. Kobayasi) H. Kobayasi, (12-14) *Achnanthidium minutissimum* (Kützing) Czarnecki, (15-16) *Eolimna minima* (Grunow) Lange-Bertalot, (17-18) *Eolimna subminuscula* (Manguin) Gerd Moser, (19-20) *Mayamaea atomus* (Kützing) H. Lange-Bertalot,
(21-22) *Cymbella sumatrensis* Hustedt, (23) *Cymbella* sp.1, (24) *Encyonema* sp.1, (25-26) *Planothidium frequentissimum* (Lange-Bertalot) Round & L. Bukhtiyarova, (27) *Melosira varians* C. Agardh

The water quality in the Mekong River and its tributaries was classified in the fourth category according to the standards for surface water quality of Thailand certified by the Pollution Control Department [39], and can be used for household consumption after a disinfection process and special water treatment.

Table 2. Physicochemical properties of water at 14 sampling sites (average values and min-max values, n=14)

Sampling Site	Temperature (°C)	Velocity (m/s)	pH	Conductivity (µS/cm)	Turbidity (NTU)	Alkalinity (mg/L as $CaCO_3$)	DO (mg/L)	BOD (mg/L)	NO_3^--N (mg/L)	NH_4^+-N (mg/L)	SRP (mg/L)
GT	25.6 (18.1-30.8)	5.4 (1.8-9.2)	7.7 (7.3-8.0)	218.8 (153.0-312.0)	137.1 (54.0-301.0)	55.70 (9.90-103.00)	8.00 (5.40-10.00)	2.60 (1.80-4.10)	0.78 (0.10-1.90)	0.21 (0.04-0.47)	0.14 (0.06-0.55)
KO	26.0 (20.5-29.2)	5.8 (4.0-7.8)	7.2 (6.9-7.8)	138.5 (78.9-198.2)	199.1 (57.0-305.0)	41.05 (6.90-70.20)	8.20 (5.20-11.00)	3.10 (2.00-5.00)	1.57 (0.80-3.00)	0.37 (0.29-0.46)	0.24 (0.10-1.19)
HK	25.3 (18.5-29.8)	7.8 (3.0-12.3)	7.6 (7.2-8.1)	221.0 (162.0-270.0)	212.6 (48.0-419.0)	60.80 (17.60-97.00)	7.80 (5.20-9.80)	1.50 (0.20-3.10)	1.55 (0.20-3.40)	0.31 (0.13-0.67)	0.15 (0.02-0.67)
HG	30.2 (23.3-35.8)	6.7 (0.5-14.3)	7.6 (7.2-8.1)	180.4 (64.0-389.0)	82.5 (3.0-438.0)	57.80 (19.00-101.00)	7.00 (4.20-8.40)	2.70 (0.40-6.40)	0.88 (0.00-1.60)	0.42 (0.15-0.72)	0.22 (0.10-0.61)
KK	28.9 (23.9-32.8)	3.5 (0.1-5.6)	7.6 (7.0-8.7)	192.8 (49.0-325.0)	205.2 (105.0-453.0)	67.80 (35.00-104.00)	5.90 (4.80-8.60)	2.30 (0.00-5.60)	1.20 (0.20-2.00)	0.28 (0.14-0.43)	0.19 (0.14-0.29)
PS	30.0 (26.0-33.0)	2.74 (0.0-6.2)	7.4 (7.0-7.8)	249.7 (147.0-349.0)	183.4 (96.0-367.0)	65.80 (25.00-107.00)	5.60 (4.40-8.20)	1.20 (0.20-4.40)	1.12 (0.60-1.80)	0.38 (0.16-0.58)	0.19 (0.07-0.26)
LG	31.5 (26.5-34.1)	1.3 (0.0-6.3)	7.2 (6.4-8.1)	292.0 (146.0-401.0)	53.3 (12.0-125.0)	36.00 (8.00-85.00)	4.40 (2.60-5.80)	1.30 (0.10-3.00)	0.79 (0.50-1.10)	0.41 (0.20-0.74)	0.20 (0.07-0.40)
NP	30.6 (25.1-32.9)	1.4 (0.0-4.4)	7.4 (6.7-7.8)	195.7 (91.0-263.0)	127.4 (28.0-266.0)	61.20 (20.50-95.00)	5.70 (4.00-8.20)	1.70 (0.20-4.90)	0.76 (0.00-1.30)	0.36 (0.17-0.55)	0.13 (0.00-0.33)
SK	31.4 (27.0-34.8)	3.7 (0.1-10.4)	6.8 (6.0-7.5)	341.1 (127.0-759.0)	70.1 (10.0-288.0)	23.30 (4.10-45.00)	4.60 (2.20-7.00)	1.60 (0.00-3.60)	0.99 (0.20-1.80)	0.40 (0.18-0.73)	0.09 (0.01-0.20)
KB	30.4 (24.5-32.6)	8.3 (2.0-16.5)	7.5 (6.8-8.0)	193.2 (133.5-255.0)	134.1 (23.0-271.0)	51.40 (17.00-92.00)	6.00 (4.60-8.40)	1.90 (0.30-4.60)	0.68 (0.10-1.90)	0.30 (0.14-0.54)	0.15 (0.04-0.29)
HW	31.0 (27.1-34.8)	6.9 (0.1-14.9)	7.4 (6.8-7.9)	166.3 (66.0-255.0)	136.0 (16.0-303.0)	49.20 (18.50-87.00)	6.10 (4.60-8.60)	1.10 (0.00-4.90)	0.55 (0.10-1.20)	0.31 (0.10-0.60)	0.15 (0.00-0.37)
KH	30.3 (22.4-36.4)	2.7 (0.0-7.1)	7.5 (6.8-7.8)	134.9 (43.0-250.0)	144.1 (22.0-325.0)	52.50 (20.00-90.00)	5.89 (4.00-8.40)	1.40 (0.10-4.80)	0.55 (0.10-1.10)	0.31 (0.16-0.61)	0.17 (0.00-0.70)
KP	32.1 (28.0-36.0)	5.2 (0.1-8.8)	6.9 (6.2-7.9)	175.7 (80.0-265.0)	72.6 (13.0-119.0)	43.90 (10.00-73.20)	4.86 (3.60-7.20)	1.44 (0.00-5.20)	0.65 (0.00-1.90)	0.53 (0.17-0.85)	0.10 (0.02-0.30)
KJ	31.5 (27.0-34.8)	1.7 (0.0-4.7)	7.9 (6.6-8.2)	141.8 (44.0-243.0)	119.9 (14.0-260.0)	59.80 (21.00-85.00)	6.29 (4.60-8.50)	2.36 (0.60-5.10)	0.68 (0.00-1.30)	0.40 (0.11-1.07)	0.14 (0.01-0.34)

Correlation between Physico-Chemical Variables

There were significant positive and negative correlations between some of the physico-chemical variables of water as shown in Table 3. Significant positive correlation between SRP and NO_3^--N was observed ($P<0.001$): the SRP concentration increased with higher NO_3^--N concentration. The pH positively correlated with NO_3^--N ($P<0.01$), NH_4^+-N ($P<0.001$) and SRP ($P<0.001$). It increased with higher NO_3^--N, NH_4^+-N and SRP concentrations. The alkalinity positively correlated with NO_3^--N ($P<0.01$), SRP ($P<0.001$), pH ($P<0.001$) and conductivity ($P<0.001$), but negatively correlated with NH_4^+-N ($P<0.001$). Alkalinity increased with higher NO_3^--N and SRP concentrations as well as pH and conductivity. On the other hand, it decreased with higher NH_4^+-N concentration. The BOD positively correlated with NO_3^--N ($P<0.001$), SRP ($P<0.001$), pH ($P<0.001$), alkalinity ($P<0.001$) and DO ($P<0.001$). However, it showed negative

correlation with NH_4^+-N ($P<0.05$). The BOD increased with higher NO_3^--N and SRP concentrations, pH, alkalinity and DO, whereas it decreased with higher NH_4^+-N concentration.

Table 3. Pearson's correlation coefficients (r) between water physico-chemical variables. Significant values of r: * = $P < 0.05$; ** = $P < 0.01$; *** = $P < 0.001$ (n = 194)

	NO_3^--N	NH_4^+-N	SRP	pH	Conductivity	Alkalinity	DO	BOD	Temperature	Velocity	Turbidity
NO_3^--N	1										
NH_4^+-N	−0.040	1									
SRP	0.360 (***)	−0.032	1								
pH	0.200 (**)	0.446 (***)	0.353 (***)	1							
Conductivity	0.146 (*)	−0.072	0.162 (*)	0.206 (**)	1						
Alkalinity	0.212 (**)	−0.311 (***)	0.313 (***)	0.644 (***)	0.260 (***)	1					
DO	0.069	−0.495 (***)	0.005	0.492 (***)	0.046	0.349 (***)	1				
BOD	0.293 (***)	−0.178 (*)	0.265 (***)	0.382 (***)	0.047	0.310 (***)	0.360 (***)	1			
Temperature	−0.090	0.515 (***)	0.017	−0.337 (***)	−0.053	−0.090	−0.716 (***)	−0.233 (***)	1		
Velocity	0.004	0.041	0.165 (*)	0.057	0.024	0.006	0.149 (*)	0.102	−0.020	1	
Turbidity	0.129	0.177 (*)	−0.032	−0.219 (**)	−0.305 (***)	−0.325 (***)	−0.139 (*)	−0.079	−0.078	0.079	1

Human activities in the Mekong River basin include small-scale livestock keeping, fish farming, subsistence farming and horticultural farming. All these activities are the source of pollution, especially in the tributaries which are frequently disturbed by domestic animals and riparian human communities. Sampling sites such as LG, SK and KP, where the water passes through a city, are directly affected by human activities. On the contrary, at KO where the river runs through a rural area, or at HG where the river runs through mountains, the water is not affected by such activities.

Relationship between Diatom Species and Physico-Chemical Variables by CCA

Twenty-nine common species of benthic diatoms were subjected to CCA to find the relationship between water physico-chemical properties and diatom species using MVSP statistical program. The results of CCA are shown in Figure 4. It was found that *Achnanthidium minutissimum* (Achmin) positively correlated with conductivity; the amount of this alga increased with higher conductivity. *Navicula menisculus* (Navmen) positively correlated with alkalinity (Alk) but it negatively correlated with NH_4^+-N (NH4). The number of *Navicula menisculus* increased with higher alkalinity but decreased with higher NH_4^+-N. *Nitzschia clausii* (Nitcla), *Luticola goeppertiana* (Lutgeo), *Achnanthidium convergens* (Achcon), *Eolimna minima* (Eolmin) and *Ulnaria ulna* (Ulnuln) positively correlated with SRP and NO_3^--N but negatively correlated with BOD. They increased with higher SRP and NO_3^--N but decreased with higher BOD.

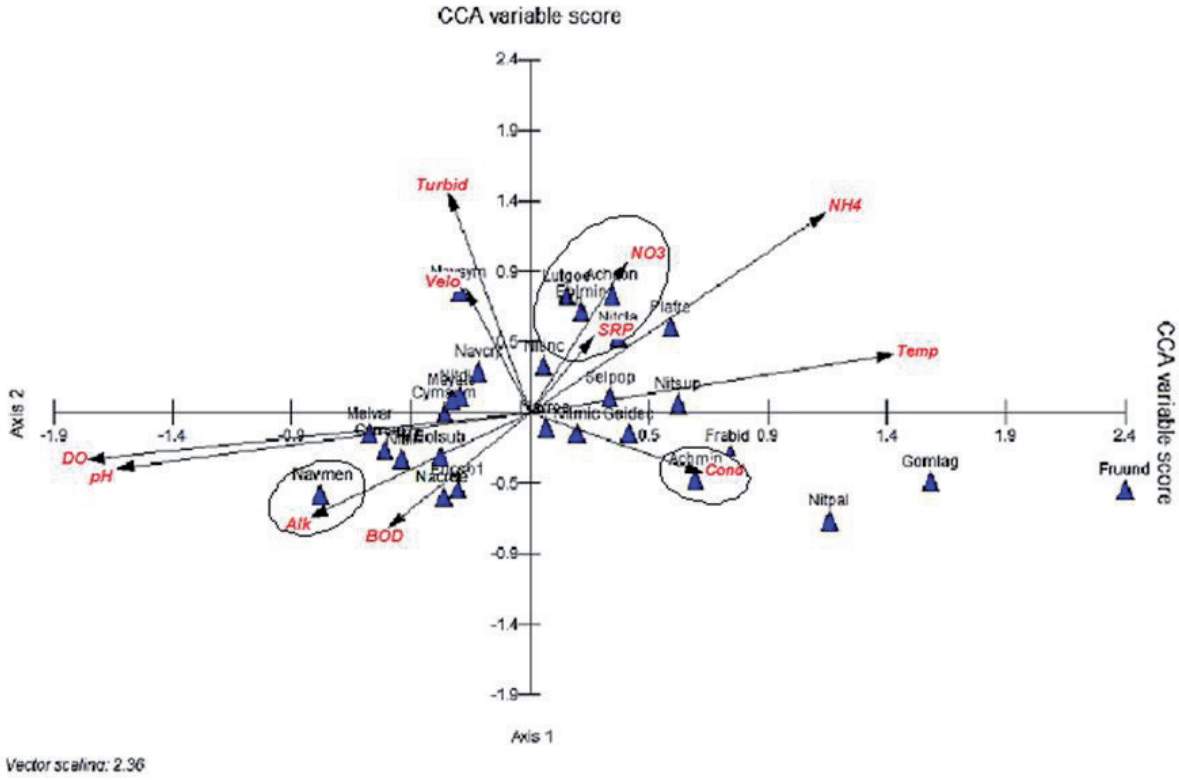

Figure 4. CCA of the relationship between water quality and common species of diatom (% of relative abundance > 1)

There are many environmental conditions which influence the growth of algae. In a lotic ecosystem, almost all algae live in benthic forms [40] and they usually grow on any surface of the substratum. Each type of substratum, either rock, mud, sand or silt, affects the benthic behaviour [41]. The substratum type is related to the current velocity and water volume [33]. The substratum characteristic has a direct impact on the distribution of benthic algae [42]. In this study, the lowest amounts of diatoms at all sampling times were recorded at HK sampling site (Figure 2). This observation was probably due to a high level of water in the wet season and the substrata along the bank being soft sediment of sand and silt, which is not suitable for diatom growth [43]. Furthermore, blooms of macroalgae, namely *Cladophora* spp. and *Microspora* spp., appeared in cool dry season and there were fewer suitable substrata for the attachment of benthic diatoms. Mpawenayo and Mathooko [44] published the structure of the diatom assemblage associated with *Cladophora* macroalgae and sediment in a highland stream of Kenya. The dominant species of diatoms were *Nitzschia amphibia* and *Gomphonema parvulum*. Similary, *G. parvulum* was found at HK where there was a full bloom of *Cladophora* spp. Jüttner et al. [45] reported that *G. parvulum* in particular preferred vegetation as its habitat. However, *G. parvulum* was found equally often on sediment because of transportation and contamination. Persistent stability and protection of diatoms attached on *Cladophora* could explain the existence of higher diatom species richness on *Cladophora* than in a more unstable sediment habitat.

In fast-flowing water, there are diatoms such as *Achnanthes* and *Cocconeis* that can attach on rocks and other hard surfaces [24]. Similarly, in this study, *Cocconeis* spp. were found as dominant species at HG during summer 2007 with high water velocity. In slower flowing water, *Melosira varians* and various species of *Synedra*, *Gomphonema* and *Cymbella* are found on hard substrata [24]. Throughout the sampling period, *Gomphonema* spp. were also observed at LG located about 100 metres downstream from a small dam, where the flow rate of water was extremely low.

Species of Benthic Diatoms in Relation to Physico-Chemical Properties of Water by Cluster Analysis

Twenty nine common diatom species were arranged in groups of sampling sites detected by cluster analysis of physico-chemical parameters of water quality at 80% similarity. The number of benthic diatoms in each group was calculated by Minitab program to find the significant difference and significant correlation between groups. The relationship between diatom community composition and water quality variables was determined using statistical techniques. Each sampling site had distinct water physico-chemical properties. At 80% similarity, the dendrogram divided sampling sites into eleven distinct clusters of characteristic water quality types: groups A to I_2 (Figure 5 and Table 4). It was found that all sampling sites in groups A (n=3) and B (n=9) and some in group C (n=3) were those during December 2006 (cool dry season). Group E, the biggest group (n=54), was composed of sampling sites during May 2006 (summer) and some sites in two cool dry seasons.

The values of physico-chemical parameters in each group were calculated by Minitab program to find significant differences and correlations between groups A to I_2 as shown in Table 5. It was found that groups A, C, G and H showed a non-significant correlation with NO_3^--N concentration. Group F_1 showed higher concentrations of NO_3^--N (average of 1.33 mg/L) than groups B, D, E, F_2 and I_1 ($P < 0.05$). Group D ($P<0.05$) was high in NH_4^+-N concentration (average of 0.59 mg/L). There was a non-significant correlation with NH_4^+-N concentration in group A ($P<0.05$)

Significantly high concentrations of SRP (average of 0.39 mg/L) in group H ($P<0.05$) compared to other groups were observed while groups C and G showed a non-significant correlation with the same parameter. The study showed significantly high pH (average of 7.75) in group C ($P<0.05$) and significantly low pH (average of 6.59) in group G ($P<0.05$). The pH values of all sampling sites in groups A and H were not significantly different within each group. As for conductivity, there were significant differences in all groups ($P<0.05$). Group A showed high conductivity values (average of 753.00 µS/cm), whereas low conductivity values (average of 47.78 µS/cm) were observed in group B.

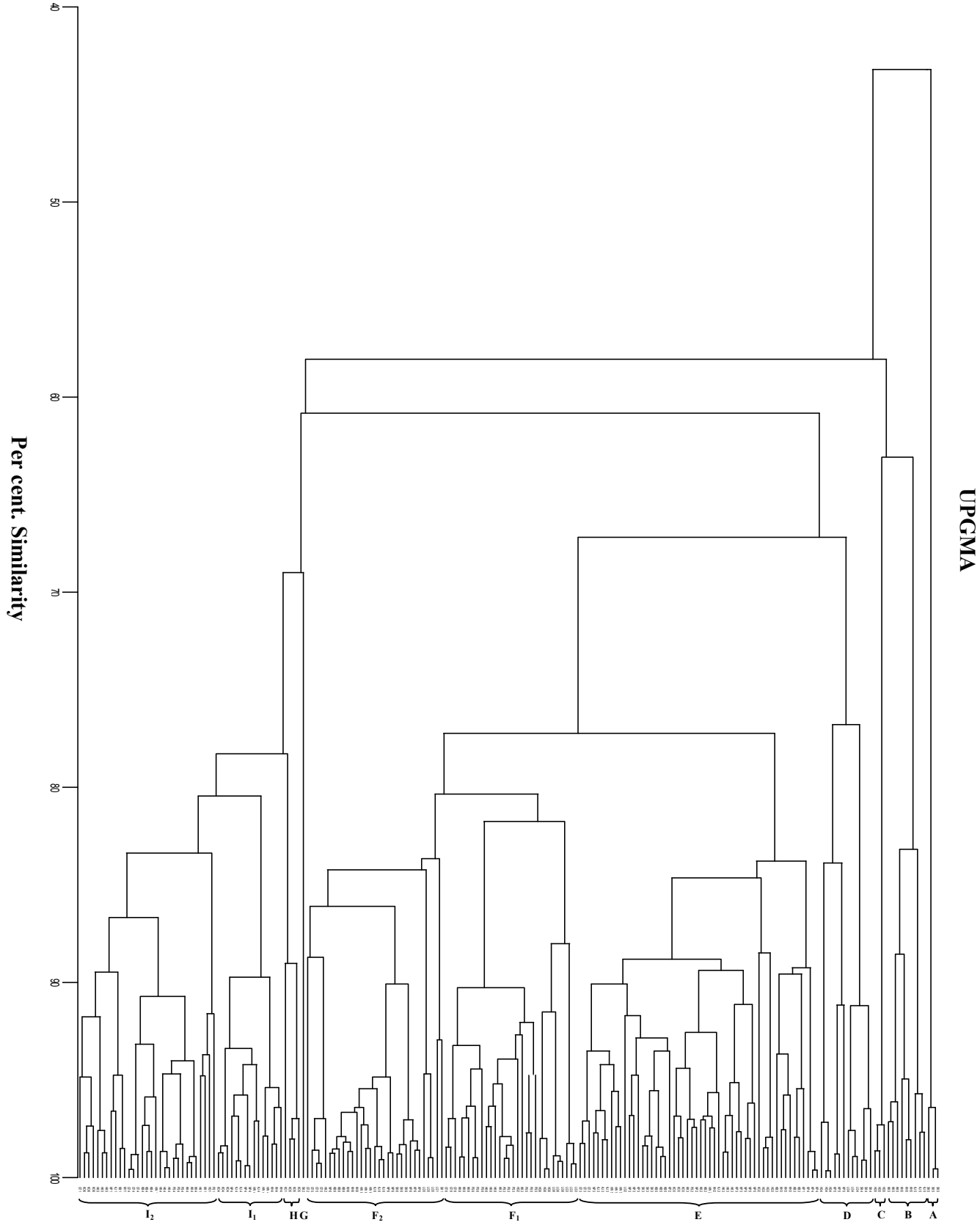

Figure 5. Dendrogram of similarities between investigated sites according to physico-chemical parameters of water; 252 cases, 11 variables

Table 4. Groups of sampling sites detected by cluster analysis of physico-chemical parameters of water quality at 80% similarity

Group	Sampling site	Description
A	SK5.1, SK5.2, SK5.3	Tributaries in north-eastern Thailand in cool dry season (second year)
B	KK5.1, KK5.2, KK5.3, KH5.1, KH5.2, KH5.3, KJ5.1, KJ5.2, KJ5.3	Mekong River in north-eastern Thailand in cool dry season (second year)
C	HG5.1, HG5.2, HG5.3	Tributaries in north-eastern Thailand in cool dry season (second year)
D	HG4.1, HG4.2, HG4.3, LG4.1, LG4.2, LG4.3, SK4.1, SK4.2, SK4.3, KP5.1, KP5.2, KP5.3	Tributaries in north-eastern Thailand in summer (second year) and cool dry season (second year)
E	GT3.1, GT3.2, GT3.3, KO2, KO3.1, KO3.2, KO3.3, HK3.1, HK3.2, HK3.3, HG3.1, HG3.2, HG3.3,KK2, KK3.2, PS2, LG2, NP2, NP3.1, NP3.2,NP3.3, NP5.1, NP5.2, NP5.3, SK3.1, SK3.2, SK3.3, KB2, KB3.1, KB3.2, KB3.3, KB5.1, KB5.2, KB5.3, HW2, HW5.1, HW5.2, HW5.3, KH2, KH3.1, KH3.2, KH3.3, KP1, KP2, KP3.1, KP3.2, KP3.3, KP4.1, KP4.2, KP4.3, KJ2, KJ3.1, KJ3.2, KJ3.3	Mekong River and its tributaries in summer (first year) and some of two cool dry seasons
F_1	GT6.1,GT6.2,GT6.3, HK6.1,HK6.2,HK6.3,HG2, HG6.1, HG6.2, HG6.3, KK3.1, KK3.3, K6.1, KK6.2, KK6.3, PS3.1, PS3.2, PS3.3,PS5.1,PS5.2,PS5.3, PS6.1, PS6.2, PS6.3,LG3.1, LG3.2, LG3.3,LG6.1, LG6.2, LG6.3	Mekong River and its tributaries in two summers
F_2	GT2, GT5.1, GT5.2, GT5.3, HK2, LG1, LG5.1,LG5.2, LG5.3, NP6.1, NP6.2, NP6.3, SK1, SK6.1, SK6.2, SK6.3, KB6.1, KB6.2, KB6.3, HW6.1, HW6.2, HW6.3, KH6.1, KH6.2, KH6.3, KP6.1, KP6.2, KP6.3, KJ6.1, KJ6.2,KJ6.3	Mekong River and its tributaries in summer (second year) and some of cool dry season (second year)
G	SK2	Tributaries in north-eastern Thailand in cool dry season (first year)
H	KO1, KO5.1, KO5.2, KO5.3	Tributaries in northern Thailand in rainy season (first year) and cool dry season (second year)
I_1	KO4.1, KO4.2, KO4.3, NP4.1, NP4.2, NP4.3,HW4.1, HW4.2, HW4.3, KH4.1, KH4.2, KH4.3, KJ4.1, KJ4.2, KJ4.3	Mekong River and its tributaries in rainy season (second year)
I_2	GT1, GT4.1, GT4.2, GT4.3, KO6.1, KO6.2, KO6.3, HK1, HK4.1, HK4.2, HK4.3, HK5.1, HK5.2, HK5.3, HG1, KK1, KK4.1, KK4.2, KK4.3, PS1, PS4.1, PS4.2, PS4.3, NP1,KB1, KB4.1, KB4.2, KB4.3, HW1, KH1, KJ1	Mekong River and its tributaries in two rainy seasons and some of cool dry season (second year) and summer (second year)

There were significant differences ($P<0.05$) in alkalinity in all groups. High values of alkalinity (average of 83.17 mg/L) were observed in group F_1 ($P<0.05$). The DO values of all sampling sites in groups A and G were not significantly different within each group. High DO values (average of 9.50 mg/L) were observed in group H while low values (average of 4.67 mg/L and 4.71 mg/L) were observed in groups D and I_1 respectively. For BOD, the values were not significantly different in group G while significantly high values (average of 4.47 mg/L) were observed in group C and significantly low values (average of 0.23 mg/L) were in group A.

There were non-significant correlation with water temperature in groups A and G. Group D ($P<0.05$) and group I_1 ($P<0.05$) had significantly high water temperatures (average of 33.5^{o}C and 32.8^{o}C respectively). Low water temperatures (average of 22.3^{o}C) were observed in group H ($P<0.05$). Significant difference in turbidity was observed for all groups ($P<0.05$). The lowest

turbidity (average of 4.33 NTU) was recorded for group C while the highest (average of 314.16 NTU) was recorded for group I_2.

Table 5. Values of average ($\bar{X}$) and standard error (se) of physico-chemical parameters ($P<0.05$) and correlation (cor) between groups A-I_2

Parameter	A	B	C	D	E
NO_3^--N	$\bar{X}$ = 0.57	$\bar{X}$ = 0.56	$\bar{X}$ = 0.80	$\bar{X}$ = 0.47	$\bar{X}$ = 0.88
(mg/L)	se = 0.19	se = 0.20	se = 0.36	se = 0.07	se = 0.07
	n = 3	n = 9	n = 3	n = 12	n = 54
	cor ns	cor B<F_1	cor ns	cor D<F_1, H, I_2	cor E< F_1
NH_4^+-N	$\bar{X}$ = 0.41	$\bar{X}$ = 0.18	$\bar{X}$ = 0.22	$\bar{X}$ = 0.59	$\bar{X}$ = 0.32
(mg/L)	se = 0.03	se = 0.01	se = 0.06	se = 0.04	se = 0.02
	n = 3	n = 9	n = 3	n = 12	n = 54
	cor ns	cor B<D,I_1,I_2	cor C<D,I_1	cor D>B,E,F_1,F_2,H,I_2	cor E<D,I_1
SRP	$\bar{X}$ = 0.04	$\bar{X}$ = 0.07	$\bar{X}$ = 0.18	$\bar{X}$ = 0.07	$\bar{X}$ = 0.14
(mg/L)	se = 0.03	se= 0.03	se= 0.04	se = 0.01	se = 0.01
	n = 3	n=9	n=3	n = 12	n = 54
	cor A<F_1,H	cor B<F_1,F_2,H	cor ns	cor D< F_1,F_2,H	cor E< F_1,H
pH	$\bar{X}$ = 7.09	$\bar{X}$ = 7.56	$\bar{X}$ = 7.75	$\bar{X}$ = 6.73	$\bar{X}$ = 7.40
	se = 0.06	se= 0.06	se= 0	se = 0.13	se = 0.07
	n = 3	n=9	n=3	n = 12	n = 54
	cor ns	cor B>D,I_1	cor C>D,I_1	cor D<B,C,E,F_1,F_2,I_2	cor E> D,I_1
Conductivity	$\bar{X}$ = 753.00	$\bar{X}$ = 47.78	$\bar{X}$ = 65.17	$\bar{X}$ = 110.86	$\bar{X}$ = 186.81
(µS/cm)	se = 5.03	se= 1.33	se= 0.09	se = 8.77	se = 3.80
	n = 3	n=9	n=3	n = 12	n = 54
	cor A>B,C,D,E,F_1,F_2,G,H,I_1,I_2	cor B<A,D,E,F_1,F_2,G,H,I_2	cor C<A,E,F_1,F_2,G,H,I_2	cor B<D<A,E,F_1,F_2,G,I_2	cor B,C,D,H,I_1<E=I_2<A,F_1,F_2,G
Alkalinity	$\bar{X}$ = 4.25	$\bar{X}$ = 55.56	$\bar{X}$ = 48.33	$\bar{X}$ = 21.17	$\bar{X}$ = 55.89
(mg/L as $CaCO_3$)	se = 0.12	se= 6.40	se= 0.44	se =5.17	se = 2.78
	n = 3	n=9	n=3	n = 12	n = 54
	cor A<B,D,F_1,F_2,I_2	cor A,D,I_1<B<F_1	cor C<F_1	cor D<B,E,F_1,F_2,I_2	cor A,D,I_1,I_2<E< F_1
DO	$\bar{X}$ = 6.47	$\bar{X}$ = 7.36	$\bar{X}$ = 8.13	$\bar{X}$ = 4.67	$\bar{X}$ = 6.48
(mg/L)	se = 0.07	se= 0.09	se= 0.13	se= 0.41	se = 0.23
	n = 3	n=9	n=3	n=12	n = 54
	cor ns	cor B> D,I_1,I_2	cor C> D,I_1,I_2	cor D<E,F_1,F_2,H	cor D,I_1<E<H
BOD	$\bar{X}$ = 0.23	$\bar{X}$ = 0.69	$\bar{X}$ = 4.47	$\bar{X}$ = 0.54	$\bar{X}$ = 2.62
(mg/L)	se = 0.03	se= 0.19	se= 1.30	se = 0.18	se = 0.18
	n = 3	n=9	n=3	n = 12	n = 54
	cor A<C,E,F_1,H	cor B<C,E,F_1,H	cor C>A,B,D,E,F_1,F_2,I_1,I_2	cor D<C,E,F_1,F_2,H,I_2	cor E>A,B,D,F_2,I_1,I_2
Temperature	$\bar{X}$ = 28.00	$\bar{X}$ = 24.71	$\bar{X}$ = 27.30	$\bar{X}$ = 33.49	$\bar{X}$ = 29.96
(^oC)	se = 0.90	se= 0.79	se= 0	se = 0.61	se = 0.41
	n = 3	n=9	n=3	n = 12	n = 54
	cor ns	cor B<D,E,F_1,F_2,I_1,I_2	cor C<D,I_1	cor D>B,C,E,F_1,F_2,H,I_1,I_2	cor B,H<E<D,I_1
Turbidity	$\bar{X}$ = 41.00	$\bar{X}$ = 126.33	$\bar{X}$ = 4.33	$\bar{X}$ = 65.78	$\bar{X}$ = 95.35
(NTU)	se = 14.05	se= 10.48	se= 0.88	se = 4.79	se = 3.18
	n = 3	n=9	n=3	n = 12	n = 54
	cor A<B,E,F_1,G,H,I_1,I_2	cor A,C,D,E,F_1,F_2<B<G,H,I_1,I_2	cor C<B,D,E,F_1,G,H,I_1,I_2	cor C,F_2<D<B,E,F_1,G,H,I_1,I_2	cor A,C,D,F_2<E=F_1<B,G,H,I_1,I_2

Note: ns = not significant

Table 5. (continued)

Parameter	F_1	F_2	G	H	I_1	I_2
NO_3^--N (mg/L)	$\bar{X}$ = 1.33 se = 0.08 n = 30 cor F_1>B,D,E,F_2,I_1	$\bar{X}$ = 0.82 se = 0.08 n = 31 cor F_2 < F_1	$\bar{X}$ = 1.80 se = 0 n = 1 cor ns	$\bar{X}$ =1.38 se = 0.54 n=4 cor ns	$\bar{X}$ =0.68 se = 0.23 n=15 cor I_1< F_1	$\bar{X}$ =1.04 se=0.15 n=31 cor I_2>D
NH_4^+-N (mg/L)	$\bar{X}$ = 0.32 se = 0.03 n = 30 cor F_1=F_2<D,I_1	$\bar{X}$ = 0.32 se = 0.04 n = 31 cor F_2= F_1<D,I_2	$\bar{X}$ = 0.38 se = 0 n = 1 cor ns	$\bar{X}$ = 0.32 se = 0.01 n = 4 cor H< D	$\bar{X}$ = 0.49 se = 0.02 n = 15 cor I_1>B,C,E,F_1,F_2	$\bar{X}$ = 0.41 se = 0.02 n = 31 cor B,E<I_2<D
SRP (mg/L)	$\bar{X}$ = 0.23 se = 0.02 n = 30 cor F_1> A,B,D,E,I_1	$\bar{X}$ = 0.21 se = 0.03 n = 31 cor B,D,I_1<F2<H	$\bar{X}$ = 0.07 se = 0 n = 1 cor ns	$\bar{X}$ = 0.39 se = 0.27 n = 4 cor H>A,B,D,E,F_2,I_2	$\bar{X}$ = 0.09 se = 0.01 n = 15 cor I_2<F_1,F_2,H	$\bar{X}$ = 0.17 se = 0.03 n = 31 cor I_2<H
pH	$\bar{X}$ = 7.60 se = 0.06 n = 30 cor F_1=F_2>D,E,G,I_1	$\bar{X}$ = 7.63 se = 0.08 n = 31 cor F_2=F_1>D,E,G,I_1	$\bar{X}$ = 6.59 se = 0 n = 1 cor G<F_1,F_2	$\bar{X}$ = 7.16 se = 0.21 n = 4 cor ns	$\bar{X}$ = 6.81 se = 0.03 n = 15 cor I_1<B,C,E,F_1,F_2,I_2	$\bar{X}$ = 7.36 se = 0.06 n = 31 cor D,I_1<F_1,F_2
Conductivity (µS/cm)	$\bar{X}$ = 316.44 se = 9.53 n = 30 cor B,C,D,E,F_2,H,I_1,I_2<F_1 <A,G	$\bar{X}$ = 254.71 se = 3.89 n = 31 cor B,C,D,E ,H,I_1,I_2<F_2 <A,F_1,G	$\bar{X}$ = 484.00 se = 0 n = 1 cor B,C,D,E,F_1,F_2,H,I_1,I_2 <E<A	$\bar{X}$ = 121.45 se = 6.21 n = 4 cor B,C,I_1<H<A,E,F_1, F_2,G,I_2	$\bar{X}$ = 78.42 se = 2.35 n = 15 cor I_1>A,E,F_1,F_2,G,H,I_2	$\bar{X}$ = 175.96 se = 6.21 n = 31 cor B,C,D,H,I_1<I_2=E <A,F_1,F_2,G
Alkalinity (mg/L as $CaCO_3$)	$\bar{X}$ = 83.17 se = 4.05 n = 30 cor F_1>A,B,C,D,E,F_2,G,H,I_1,I_2	$\bar{X}$ = 62.90 se = 4.93 n = 31 cor A,D,I_1,I_2<F_2<F_1	$\bar{X}$ = 23.00 se = 0 n = 1 cor G<F_1	$\bar{X}$ = 33.00 se = 2.08 n = 4 cor H<F_1,F_2	$\bar{X}$ = 17.95 se = 1.48 n = 15 cor I_1< B,E,F_1,F_2,I_2	$\bar{X}$ = 39.41 se = 3.71 n = 31 cor D,I_1<I_2< E,F_1,F_2
DO (mg/L)	$\bar{X}$ = 6.38 se = 0.29 n = 30 cor D,I_1<F_1<H	$\bar{X}$ = 6.16 se = 0.34 n = 31 cor D,I_1<F_2<H	$\bar{X}$ = 7.00 se = 0 n = 1 cor ns	$\bar{X}$ = 9.50 se = 1.43 n = 4 cor H>D,E,F_1,F_2,I_1,I_2	$\bar{X}$ = 4.71 se = 0.19 n = 15 cor I_1<B,E,F_1,F_2,H	$\bar{X}$ = 5.79 se = 0.27 n = 31 cor I_2<B,C,H
BOD (mg/L)	$\bar{X}$ = 2.26 se = 0.27 n = 30 cor A,B,D,F_2,I_1<F_1<C	$\bar{X}$ = 1.25 se = 0.18 n = 31 cor F_2<C,H	$\bar{X}$ = 3.60 se = 0 n = 1 cor ns	$\bar{X}$ = 3.05 se = 0.34 n = 4 cor H>A,B,D,F_2,I_1	$\bar{X}$ = 0.91 se = 0.35 n = 15 cor I_1< C,E,F_1,H	$\bar{X}$ = 1.70 se = 0.26 n = 31 cor D<I_2<C,H
Temperature (^{0}C)	$\bar{X}$ = 30.17 se = 0.36 n = 30 cor B,H<F_1<D	$\bar{X}$ = 29.33 se = 0.87 n = 31 cor B,H<F_2<D,I_1	$\bar{X}$ = 27.00 se = 0 n = 1 cor ns	$\bar{X}$ = 22.33 se = 1.76 n = 4 cor H<D,E,F_1,F_2,I_1,I_2	$\bar{X}$ = 32.83 se = 0.99 n = 15 cor I_1>B,C,E,F_2,H,I_2	$\bar{X}$ = 28.41 se = 0.76 n = 31 cor B,H<I_2<D,I_1
Turbidity (NTU)	$\bar{X}$ = 101.60 se = 7.08 n = 30 cor A,C,D,F_2<F_1=E <B,G,H,I_1,I_2	$\bar{X}$ = 28.06 se = 3.15 n = 31 cor F_2<B,D,E,F_1,G,H,I_1,I_2	$\bar{X}$ = 288.00 se = 0 n = 1 cor G>A,B,C,D,E,F_1,F_2,H	$\bar{X}$ = 183.00 se = 9.60 n = 4 cor A,B,C,D,E,F_1,F_2<H <G,I_1,I_2	$\bar{X}$ = 265.80 se = 8.64 n = 15 cor A,B,C,D,E,F_1,F_2,H <I_1<I_2	$\bar{X}$ = 314.16 se = 10.20 n = 31 cor I_1>A,B,C,D,E,F_1,F_2, H,I_2

It was found that from cluster analysis, only 4 from 29 species had a significant correlation with water physico-chemical properties. From Table 5, there was a significant correlation ($P<0.05$) between *Luticola goeppertiana* in most sampling sites in Group I_2 in wet season and low conductivity. The presence of *L. goeppertiana* thus seemed to indicate low conductivity.

There was also a significant correlation ($P<0.05$) of *Eolimna minima* in group H (a tributary in northern Thailand) in wet season with high SRP. Therefore, *E. minima* seemed to indicate a high concentration of SRP. In the same manner, *Mayamaea atomus* and *Ulnaria ulna* in Group C (a tributary in north-eastern Thailand) could be indicators of a high BOD.

CONCLUSIONS

The number of benthic diatom species found (252 species from 53 genera) in Mekong River and its tributaries in north and north-eastern Thailand is similar to those reported for other river systems of comparable size. Determination of the relationship between diatom community composition and water quality variables shows that many species, notably *Achnanthidium minutissimum*, *A. convergens*, *Navicula menisculus*, *Nitzschia clausii*, *Luticola goeppertiana*, *Eolimna minima*, *Ulnaria ulna* and *Mayamaea atomus*, can act as indicators of some of the river-water qualities, viz. conductivity, alkalinity, NH_4^+-N, NO_3^--N, soluble reactive phosphorus, and BOD.

ACKNOWLEDGEMENTS

The authors would like to thank Thailand Research Fund (TRF) for its support in the form of a research grant (Grant No. PHD/0129/2547) through the Royal Golden Jubilee PhD Program. They are also grateful to Dr. Ingrid Jüttner from National Museum Cardiff, U.K. for her suggestions and assistance in diatom identification.

REFERENCES

1. A. Chovanec, P. Jäger, M. Jungwirth, V. Koller-Kreimel, O. Moog, S. Muhar and S. Schmutz, "The Austrian way of assessing the ecological integrity of running waters – a contribution to the EU water framework directive", *Hydrobiol.*, **2000**, *422/423*, 445-452.
2. F. E. Round, "Use of diatoms for monitoring rivers", in "Use of Algae for Monitoring Rivers" (Ed. B. A. Whitton, E. Rott and G. Friedrich), Institut fur Botanik, Universitat, Innsbruck, **1991**, pp.25-32.
3. B. A. Whitton, E. Rott and G. Friedrich, "Use of algae for monitoring rivers", Proceedings of International Symposium on Use of Algae for Monitoring Rivers I, **1991**, Düsseldorf, Germany, pp.10-18.
4. E. Rott, E. Pipp and P. Pfister, "Diatom methods developed for river quality assessment in Austria and a cross-check against numerical trophic indication methods used in Europe", *Algol. Stud.*, **2003**, *110*, 91-115.
5. J. Prygiel, M. Coste and J. Bukowska, "Review of the major diatom-based techniques for the quality assessment of river-state of the art in Europe", Proceedings of International Symposium on Use of Algae for Monitoring Rivers III, **1999**, Douai, France, pp.224-238.
6. M. Ohno, H. Fukushima and T. Ko-Bayashi, "Diatom flora of the Mekong water system, Cambodia", *Nat. Sci.*, **1972**, *20*, 1-11.
7. Mekong River Commission, "Biomonitoring of the lower Mekong River and selected tributaries", MRC technical paper No.13, Mekong River Comission, Vientiane, Lao PDR, **2006**.
8. S. Pruethiworanon, "Diversity of macroalgae and benthic diatoms in Mekong River passing Thailand and their application for water quality", *MS Thesis*, **2008**, Chiang Mai University, Thailand.

9. I. Renberg, "A procedure for preparing large sets of diatom slides from sediment cores", *J. Paleolimnol.*, **1990**, *4*, 87-90.
10. M. G. Kelly, A. Cazaubon, E. Coring, A. Dell'Uomo, L. Ector, B. Goldsmit, H. Guasch, J. Hürlimann, A. Jarlman, B. Kaweeka, J. Kwandrans, R. Laugaste, E.- A. Lindstrom, M. Leitao, P. Marvan, J. Padisak, E. Pipp, J. Prygiel, E. Rott, S. Sabater, H. van Dam and J. Vizinet, "Recommendations for the routine sampling of diatoms for water quality assessments in Europe", *J. Appl. Phycol.*, **1998**, *10*, 215-224.
11. K. Krammer and H. Lange-Bertalot, "Bacillariophyceae Teil 1: Naviculaceae, Süsswasserflora von Mitteleuropa Band 2/1", Gustav Fisher Verlag, Stuttgart, **1986**.
12. K. Krammer and H. Lange-Bertalot, "Bacillariophyceae Teil 2: Epithemiaceae Surirellaceae, Süsswasserflora von Mitteleuropa Band 2/2", Gustav Fisher Verlag, Stuttgart, **1988**.
13. K. Krammer and H. Lange-Bertalot, "Bacillariophyceae Teil 3: Centrales Fragilariaceae Eunotiaceae, Süsswasserflora von Mitteleuropa Band 2/3", Gustav Fisher Verlag, Stuttgart, **1991a**.
14. K. Krammer and H. Lange-Bertalot, "Bacillariophyceae Teil 4: Achnanthaceae, Süsswasserflora von Mitteleuropa Band 2/4", Gustav Fisher Verlag, Stuttgart, **1991b**.
15. H. Lange-Bertalot, "Diatoms of Europe", A.R.G. Gantner Verlag K.G., Ruggell, **2001**.
16. T. Watanabe, T. Ohtsuka, A. Tuji and A. Houki, "Picture Book and Ecology of the Freshwater Diatoms", Uchida-rokakuho, Tokyo, **2005**.
17. H. Lange-Bertalot, "Iconographia Diatomologica: Annotated Diatom Micrographs", Vol.13, A.R.G. Gantner Verlag K.G., Ruggell, **2004**.
18. A. D. Eaton, L. S. Clesceri, E. W. Rice and A. E. Greenberg, "Standard Methods for Examination of Water and Wastewater: Centennial Edition", 21st Edn., American Public Health Association, Washington D. C., **2005**.
19. N. T. H. Holmes and B. A. Whitton, "Phytobenthos of the River Tees and its tributaries", *Freshwater Biol.*, **1981**, *11*, 139-163.
20. R. E. M. Archibald, "The diatoms of the Sundays and Great Fish Rivers in the Eastern Cape Province of South Africa", A.R.G. Gantner Verlag K.G., Ruggell, **1983**.
21. B. C. Chessman, "Diatom flora of an Australian river system: Spatial patterns and environment relationships", *Freshwater Biol.*, **1986**, *16*, 805-819.
22. I. Jüttner, S. Sharma, B. M. Dahal, S. J. Ormerod, P. J. Chimonides and E. J. Cox, "Diatoms as indicators of stream quality in the Kathmandu Valley and Middle Hills of Nepal and India", *Freshwater Biol.*, **2003**, *48*, 2065-2084.
23. T. T. Duong, M. Coste, A. Feurtet-Mazel, D. K. Dang, C. Gold, Y. S. Park and A. Boudou, "Impact of urban pollution from the Hanoi area on benthic diatom communities collected from the Red, Nhue and Tolich Rivers (Vietnam)", *Hydrobiol.*, **2006**, *563*, 201-216.
24. R. Patrick, "Ecology of freshwater diatoms and diatom communities", in "The Biology of Diatoms" (Ed. D. Werner), Blackwell Scientific Publications, Oxford, **1977**, pp.284-322.
25. N. Foged, "Freshwater Diatoms in SriLanka", Odense Publisher, Odense (Denmark), **1976**.
26. A. M. Silva-Benavides, "The epilithic diatom flora of a pristine and a polluted river in Costa Rica, Central America", *Diatom Res.*, **1996**, *11*, 105-142.

27. R. Patrick and C. W. Reimer, "The Diatoms of the United States", The Academy of Natural Science of Philadelphia, Philadelphia, **1966**.
28. T. Pekthong, "Diversity of phytoplankton and benthic algae in Mae Sa stream, Doi Suthep-Pui National Park, altitude 330-550 meters", *MS Thesis*, **1998**, Chiang Mai University, Thailand.
29. T. Pekthong, "Fifty one new record species of freshwater diatoms in Thailand", *Chiang Mai J. Sci.*, **2002**, *28*, 97-112.
30. P. Waiyaka, "Diversity of phytoplankton and benthic algae in Mae Sa stream, Doi Suthep-Pui National Park, altitude 550-1050 meters", *MS Thesis*, **1998**, Chiang Mai University, Thailand.
31. T. Kunpradid, "Biodiversity of phytoplankton and macroalgae in Mae Sa stream, Doi Suthep-Pui National Park, Chiang Mai province", *MS Thesis*, **2000**, Chiang Mai University, Thailand.
32. T. Kunpradid, "Diversity of macroalgae and benthic diatoms and their relationship with nutrient compounds in Ping and Nan Rivers", *PhD Thesis*, **2005**, Chiang Mai University, Thailand.
33. Y. Peerapornpisal, T. Pekthong, P. Waiyaka and S. Promkutkaew, "Diversity of phytoplankton and benthic algae in Mae Sa stream, Doi Suthep-Pui National Park, Chiang Mai", *Siam Soc.*, **2000**, *48*, 193-211.
34. S. Suphan, "Diversity of macroalgae and benthic diatoms in the area of Golden Jubilee Thong Pha Phum Project, Thong Pha Phum district, Kanchanaburi province", *MS Thesis*, **2004**, Chiang Mai University, Thailand.
35. T. Inthasotti, "Seasonal distribution of macroalgae and benthic diatoms in Mae Tang River, Wiang Haeng district, Chiang Mai province between March 2004-January 2005", Independent Study for Master Degree, **2006**, Chiang Mai University, Thailand.
36. T. Inthasotti, "Diversity of macroalgae and benthic diatoms in Kham watershed, Chiang Rai province", *MS Thesis*, **2006**, Chiang Mai University, Thailand.
37. P. Leelahakriengkrai, "Usage of macroalgae and benthic diatoms to monitor the water quality of Kok River and tributaries", Independent study for Master Degree, **2006**, Chiang Mai University, Thailand.
38. P. Leelahakriengkrai, "Diversity and usage of macroalgae and benthic diatoms to monitor water quality of Ping River, 2004-2005", *MS Thesis*, **2006**, Chiang Mai University, Thailand.
39. National Environmental Board, "Surface water quality standards" (in Thai), the Royal Government Gazette, Vol. 111, Part 16 (February 24, **1994**).
40. H. B. N. Hynes, "The Ecology of Running Waters", Liverpool University Press, Liverpool, **1970**, pp.53-77.
41. S. Panha, "A new species of Amphidromus from Thailand (Stylommatophora: Camaenidae)", *Malacol. Rev.*, **1996**, *29*, 131-132.
42. V. J. Chapman and D. J. Chapman, "The Algae", Macmillan, London, **1973**, pp.388-395.
43. F. E. Round, "The Biology of the Algae", 2nd Edn., Edward Arnold Ltd., London, **1973**, pp.64-69.
44. B. Mpawenayo and J. M. Mathooko, "The structure of diatom assemblages associated with *Cladophora* and sediments in a highland stream in Kenya", *Hydrobiol.*, **2005**, *544*, 55-67.

45. I. Jüttner, H. Rothfritz and S. J. Ormerod, "Diatoms as indicators of river quality in the Nepalese Middle Hills with consideration of the effects of habitat-specific sampling", *Freshwater Biol.*, **1996**, *36*, 475-486.

Maejo Int. J. Sci. Technol. **2012**, *6*(01), 47-61

Maejo International Journal of Science and Technology

ISSN 1905-7873

Available online at www.mijst.mju.ac.th

Full Paper

Fourteen new records of cercosporoids from Thailand

Pheng Phengsintham[1,2], Ekachai Chukeatirote[1], Eric H. C. McKenzie[3], Mohamed A. Moslem[4], Kevin D. Hyde[1, 4, *] and Uwe Braun [5]

[1] School of Science, Mae Fah Luang University, Chiang Rai 57100, Thailand

[2] Department of Biology, Faculty of Sciences, National University of Laos, Laos

[3] Landcare Research, Private Bag 92170, Auckland, New Zealand

[4] King Saud University, College of Science, Department of Botany and Microbiology, P.O. Box: 2455, Riyadh 1145, Saudi Arabia

[5] Martin-Luther-Universität, Institut für Biologie, Bereich Geobotanik und Botanischer Garten, Herbarium, Neuwerk 21 D-06099 Halle/S, Germany

[*] Corresponding author: kdhyde3@gmail.com

Received: 24 July 2010 / Accepted: 27 January 2012 / Published: 1 February 2012

Abstract: Comprehensive examination of cercosporoid leaf-spotting hyphomycetes was carried out in northern Thailand. Fourteen species assigned to the genera *Cercospora* (5), *Passalora* (3), *Pseudocercospora* (5) and *Zasmidium* (1) are new records for Thailand. *Cercospora verniciferae* and *Zasmidium cassiicola* are poorly known species and are fully described.

Keywords: anamorphic fungi, cercosporoid hyphomycetes, South-East Asia, taxonomy, new records

INTRODUCTION

Cercospora sensu lato is one of the largest genera of hyphomycetes and is almost cosmopolitan in distribution. It causes leaf-spots and other lesions on a wide range of host plants. Species of this genus are important pathogens responsible for severe damage to beneficial plants such as maize, rice, grasses, vegetables, forest trees and ornamentals [1-3].

There have been several recent comprehensive accounts of the fungi of Thailand which are among the best documented in the region [4, and references therein]. In Thailand, the study of *Cercospora* and allied genera can be traced back to 1980 [5, 6]. Sixty cercosporoids were listed, including 13 unidentified species of *Cercospora* in the host index of plant diseases in Thailand [5],

whereas 21 species of *Cercospora* were specified as plant pathogens [6]. In 1989, 49 cercosporoid species were further identified in southern Thailand [7]. These reports, however, were based on the old generic characters, i.e. *Cercospora sensu lato*. Subsequently, 112 species of *Cercospora* as well as their synonyms were recorded in 'The host index of plant diseases in Thailand' [8]. It should also be noted that, according to the list, species names used were ambiguous since the criteria used for classification were based on both old and new criteria. In 2007, three new species of *Cercospora* were discovered; these included 11 species that were new to Thailand [9]. Forty-three cercosporoid species were included in an annotated list of cercosporoid fungi in northern Thailand [10], and two taxa associated with necrotic leaflets of an areca palm (*Areca cathecu*) were reported [11]. A PhD thesis on "Diversity and phylogeny of true cercosporoids fungi from northern Thailand" available in 2009 encompassed 166 cercosporoids [12]. Recently, many new *Cercospora* species have been discovered, including *Cercospora cristellae*, a new cercosporoid species associated with the weed *Cristella parasitica* from northern Thailand [13], and three new records of cercosporoid fungi (*Cercospora diplaziicola, Pseudocercospora duabangae* and *Pseudocercospora trematicola*) from Thailand [14].

The genus *Cercospora* Fresen. *s. lat.*, which is one of the largest genera of hyphomycetes, has been monographed with over 3000 names [15]. Similar to other fungal group, the classification and identification of *Cercosporoid* fungi are mainly based on morphological characteristics. Currently, an identification key of *Cercosporoid* proposed in 2003 has been widely accepted [16]. In this present study, we explored the diversity of *Cercospora* and allied genera by using this identification key. The objectives of this paper are to investigate the cercosporoid fungi of Thailand and Laos, and to provide data on Thailand's fungi in comparison with the diversity of these fungal groups in neighbouring countries.

MATERIALS AND METHODS

Sample Collections and Examination of Fungal Structures

Plants leaves with leaf spots or other lesions were collected during field trips in northern Thailand. Photographs of symptoms, including fungal colonies or fruiting bodies, were taken.

Macroscopic characters were observed using a stereomicroscope to check lesions/leaf spots (shape, size, colour, margin) and colonies/caespituli (with details, i.e. amphigenous/epiphyllous, punctiform/pustulate/inconspicuous, effuse, loose, dense, brown/blackish, and others.)

Microscopic examination, measurement, description and presentation of drawings followed the standard procedures [16,17]. In the illustrations, thin-walled structures were depicted by a single line, thick-walled ones by double lines, and stippling was used to accentuate shape and pigmentation.

Identification of Fungi

The species of cercosporoid hyphomycetes were determined using the key available in the current taxonomic publications cited in the list of references.

Dried specimens were prepared and stored at the herbarium of the School of Science, Mae Fah Luang University (MFU). Duplicates were preserved at the herbarium of the Institute of Biology, Geobotany and Botanical Garden, Halle (Saale), Germany (HAL).

RESULTS AND DISCUSSION

Fourteen cercosporoid hyphomycetes were identified and assigned to species of the genera *Cercospora* (5), *Passalora* (3), *Pseudocercospora* (5) and *Zasmidium* (1). The cercosporoid species and their habitats are listed in Table 1.

Table 1. Cercosporoid species examined in this study

Fungal species	F	DD	G	U
Cercospora malloti	×			
Cercospora senecionicola	×			
Cercospora sidicola	×			
Cercospora verniciferae				×
Cercospora zizphigena		×		
Passalora broussonetiae	×			
Passalora fusimasculans	×		×	
Passalora graminis	×			
Pseudocercospora cycleae	×			
Pseudocercospora malloticola	×			
Pseudocercospora olacicola		×		
Pseudocercospora paederiae	×			
Pseudocercospora polysciatis				×
Zasmidium cassiicola				×

Note: F = fallow land; DD = dry dipterocarp forest; G = garden; U = urban area

Cercospora malloti [18]

Notes: The collection no. MFLU10-0310 from Tadsak waterfall, Ching Rai province agrees well with *Cercospora malloti* as previously circumscribed [15,16] (conidiophores 10–50 × 3–5 µm and conidia 40–75 × 1.5–3 µm). *C. malloti* is part of the *C. apii* Fesen. complex from which it is morphologically barely distinguishable [16]. The collection from Thailand has conidiophores which are 32–140 × 5–6 µm, and conidia which are 20–146 × 2–4 µm.

Known hosts: *Mallotus apelta* (Lour.) Müll. Arg., *M. japonicus* (L. f.) Müll. Arg., and *M. repandus* (Rotter) Müll. Arg. (Euphorbiaceae) [15,16].

Known distribution: **Asia** - China, Japan [15,16], Thailand (this paper); **North America** - USA (MS) [15,16].

Material examined: Phengsintham (MFLU10-0310) on leaf of *Mallotus repandus* (Euphorbiaceae) (Thailand: Chiang Rai province, Wiang Chiang Rung district, Tadsak waterfall), 23 December 2009.

Cercospora senecionicola [19]

Notes: The collection no. MFLU10-0318 from Sri Pangsang village, Chiang Rai province agrees with *Cercospora senecionicola* as circumscribed in Chupp [15]. Brief description of the collection from Thailand: **Leaf spots/Lesions** circular to slightly irregular, 2–3 mm diam., at first dark green, later becoming brown to dark brown in the centre, dark brown margin. **Caespituli/Colonies** amphigenous, conspicuous, scattered, dark brown. **Conidiophores** single or fasciculate, arising from stromata (1–8 per fascicle), 0–5-geniculate, cylindrical, straight to curved, 67–170 × 5–6 µm, 0–8-septate. **Conidia** acicular to obclavate, straight to curved, 17–82 × 4–7 µm, 0–8-sepate, slightly constricted at the septa, hyaline to subhyaline, smooth, wall 0.3–0.5 µm thick, apex acute, based truncate to subtruncate, hila 2–3 µm wide, wall of the hila 0.5 µm wide, darkened.

Known hosts: *Senecio aureus* L., *S. aureus* var. *balamitea* Toir. & Gray, and *S. walkeri* Arn. (Compositae = Asteraceae) [15,16].

Known distribution: **Asia -** China, Laos, Thailand [15].

Material examined: 1) Phengsintham (MFLU10-0318) on leaf of *Senecio walkeri* (Asteraceae) (Thailand: Chiang Rai province, Muang district, Sri Pangsang village), 11 August 2009; 2) Phengsintham (P567) on leaf of *Senecio walkeri* (Asteraceae) (Laos: Bokeo province, Phimonsine village), 20 February 2010.

Cercospora sidicola [20]

Notes: The collection no. MFLU10-0312 from Tadsak waterfall, Chiang Rai province agrees with *Cercospora sidicola* as circumscribed by Chupp [15], but differs in formation of leaf spots.

Known hosts: *Sida acuta* Burm. F., *S. cordifolia* (DC.) Fryxell , *S. mysorensis* Wight & Arn., *S. rhombifolia* L., *S. spinosa* L., and *Sida* sp. (Malvaceae) [15,16].

Known distribution: **Asia** - China, India, Thailand (this paper); **North America** - Cuba, Dominican Republic, Panama, Puerto Rico, USA (FL, LA, TX), Virgin Islands; **South America** - Argentina, Brazil [16].

Material examined: Phengsintham (MFLU10-0312) on leaf of *Sida mysorensis* (Malvaceae) (Thailand: Chiang Rai province, Wiang Chiang Rung district, Tadsak waterfall), 23 December 2009.

Cercospora verniciferae [21] (Figure 1; Redescribed because this species is poorly known.)

Leaf spots/Lesions small to medium, suborbicular to irregular, 1–4 mm in diam., brown in the centre, and with brown-yellow margin. **Caespituli/Colonies** hypophyllous, scattered, dark brown. **Mycelium** internal; **hyphae** branched, 3–5 µm wide ($\bar{x}$ = 3.57 µm, n = 7), septate, constricted at the septa, distance between septa 7–12 µm ($\bar{x}$ = 8.42 µm, n = 7), brownish or green-hyaline, wall 0.5–0.8 µm wide ($\bar{x}$ = 0.54 µm, n = 7), smooth, forming plate-like plectenchymatous stromatic hyphal aggregations. **Stromata** developed, small to medium-sized, globular to subglobular, substomatal and intraepidermal, 16–33 µm in diam. ($\bar{x}$ = 23.6 µm, n = 8), dark brown to black in

mass, composed of swollen hyphal cells, subglobose, rounded to angular in outline, 5–10 µm wide ($\bar{x}$ = 7.9 µm, n = 13), brown to dark brown, wall 0.5–0.8 µm wide ($\bar{x}$ = 0.68 µm, n = 13), smooth. **Conidiophores** fasciculate, arising from stromata (1–4 per fascicle), emerging through stomata, not branched, straight to curved, cylindrical, 45–89 × 5–7 µm ($\bar{x}$ = 71.2 × 5.4 µm, n = 5), 2–5-septate, distance between septa 5–30 µm ($\bar{x}$ = 16.2 µm, n = 16), medium brown, paler at the apex, wall 0.5–0.8 µm wide ($\bar{x}$ = 0.63 µm, n = 16), smooth, 0–2-times geniculate. **Conidiogenous cells** integrated, terminal, cylindrical, 16–30 × 4–5 µm ($\bar{x}$ = 24.5 × 4.5 µm, n = 4), pale brown; **conidiogenous loci** conspicuous, subcircular, 2–2.5 µm wide ($\bar{x}$ = 2.12 µm, n = 4), wall 0.5–0.8 µm thick ($\bar{x}$ = 0.57 µm, n = 4), thickened and darkened. **Conidia** solitary, acicular to obclavate, straight to curved, 23–105 × 2–4 µm ($\bar{x}$ = 64 × 2.8 µm, n = 5), 5–12-septate, hyaline to subhyaline, thin-walled 0.3–0.5 µm ($\bar{x}$ = 0.31 µm, n = 5), smooth; tip acute; base truncate, hila thickened and darkened 1–1.5 µm wide ($\bar{x}$ = 1.1 µm, n = 5), wall of the hila 0.3–0.35 µm ($\bar{x}$ = 0.31 µm, n = 5) thick.

Known hosts: *Rhus vernicifera* DC., *Spondias dulcis* Parkinson, and *S. pinnata* (L. F.) Kurz (Anacardiaceae) [15,16].

Known distribution: **Asia** - Thailand (this paper); **Oceania** - American Samoa; **South America** - Brazil [15,16].

Material examined: Phengsintham (MFLU10-0313) on leaf of *Spondias pinnata* (Anacardiaceae) (Thailand: Chiang Rai province, Muang district, Sri Pangsang village), 22 December 2009.

Notes: The collection from Thailand agrees well with *Cercospora verniciferae* as circumscribed by Chupp [15]. *C. verniciferae* has conidiophores that are 45–89 × 5–7 µm and conidia that are 23–105 × 2–4 µm. *C. verniciferae* is part of the *C. apii* Fesen. complex from which it is morphologically barely distinguishable [16].

Cercospora ziziphigena [22]

Notes: The collection no. MFLU11-0019 from Mae Puem National Park, Pha Yao province (conidiophores 40–320 × 4–6 µm and conidia 163–195 × 2.5–3 µm) having a long conidia, differs from the *Cercospora ziziphigena* previously described [22] (conidiophores 13.8–92.5 × 3.5–6.3 µm and conidia 17.5–76.8 × 3.1–5.3 µm). A true *Cercospora s. str.* is quite distinct from *Cercospora apii s. lat.* [16].

Known hosts: *Ziziphus incurva* Roxb. and *Ziziphus* sp. (Rhamnaceae) [16, 22].

Known distribution: **Asia** - China [16, 22], Thailand (this paper).

Material examined: Phengsintham (MFLU11-0019) on leaf of *Ziziphus* sp. (Rhamnaceae) (Thailand: Pha Yao province, Mae Jai district, Mae Puem National Park), 22 August 2010.

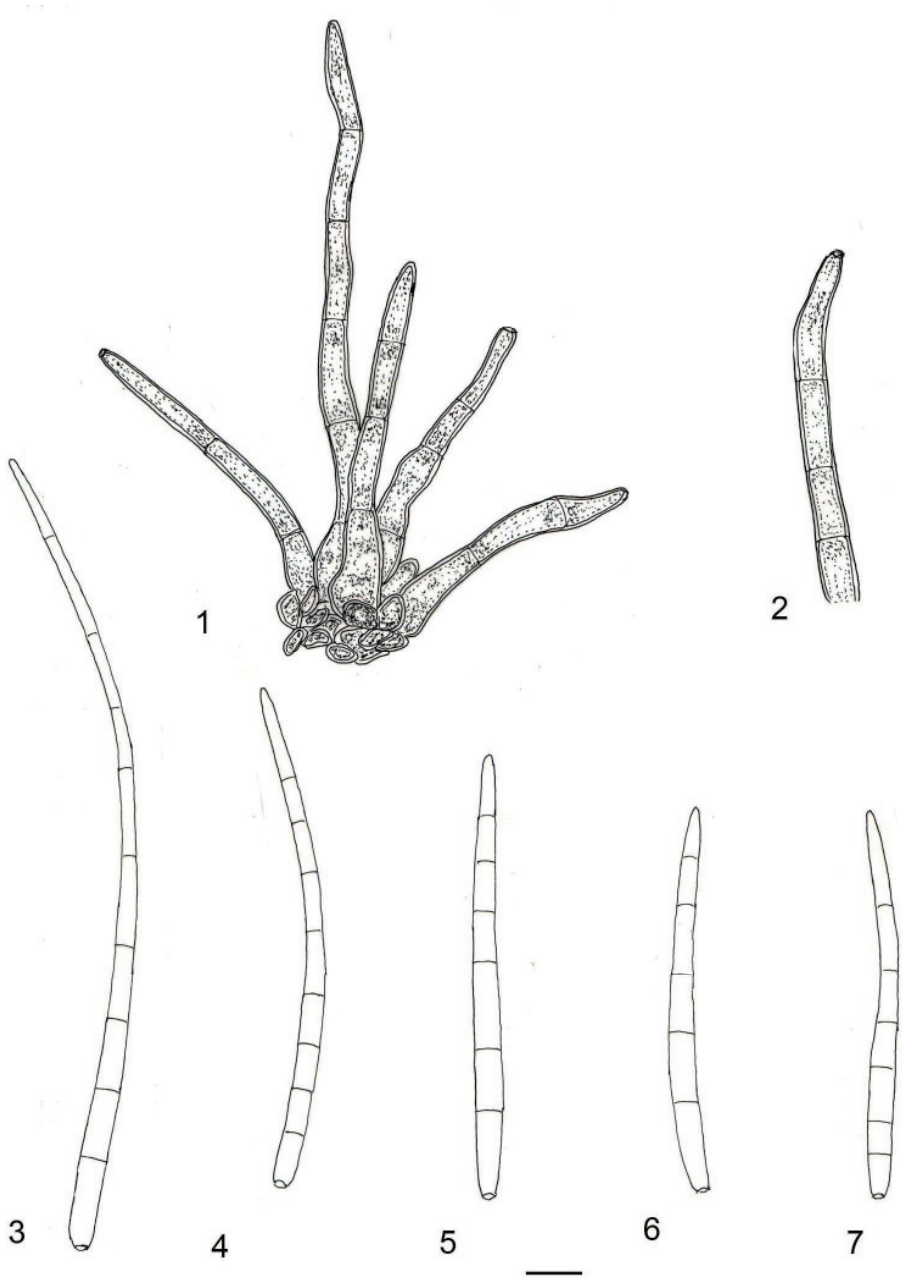

Figure 1(a). *Cercospora verniciferae* on *Spondias pinnata* from leaf spots: 1. Stroma with attached conidiophores; 2. Conidiophore; 3–7. Conidia. (Scale bar = 10 µm)

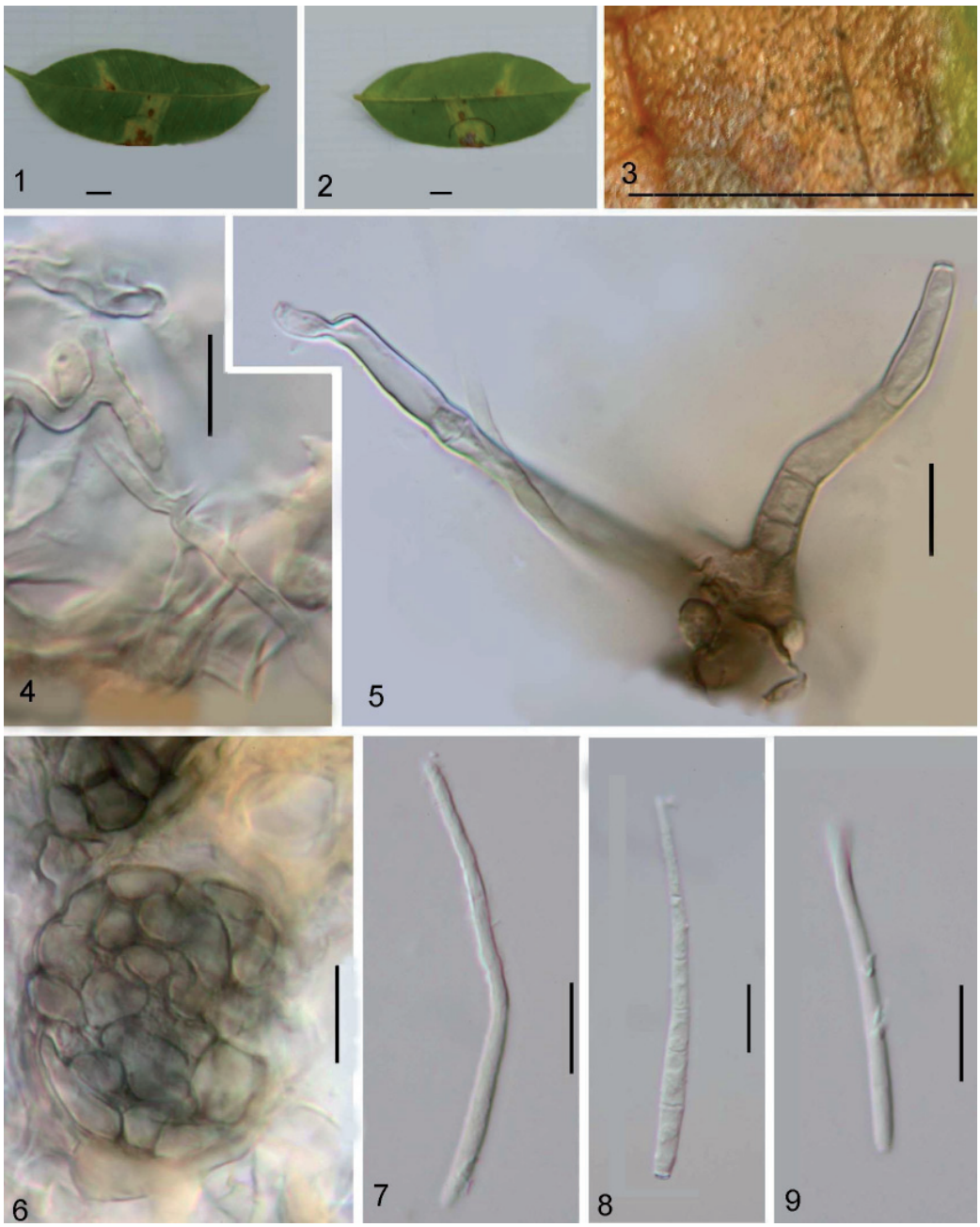

Figure 1(b). *Cercospora verniciferae* on *Spondias pinnata* from leaf spots: 1–2. Lesions on host leaves (1. upper surface and 2. lower surface); 3. Caespituli; 4. Internal mycelium; 5. Stroma with attached conidiophores; 6. Stroma; 7–9. Conidia. (Scale bar: 1–2. = 10 mm; 3. = 3 mm; 4–9. = 10 μm)

Passalora broussonetiae [16]

Notes: The collection no. MFLU10-0314 from Tadsak waterfall, Chiang Rai province agrees well with *Passalora broussonetiae* [16], but the hyphae are smooth to distinctly verruculose (described to be smooth by Hsieh and Goh [3]). Brief description of *Passalora broussonetiae* from Thailand: **Leaf spots/Lesions** irregular, 1–9 mm diam., at first reddish brown, later becoming dark brown in the centre, gray to reddish brown margin. **Caespituli/Colonies** amphigenous, conspicuous. **Conidiophores** 170–390 × 2–5 µm, 5–17-septate. **Conidia** 6–28 × 4–6 µm, 0–3-septate.

Known host: *Broussonetia papyrifera* (L.) L'Hér. ex Vent.[3, 23].

Known distribution: **Asia** - Taiwan [3,16], Thailand (this paper).

Material examined: Phengsintham (MFLU10-0314) on leaf of *Broussonetia papyrifera* (Moraceae) (Thailand: Chiang Rai province, Wiang Chiang Rung district, Tadsak waterfall), 23 December 2009.

Passalora fusimaculans [16] ≡ *Cercospora fusimaculans* [24]

Notes: The collection no. MFLU10-0315 from Sri Pangsang village garden and no. MFLU10-0316 from Huay Kang Pah National Park, Chiang Rai province agree well with *Passalora fusimaculans* as circumscribed previously [3, 15, 25], but differ in having rather long conidiophores (up to 130 µm) and shorter conidia (up to 85 µm).

Known hosts: *Agrostis*, *Brachiaria*, *Brachia, Beckeropsis, Chasmopodium, Digitaria, Echinochloa*, *Eleusine, Entolasia*, *Ichnanthus, Leptoloma, Oplismenus, Panicum, Paspalidium*, *Pennisetum*, *Rottboellia*, *Setaria*, *Sorghum*, *Stenotaphrum*, *Urochloa*, and *Zea* (Poaceae) [16].

Known distribution: **Africa** - Botswana, Ethiopia, Ghana, Guinea, Ivory Coast, Kenya, Malawi, Nigeria, Rwanda, Sierra Leone, South Africa, Sudan, Tanzania, Togo, Uganda, Zambia, Zimbabwe; **Asia** - Brunei, China, India, Japan, Malaysia, Philippines, Taiwan, Thailand (this paper); **Europe** - Azerbaijan, France, Georgia; **North America** - Costa Rica, Cuba, Dominican Rep., El Salvador, Guatemala, Honduras, Jamaica, Mexico, Nicaragua, Panama, Trinidad & Tobago, USA (AL, PL, IA, ID, KS, NC, ND, OK, OR, TX, VA, WI); **Oceania** - Australia, Fiji, New Zealand, Palau, Papua New Guinea, Samoa, Solomon Islands, Vanuatu; **South America** - Bolivia, Brazil, Colombia, Ecuador, Guyana, Peru, Venezuela [16].

Material examined: 1) Phengsintham (MFLU10-0315) on leaf of *Echinochloa esculenta* (Poaceae) (Thailand: Chiang Rai province, Muang district, Sri Pangsang village), 15 September 2009; 2) Phengsintham (MFLU10-0316) on leaf of *Echinochloa esculenta* (Poaceae) (Thailand: Chiang Rai province, Huay Kang Pah National Park), 4 December 2009.

Passalora graminis [26]

Notes: The collection no. MFLU10-0317 from Doi Tung National Park, Chiang Rai province agrees well with *Passalora graminis* as circumscribed previously [15, 23]. *Passalora graminis* has conidiophores of 10–52 × 3–5 µm and conidia of 18–38 × 1.5–2 µm.

Known hosts: *Agrobardeum*, *Agropyron, Agrositanion*, *Agrostis*, *Alopecurus*, *Ammophila*, *Anthoxanthum, Arctagrostis*, *Arrhenatherum, Arundinaria, Avena, Beckmannia, Bromus*,

Calamagrostis, Cinna, Cynodon, *Cynosurus*, *Dactylis, Danthonia, Deschampsia*, *Digitaria, Elymus*, *Elysitanion, Elytrigia, Egagrostis, Festuca, Glyceria, Hierochloe, Hordeum, Hystrix, Koeleria, Leersia, Leucopoa, Lolium*, *Melica*, *Milium*, *Miscanthus*, *Muhlenbergia, Oryzopsis*, *Panicum*, *Pennisetum, Phleum*, *Phragmities, Poa, Puccinella, Roegneria, Secale, Sitanion*, *Sparlina*, *Stenotaphrum, Stipa, Trisetum,* and *Zea* (Poaceae) [16].

Known distribution: **Asia** - Thailand (this paper) and worldwide [16].

Material examined: Phengsintham (MFLU10-0317) on leaf of *Agrostis* sp. (Poaceae) (Thailand: Chiang Rai province, Doi Tung National Park), 18 August 2009.

Pseudocercospora cycleae [23]

Notes: The collection no. MFLU10-0319 from Khun Korn waterfall, Chiang Rai province agrees with the previous description of this species [27], but differs in having longer conidiophores.

Known hosts: *Cyclea fissicalyx* Dunn, *C. peltata* Hook. f. & Thomson, and *Cyclea* sp. (Menispermaceae) [27].

Known distribution: **Asia** - China, India [27], Thailand (this paper).

Material examined: Phengsintham (MFLU10-0319) on leaf of *Cyclea peltata* (Menispermaceae) (Thailand: Chiang Rai province, Khun Korn waterfall), 18 December 2009.

Pseudocercospora malloticola [3]

Notes: The collection no. MFLU10-0320 from Sri Pangsang village, Chiang Rai province (Thailand) and no. NUOL P588 from Naloumai village, Savannakhet province (Laos) are similar to *Pseudocercospora malloticola* from Taiwan previously described [3]. Brief description of the collection from Thailand: **Leaf spots/Lesions** discoid to irregular, 1–6 mm diam., at first yellowish, later becoming brown or dark brown, and with yellowish margin. **Conidiophores** fasciculate, arising from stromata (2–11 per fascicle), emerging through stomata, nearly straight, cylindrical, unbranched, 10–40 × 3–5 µm. **Conidia** formed singly, cylindric, straight to slightly curved, 33–75 × 3–4 µm.

Known hosts: *Mallotus barbatus* (Wall.) Müll. Arg., *M. japonicus* (L. F.) Müll. Arg., and *M. thorelii* Gagnep [3].

Known distribution: **Asia** - Laos (this paper), Taiwan [3], Thailand (this paper).

Material examined: 1) Phengsintham (MFLU10-0320) on leaf of *Mallotus barbatus* (Euphorbiaceae) (Thailand: Chiang Rai province, Muang district, Sri Pangsang village), 30 August 2009; 2) Phengsintham (P588) on leaf of *Mallotus thorelii* (Euphorbiaceae) (Laos: Savannakhet province, Vilaboury district, Naloumai village), 23 June 2010.

Pseudocercospora olacicola [28]

Notes: The collection no. MFLU11-0020 from Mae Puem National Park, Pha Yao province (conidiophores 12–35 × 3–5 µm and conidia 11–58 × 2–3 µm) agrees with *Pseudocercospora olacicola* previously described [28] (conidiophores 10.5–40.5 × 2.5–5 µm and conidia 16–30.5 × 2.5–4 µm).

Known hosts: *Olax scandens* Roxb., *Olax wightiana* Wall. ex Wight & Arn., *O. zeylanica* L., *Olax* sp., and *Ximenia* sp. (Olacaceae) [16, 28].

Known distribution: **Asia** - India [16, 28], Thailand (this paper).

Material examined: Phengsintham (MFLU11-0020) on leaf of *Olax scandens* (Olacaceae) (Thailand: Pha Yao province, Mae Jai district, Mae Puem National Park), 22 August 2010.

Pseudocercospora paederiae [3]

Notes: The collection no. MFLU10-0321 from Tadsak waterfall, Chiang Rai province (conidiophores 5–20 × 3–5 µm and conidia 42–75 × 2–3 µm) is similar to the original description of this species, based on material from Taiwan, but there are slight differences in the size of the conidiophores and conidia. The collection from Taiwan has conidiophores that are densely fasciculate, 20–120 × 3–4 µm, subhyaline to pale brown and conidia that are obclavate, straight to moderately curved, 30–80 × 3.5–5 µm and medium olivaceous [3, 15, 27].

Known hosts: *Paederia chinensis* Hance, *P. foetida* L., *P. scandens* (Lour.) Merr., and *P. tomentosa* Blume (Rubiaceae) [3,27].

Known distribution: **Asia** - China, Japan, Korea, Taiwan [3, 27], Thailand (this paper).

Material examined: Phengsintham (MFLU10-0321) on leaf of *Paederia tomentosa* (Rubiaceae) (Thailand: Chiang Rai province, Wiang Chiang Rung district, Tadsak waterfall), 23 December 2009.

Pseudocercospora polysciatis [29]

Notes: The collection no. MFLU10-0322 from Sri Pangsang village, Chiang Rai province agrees well with *Pseudocercospora polysciatis* described previously [3, 27] but differs in having distinct constriction at the septa.

Known hosts: *Polyscias balfouriana* (André) L.H. Bailey, *P. guilfoylei* (W. Bull) L.H. Bailey, and *Polyscias* sp. (Araliaceae) [3, 16, 27].

Known distribution: **Africa** - Mauritius, Ivory Coast; **Asia** - Brunei, Philippines, Taiwan, Thailand (this paper); **North America** - Cuba; **Oceania** - American Samoa, Cook Islands, Fiji, Kiribati, Marshall Islands, Micronesia, Niue, Samoa, Solomon Islands, Tonga [16].

Material examined: Phengsintham (MFLU10-0322) on leaf of *Polyscias balfouriana* (Araliaceae) (Thailand: Chiang Rai province, Muang district, Sri Pangsang village), 16 January 2010.

Zasmidium cassiicola [30] ≡ *Stenella cassiicola* [31] (Figure 2; Redescribed because this species is poorly known.)

Leaf spots/Lesions variable, more or less irregularly orbicular, 1–8 mm diam., typically deep brown. **Caespituli/Colonies** hypophyllous, conspicuous. **Mycelium** external; **hyphae** branched, 2–4 µm wide ($\bar{x}$ = 3.2 µm, n = 9), septate, constricted at the septa, distance between septa 8–30 µm ($\bar{x}$ = 18.56 µm, n = 9), pale olivaceous-brown, thin-walled 0.3–0.5 µm wide ($\bar{x}$ = 0.41 µm, n = 9), verruculose. **Stromata** absent. **Conidiophores** borne on external mycelial hyphae, unbranched, cylindrical, 30 – 117 × 3 – 4 µm ($\bar{x}$ = 65.9 × 3.17 µm, n = 18), 3 – 8-septate, distance between

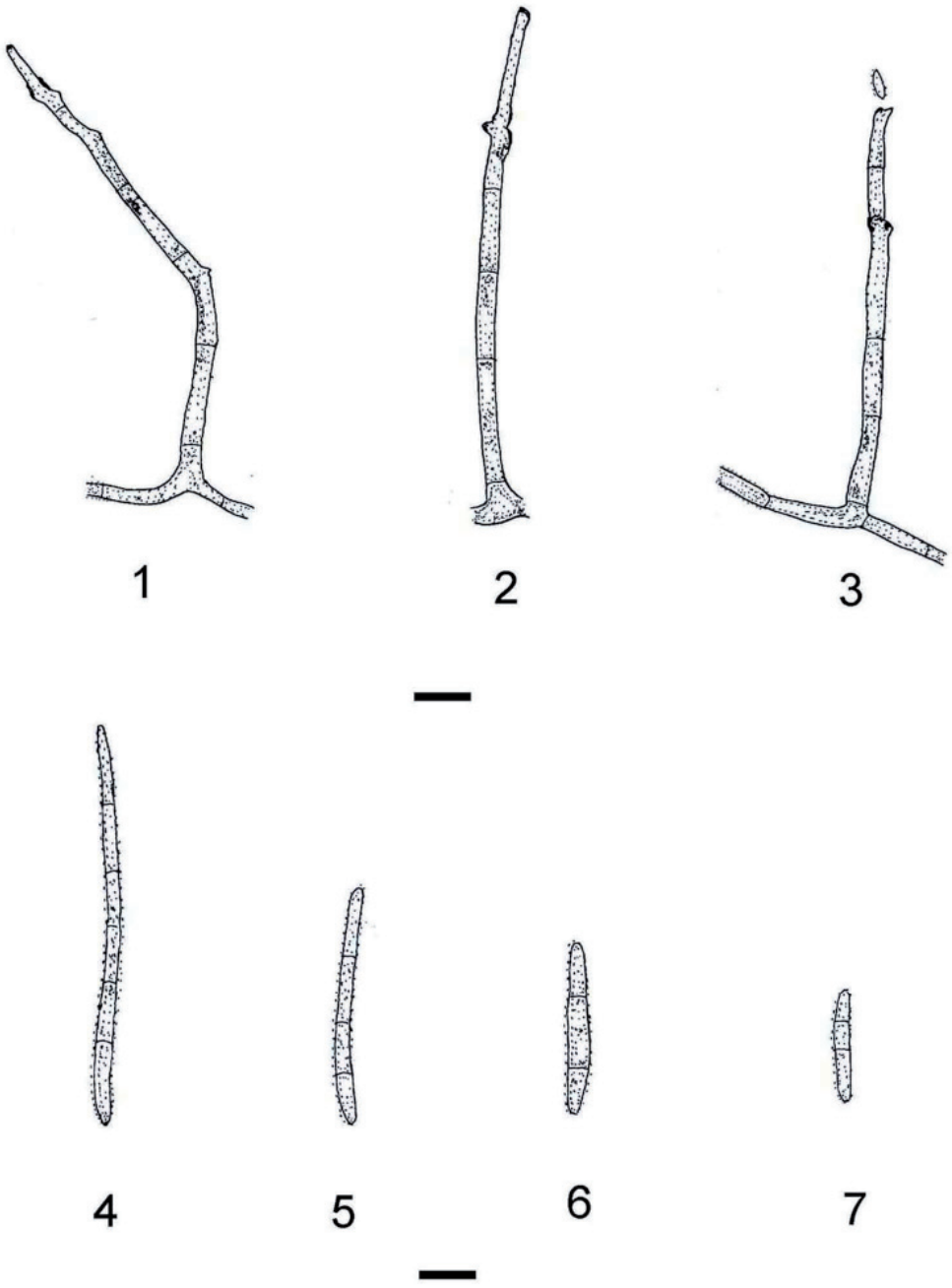

Figure 2(a). *Zasmidium cassiicola* on *Cassia fistula*: 1–3. External mycelia with attached conidiophores; 4–7. Conidia. (Scale bar = 10 µm)

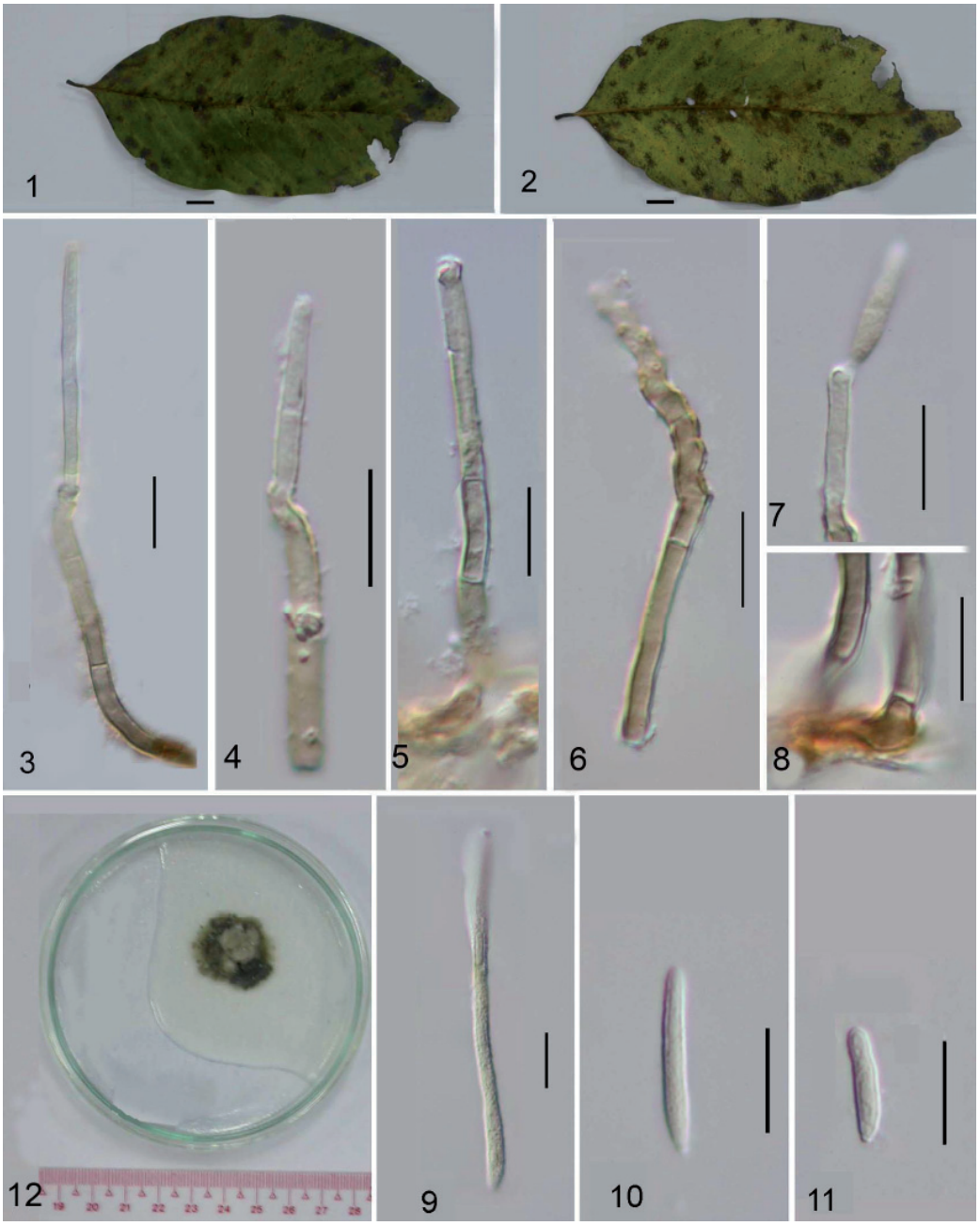

Figure 2(b). *Zasmidium cassiicola* on *Cassia fistula* from leaf spot: 1–2. Lesions on host leaves (1. upper surface and 2. lower surface); 3–6. Conidiophores; 7. Apex with attached conidium; 8. External mycelium; 9–11. Conidia; 12. Living culture. (Scale bars: 1–2. = 10 mm, 3–11. = 10 µm)

septa 7–25 µm ($\bar{x}$ = 15.8 µm, n = 30), mid pale golden brown, wall 0.5–0.8 µm ($\bar{x}$ = 0.48 µm, n = 30), smooth. **Conidiogenous cells** integrated, terminal or intercalary, 7–20 × 2–4 µm ($\bar{x}$ = 13 × 2.63 µm, n = 8), cylindrical, swollen and curved at the apex; **conidiogenous loci** forming minute, dark or refractive scars on lateral and terminal denticles, 1–2 µm diam. ($\bar{x}$ = 1.4 µm, n = 7), giving rise to branched conidial chains, wall 0.3–0.5 µm wide ($\bar{x}$ = 0.4 µm, n = 7), thickened, darkened.

Conidia solitary or catenate, sometimes ellipsoidal-ovoid or subcylindrical, but mostly slightly obclavate, straight or slightly curved or sinuous, 11–70 × 2–4 µm ($\bar{x}$ = 34.16 × 2.9 µm, n = 24), 1–5-septate, pale olivaceous, wall 0.3–0.5 µm wide ($\bar{x}$ = 0.33 µm, n = 24), smooth or finely verruculose; apex rounded or subtruncate, 1–1.5 µm wide, wall 0.3–0.5 µm wide; base short tapered at the base to the hilum, 1–2 µm wide ($\bar{x}$ = 1.3 µm, n = 9), wall 0.3–0.5 µm wide ($\bar{x}$ = 0.41 µm, n = 9), thickened and darkened.

Known host: *Cassia fistula* L. (Leguminosae) [31].

Known distribution: **Asia** - India [31], Thailand (this paper).

Material examined: Phengsintham (MFLU10-0324) on leaf of *Cassia fistula* (Leguminosae) (Thailand: Chiang Rai province, Muang district, Sri Pangsang village), 16 January 2010.

Cultural characteristics: **Colonies** on potato dextrose agar after three weeks at 25°C with spreading mycelium, surface ridged, black and wavy in the centre and gray margin, reaching 5–15 mm diam.; **hyphae** often constricted at the septa, distances between septa 6–16 × 3–5 µm ($\bar{x}$ = 10.5 × 3.6 µm, n = 30), thin-walled, 0.3–0.5 µm wide ($\bar{x}$ = 0.45 µm, n = 30), hyaline, smooth or verruculose; **Conidiophores** and **conidia** not formed in culture.

Notes: The collection from Thailand agrees well with the Indian *Zasmidium cassiicola* (*Stenella cassiicola* [13, 31]. This is the first record outside India. *Zasmidium cassiae-fistulae* is a similar species but differs in forming its conidia consistently singly [32].

CONCLUSIONS

Cercosporoid fungi are one of the largest groups of pathogenic hyphomycetes causing leaf spots on a wide range of crops, fruit trees and other plants. The damage to living leaves and fruits may cause reduced yield. Fourteen species assigned to the genera *Cercospora* (5), *Passalora* (3), *Pseudocercospora* (5) and *Zasmidium* (1) are new records for Thailand. *Cercospora verniciferae* and *Zasmidium cassiicola* are poorly known species and are fully described.

ACKNOWLEDGEMENTS

The authors would like to thank the Global Research Network for Fungal Biology and King Saud University and the Mushroom Research Foundation (MRF) for supporting this research. Special thanks also go to the Mushroom Research Foundation.

REFERENCES

1. G. N. Agrios, "Plant Pathology", 5th Edn., Academic Press, San Diego, **2005**.
2. P. W. Crous, "Taxonomy and phylogeny of the genus *Mycosphaerella* and its anamorphs", *Fungal Divers.*, **2009**, *38*, 1-24.
3. W. H. Hsieh and T. K. Goh, "*Cercospora* and Similar Fungi from Taiwan", Maw Chang Book Co., Taipei, **1990**.
4. E. B. G. Jones, M. Tanticharoen and K. D. Hyde (Ed.), "Thai Fungal Diversity", Biotec, Bangkok, **2005**.

5. P. Giatgong, "Host Index of Plant Diseases in Thailand", Ministry of Agriculture and Cooperatives, Bangkok, **1980**.
6. P. Sontirat, P. Pitakpraiwan, W. Choonbamroong and U. Kueprakone, "Plant Pathogenic Cercosporoids in Thailand", Ministry of Agriculture and Cooperatives, Bangkok, **1980**.
7. V. Petcharat and M. Kajanamaneesathian, "Species of plant pathogenic *Cercospora* in southern Thailand", *Thai J. Phythopathol.*, **1989**, *9*, 23-27.
8. P. Sontirat, P. Pitakpraivan, T. Khamhangridthrirong, W. Choonbamroong and U. Kueprakone, "Host Index of Plant Diseases in Thailand", Ministry of Agriculture and Cooperatives, Bangkok, **1994**.
9. C. Nakashima, K. Motohashi, J. Meeboon and C. To-anun, "Studies on *Cercospora* and allied genera in northern Thailand", *Fungal Divers.*, **2007**, *26*, 257-270.
10. J. Meeboon, I. Hidayat and C. To-anun, "An annotated list of cercosporoid fungi in northern Thailand", *J. Agric. Technol.*, **2007**, *3*, 51-63.
11. C. To-anun, J. Nguenhom, J. Meeboon and I. Hidayat, "Two fungi associated with necrotic leaflets of areca palms (*Areca catechu*)", *Mycol. Prog.*, **2009**, *8*, 115-121.
12. J. Meeboon, "Diversity and phylogeny of true cercosporoid fungi from northern Thailand", *PhD Thesis*, **2009**, Chiang Mai University, Thailand.
13. C. To-anun, I. Hidayat and J. Meeboon, "*Cercospora cristellae*, a new cercosporoid fungus associated with weed *Cristella parasitica* from northern Thailand", *J. Agric. Technol.*, **2010**, *6*, 331-339.
14. P. Phengsintham, E. Chukeatirote, K. A. Abdelsalam, K. D. Hyde and U. Braun, "*Cercospora* and allied genera from Laos 3", *Cryptogamie Mycol.*, **2010**, *31*, 305-322.
15. C. Chupp, "A Monograph of the Fungus Genus *Cercospora*", Charles Chupp, Ithaca (New York), **1954**.
16. P. W. Crous and U. Braun, "*Mycosphaerella* and Its Anamorphs: 1. Names Published in *Cercospora* and *Passalora*", Centraalbureau voor Schimmelcultures, Utrecht, **2003**.
17. U. Braun, "A Monograph of *Cercosporella, Ramularia* and Allied Genera (Phytopathogenic Hyphomycetes)", Vol. 1, IHW Verlag, Eching (Germany), **1995**.
18. J. B. Ellis and B. M. Everhart, "New species of fungi from various localities", *J. Mycol.*, **1888**, *4*, 113-118.
19. J. J. Davis, "Notes on parasitic fungi in Wisconsin XX", *Trans. Wisc. Acad. Sci.*, **1937**, *30*, 1-16.
20. J. B. Ellis and B. M. Everhart, "New species of hyphomycetes fungi", *J. Mycol.*, **1889**, *5*, 68-72.
21. A. P. Viegas, "Alguns fungos do Brasil, Cercosporae", *Bol. Soc. Bras. Agron.*, **1945**, *8*, 1-160.
22. L. Xu and Y. L. Guo, "Studies on *Cercospora* and allied genera in China XIII", *Mycosystema*, **2003**, *22*, 6-8.
23. F. C. Deighton, "Studies on *Cercospora* and allied genera. VI. *Pseudocercospora* Speg., *Pantospora* Cif. and *Cercoseptoria* Petr.", *Mycol. Papers*, **1976**, *140*, 1-168.
24. G. F. Atkinson, "Some Cercosporae from Alabama", *J. Elisha Mitchel Sci. Soc.*, **1891**, *8*, 33-67.

25. M. B. Ellis, "More Dematiaceous Hyphomycetes", Commonwealth Mycological Institute, Kew, Surrey, **1976**.
26. P. Srivastava, "Recombinations in genus *Passalora* Fries", *J. Living World*, **1994**, *1*, 112-119.
27. Y. L. Guo and W. H. Hsieh, "The Genus *Pseudocercospora* in China", International Academic Publishers, Beijing, **1995**.
28. Kamal, M. K. Khan and R. K. Verma, "New species and combinations in *Pseudocercospora* from India", *Mycol. Res.*, **1990**, *94*, 240-242.
29. U. Braun and A. Sivapalan, "Cercosporoid hyphomycetes from Brunei", *Fungal Divers.*, **1999**, *3*, 1-27.
30. Kamal, "Cercosporoid Fungi of India", Bishen Singh Mahendra Pal Singh, Dehradun (India), **2010.**
31. S. Misra, A. K. Srivastava and Kamal, "Further additions to *Stenella* from India and Nepal", *Mycol. Res.*, **1999**, *103*, 268-270.
32. U. Braun, P. Crous and Kamal, "New species of *Pseudocercospora, Pseudocercosporella, Ramularia* and *Stenella* (cercosporoid hyphomycetes)", *Mycol. Prog.*, **2003**, *2*, 197-208.

Maejo Int. J. Sci. Technol. **2012**, *6*(01), 62-69

Maejo International Journal of Science and Technology

ISSN 1905-7873
Available online at www.mijst.mju.ac.th

Short Communication

On the security of an anonymous roaming protocol in UMTS mobile networks

Shuhua Wu [1, 2, *], Qiong Pu [2, 3] and Ji Fu [1]

[1] Department of Network Engineering, Information Engineering University, Zhengzhou, China
[2] State Key Laboratory of Information Security, Graduate University of Chinese Academy of Sciences, Beijing, China
[3] CIMS Research Centre, Tongji Univerity, Shanghai, China

* Corresponding author, e-mail: pqwsh@yahoo.com.cn

Received: 21 April 2011 / Accepted: 4 February 2012 / Published: 10 February 2012

Abstract: In this communication, we first show that the privacy-preserving roaming protocol recently proposed for mobile networks cannot achieve the claimed security level. Then we suggest an improved protocol to remedy its security problems.

Keywords: cryptanalysis, anonymous roaming, authentication, UMTS

INTRODUCTION

With the advancement and tremendous development of computer networks and telecommunications, user mobility has become a highly desirable network feature nowadays, especially in wireless networks (e.g. cellular networks [1-3]). This technology enables users to access services universally and without geographical limitations. In other words, they can go outside the coverage zone of their home networks, travel to foreign networks and access services provided by the latter as a visiting user or a guest. This capability is usually called roaming. Security is one of the major requirement in roaming networks. In addition to authentication, user's privacy is equally important in such networks. To preserve this feature, not only should the user's identity be protected (anonymity requirement), but also his location and the relation between his activities should be kept secret (untraceability requirement). The violation of either of the mentioned requisites can seriously endanger the user's privacy. Samfat et al. [1] have proposed a comprehensive classification for different levels of privacy protection according to the knowledge of different entities about the user's identification information. The classification is as follows:

- C1: Each user is anonymous to eavesdroppers and his activities are unlinkable to them.
- C2: In addition to C1, each user is anonymous to the foreign servers and his activities are unlinkable to them.
- C3: In addition to C2, the relationship between the user and servers (the home server and the foreign servers) is anonymous for eavesdroppers.
- C4: In addition to C3, the home server of the user is anonymous to the foreign servers.
- C5: In addition to C4, each user is anonymous and his activities are unlinkable to his home server.

In the standard universal mobile telecommunication system (UMTS) [2], the home server must be always aware of the mobile user's location in order to route the incoming calls towards the user. Moreover, the foreign server should know the identity of the home server for billing purpose. Therefore, it seems that the admissible level of privacy protection in this scenario is C3. In the last decades, several schemes addressed the privacy of users in mobile networks [3-15]. However, the most perfect and practical scheme that has been proposed so far only achieves the C2 class of anonymity and the possible C3 class has not been provided in UMTS yet. To fill this blank, Fatemi et al. [2] recently proposed a privacy-preserving roaming protocol based on hierarchical identity-based encryption (IBE) [16] for mobile networks. This protocol was claimed to achieve the acceptable C3 level of privacy. In this communication, we first show that it has some security weakness and thus the claimed security level is not achieved. Finally, we propose an enhanced protocol to remedy the existing security loopholes.

PRELIMINARY

In this section we recall the concept of Identity-Based Encryption (IBE) and hierarchical IBE (HIBE) schemes, upon which Fatemi et al.'s scheme builds. Here we just follow their description [2]. At first, we introduce the concept of a bilinear map between two groups, which will be used in the IBE scheme. Let G_1 be an additive group and G_2 be a multiplicative group, both of order q (q should be some large prime, e.g. 160 bits). We say that a map $e: G_1 \times G_1 \to G_2$ is an admissible bilinear map if all the three following conditions are satisfied:

1) $e(aP, bQ) = e(P, Q)^{ab}$ for all $a, b \in Z_q$ and $P, Q \in G_1$ (bilinear condition);
2) the map does not send all elements of $G_1 \times G_1$ to the identity element of G_2 (non-degeneracy condition); and
3) there is an efficient algorithm to compute $e(P, Q)$ for all $P, Q \in G_1$ (computability condition).

Throughout this communication, the Bilinear Diffie-Hellman (BDH) in $< G_1, G_2, e >$ is believed to be hard (i.e. it is hard to compute $e(P, P)^{abc} \in G_2$, given $< P, aP, bP, cP >$ for some $a, b, c \in Z_q$). Since the BDH problem is not harder than the computational Diffie-Hellman (CDH) problem in G_1 or G_2, the CDH problem in G_1 or G_2 is also believed to be hard. The CDH problem in G_1 is as follows: given random $< P, aP, bP >$ for $a, b \in Z_q$, compute abP; the CDH problem in G_2 is defined similarly. In addition, for a point $Q \in G_1^*$, the isomorphism $f_Q: G_1 \to G_2$ by $f_Q(P) = e(P, Q)$ is considered as a one-way function (P cannot be inferred from $e(P, Q)$ and Q)

since an efficient algorithm for inverting f_Q for some Q results in an efficient algorithm for solving CDH problem in G_2.

Now we begin to introduce the IBE system. An IBE is a public key cryptosystem in which the public key takes any arbitrary string such as a name or an e-mail address, and the private key generator (PKG) can produce a private key corresponding to each string. Hence, one can encrypt a message by a public key even if the public key's owner has not yet set up his private key. An efficient IBE is presented [17], which is called a Boneh-Franklin scheme. Let P be a generator of G_1 and $s \in Z_q^*$ be the PKG's master key. Then in the Boneh-Franklin scheme, each user's identity-based private key should be computed as $k_U = sH_1(U)$, where $H_1 : \{0,1\}^* \to G_1$ is a cryptographic hash function and U is the user's identity. Then one can encrypt a message using the public key U, and U can decrypt the ciphertext using the private key k_U. The BF scheme is resistant to the chosen ciphertext attack, assuming the hardness of the BDH problem [17].

Similar to the public key cryptosystems, a hierarchy of PKGs is desirable in an IBE system to reduce the workload of the master servers. A two-level HIBE (2-HIBE) is presented [16]. There are three entities involved in a 2-HIBE scheme: a root PKG which possesses a master key s, the domain PKGs which gain their domain keys from the root PKG, and the users with private keys generated by their domain PKGs. The 2-HIBE scheme benefits from a linear one-way function $h : G_1 \times Z_q^* \to G_1$ with the following properties:

1) For all $P \in G_1, a, x \in Z_q^*, h(aP, x) = ah(P, x)$,
2) Given $x, x_i \in Z_q^*, P \in G_1$ and $< x_i, h(aP, x_i) >$ for $i = 1, \cdots, n$, $h(aP, x)$ cannot be computed with any probabilistic polynomial-time algorithm.

The function h defined above is a one-way function with respect to its first argument, i.e. P cannot be inferred from $h(P, x)$ and x. Then the key for domain S is $k_S = sH_1(S) \in G_1$ and the key for user U in domain S is $k_U = h(k_S, H_2(S \| U)) \in G_1$, where $H_2 : \{0,1\}^* \to Z_q^*$ is a cryptographic hash function and $\|$ denotes concatenation. Finally, one can encrypt a message by a public key $< S, U >$ and U can decrypt the ciphertext using k_U.

FATEMI ET AL.' S ROAMING PROTOCOL

Review of Protocol

Here we just follow the description of Fatemi et al [2]. Like Wan et al.'s scheme [18], they also assume that a 2-HIBE is implemented in the system and the domain servers have received their private keys $\{K_{S_i} = sH_1(S_i)\}$ from a root server. Also, they suppose that the user U obtains his private key $K_U = h(K_{HS}, H_2(HS \| U))$ during the registration at his home domain server HS. In addition, a temporary key $K = e(h(h(H_1(HS), H_2(HS \| Nym)), H_2(HS)), sH_1(HS))$ corresponding to a pseudonym Nym will be computed by the user during the roaming protocol and will be used for the authentication and key agreement purposes when he enters a foreign network domain.

As shown in Figure 1, the protocol is as follows:

Step 1. When the foreign server (FS) detects a new user in his domain, it generates a nonce N_s and a random number r_s (both from Z_q^*) and computes r_sP. Then it stores the values N_s and r_sP in his database and sends the first message including his identity ID_{FS}, N_s and r_sP to the user.

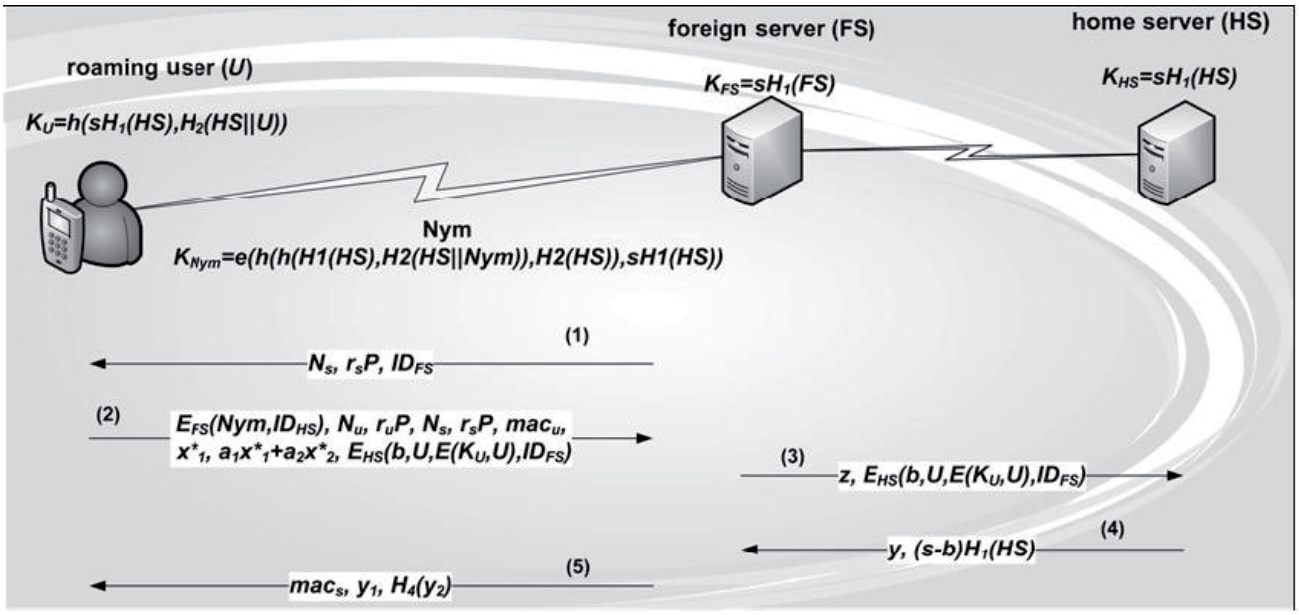

Figure. 1. Fatemi et al.'s roaming protocol [2]

Step 2. Similarly, the user U generates a nonce N_u and a random number r_u and computes $k'_u = r_u r_s P$. Then he fetches the only unused pair of (Nym, K) from his memory and computes the session key to be shared with the foreign server as $sk_u = H_4(K \| k'_u \| FS \| Nym \| N_u \| N_s \| 1)$ and a verifier $mac_u = H_4(K \| k'_u \| FS \| Nym \| N_u \| N_s \| 0)$, where H_4 is a hash function which maps $\{0,1\}^*$ to $\{0,1\}^l$ for some security parameter l. After that, he selects an arbitrary Nym_{next} to be used in the next execution of the roaming protocol (either in the current FS or another FS). In order to compute the corresponding key K_{next} with the help of FS and HS, the user selects a random number $a^* \in Z_q^*$ and computes the following values: $x_1^* = h(h(a^* H_1(HS), H_2(HS \| Nym_{next})), H_2(HS))$, $x_2^* = h(h(a^* H_1(HS), H_2(HS \| U)), H_2(HS))$. Also, he chooses random numbers $b, a_1, a_2 \in Z_q^*$ and computes $a_1 x_1^*, a_2 x_2^*$ and $E_{HS}(b, U, E(K_U, U), ID_{FS})$, where $E_S(M)$ denotes the ID-based encryption of message M with the public key S (e.g. HS or FS), and $E(K_U, U)$ denotes the symmetric encryption of U with the key K_U. Next, he sends the values $E_{FS}(Nym, ID_{HS}), N_u, r_u P, N_s, r_s P, mac_u, x_1^*, a_1 x_1^* + a_2 x_2^*$ and $E_{HS}(b, U, E(K_U, U), ID_{FS})$ to the foreign server.

Step 3. Upon receiving the above values, the foreign server checks if N_s and r_sP exist in its database and aborts the connection if it does not find such values. Otherwise, it decrypts $E_{FS}(Nym, ID_{HS})$ with its private key $sH_1(FS)$ and obtains the Nym and ID_{HS}. Then it generates a random number $c \in Z_q^*$ and computes $z = h(h(cH_1(HS), H_2(HS \| Nym)), H_2(HS))$. Subsequently, the FS sends z and $E_{HS}(b, U, E(K_U, U), ID_{FS})$ to the HS.

Step 4. The home server decrypts the message $E_{HS}(b,U,E(K_U,U),ID_{FS})$ with its private key $sH_1(HS)$ and checks whether it has received the messages from the server with the identity ID_{FS}. Then it authenticates the user U by verifying the correctness of $E(K_U,U)$. The home server terminates the connection if any of these verifications fails. Otherwise, it computes $y = e(z, sH_1(HS))$ $(s-b)H_1(HS) = sH_1(HS)$ $-bH_1(HS)$ and sends them back to the FS.

Step 5. The FS computes $k'_s = r_s r_u P$ and the values $K^* = y^{c^{-1}}$, $mac_u^* = H_4(K^* \| k'_s \| FS \| Nym \| N_u \| Ns \| 0)$. The FS rejects the connection if the equality $mac_u = mac_u^*$ does not hold. Otherwise, it accepts K^* as the user's key corresponding to *Nym* and authenticates the user. The computed K^* together with the message $E_{HS}(b,U,E(K_U,U),ID_{FS})$ are credentials by which the foreign server will be able to request the user's home server for service charge. Indeed, these values become a proof for payment request. In the next step the foreign server computes the session key $sk_s = H_4(K^* \| k'_s \| FS \| Nym \| N_u \| Ns \| 1)$ and the authenticator $mac_s = H_4(K^* \| k'_s \| FS \| Nym \| N_u \| Ns \| 2)$. Moreover, the foreign server calculates $y_1 = e(x_1^*, (s-b)H_1(HS))$ and $y_2 = e(a_1 x_1^* + a_2 x_2^*, (s-b)H_1(HS))$ to make the computation of K_{next} feasible for the user. Finally, it returns mac_s, y_1 and $H_4(y_2)$ to the user.

Step 6. When the user receives the messages from the foreign server, he computes $mac_s^* = H_4(K \| k'_U \| FS \| Nym \| N_u \| Ns \| 2)$ and checks the equality $mac_s = mac_s^*$. If it does not hold, the user aborts the connection. Otherwise, he authenticates the foreign server and computes the following values: $y_1^* = y_1 \cdot e(x_1^*, bH_1(HS))$, $y_2^* = (y_1)^{a_1}[e(h(a \cdot K_U, H_2(HS)), H_1(HS))e(x_2^*, -bH_1(HS))]^{a_2}$, $K_{next} = (y_1^*)^{(a^*)^{-1}}$. Afterwards, the user considers whether $H_4(y_2) = H_4(y_2^*)$. If the equation holds, he accepts K_{next} as the key corresponding to Nym_{next}. If not, he rejects the connection.

At the end of the protocol, $sk_u = sk_s$ is the key that the user and the home server have agreed upon to be used for security purpose.

Weakness of Fatemi et al.'s Protocol

We assume the adversary has totally controlled a mobile user $\overline{U}$ or equivalently he has revealed the secret keys $K_{\overline{U}}$ through side channel attacks [19]. We further assume the adversary has corrupted one of foreign networks, e.g. $\overline{FN}$. Let $\overline{HS}$ be the home server of $\overline{U}$ and $\overline{FS}$ be the server of $\overline{FN}$. The adversary impersonated $\overline{U}$ to visit $\overline{FN}$ and initiated an execution of Fatemi et al.'s roaming protocol. He obtained from the corrupted network the message transmitted from $\overline{HA}$ to $\overline{FS}$ in Step 4: $(s-\overline{b})H_1(\overline{HS})$, where $\overline{b}$ is the random number chosen by the adversary in Step 2. He could then compute $\overline{HS}$'s secret key $K_{\overline{HS}}$ through $K_{\overline{HS}} = sH_1(\overline{HS}) = (s-\overline{b})H_1(\overline{HS}) + \overline{b}H_1(\overline{HS})$. When the adversary knows $K_{\overline{HS}}$, the problem of Fatemi et al.'s roaming protocol becomes evident:

- Firstly, the adversary can reveal the real identity of any other subscriber of $\overline{HS}$. When a mobile user U ($\neq \overline{U}$) performs the authentication procedure with a foreign server FS ($\neq \overline{FS}$), the adversary eavesdrops their communication and can easily get the message transmitted between

U and FS : ID_{FS} in Step 1 and $E_{HS}(b,U,E(K_U,U),ID_{FS})$ in Step 2. Then the adversary just guesses that U is a subscriber of $\overline{HS}$ and attempts to decrypt the message $E_{HS}(b,U,E(K_U,U),ID_{FS})$ with $K_{\overline{HS}} = sH_1(\overline{HS})$. If he can retrieve ID_{FS} from the decrypted message, he confirms his guess is correct, i.e. $HS = \overline{HS}$, because otherwise the probability that he gets any meaningful results from decryption for verification is next to zero. Then he further retrieves item U from the decrypted message and thus knows the user's real identity U. This even contradicts the C1 security requirements. However, if U is not a subscriber of $\overline{HS}$, his attack cannot succeed, but he will always succeed for any subscriber of $\overline{HS}$.

- Secondly, the adversary can impersonate any other subscriber of $\overline{HS}$ (e.g. U) because he may derive K_U from $K_{\overline{HS}}$ as follows: $K_U = h(K_{\overline{HS}}, H_2(\overline{HS}\square U))$. In other words, the authentication mechanism of the protocol is completely compromised.

IMPROVED ROAMING PROTOCOL

The above demonstrated attacks show that Fatemi et al.'s protocol does not seem to achieve authentication or anonymity. In this section we present an enhanced protocol to remedy the security loopholes. As shown in Figure 2, our protocol is based on that of Fatemi et al. and it has the following changes:

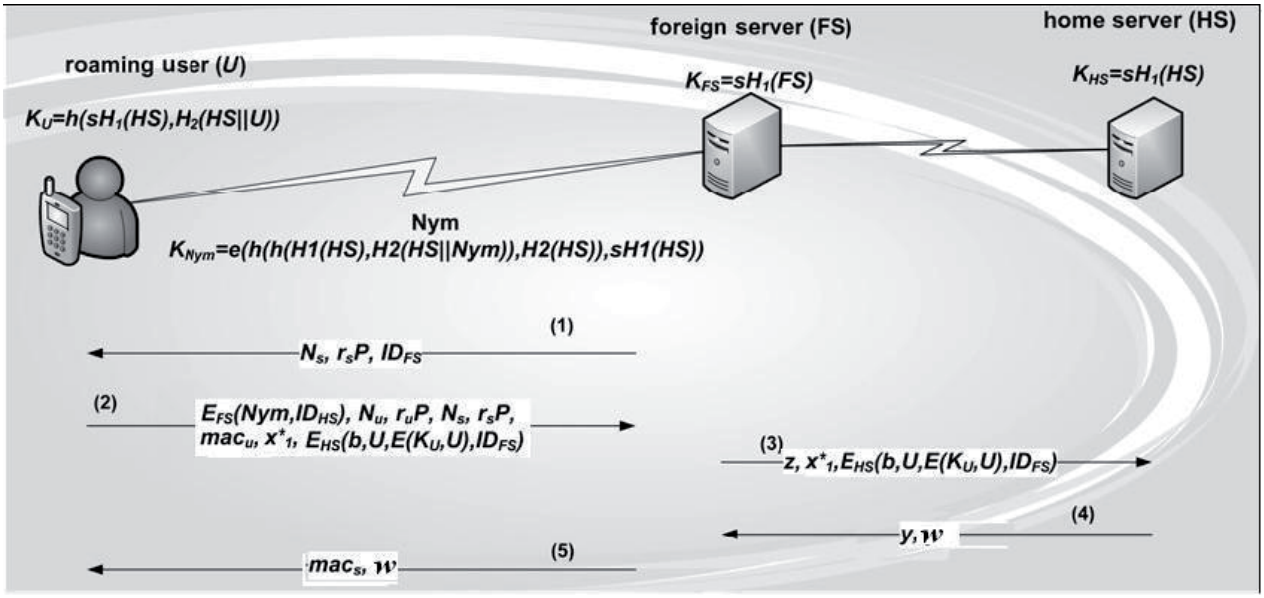

Figure 2. Improved roaming protocol

- In Step 2 the computation of $a_1x_1^* + a_2x_2^*$ is not needed any longer and finally the user U sends the values $E_{FS}(Nym, ID_{HS}), N_u, r_uP, N_s, r_sP, mac_u, x_1^*$ and $E_{HS}(b,U,E(KU,U),ID_{FS})$ to the foreign server.
- In Step 3 the FS also forwards x_1^* to the *HS*. That is, the FS sends *z*, $E_{HS}(b,U,E(K_U,U),ID_{FS})$ and x_1^* to the *HS*.

- In Step 4 the computation of $(s-b)H_1(HS) = sH_1(HS) - bH_1(HS)$ is not needed. Instead, the home server computes a new item $w = E(K_U, e(x_1^*, sH_1(HS)) \square x_1^*)$ to make the computation of K_{next} feasible for the user and finally sends w along with y back to the FS.
- In Step 5 the computation of y_1 and y_2 is not needed and the foreign server returns mac_s and w to the user.
- In Step 6 the computation of y_1^* and y_2^* is not needed. After the verification of mac_s is passed and the foreign server is authenticated, the user U decrypts w using his own secret key K_U to retrieve the two items $e(x_1^*, sH_1(HS)) \square x_1^*$. If the decrypted x_1^* is the same as x_1^* computed in Step 1, he proceeds to compute $K_{next} = (e(x_1^*, sH_1(HS)))^{(a^*)^{-1}}$ and accepts K_{next} as the key corresponding to Nym_{next}. If not, he rejects the connection.

In our improved protocol, the item $e(x_1^*, sH_1(HS))$ is used to make the computation of K_{next} feasible for the user. Given $e(x_1^*, sH_1(HS))$, it is impossible for the adversary to compute $sH_1(HS)$ since the isomorphism f_Q (here $Q = x_1^*$) is a one-way function. Therefore, the attacks described previously will not work any more. Although the changes introduce some computation overhead on the side of HS due to the computation of w, the computation cost of FS or U is significantly reduced since both FS and U omit several costly operations (including bilinear map and exponentiation). In practice the device of the mobile user is much less powerful than the servers'. Our protocol, therefore, would be more practical.

ACKNOWLEDGEMENTS

This work was supported in part by the National Natural Science Foundation of China (Project No. 61101112) and China Postdoctoral Science Foundation (Project No. 2011M500775).

REFERENCES

1. D. Samfat , R. Movla and N. Asokan , "Untraceability in mobile networks", Proceedings of the 1st International Conference on Mobile Computing, **1995**, Santa Barbara, California, USA, pp.26-36.
2. M. Fatemi, S. Salimi and A. Salahi, "Anonymous roaming in universal mobile telecommunication system mobile networks", *IET Inf. Secur.*, **2010**, *4*, 93-103.
3. W.-S. Juang and J.-L. Wu, "Efficient 3GPP authentication and key agreement with robust user privacy protection", Proceedings of IEEE Wireless Communications and Networking Conference, **2007**, Hong Kong, China, pp.2720-2725.
4. B. Sattarzadeh, M. Asadpour and R. Jalili, "Improved user identity confidentiality for UMTS mobile networks", Proceedings of 4th European Conference on Universal Multiservice Networks, **2007**, Toulouse, France, pp.401-409.
5. Y. Jiang, C. Lin, X. Shen and M. Shi, "Mutual authentication and key exchange protocols for roaming services in wireless mobile networks", *IEEE Trans. Wireless Comm.*, **2006**, *5*, 2569-2577.

6. G. Yang, D. S. Wong and X. Deng, "Efficient anonymous roaming and its security analysis", Proceedings of the 3rd International Conference on Applied Cryptography and Network Security, **2005**, New York, USA, pp.334-349.
7. C.-T. Li and C.-C Lee, "A novel user authentication and privacy preserving scheme with smart cards for wireless communications", *Math. Comp. Model.*, **2012**, *55*, 35-44.
8. S. Wu, Y. Zhu and Q. Pu, "Security analysis of a cocktail protocol with the authentication and key agreement on the UMTS", *IEEE Comm. Lett.*, **2010**, *14*, 366-369.
9. S. Wu,. Y. Zhu and Q. Pu, "A novel lightweight authentication scheme with anonymity for roaming service in global mobility networks", *Int. J. Network Manage.*, **2011**, *21*, 384-401.
10. C.-C. Chang and H.-C. Tsai, "An anonymous and self-verified mobile authentication with authenticated key agreement for large-scale wireless networks", *IEEE Trans. Wireless Comm.*, **2010**, *9*, 3346-3353.
11. T.-Y. Youn and J. Lim, "Improved delegation-based authentication protocol for secure roaming service with unlinkability", *IEEE Comm. Lett.*, **2010**, *14*, 791-793.
12. D. He, J. Bu, S. Chan, C. Chen and M. Yin, "Privacy-preserving universal authentication protocol for wireless communications", *IEEE Trans. Wireless Comm.*, **2011**, *10*, 431-436.
13. D. He, M. Ma, Y. Zhang, C. Chen and J. Bu, "A strong user authentication scheme with smart cards for wireless communications", *Comp. Comm.* , **2011**, *34*, 367-374.
14. J. Xu, W-T. Zhu and D-G. Feng, "An efficient mutual authentication and key agreement protocol preserving user anonymity in mobile networks", *Comp. Comm.*, **2011**, *34*, 319-325.
15. C. Chen, D. He, S. Chan, J. Bu, Y. Gao and R. Fan, "Lightweight and provably secure user authentication with anonymity for the global mobility network", *Int. J. Comm. Syst.*, **2011**, *24*, 347-362.
16. J. Horwitz and B. Lynn, "Toward hierarchical identity-based encryption", Proceedings of the 21st International Conference on the Theory and Applications of Cryptographic Techniques, **2002**, Amsterdam, Netherlands, pp.466-481
17. D. Boneh and M. Franklin, "Identity-based encryption from the weil pairing", Proceedings of the 21st International Cryptology Conference on Advances in Cryptology, **2001**, Santa Barbara, California, USA, pp.213-229
18. Z. Wan, K. Ren and B. Preneel, "A secure privacy-preserving roaming protocol based on hierarchical identity-based encryption for mobile networks", Proceedings of the 1st ACM Conference on Wireless Network Security, **2008**, New York, USA, pp.62-67.
19. P. Kocher, J. Jaffe and B. Jun, "Differential power analysis", Proceedings of the 19th Annual International Cryptology Conference, **1999**, Santa Barbara, California, USA, pp.388-397.

Maejo Int. J. Sci. Technol. **2012**, *6*(01), 70-76

Maejo International Journal of Science and Technology

ISSN 1905-7873
Available online at www.mijst.mju.ac.th

Full Paper

Influence of MeV H^+ ion beam flux on cross-linking and blister formation in PMMA resist

Somrit Unai [1, 2, *], Nitipon Puttaraksa[1, 3], Nirut Pussadee[1, 2], Kanda Singkarat [4], Michael W. Rhodes [5], Harry J. Whitlow [3] and Somsorn Singkarat [1, 2]

[1] Plasma and Beam Physics Research Facility, Department of Physics and Materials Science, Faculty of Science, Chiang Mai University, Chiang Mai 50200, Thailand
[2] Thailand Centre of Excellence in Physics, CHE, 328 Si Ayutthaya Road, Bangkok 10400, Thailand
[3] Department of Physics, University of Jyväskylä, P.O. Box 35 (YFL), FIN – 40014, Finland
[4] Department of Physics and Materials Science, Faculty of Science, Chiang Mai University, Chiang Mai 50200, Thailand
[5] Science and Technology Research Institute, Chiang Mai University, Chiang Mai 50200, Thailand

* Corresponding author, e-mail: somrit@fnrf.science.cmu.ac.th

Received: 31 March 2011 / Accepted: 13 February 2012 / Published: 14 February 2012

Abstract: In soft lithography, a pattern is produced in poly(dimethylsiloxane) (PDMS) elastomer by casting from a master mould. The mould can be made of poly(methylmethacrylate) (PMMA) resist by utilising either its positive or negative tone induced by an ion beam. Here we have investigated the irradiation conditions for achieving complete cross-linking and absence of blister formation in PMMA so that its negative characteristic can be used in making master moulds. PMMA thin films approximately 9 μm thick on Si were deposited by spin coating. The 2-MeV H^+ ion beam was generated using a 1.7-MV tandem Tandetron accelerator. The beam was collimated to a 500×500 μm^2 cross section using programmable proximity aperture lithography system with a real-time ion beam monitoring system and a high precision current integrator. The irradiated areas were investigated by a standard scanning electron microscope and a profilometer. It was found that both the ion beam flux and the stopping power of the ions in the polymer have a critical influence on the blister formation.

Keywords: soft lithography, H^+ ion irradiation, PMMA resist, blister formation

INTRODUCTION

Numerous studies of ion-beam-induced modification of polymers have been performed in the last three decades because of its potential for technological applications [e.g. 1-3]. In recent years, ion beam lithography on a resist for the development of microfluidic devices has been extensively investigated [4-6]. The resist that has the tendency to form cross-linkage of the main polymer chains or pendant side chains during irradiation is of the negative type (also called negative tone). This is because the irradiated area becomes less soluble in developing solutions compared to an unirradiated region. On the other hand, the predominant modification in a positive resist (also called positive tone) is chain scissioning of the main and side polymer chains, which enhances the solubility rate in the exposed region [7]. Typically, the master mould for soft lithography is fabricated from either an ion-irradiated negative resist such as SU-8 [8] or a positive resist such as poly(methyl methacrylate) (PMMA) [5]. In addition, Licciardello et al. [9] found that the PMMA would undergo a changeover from a positive to a negative tone by the action of high fluence irradiation, but the utilisation of PMMA as a negative tone resist for master mould fabrication has been little used [10]. For both positive and negative resists, a good master mould used in a direct replica moulding technique must have smooth surfaces. However, blisters or craters have been observed on irradiated polymer surfaces [11-12]. These defects can spoil the mould since they may introduce blockages into poly(dimethylsiloxane) (PDMS) replicas for microfluidic networks. Consequently, blisters and craters must be avoided. This paper reports on an experimental study to control defects from 2-MeV H^+ ion irradiation until the dominance of cross-linking in PMMA has been achieved. Some effects of 1-MeV H^+ ion beam are also included for comparison.

PRINCIPLE

According to the stopping and range of ions in matter (SRIM) simulation program, version SRIM-2008 [13], for the projected range of 65 μm, the tracks of 2-MeV H^+ ions in PMMA is straight, especially in the first 10 μm. An individual ion loses about 200 keV of kinetic energy during its passage through the first 10 μm within 0.5 ps. For light incident ions with a velocity much greater than the Bohr velocity (2.2×10^6 m/s) in thin polymer targets, the energy deposited by the ion mainly results in the excitation and ionisation of atoms and molecules of the polymer in the ion-track zone. These initial physical processes of ion-solid interaction can cause chain scission, cross-linking and gas evolution [14]. In the case of PMMA, several simple low-mass gas products such as H_2, CO, CO_2 and CH_4 have been detected, with carbon monoxide as the dominant product [15-16]. This is indicative of bond breaking, which is a precursor of both the chain scission and cross-linking. There were reports that the gas yield from the polymers is strongly dependent on the linear energy transfer (LET) of the ions [17] and on the incident ion fluence [18]. Although the fundamental mechanism is still not fully understood, the proposed models [11-12] agree that blisters and craters on the surface of a polymer are formed by the gas products as they pass into the surrounding vacuum.

MATERIALS AND METHODS

The PMMA used in this work had a molecular weight of 950 kDa (950 PMMA A11, MicroChem). All PMMA films were spin-coated on clean 1×1-cm^2 silicon substrates at a spin speed of 2,500 rpm for 45 sec. by using a self-made spin coater. Subsequently, the films were soft-baked on a hot-plate at 160^{o}C for 2 min. This process was repeated three times to attain a total film thickness of 8.8±0.1 μm as measured with a stylus profilometer (P-15 Profiler, KLA-Tencor, USA). The 1.7-MV tandem accelerator (1.7 MV high current Tandetron, High Voltage Engineering Europa B. V., the Netherlands) was used to irradiate the polymer with 1- and 2-MeV H^+ ion beams. The pressure during irradiation was about 5×10^{-6} mbar. The irradiated area was 500×500 μm^2 for all experiments and was defined by two computerised L-shaped blade apertures of the programmable proximity aperture lithography (PPAL) system [10]. The experimental set-up when utilising the PPAL technique is shown in Figure 1. The two L-shaped blades were made of copper plates 100 μm thick with well-polished edges. Each of the L-shaped blades was mounted on a computerised micro-stepper motor that independently moved with high precision in either vertical or horizontal direction. In this manner, the PPAL system could produce any rectangular pattern with dimensions between 1-1000 μm^2. The aperture was located at ~2 mm in front of the sample. The PMMA film on silicon substrate was mounted to the translation stage holder, which could move in both x and y directions with a resolution of 1 μm.

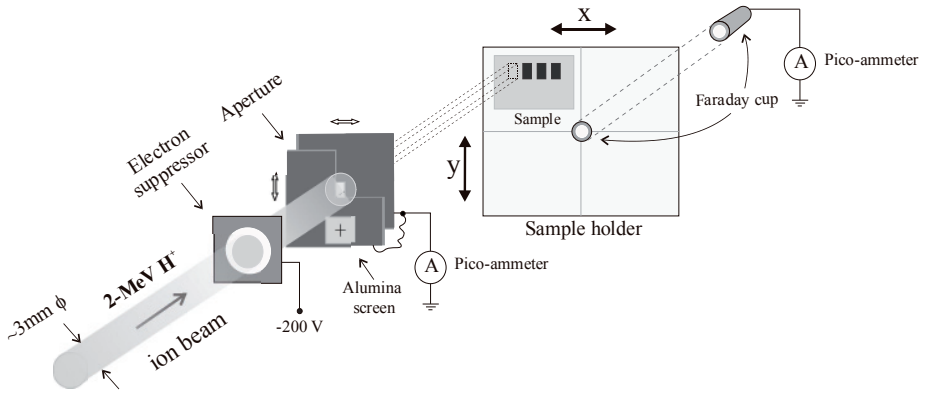

Figure 1. Schematic illustration of an experimental set-up using the PPAL technique for H^+ ion beam irradiation (not to scale)

The key parameters in this study were the values of ion beam fluence (ions/cm^2) and ion beam flux (ions/cm^2·s) at the irradiated areas. To ensure the accuracy of these measurements, the ion beam current at two different positions, as shown in Figure 1, was measured with high precision. A picoammeter with 4.8-pC resolution was specially designed for this purpose. To assure correctness in measuring, an electron suppressor with a 5-mm-diameter hole and a -200V potential was placed in front of the aperture to prevent secondary electrons from leaving the copper blades.

The picoammeter was used to measure the ion beam current detected by an 8-mm-inner-diameter, 65-mm-long Faraday cup. The Faraday cup was isolated and buried in the sample holder. The ion beam current was collected every second from start to stop. Together with the known hole area

at the aperture, the ion beam fluence and flux could be easily calculated. Moreover, the major part of the incident ion beam blocked by the aperture was monitored also; this was used to fine-tune the accelerator for a stable ion beam current.

After irradiation, the surface morphology of the irradiated areas was investigated by an optical microscope and a scanning electron microscope (SEM) (JSM-5410LV, JEOL, Japan), while the shrinkage of the irradiated areas was measured by the profilometer.

RESULTS AND DISCUSSION

It was found that for 2-MeV H^+ ions, the cross-linking of PMMA within the entire pattern occurred when the fluence exceeded 3.5×10^{14} ions/cm^2, which is consistent with a previous report [19]. Therefore, all the incident fluences used in this work were above this value. Accordingly, in Figure 2 both a and d, b and e, and c and f patterns were irradiated by the 2-MeV H^+ ion beam with the same fluence, viz. 1.0×10^{15}, 1.25×10^{15} and 1.75×10^{15} ions/cm^2 respectively, while the ion beam flux used for patterns a-c and d-f was 4.7×10^{11} and 3.0×10^{12} ions/cm^2·s respectively. It was clearly seen that flaws on the PMMA surface were strongly dependent on the ion beam flux. For the same irradiation fluence but with small values of ion current, the flaws were absent. Figure 3(a) shows that the flaws are blisters and not craters. Each isolated blister has a common appearance of a round shape with about the same diameter.

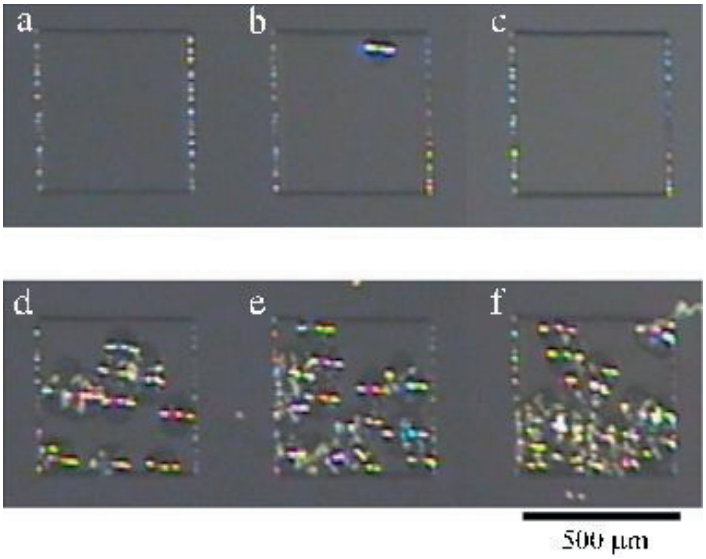

Figure 2. Optical microscope images (13×) of the six 500×500 μm^2 patterns of irradiated areas on the PMMA thin film

The surface profiles of patterns a, b and c in Figure 2 were measured by the profilometer. As shown in Figure 4, the surface regions modified by the 2-MeV H^+ ion beam are remarkably lower than those in the unirradiated regions. Also, the compaction or shrinking occurs even at the smooth patterns and increases with ion fluence. Hnatowicz and Fink [20] reported that the compaction of a polymer is initiated by cross-linking and tends to increase the material density. Experimental evidence from this study suggests that the gas evolution always occurs during irradiation even though no blister is

observed, as shown in Figure 2 (a-c). However, the gas-release mechanisms for low-flux and high-flux irradiation may be different. More information can be found in a comparison of the smooth pattern a with the blister-filled pattern d, for example. Both of them experienced the same fluence but the irradiation duration of pattern a was 1.72 times longer than that of pattern d.

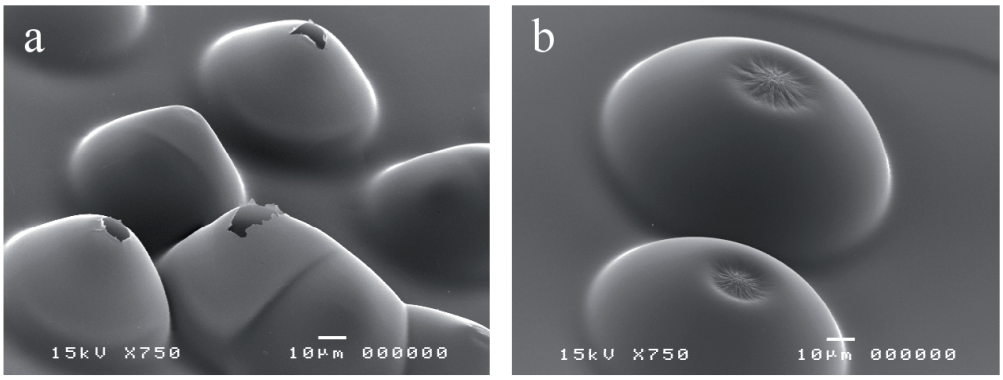

Figure 3. Tilted SEM images of the blisters created by (a) 2-MeV H^+ ions and (b) 1-MeV H^+ ions. The average blister diameters are (a) 61.0±5.8 µm and (b) 92.8±2.5 µm.

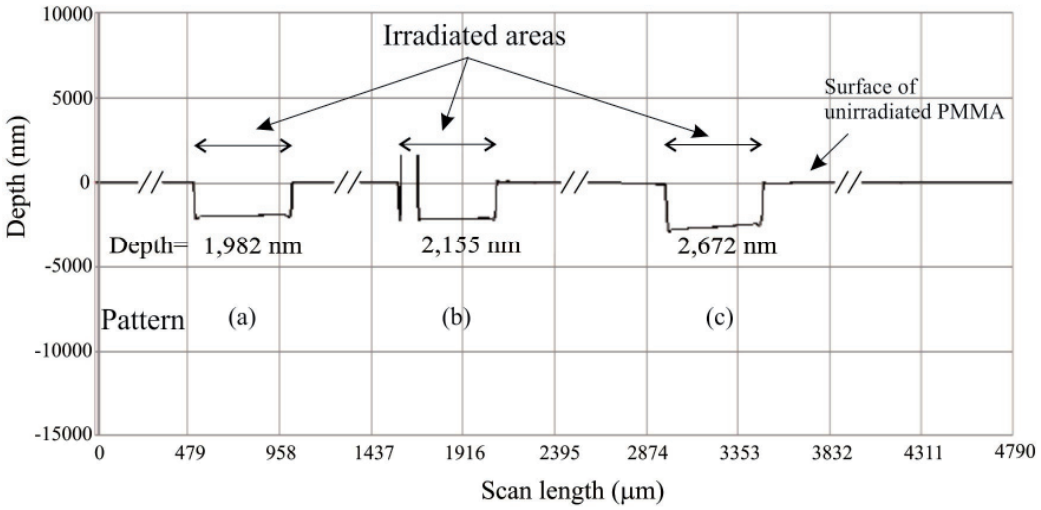

Figure 4. The surface profile of the 3 irradiated areas in the top row of Figure 2

It is reasonable to draw a conclusion that each ion track can be considered isolated in the case of low flux. Degassing due to the pressure gradient is thought to be the main mechanism. Moreover, the very thin PMMA film would allow the gases to leave the polymer easily without much build-up. On the other hand, in the high ion flux case, the temporal interval between the closely-spaced incident ion tracks would allow a build-up of dense low-molecular-weight fragments from intense main-chain scissions. This might nucleate gas bubbles in the whole irradiated volume of the polymer and accumulate gases which eventually converted it into a 'foamed' structure [21]. In this case, the gas bubbles that reached the polymer surface would form blisters.

It was also found that a 1-MeV H^+ ion beam creates blisters at lower ion beam flux than does a 2-MeV H^+ ion beam. By comparing Figure 3(b) with Figure 3(a), we can see that although each isolated blister has the same shape, the blisters from 1-MeV irradiation are significantly larger in diameter than those from 2-MeV irradiation. From the SRIM code, the stopping power is 1.5 times and the displacement damage 2.4 times greater in 1-MeV than in 2-MeV proton irradiation.

CONCLUSIONS

At an ion irradiation fluence of 10^{14} ions/cm^2 of 2-MeV H^+ ions, the cross-linking process in PMMA started to overcome the chain scission process. The full cross-linking began at an ion fluence of 6.6×10^{14} ions/cm^2. The formation of blisters was strongly dependent on the ion beam flux and stopping power of the polymer for the ions. A 2-MeV proton flux of less than 4.7×10^{11} ions/cm$^2\cdot$s achieved a blister-free condition for the PMMA film ~9 μm thick. This work has confirmed that blisters are created by gas evolution due to chain scissions induced by the ion beams, especially in the early stage of irradiation.

ACKNOWLEDGEMENTS

This work was partly supported by the CoE Program of Chiang Mai University and the International Atomic Energy Agency (IAEA, Vienna). S.U. gratefully acknowledges a scholarship from the ThEP Centre. N. P. (N. Puttaraksa) gratefully acknowledges financial support from Thailand Research Fund (TRF) in the form of an RGJ scholarship. H. J. W.'s and N. P.'s work was carried out under the Academy of Finland Centre of Excellence in Nuclear and Accelerator Based Physics (Ref. 213503). H. J. W. is grateful for a senior researcher grant from the Academy of Finland (Ref. 129999). The authors also wish to thank Mr. Chome Thongleurm and Mr. Witoon Ginamoon for their technical support.

REFERENCES

1. T. M. Hall, A. Wagner and L. F. Thompson, "Ion beam exposure characteristics of resists: Experimental results", *J. Appl. Phys.*, **1982**, *53*, 3997-4010.
2. S. V. Springham, T. Osipowicz, J. L. Sanchez, L. H. Gan and F. Watt, "Micromachining using deep ion beam lithography", *Nucl. Instr. Meth. Phys. Res. B*, **1997**, *130*, 155-159.
3. F. Menzel, D. Spemann, S. Petriconi, J. Lenzner and T. Butz, "Proton beam writing of submicrometer structures at LIPSION", *Nucl. Instr. Meth. Phys. Res. B*, **2007**, *206*, 419-425.
4. P. G. Shao, J. A. van Kan, K. Ansari, A. A. Bettiol and F. Watt, "Poly(dimethylsiloxane) micro/nanostructure replication using proton beam written masters", *Nucl. Instr. Meth. Phys. Res. B*, **2007**, *260*, 479-482.
5. S. Gorelick, N. Puttaraksa, T. Sajavaara, M. Laitinen, S. Singkarat and H. J. Whitlow, "Fabrication of microfluidic devices using MeV ion beam Programmable Proximity Aperture Lithography (PPAL)", *Nucl. Instr. Meth. Phys. Res. B*, **2008**, *266*, 2461-2465.
6. C. Udalagama, E. J. Teo, S. F. Chan, V. S. Kumar, A. A. Bettiol and F. Watt, "Proton beam writing of long, arbitrary structures for micro/nano photonics and fluidics applications", *Nucl. Instr. Meth. Phys. Res. B*, **2011**, *269*, 2417-2421.

7. M. J. Madou, "Fundamentals of Microfabrication: The Science of Miniaturization", 2nd Edn., CRC Press, Boca Raton, **2002**, pp.6-7.
8. V. Auzelyte, M. Elfman, P. Kristiansson, C. Nilsson, J. Pallon, N. A. Marrero and M. Wegdén, "Exposure parameters for MeV proton beam writing on SU-8", *Microelectron. Eng.*, **2006**, *83*, 2015-2020.
9. A. Licciardello, M. E. Fragalà, G. Foti, G. Compagnini and O. Puglisi, "Ion beam effects on the surface and on the bulk of thin films of polymethylmethacrylate", *Nucl. Instr. Meth. Phys. B*, **1996**, *116*, 168-172.
10. N. Puttaraksa, S. Unai, M. W. Rhodes, K. Singkarat, H. J. Whitlow and S. Singkarat, "Fabrication of a negative PMMA master mold for soft-lithography by MeV ion beam lithography", *Nucl. Instr. Meth. Phys. B*, **2012**, *272*, 149-152.
11. J. Kaur, S. Singh, D. Kanjilal and S. K. Chakarvarti, "Nano/micro surface structures by swift heavy ion irradiation of polymeric thin films on GaAs", *Digest J. Nanomater. Biostruct.*, **2009**, *4*, 729-737.
12. D. He and M. N. Bassim, "Atomic force microscope study of crater formation in ion bombarded polymer", *J. Mater. Sci.*, **1998**, *33*, 3525-3528.
13. J. F. Ziegler and J. P. Biersack, "The stopping and range of ions in matter", **2008**, http://www.srim.org.
14. M. E. Fragalà, G. Compagnini, A. Licciardello and O. Puglisi, "Track overlap regime in ion-irradiated PMMA", *J. Polym. Sci. B*, **1998**, *36*, 655-664.
15. Z. Chang and J. A. LaVerne, "The gases produced in gamma and heavy-ion radiolysis of poly(methyl methacrylate)", *Radiat. Phys. Chem.*, **2001**, *62*, 19-24.
16. M. E. Fragalà, G. Compagnini, L. Torrisi and O. Puglisi, "Ion beam assisted unzipping of PMMA", *Nucl. Instr. Meth. Phys. B*, **1998**, *141*, 169-173.
17. M. B. Lewis and E. H. Lee, "G-values for gas production from ion-irradiated polystyrene", *J. Nucl. Mater.*, **1993**, *203*, 224-232.
18. F. Schrempel and W. Witthuhn, "Deep light ion lithography in PMMA—a parameter study", *Nucl. Instr. Meth. Phys. B*, **1997**, *132*, 430-438.
19. N. Puttaraksa, R. Norarat, M. Laitinen, T. Sajavaara, S. Singkarat and H. J. Whitlow, "Lithography exposure characteristics of poly(methyl methacrylate) (PMMA) for carbon, helium and hydrogen ions", *Nucl. Instr. Meth. Phys. B*, **2012**, *272*, 162-164.
20. V. Hnatowicz and D. Fink, "Macroscopic changes in ion-irradiated polymers", in "Fundamentals of Ion-Irradiated Polymers" (Ed. D. Fink), Springer-Verlag, Berlin, **2004**, pp.349-375.
21. A. Chapiro, "Chemical modifications in irradiated polymers", *Nucl. Instr. Meth. Phys. B*, **1988**, *32*, 111-114.

Maejo Int. J. Sci. Technol. **2012**, *6*(01), 77-94

Maejo International Journal of Science and Technology

ISSN 1905-7873
Available online at www.mijst.mju.ac.th

Full Paper

Degradation of bisphenol A by ozonation: rate constants, influence of inorganic anions, and by-products

Kheng Soo Tay *, Noorsaadah Abd. Rahman and Mhd. Radzi Bin Abas

Environmental Research Group, Department of Chemistry, Faculty of Science, University of Malaya, 50603 Kuala Lumpur, Malaysia

* Corresponding author, e-mail: khengsoo@um.edu.my

Received: 8 February 2011 / Accepted: 23 February 2012 / Published: 27 February 2012

Abstract: The second-order rate constants for the reaction between bisphenol A (BPA) and ozone were evaluated over the pH range of 2-12. The rate constants showed minimum values ($\times 10^4$ $M^{-1}s^{-1}$) under acidic condition (pH < 4) and were of maximum values ($\times 10^9$ $M^{-1}s^{-1}$) under basic condition (pH >10). From pH 4 to 7, the second-order rate constants were found to increase by a magnitude of almost 10^2 and this was due to the increase in anionic BPA species in the solution. The rate constants increased almost twofold when pH increased from 9.6 to 10.2. The presence of common inorganic anions at levels commonly found in the environment did not affect the rate of degradation of BPA.

The degradation by-products from the ozonation of BPA were identified as 4-(prop-1-en-2-yl)phenol, hydroquinone, 4-hydroxyacetophenone, 2-(2-(4-hydroxyphenyl)propan-2-yl)succin-aldehyde, 2-(1-(4-hydroxyphenyl)vinyl)pent-2-enal, 3-formyl-4-(4-hydroxyphenyl)-4-methylpent-2-enoic acid, monohydroxy-BPA and dihydroxy-BPA. In conclusion, ozonation was found to be an effective method for the removal of BPA even in the presence of common inorganic anions at environmental concentrations. However, incomplete treatment of BPA might produce a variety of degradation by-products.

Keywords: bisphenol A, ozonation, rate constant, anions, competitive kinetics, OH radical

INTRODUCTION

Bisphenol-A (BPA; 2,2-bis(4-hydroxylphenyl)propane) is a commonly used chemical in the synthesis of polymers, especially for food and beverage packages. BPA has been reported to have developmental toxicity, carcinogenicity, possible neurotoxicity [1] and estrogenic effects [2]. This

chemical can leach from plastic products under normal and high temperatures [2-3]. Thus, the leaching of BPA into the environment from disposed plastic materials is expected. So far, legislation on the use of BPA and its discharge into the environment is sorely lacking. Consequently, the occurrences of BPA in the environment have been widely reported [e.g. 4-6]. The presence of BPA in coastal waters and supermarket seafood from Singapore and mussels from South and South-east Asia [7-8] indicates that BPA pollution is severe not only in developed countries but also in the Asian region.

Since BPA has the potential to cause undesirable ecological and human health effects, various treatment technologies have been developed for its removal from water. The oxidative degradation methods for BPA such as ozonation [9-14], photo-Fenton reaction [15], photocatalytic reaction by TiO_2 [16] and ultrasound-UV-iron(II) treatment [17] have been reported. Among the treatment methods, ozonation has been projected to be one of the fastest growing water disinfection technologies in the market [18-19]. It has been shown to be effective in the removal of organic pollutants from water and wastewater [20-24]. During ozonation, organic pollutants undergo a series of oxidation processes by ozone (O_3) and hydroxyl radical (•OH) formed by the decomposition of O_3 in water [25]. In some cases, toxic by-products may be generated [22]. Therefore, evaluation and determination of degradation by-products from the ozonation of organic pollutants is an important consideration.

Although the ozonation of BPA has been widely reported, based on our literature review the influence of inorganic anions on the removal of BPA by ozonation has not been evaluated. The influence of inorganic anions is important since chloride and phosphate ions, for example, can react with O_3 and •OH, thus affecting the rate of removal of the organic pollutants in water [26-27]. The increase in salt concentration has also been reported to affect O_3 solubility in water [28]. The main objective of this study, therefore, is to evaluate the effect of inorganic anions, namely phosphate, nitrate, sulphate and chloride ions. In addition, the second-order rate constants for the reaction between BPA and O_3 at pH 2-12 were determined. The variation in the rate constant at different pH values, especially within the two pK_a values (9.6 and 10.2) of BPA, was studied in detail in order to compare the reactivity of anionic and dianionic species of BPA in aqueous solution towards O_3. The degradation by-products (DBPs) of BPA were also identified. Some DBPs of BPA have already been determined by previous studies [11,13]. However, in this study, we managed to identify a few additional compounds and degradation pathways of BPA during ozonation were proposed.

MATERIALS AND METHODS

Chemicals

BPA (>99% purity) was obtained from Aldrich and used without further purification. Its stock solution (200 mg/L) was prepared by dissolving in boiling ultrapure deionised water (Elcagan, UK). All chemicals were used without further purification. Sodium phosphate (96%) and sodium dihydrogen phosphate (99%) was obtained from Aldrich. Sodium chloride (≥99.5%), sodium nitrate (99%) sodium sulphate decahydrate (>99%), sodium phosphate monobasic (99%) and *tert*-butyl alcohol (*t*-BuOH) (99.5%) were purchased from Sigma. Sodium phosphate dibasic (99%) and disodium hydrogen phosphate (99%) were purchased from Riedel-de-Haën. A mixture of BSTFA

(*N*,*O*-bis(trimethylsilyl)trifluoroacetamide) and TMCS (trimethylchlorosilane) in a ratio of 99:1 was obtained from Supelco. All solvents (HPLC grade) and phosphoric acid (85%) were obtained from Merck. Sodium hydroxide (>98%) was purchased from Fluka. Purified oxygen (99.8%) was obtained from MOX-linde (Malaysia). Phosphate buffer (0.5 mol/L) was prepared using sodium dihydrogen phosphate and/or disodium hydrogen phosphate and the pH was adjusted using either phosphoric acid or sodium hydroxide solutions. O_3 was produced from purified oxygen by an ozone generator (model OZX03K, Enaly Trade Co. Ltd., Canada). All tubing from the ozone generator was of ozone-inert silicone material.

Ozonation of BPA

Determination of second-order rate constant for reaction of BPA with O_3

A detailed description of the rate constant determination was given in our previous study [29]. Briefly, a competitive kinetic method was applied using phenol as a reference compound. Experiments were performed at room temperature (27-30ºC) in 20-mL vials with solution containing equal concentration of BPA and phenol (4 µmol/L) as well as 20 mmol/L of *t*-BuOH. The pH of the solution was adjusted using 20 mmol/L of phosphate buffer. Ozone solutions with concentrations ranging from 1.5 to 7.5 µmol/L were added. The aqueous O_3 stock solution was prepared by sparging O_3 at a rate of 0.70 g/hr into deionised water placed inside a water-jacketed beaker at 2ºC. The concentration of O_3 was measured by the indigo method [30]. The final volume of the mixtures was 20 mL, which also minimised the headspace. Each vial was then shaken vigorously. The time of total ozone consumption was estimated from the half-life of ozone in the BPA solution under different pH conditions. The half-lives for ozone in BPA solution were found to be 28, 9 and <2 min. at pH 2, 7 and 12 respectively. To ensure the reaction was completed, the reaction mixtures were shaken for 12 hr using a shaker. The remaining concentrations of BPA and phenol were determined by high performance liquid chromatography (HPLC).

Effect of selected anions on ozonation of BPA

All experiments were performed under heterogeneous conditions in which O_3 was bubbled at a rate of 0.70 g/hr through a gas dispersion tube into a 1000-mL jacketed beaker containing 1000 mL of magnetically-stirred BPA solution (100 mg/L) and an anion. The reaction temperature was maintained by means of a circulating water bath at 25 ± 0.1°C. Aliquots were withdrawn at defined time intervals and analysed by HPLC in order to monitor the remaining concentrations of BPA.

Extraction of degradation by-products of BPA ozonation

Ozone was bubbled at a rate of 0.70 g/hr through a gas dispersion tube into a 1000-mL jacketed beaker containing 1000 mL of magnetically-stirred BPA solution (100 mg/L). In this experiment, ozonation was carried out without *t*-BuOH in order to study the contribution of both O_3 and •OH in the degradation of BPA. The reaction temperature was maintained by means of a circulating water bath at 25 ± 0.1°C. A 10-mL aliquot was withdrawn every 2 min. for a period of 10 min. and, after removing residual ozone with nitrogen gas [31], subjected to a liquid-liquid extraction using ethyl acetate. The organic extract was then silylated with BSTFA + TMCS (99:1) at 70ºC for 4

hr. The silylated extract was dried with nitrogen stream and redissolved in 30 μL of dichloromethane,1.2 μL of which was analysed by gas chromatography-mass spectrometry (GC-MS).

Analytical methods

The concentration of BPA in the reaction mixture was determined using HPLC (Thermo Separation Product HPLC System P2000, HiTech Trader, USA) equipped with a UV detector and a degasser. A 250×4.6mm RP-8 (5μm) Lichrospher-100 analytical column (Merck) was used for separation. Acetonitrile (65%) in deionised water with 0.1% trifluoroacetic acid was used as the mobile phase. The separation was carried out under isocratic condition. The separated components were detected at 230 nm. The flow rate was maintained at 1.0 mL/min for all runs and the sample volume for HPLC analysis was 20 μL.

The analysis of the degradation by-products was carried out using a Hewlett-Packard HP 6890 gas chromatograph coupled with HP5972 mass spectrometer. The column was HP-5 (5% phenylmethylpolysiloxane) column with the dimension of 30 m × 0.25 mm and 0.25 μm of film thickness. Helium was used as the carrier gas with an average flow rate of 40 cm/sec., and the GC oven temperature was initially 60°C (maintained for 2 min.) and increased to 280°C at the rate of 6°C/min and maintained at this temperature for 2 min. The temperatures of the injection port and the transfer line were set at 290°C and 300°C respectively. The data for quantitative analysis was acquired in the electron impact mode (70 eV) with scanning in the range of 50-600 amu at 1.5 sec./scan.

RESULTS AND DISCUSSION

Kinetics of Degradation of BPA by Ozonation

The reaction of ozone with an organic compound has been reported to be of first order with respect to both ozone and the organic compound. Thus, the kinetics of ozonation can be expressed as a second-order reaction [32]. The determination of its rate constants was performed using a competitive kinetics method with phenol as reference compound [20, 29, 33-34]. Phenol was selected because it was expected to have a similar decomposition pathway and rate constant as BPA in the ozonation [34]. For phenol, the second-order rate constants for the reaction with O_3 at different pH values ($k_{\text{app,Phenol-O}_3}$) were calculated using equation 1:

$$k_{\text{app,Phenol-O}_3} = k_{\text{O}_3,\text{Phenol}}\left(\frac{10^{-\text{pH}}}{10^{-\text{p}Ka}+10^{-\text{pH}}}\right) + k_{\text{O}_3,\text{Phenolate}}\left(\frac{10^{-\text{p}Ka}}{10^{-\text{p}Ka}+10^{-\text{pH}}}\right) \quad (1)$$

where pK_a of phenol was 9.9 and the intrinsic rate constants for phenol and phenolate were 1.3×10^3 M^{-1} s^{-1} ($k_{\text{O}_3,\text{Phenol}}$) and 1.4×10^9 M^{-1} s^{-1} ($k_{\text{O}_3,\text{Phenolate}}$) respectively [9, 34]. The rate constants for the reaction between O_3 and BPA ($k_{\text{O}_3-\text{BPA}}$) were estimated using competitive kinetics method derived from equation 2 [35, 36]:

$$\ln\left(\frac{[\text{BPA}]_n}{[\text{BPA}]_0}\right) = \frac{k_{\text{O}_3-\text{BPA}}}{k_{\text{app,O}_3\text{-Phenol}}} \ln\left(\frac{[\text{Phenol}]_n}{[\text{Phenol}]_0}\right) \quad (2)$$

where $[\text{BPA}]_0$ and $[\text{Phenol}]_0$ represent the initial concentration of BPA and phenol and $[\text{BPA}]_n$ and $[\text{Phenol}]_n$ represent the concentration of BPA and phenol after the ozonation reaction at different ozone dose, *n*.

Ozonation of BPA was carried out at pH 2.0-12.0 in the presence of excess *t*-BuOH ([*t*-BuOH] / [O_3] > 300). *t*-BuOH is a radical scavenger added to scavenge the •OH radical, thus allowing BPA to react only with O_3 during ozonation. Lee et al. [9] and Deborde et al. [34] reported $k_{\text{o}_3\text{-BPA}}$ at 20°C = 1.68×10^4 and 1.30×10^4 M^{-1} s^{-1} at pH 2, and 1.11×10^9 and 1.60×10^9 M^{-1} s^{-1} at pH 12 respectively. In this work, somewhat higher values of $k_{\text{o}_3\text{-BPA}}$ were obtained, viz. $(1.7\pm0.5)\times10^4$ and $(9.0\pm0.5)\times10^9$ $M^{-1}s^{-1}$ at pH 2 and 12 respectively. This difference might be due to a large error that can occur in the competitive kinetics method [20] and also to a higher reaction temperature that was selected in this study.

According to Staples et al. [37], the two dissociation constants of BPA are 9.6 (pK_a1) and 10.2 (pK_a2). BPA is therefore a weak organic acid which can dissociate in solution as either an anionic or dianionic species. Generally, when pH = pK_a, the undissociated and ionic species exist at equal concentration in solution. When pH < pK_a, the undissociated species is predominant and when pH > pKa, the ionic species is predominant [38]. Therefore, for BPA, when pH < pK_a1, undissociated BPA exists predominantly in water. When pK_a1 < pH < pK_a2, anionic BPA is the predominant species and when pH > pK_a2, dianionic BPA are predominant (Figure 1).

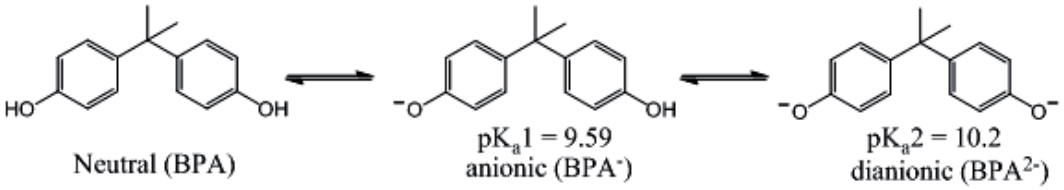

Figure 1. Dissociation of BPA

It has been previously shown that in the presence of the •OH radical, the rate of BPA degradation by ozone increases from pH 2 to 7 and then decreases at pH 10 due to •OH scavenging by carbonate and bicarbonate ions [14]. In this study, *t*-BuOH was added to scavenge the •OH radical from the beginning in order to study the rate constants for BPA degradation by O_3 only. The results are shown in Figure 2, indicating that the reactivity increases as the pH increases from 2 to 12. Under acidic condition (pH < 7), the reaction would be mainly between O_3 and undissociated BPA. Between pH 4-7, the rate constant was observed to increase by a magnitude of almost 10^2 and this would be due to the increase of anionic species of BPA in the solution. The rate constant increased almost twofold when the pH increased from 9.6 (= pK_a1) to 10.2 (= pK_a2).

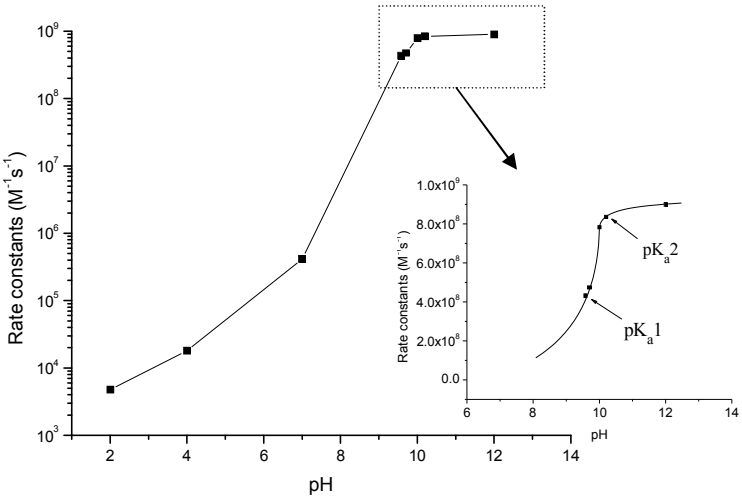

Figure 2. Variation of second-order rate constant of BPA-ozone reaction at different pH values

In order to study the effect of the ratio of $[BPA^{2-}]$ / $[BPA^{-}]$ on the rate constant, the obtained second-order rate constants were plotted against $[BPA^{2-}]$ / $[BPA^{-}]$ values at pH between 9.6-10.3 (Figure 3). The ratio of $[BPA^{2-}]$ / $[BPA^{-}]$ was estimated using Henderson-Hasselbach equation as follows [39]:

$$pH = pK_a 2 + \log\left[\frac{[BPA^{2-}]}{[BPA^{-}]}\right] \quad (3)$$

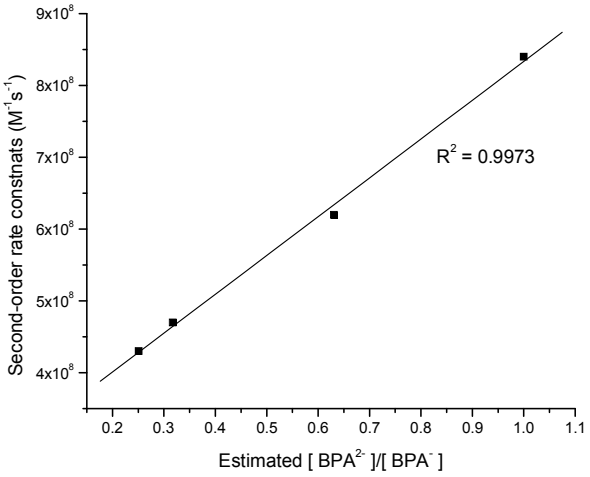

Figure 3. Effect of $[BPA^{2-}]$ / $[BPA^{-}]$ on second-order rate constant of BPA-ozone reaction at the pH 9.6-10.3

From Figure 3, the rate constant increases proportionally with $[BPA^{2-}]$ / $[BPA^{-}]$, which implies that the dianionic species of BPA (BPA^{2-}) is more easily oxidised by O_3 compared to its anionic counterpart (BPA^{-}). From Figure 2, it can be clearly observed that when the pH value

increases further from 10.2 to 12.0, the reactivity of BPA with O_3 remains almost constant. This is most likely due to the fact that the maximum fraction of BPA^{2-} has been reached at pH 10.2 and further increasing of pH does not influence the amount of BPA^{2-} anymore.

Influence of Inorganic Anions

Most wastewaters normally contain inorganic anions coexisting with organic pollutants. The effects of the anions on the rate of BPA degradation was studied at concentrations found in wastewaters [40-42]. Figure 4 shows plots of BPA degradation in the presence of phosphate, nitrate, chloride and sulphate ions. The results indicate that the presence of common inorganic anions at concentration levels in the wastewaters does not significantly affect the rate of BPA degradation. This might be due to the fast reaction between O_3 and BPA as indicated by the determined second-order rate constants.

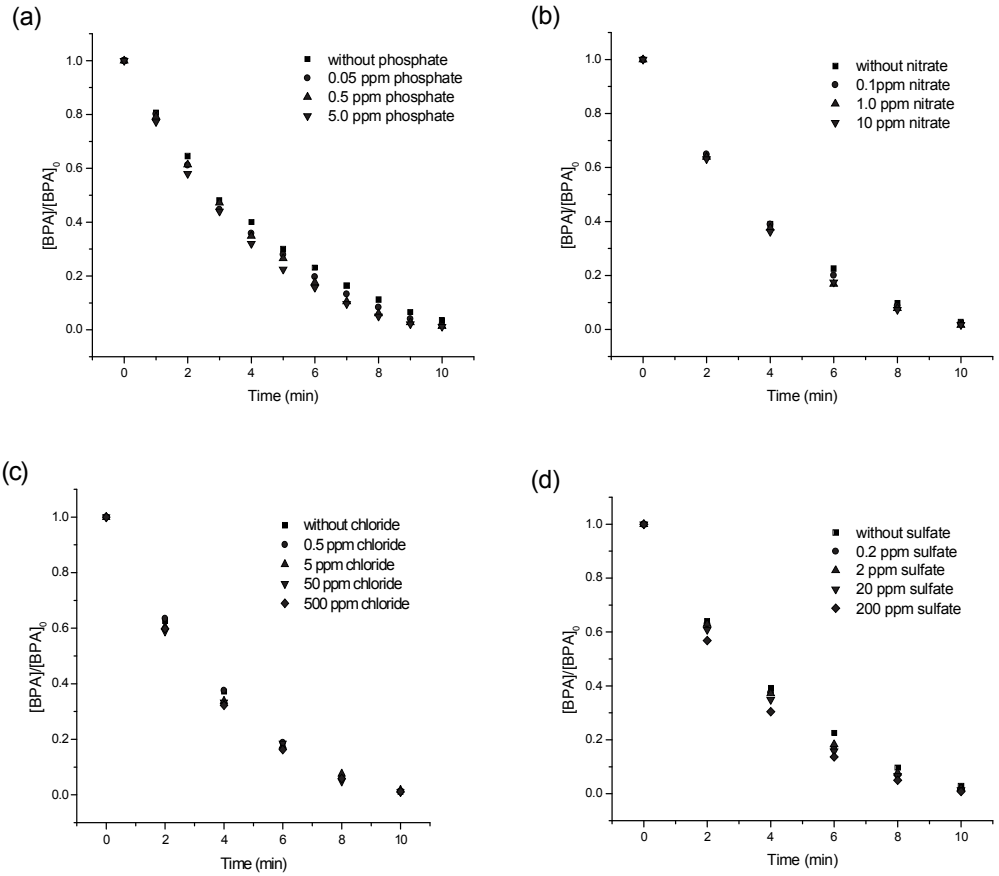

Figure 4. Effect of (a) phosphate, (b) nitrate, (c) chloride and (d) sulphate ions on the degradation of BPA (temperature = 25ºC; O_3 dose = 0.69 g/h; pH = 6.5; $[BPA]_0$ = 100 mg/L)

Degradation By-Products (DBPs) of BPA

GCMS analyses were performed by comparing the chromatogram of BPA with those of the aliquots taken at different ozonation times. All samples were subjected to similar derivatisation

procedure as mentioned in the experimental section. A chromatogram showing the distribution of DBPs of BPA is presented in Figure 5 and the proposed DBPs are presented in Table 1. All derivatised compounds occurred as trimethylsilyl derivatives characterised by the peak at *m/z* 73 in the mass spectrum. Identification of DBPs was carried out based on fragmentation patterns in the mass spectrum and/or by comparing the mass spectrum with the library available in the instrument database.

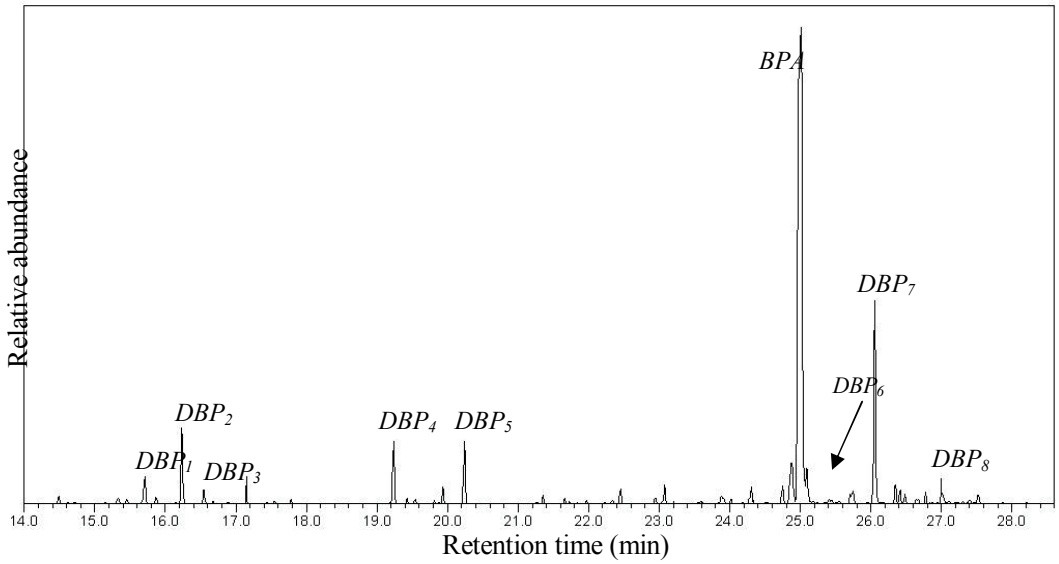

Figure 5. Gas chromatogram of BPA after 4 min. of ozonation time ($[BPA]_0$ = 100 mg/L, pH = 6.5, temperature = 25 ºC, O_3 dose = 0.70 g/hr)

The mass spectrum of BPA shows the molecular ion peak at *m/z* 372 (Figure 6a). Besides the peak at *m/z* 357 representing the loss of methyl group from trimethylsilyl group ($(M\text{-}CH_3)^+$), the other significant peak is at *m/z* 207 representing the loss of trimethyl(phenoxy)silane from silylated BPA. DBP_1, DBP_2 and DBP_3 represent the breakdown products of BPA and their mass spectra (as silylated derivatives) are presented in Figures 6 (b-d). The formation of DBP_1, DBP_2 and DBP_3 has also been detected in previous studies [13,15,16].

The mass spectra of DBP_4 and DBP_5, formed by aromatic-ring opening during the ozonation process, are presented in Figures 7a and 7b respectively. Silylated DBP_5 with a molecular weight of 292 amu shows a peak representing $(M-1)^{+\cdot}$ at *m/z* 291 (Figure 7b). DBP_6 is a BPA degradation by-product proposed by Deborde et al. [11]. The structure of this compound was derived based on its fragmentation pattern in the mass spectrum (Figure 7c). The peak at *m/z* 378 corresponds to the molecular ion peak of silylated DBP_6. Other major peaks are at *m/z* 212 and 217. The peak at *m/z* 212 represents the radical cation of silylated 3-formyl-4-methylpenta-2,4-dienoic acid. The peak at *m/z* 217 represents the loss of silylated carboxylic acid and aldehyde functional groups from the parent compound.

Monohydroxylated (DBP_7) and dihydroxylated (DBP_8) BPA were also detected during the ozonation process. The molecular ion peaks of DBP_7 and DBP_8 are at *m/z* 460 (Figure 7d) and *m/z* 548 (Figure 7e) respectively. Additional 88 amu and 176 amu over the molecular ion peak of

silylated BPA (*m/z* 372) indicated the addition of one and two $[(CH_3)_3SiO]^+$ groups to silylated BPA respectively.

Table 1. Degradation by-products of BPA

Compound identified	Retention time (min.) (Label)	Proposed structure of compound (Molecular weight)	Name
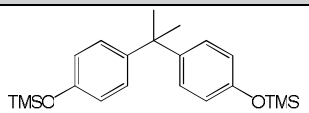 (*m/z* 372)	25.01 BPA	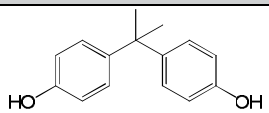 (228.3)	Bisphenol A
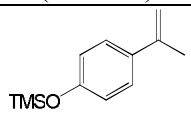 (*m/z* 206)	15.71 (*DBP*$_1$)	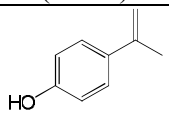 (134.1)	4-(Prop-1-en-2-yl)phenol
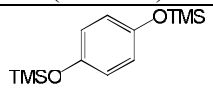 (*m/z* 254)	16.23 (*DBP*$_2$)	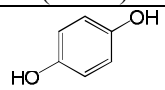 (110.0)	Hydroquinone
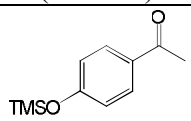 (*m/z* 208)	17.15 (*DBP*$_3$)	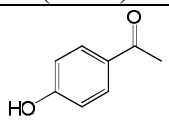 (136.1)	4-Hydroxyacetophenone
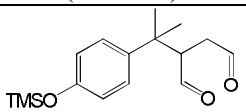 (*m/z* 292)	19.23 (*DBP*$_4$)	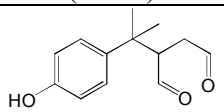 (220.1)	2-(2-(4-Hydroxyphenyl)propan-2-yl)succinaldehyde
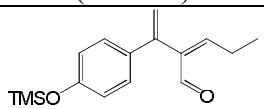 (*m/z* 274)	20.24 (*DBP*$_5$)	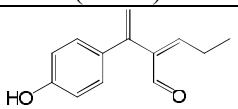 (202.1)	2-(1-(4-Hydroxyphenyl)vinyl)-pent-2-enal
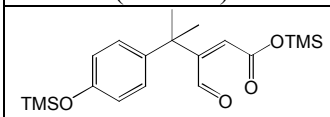 (*m/z* 378)	25.09 (*DBP*$_6$)	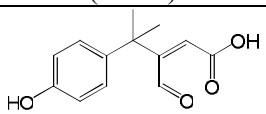 (234.1)	3-Formyl-4-(4-hydroxyphenyl)-4-methylpent-2-enoic acid
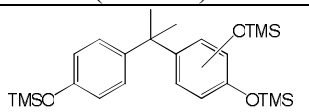 (*m/z* 460)	26.20 (*DBP*$_7$)	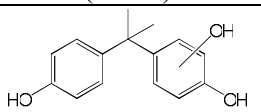 (244.1)	Monohydroxy-BPA
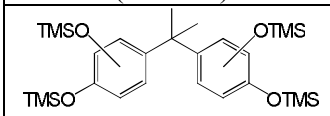 (*m/z* 548)	27.01 (*DBP*$_8$)	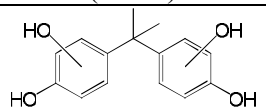 (260.1)	Dihydroxy-BPA

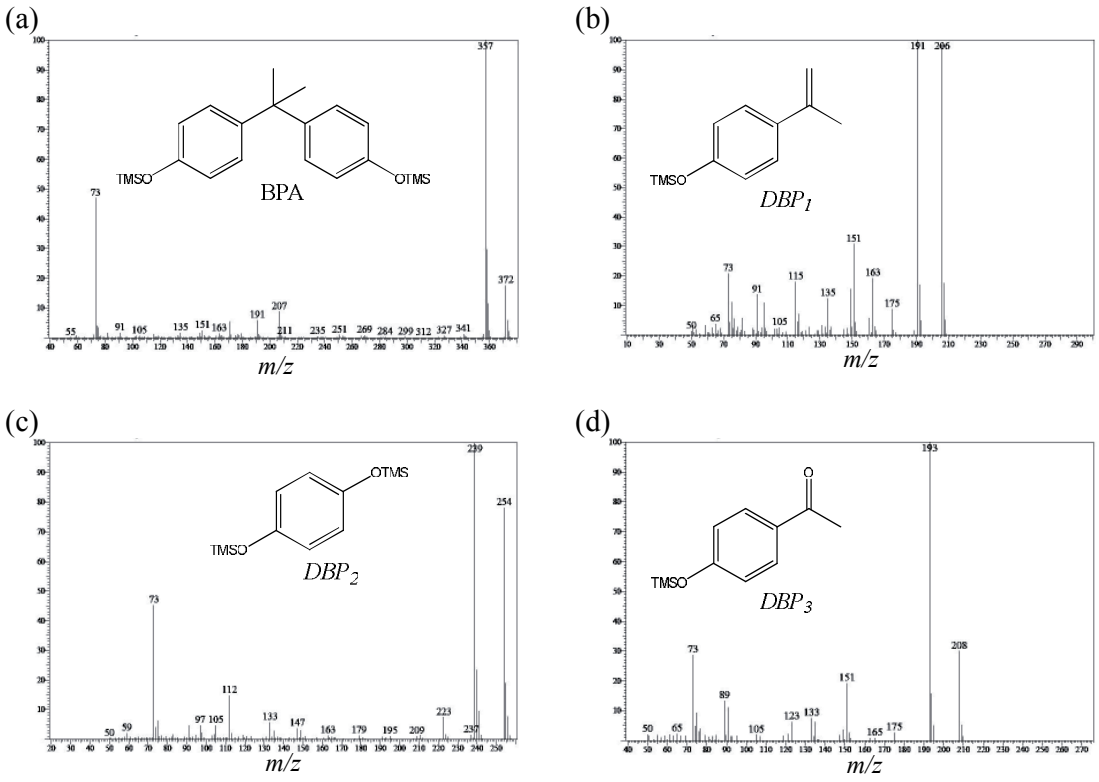

Figure 6. Mass spectra of *DBP*$_1$, *DBP*$_2$, *DBP*$_3$ and BPA

Figure 8 shows the time profiles of the major DBPs, most of which were successfully removed after 10 min. of ozonation, with the exception of *DBP*$_3$, *DBP*$_6$ and *DBP*$_8$. These three by-products thus seemed to be more resistant to ozonation compared to others. In the degradation experiment, ozonation was performed without a radical scavenger, so BPA could react with both O_3 and •OH. As compared to the reaction between O_3 and BPA [11], the results in this study show that the presence of •OH seemed to produce more species of the breakdown products such as *DBP*$_1$, *DBP*$_3$ and *DBP*$_4$, which was most likely due to the non-selective behaviour of •OH, which can also react at the aliphatic chain and aromatic ring of BPA [33, 43].

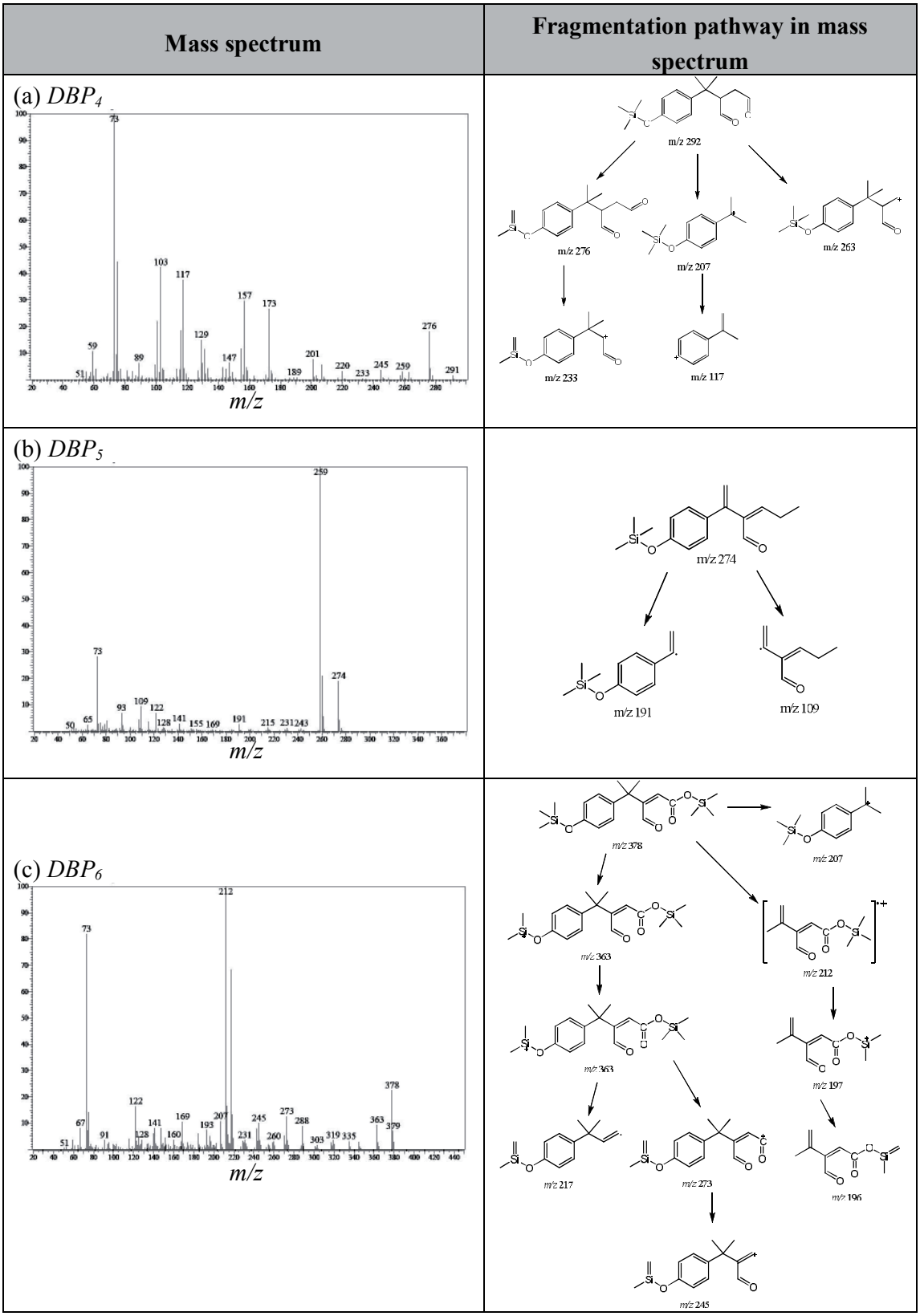

Figure 7. Mass spectra and fragmentation patterns of DBP_4, DBP_5, DBP_6, DBP_7 and DBP_8

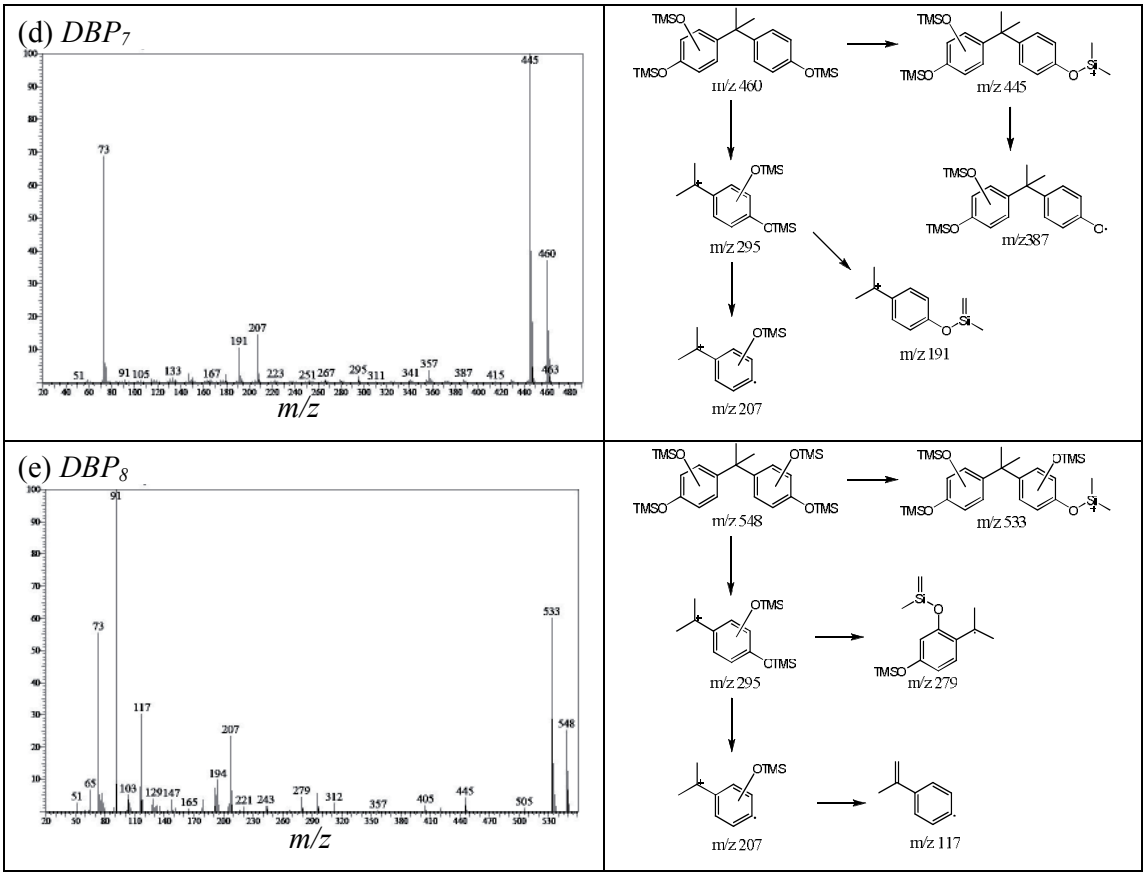

Figure 7. (continued)

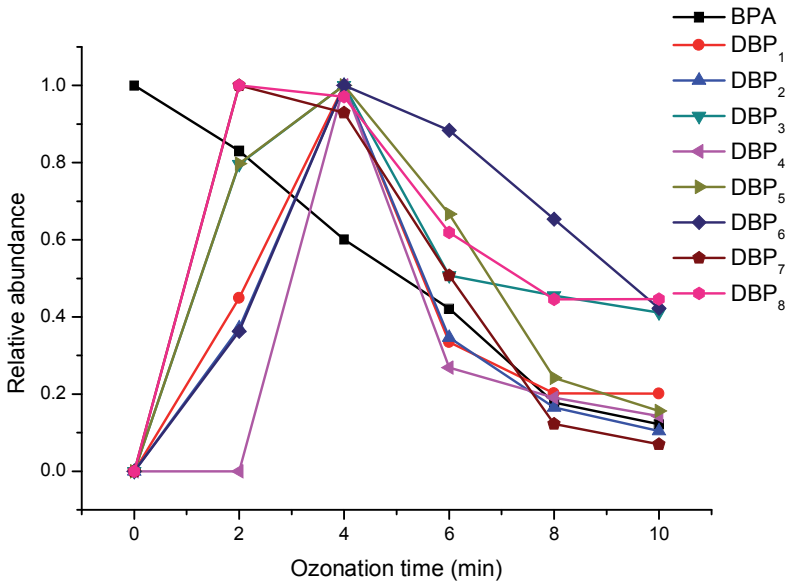

Figure 8. Time profiles of major BPA degradation by-products ($[BPA]_0$ = 100 mg/L, pH = 6.5, temperature = 25ºC, and O_3 dose = 0.69 g/h). Relative abundance of the degradation by-products was calculated by normalising the peak areas at the defined ozonation time to the highest peak areas.

Formation of Degradation By-Products

Formation of DBP_1, DBP_2, DBP_3, DBP_7 and DBP_8

Formation of DBP_7 and DBP_8 can occur through hydroxylation of BPA or via a direct reaction between BPA and O_3 (Figure 9). Hydroxylated BPA is proposed to be an important intermediate of by-products resulting from ring opening, especially DBP_4, DBP_5 and DBP_6. Formation of polyhydroxylated BPA through the reaction between BPA and •OH has also been reported during the degradation of BPA by ultrasound-UV-iron (II) treatment [17].

The formation of DBP_1, DBP_2 and DBP_3 are presented in Figure 9b. Since O_3 with its eletrophilic nature reacts selectively with an electron-rich reaction site, it is proposed that the reaction begins at the side chain of BPA with an initial attack of •OH via hydrogen abstraction and leads to the formation of radical *A*. Intramolecular rearrangement of radical *A* then leads to the cleavage of C-C bond to form DBP_1 (4-isopropenylphenol) and a phenol radical, *B*. *B* will then react with •OH to form DBP_2 (hydroquinone). DBP_1 can further react with either O_3 or •OH, leading to the formation of dihydroxylated DBP_1 (*C*). *C* would then react with •OH via hydrogen abstraction to form radical *D*, which undergoes a fragmentation to form DBP_3 (4-hydroxyacetophenone).

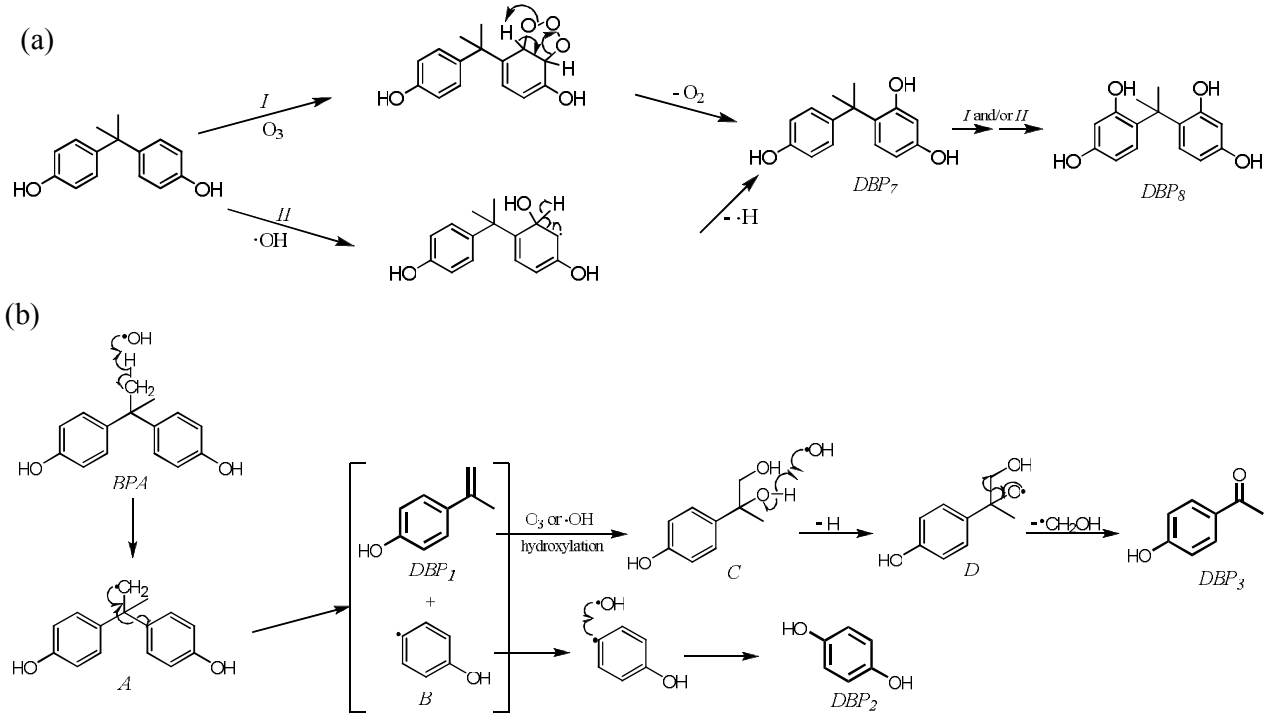

Figure 9. Proposed pathways for the formation of: (a) DBP_1, DBP_2 and DBP_3; (b) DBP_7 and DBP_8 from BPA during ozonation

Formation of DBP_4, DBP_5 and DBP_6

The formation pathway of DBP_4 is presented in Figure 10. The formation of DBP_6 is proposed to begin with the initial attack of •OH on the monohydroxylated BPA giving a radical intermediate (*F*) (Figure 11a). Intra-molecular rearrangement of *F* and cleavage of C-C bond lead to the opening of an aromatic ring, resulting in the formation of radical *G*, which then rearranges to form radical *H*, which reacts with water to form *I*. Attack of •OH at the enol site of *I* affords radical *J*, which gives radical *K* on cleavage of a C-C bond. Radical *K* further reacts with •OH to form *L*, which upon hydrogen abstraction gives radical *M*. *M* then further reacts with •OH leading to the formation of DBP_6. The formation pathway of DBP_5 is presented in Figure 11b.

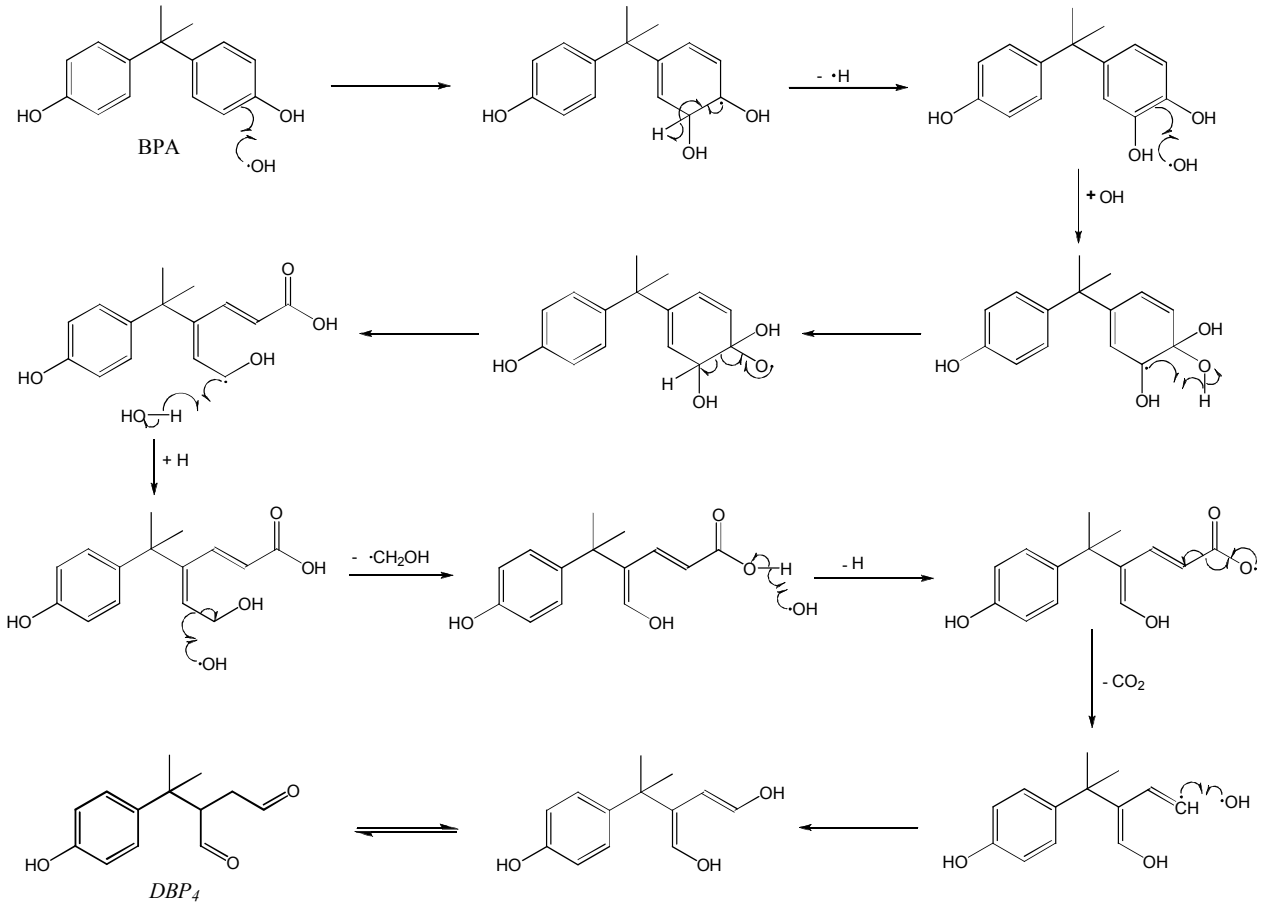

Figure 10. Proposed pathway for the formation of DBP_4

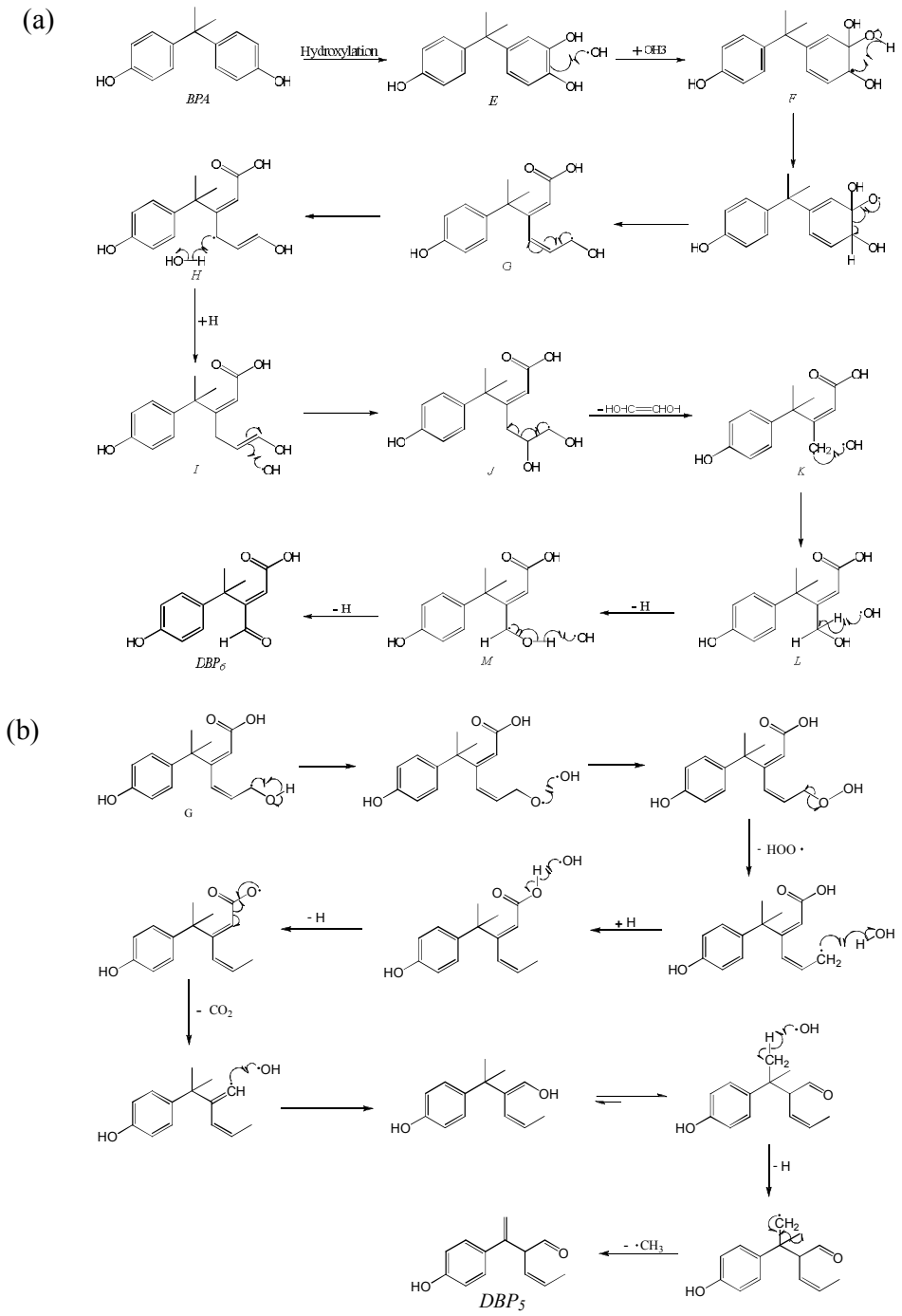

Figure 11. Proposed pathways for the formation of: (a) *DBP*$_5$ and (b) *DBP*$_6$

CONCLUSIONS

The rate constant for the reaction between BPA and ozone in aqueous solution in the presence of *t*-BuOH increased with increase in pH between pH 2-10, beyond which it was fairly constant between pH 10-12. The reactivity of BPA increased in the order: undissociated form < anionic form < dianionic form. The presence of common inorganic anions (chloride, sulphate, nitrate

and phosphate ions) at environmental levels did not significantly affect the rate of degradation of BPA by ozone.

The degradation products of BPA during ozonation were identified to be 4-(prop-1-en-2-yl)phenol, hydroquinone, 4-hydroxyacetophenone, 2-(2-(4-hydroxyphenyl)propan-2-yl)succinaldehyde, 2-(1-(4-hydroxyphenyl)vinyl)pent-2-enal, 3-formyl-4-(4-hydroxyphenyl)-4-methylpent-2-enoic acid, monohydroxy-BPA and dihydroxy-BPA.

ACKNOWLEDGEMENTS

This research was financially supported by Malaysia Toray Science Foundation (MTSF), University of Malaya (Grant No. P0266-2007A, SF025-2007A, PS153-2007B and FS305-2007C) and Ministry of Higher Education Malaysia (FRGS).

REFERENCES

1. Y. M. Lee, M. J. Seong, J. W. Lee, J. K. Lee, T. M. Kim, S. Y. Nam, D. J. Kim, Y. W. Yun, T. S. Kim, S.Y. Han and J. T. Hong, "Estrogen receptor independent neurotoxic mechanism of bisphenol A, an environmental estrogen", *J. Vet. Sci.*, **2007**, *8*, 27-38.
2. J. A. Brotons, M. F. Olea-Serrano, M. Villalobos, V. Pedraza and N. Olea, "Xenoestrogens released from lacquer coatings in food cans", *Environ. Health Perspect.*, **1995**, *103*, 608-612.
3. C. Dash, M. Marcus and P. D. Terry, "Bisphenol A: Do recent studies of health effects among humans inform the long-standing debate?", *Mutat. Res.*, **2006**, *613*, 68-75.
4. D. de A. Azevedo, S. Lacorte, P. Viana and D. Barceló, "Occurrence of nonylphenol and bisphenol-A in surface waters from Portugal", *J. Braz. Chem. Soc.*, **2001**, *12*, 532-537.
5. E. Z. Harrisson, S. R. Oakes, M. Hysell and A. Hay, "Organic chemicals in sewage sludges", *Sci. Total Environ.*, **2006**, *367*, 481-497.
6. S. Zhang, Q. Zhang, S. Darisaw, O. Ehie and G. Wang, "Simultaneous quantification of polycyclic aromatic hydrocarbons (PAHs), polychlorinated biphenyls (PCBs), and pharmaceuticals and personal care products (PPCPs) in Mississippi river water, in New Orleans, Louisiana, USA", *Chemosphere*, **2007**, *66*, 1057-1069.
7. C. Basheer, H. K. Lee and K. S. Tan, "Endocrine disrupting alkylphenols and bisphenol-A in coastal waters and supermaket seafood from Singapore", *Mar. Pollut. Bull.*, **2004**, *48*, 1161-1167.
8. T. Isobe, H. Takada, M. Kanai, S. Tsutsumi, K. O. Isobe, R. Boonyatumanond and M. P. Zakaria, "Distribution of polycyclic aromatic hydrocarbons (PAHs) and phenolic endocrine disrupting chemicals in South and Southeast Asian mussels", *Environ. Monit. Assess.*, **2007**, *135*, 423-440.
9. J. Lee, H. Park and J. Yoon, "Ozonation characteristics of bisphenol A in water", *Environ. Technol.*, **2003**, *24*, 241-248.
10. B. Xu, N. Gao, M. Rui, H. Wang and H. Wu, "Degradation of endocrine disruptor bisphenol A in drinking water by ozone oxidation", *Front. Environ. Sci. Eng. China*, **2007**, *1*, 350-356.
11. M. Deborde, S. Rabouan, P. Mazellier, J. P. Duguet and B. Legube, "Oxidation of bisphenol A by ozone in aqueous solution", *Water Res.*, **2008**, *42*, 4299-4308.

12. F. J. Rivas, Á. Encinas, B. Acedo and F. J. Beltrán, "Mineralization of bisphenol A by advanced oxidation processes", *J. Chem. Technol. Biotechnol.*, **2009**, *84*, 589-594.
13. I. Gultekin, M. Valko and H. I. Nilsun, "Degradation of bisphenol-A by ozonation", *J. Adv. Oxidat. Technol.*, **2009**, *12*, 242-248.
14. T. Garoma and S. Matsumoto, "Ozonation of aqueous solution containing bisphenol A: Effect of operational parameters", *J. Hazard Mater.*, **2009**, *167*, 1185-1191.
15. H. Katsumata, S. Kawabe, S. Kaneco, T. Suzuki and K. Ohta, "Degradation of bisphenol A in water by the photo-Fenton reaction", *J. Photochem. Photobiol. A*, **2004**, *162*, 297-305.
16. K. Nomiyama, T. Tanizaki, T. Koga, K. Arizono and R. Shinohara, "Oxidative degradation of BPA using TiO_2 in water, and transition of estrogenic activity in the degradation pathways", *Arch. Environ. Contam. Toxicol.*, **2007**, 52, 8-15.
17. R. A. Torres, C. Pétrier, E. Combet, F. Moulet and C. Pulgarin, "Bisphenol A mineralization by integrated ultrasound-UV-iron (II) treatment", *Environ. Sci. Technol.*, **2007**, *41*, 297-302.
18. J. Sowmya, "European emerging trends and technologies include UV, Ozone", Water and Waste Water International Magazine (April, **2008**), PennWell Publishing Corporation. (http://www.waterworld.com/index/display/article-display/329727/articles/water-wastewater-international/volume-23/issue-2/regional-focus/middle-east-north-africa/european-emerging-trends-amp-technologies-include-uv-ozone.html) (Accessed on 28th December 2011).
19. A. Conner, "Reducing cooling tower costs with ozone technology", CTI Bibliography of Technical Papers—Ozone, Cooling Technology Institute, **2005**, http://www.cti.org/tech_papers/ozone.php (Accessed on 28th December 2011).
20. M. M. Huber, S. Canonica, G. Y. Park and U. von Gunten, "Oxidation of pharmaceuticals during ozonation and advanced oxidation processes", *Environ. Sci. Technol.*, **2003**, *37*, 1016-1024.
21. F. J. Beltrán, "Ozone Reaction Kinetics for Water and Wastewater Systems", Lewis Publishers, Boca Raton, **2004**, pp.1-4.
22. K. Ikehata, N. J. Naghashkar and M. G. El-Din, "Degradation of aqueous pharmaceuticals by ozonation and advanced oxidation process: A review", *Ozone Sci. Eng.*, **2006**, *28*, 353-414.
23. S. A. Snyder, E. C. Wert, D. J. Rexing, R. E. Zegers and D. D. Drury, "Ozone oxidation of endocrine disruptors and pharmaceuticals in surface water and wastewater", *Ozone Sci. Eng.*, **2006**, *28*, 445-460.
24. S. Esplugas, D. M. Bila, L. G. Krause and M. Dezotti, "Ozonation and advanced oxidation technologies to remove endocrine disrupting chemicals (EDCs) and pharmaceuticals and personal care products (PPCPs) in water effluents", *J. Hazard Mater.*, **2007**, *149*, 631-642.
25. M. D. H. Guil, M. Petrović, J. Radjenovic, A. R. Fernández-Alba, A. R. Fernández-Alba and D. Barceló, "Removal of pharmaceuticals by advanced treatment technologies", in "Comprehensive Analytical Chemistry, Volume 50: Analysis, Fate and Removal of Pharmaceuticals in the Water Cycle", (Ed. M. Petrović and D. Barceló), Elsevier, Amsterdam, **2007**, pp.451-474.
26. J. Staehelin and J. Hoigné, "Decomposition of ozone in water in the presence of organic solutes acting as promoters and inhibitors of radical chain reactions", *Environ. Sci. Technol.*, **1985**, *19*, 1206-1213.
27. M. S. Siddiqui, "Chlorine-ozone interactions: Formation of chlorate", *Water Res.*, **1996**, *30*, 2160-2170.

28. M. A. Boncz, H. Bruning, W. H. Rulkens, H. Zuilhof and E. J. R. Sudhölter, "The effect of salts on ozone oxidation processes", *Ozone Sci. Eng.*, **2005**, *27*, 287-292.
29. K. S. Tay, N. A. Rahman and M. R. B. Abas, "Ozonation of parabens in aqueous solution: Kinetics and mechanism of degradation", *Chemosphere*, **2010**, *81*, 1446-1453.
30. H. Bader and J. Hoigné, "Determination of ozone in water by the indigo method", *Water Res.*, **1981**, *15*, 449-456.
31. K. S. Tay, N. A. Rahman and M. R. B. Abas, "Degradation of DEET by ozonation in aqueous solution", *Chemosphere*, **2009**, *76*, 1296-1302.
32. J. Hoigné and H. Bader, "Rate constants of reactions of ozone with organic and inorganic compounds in water – II: Dissociating organic compounds", *Water Res.*, *17*, 185-194.
33. K. S. Tay, N. A. Rahman and M. R. B. Abas, "Removal of selected endocrine disrupting chemicals and personal care products in surface waters and secondary wastewater by ozonation", *Water Environ. Res.*, **2011**, *83*, 684-691.
34. M. Deborde, S. Rabouan, J. P. Duguet and B. Legube, "Kinetics of aqueous ozone-induced oxidation of some endocrine disruptor", *Environ. Sci. Technol.*, **2005**, *39*, 6086-6092.
35. J. Benner, E. Salhi, T. Ternes and U. von Gunten, "Ozonation of reverse osmosis concentrate: Kinetics and efficiency of beta blocker oxidation", *Water Res.*, **2008**, *42*, 3003-3012.
36. F. J. Benitez, J. L. Acero, F. J. Real and G. Roldán, "Ozonation of pharmaceutical compounds: Rate constants and elimination in various water matrices", *Chemosphere*, **2009**, *77*, 53-59.
37. C. A. Staples, P. B. Dorn, G. M. Klecka, S. T. Oblock and L. R. Harris, "A review of the environmental fate, effects, and exposures of bisphenol A", *Chemosphere*, **1998**, *36*, 2149-2173.
38. C. Tian, J. T. Wang and X. L. Song, "Sediment-water interactions of bisphenol A under simulated marine conditions", *Water Air Soil Pollut.*, **2009**, *199*, 301-310.
39. J. C. Kotz, P. M. Treichel and J. R. Townsend "Chemistry and Chemical Reactivity", 7th Edn., Brooks/Cole, Belmont, **2010,** pp.810-859.
40. S. V. Karmarkar, "Analysis of wastewater for anionic and cationic nutrients by ion chromatography in a single run with sequential flow injection analysis", *J. Chromatogr. A*, **1999**, *850*, 303-309.
41. I. R. Santos, R. C. Costa, U. Freitas and G. Fillmann, "Influence of effluents from a wastewater treatment plant on nutrient distribution in a coastal creek from southern Brazil", *Braz. Arch. Biol. Technol.*, **2008**, *51*, 153-162.
42. O. A. Al-Khashman, "Chemical evaluation of Ma'an sewage effluents and its reuse in irrigation purpose", *Water Resour. Manage.*, **2009**, *23*, 1041-1053.
43. K. S. Tay, N. A. Rahman and M. R. B. Abas, "Characterization of atenolol transformation products in ozonation by using rapid resolution high-performance liquid chromatography/ quadrupole-time-of-flight mass spectrometry", *Microchem. J.*, **2011**, *99*, 312-326.

Maejo Int. J. Sci. Technol. **2012**, *6*(01), 95-104

Maejo International Journal of Science and Technology

ISSN 1905-7873
Available online at www.mijst.mju.ac.th

Full Paper

Chitinase production and antifungal potential of endophytic *Streptomyces* strain P4

Julaluk Tang-um and Hataichanoke Niamsup*

Department of Chemistry and Centre of Excellence for Innovation in Chemistry, Faculty of Science, Chiang Mai University, Chiang Mai 50200, Thailand

* Corresponding author, e-mail: hataichanoke.n@cmu.ac.th

Received: 2 August 2011 / Accepted: 11 February 2012 / Published: 29 February 2012

Abstract: The endophytic actinomycete P4 strain, previously isolated from sweet pea root, was identified as *Streptomyces* sp. by full 16S rRNA sequencing. It is mostly related to *Streptomyces griseoflavus* with a 99.7% identity score. The *Streptomyces* sp. P4 was tested for its hydrolytic activities by plate method. The result showed the presence of chitinase. The extent of chitinase activity was assessed by spectrophotometric method along with growth monitoring. Chitinase production was growth-associated and showed the highest activity on the fifth day. The dual culture method revealed that the strain was effective in restricting the radial growth of *Fusarium oxysporum* f.sp. *lycopersici*, an important phytopathogen of tomato. Scanning electronic microscopic analysis showed that the rupture of the *F. oxysporum* mycelial cell wall occurred at the area of interaction between *F. oxysporum* and *Streptomyces* sp. P4. This was possibly due to the chitinolytic activity of the P4. Thus, this actinomycete has the potential for being used as a biocontrol agent, thereby reducing the use of chemical fungicides.

Keywords: endophyte, streptomycete, chitinase, fusarium, wilt, antimicrobial activity

INTRODUCTION

As worldwide concern for the natural environment and human health has increased, so has interest in organic farming. A research institute of organic agriculture (FiBL) and the international federation of organic agriculture movements (IFOAM) reported that organic agricultural lands have expanded globally from 11.0 million hectares in 1999 to 37.2 million hectares in 2009, accounting for 0.85% of the total agricultural lands [1]. One of the criteria for organic farming is the avoidance of chemical usage. Soilborne plant diseases can be controlled through agronomic practices and microbial

biocontrol agents instead [2]. Biological controlling agents can replace chemical agents in controlling pathogenic insects, microbials and weeds. Several biofungicides are based on antibiotic metabolites and hydrolytic enzymes. For example, *Streptomyces griseoviridis* strain K61, a soilborne fungal antagonist which produces aromatic antibiotics with characteristic 7-membered rings in the molecules was commercialised as Mycostop® by Verdera Oy, a Finnish company [3], and *Streptomyces* sp. Di-944 was formulated to suppress Rhizoctonia damping-off [4].

Streptomyces is a major genus of actinimycetes, the Gram-positive terrestrial or marine bacteria found in both colony and mycelium forms. Although *Streptomyces* species with a characteristic earthy smell may be thought of as pathogens, the antibiotics that they produce have been profitably exploited [5]. For example, *S. clavuligerus* produces the β-lactam cephamycin C and clavulanic acid, a β-lactamase inhibitor. A new stereoisomeric anthracyclin with anticancer activity was isolated from *Sreptomyces* sp. Eg23 [6]. Various hydrolytic enzymes, e.g. proteases/peptidases, chitinases/chitosanases, cellulases/endoglucanases, amylases, and pectate lyases, are produced by *S. coelicolor* [7].

In this study, the hydrolytic enzyme production of the endophytic actinomycete P4 strain, previously isolated from sweet pea root [8], is investigated. Additionally, the potential use of this endophyte as a biocontrol agent is studied by assessing its antagonism against pathogenic fungi.

MATERIALS AND METHODS

Microorganism Strains and Growth Conditions

The bacterial strain P4, generously provided by Asst. Prof. Dr. Ampan Bhromsiri (Department of Soil Science and Conservation, Chiang Mai University) was previously isolated from sweet pea root. The bacteria was maintained at 30°C on an IMA-2 agar medium consisting of 5 g glucose, 5 g soluble starch, 1 g beef extract, 1 g yeast extract, 2 g N-Z-case®, 2 g NaCl and 1 g $CaCO_3$ per litre [9]. For the production of chitinase, the culture was transferred into a colloidal chitin medium, 1 litre of which consisted of 20 g colloidal chitin, 0.5 g yeast extract, 1 g $(NH_4)_2SO_4$, 0.3 g $MgSO_4 \cdot 7H_2O$ and 1.36 g KH_2PO_4, with an adjusted pH of 7.0 [10]. Colloidal chitin was prepared according to the method described by Souza et al. [11]. The liquid culture was incubated at 30°C with agitation at 160 revs/min.

The pathogenic fungi *Fusarium oxysporum f.*sp. *lycopersici*, *Corynespora cassiicola* and *Rhizoctonia solani* were obtained from the Department of Agriculture, the Ministry of Agriculture and Cooperatives (Thailand). They were maintained on potato-dextrose agar (PDA).

Identification by 16s rRNA Sequencing

An approximately 1.5-kb polymerase chain reaction (PCR) product was amplified from genomic DNA of the bacterial strain P4 using two primers, 20F (5'-GAG TTT GAT CCT GGC TCA G-3') and 1500R (5'-GTT ACC TTG TTA CGA CTT-3'), directed to the 16S rRNA region. The following conditions were used: an initial denaturation step at 94°C for 3 min., 25 cycles at 94°C (1 min.), 50°C (1 min.) and 72°C (2 min.), followed by a final extension at 72°C (3 min.). The purified PCR product was sequenced by an ABI PRISM® BigDye™ Terminator Ready Reaction Cycle Sequencing Kit (Applied Biosystems, USA) on an ABI Prism® 3730XL DNA Sequence (Applied Biosystems, USA). Homology was analysed using the BLAST program from the GenBank database [12].

Plate Screening of Hydrolytic Enzymes

The bacterial strain P4 (identified as *Streptomyces*) was screened for its capacity to produce hydrolytic enzymes using the plate method. The bacterium was allowed to grow at 30°C on nutrient agar plates supplemented with different substrates, i.e. colloidal chitin, gelatin, sodium carboxymethyl-cellulose and Tween20, for detection of chitinase, protease, cellulase and lipase respectively. The clear zone around the colonies observed after 7-14 days is an indication for enzyme production. In the cases of cellulase and protease, the plates were reacted with 0.2% Congo red and saturated $(NH_4)_2SO_4$ respectively prior to the observation of growth [13-14].

Quantification of Extracellular Chitinase Activity

The strain P4 was grown in a colloidal chitin medium broth at 30ºC with continuous shaking at 160 rpm. The supernatant fluid was harvested every two days for 17 days by filtration through Whatman no.1 filter. Chitinase activity in the supernatant was assayed using 0.6% colloidal chitin as a substrate and was based on a procedure by Taechowisan et al. [13]. The supernatant fluid (700 µl) was added with 2% colloidal chitin (300 µl) in 0.1M potassium phosphate buffer at pH 7.0, and the mixture was incubated in a water bath at 40ºC for 3 hr. One mL of Somogyi's reagent [15] was added and the reaction mixture was boiled at 100ºC for 10 min. and cooled to room temperature. Then Nelson's reagent (1 mL) was added and the mixture cooled to room temperature for 20 min. After centrifugation of the reaction mixture, the amount of N-acetyl glucosamine (GlcNAc) released in the supernatant was spectrophotometrically measured by the method of Somogyi-Nelson [15]. The method is based on the 520-nm absorbance given by a coloured complex formed between a copper-oxidised sugar and arsenomolybdate. One unit (U) of chitinase activity was defined as the amount of enzyme required to produce 1 µmol of reducing sugar per min. under the conditions of the experiment.

The cell growth was followed by measurement of the cells' dry weight. After removing the supernatant for chitinase assay, the cell pellet was dried in an oven at 80°C until a constant weight was obtained. All measurements were performed in triplicate.

In Vitro Antagonism Tests against Fungi

The identified *Streptomyces* P4 was evaluated for antagonistic activity towards three fungal phytopathogens, i.e. *F. oxysporum*, *C. cassiicola* and *R. solani*, by the dual culture method. An agar plug of 6 mm in diameter taken from a 7-day-old colony of each test fungus and that taken from a 14-day-old P4 bacterial strain were placed on PDA plates with 4-cm spacing (3 replicates each). The cultures were incubated at room temperature (30-32°C) and the diameters of the fungal colonies in the direction of the actinomycete were measured every 2 days for 14 days. The test fungi were grown alone to serve as control. Data were statistically analysed for significance ($p<0.05$) using the SPSS statistics 17.0 software.

Scanning Electronic Microscopic Analysis

A scanning electron microscope (SEM) (Model JSM-5910LV, Type LV, JEOL Ltd., Japan) was employed to monitor the effect of the *Streptomyces* P4 on the fungal cell walls. Fungal mycelia in a 14-day-old dual culture plate were taken from a free-growing area and a dual-growing area in the direction of the P4 strain. The two mycelial samples were pre-fixed with glutaraldehyde and post-fixed with

osmium tetroxide. After dehydration in ethanol, the samples were dried to their critical points with carbon dioxide [16], mounted on slides and coated with gold for observation by SEM.

RESULTS AND DISCUSSION

Identification of Bacterial Strain

A sequence of 1438-bp in length was obtained from the 1.5-kb PCR product. The DNA sequence was then submitted to GenBank database under accession no. JN102356 and was blasted against non-redundant DNA sequences in the database [12]. The 16S ribosomal DNA sequence showed the highest similarity to *Streptomyces griseoflavus* gene (accession no. EU741217) with a 99.7% identity score, followed by 99.5% score when aligned with *S. variabilis* (DQ442551, AB184884, AB184763), *S. vinaceus* (AB184186) and *S. griseoincarnatus* (AB184207, AJ781321). The P4 strain could not be definitely identified down to species level. It is worth noting that the 16S ribosomal RNA sequences are not highly variable among *Streptomyces* species and that *Streptomyces* systematics are rather complex. Lanoot et al. [17] suggested that 16S-ITS RFLP fingerprinting had a higher taxonomic resolution than 16S rDNA sequencing. A transformation reaction of progesterone has also been proposed for *Streptomyces* taxonomic classification [18].

S. griseoflavus was reported to produce many potent secondary metabolites, e.g. hormaomycin, a peptide lactone and a bacterial signalling metabolite and narrow-spectrum antibiotic [19]; okilactomycin, a polyketide antibiotic against gram-positive bacteria [20]; bicozamycin, a cyclic peptide antibiotic [21]; desferrioxamine, a precursor of iron chelator [22]; and an alkaline protease inhibitor [23]. However, there has been no report on the hydrolytic enzyme production in *S. griseoflavus*.

Chitinase Activity

From a preliminary screening of enzymes by the plant method (Figure 1), a clear zone surrounding the bacterial colonies was observed in the plate containing colloidal chitin as shown in Figure 1(A), indicating that the *Streptomyces* sp. P4 produced chitinase, whose activity was assayed during cell growth. Figure 2 shows that the activity was at a maximum on the fifth day, followed by a decrease upon approaching a stationary phase of growth. The findings imply that chitinase production is growth-associated. It should be noted that the *Streptomyces* sp. P4 strain had been pre-cultured in colloidal chitin medium prior to this experiment. As a consequence, the lag phase of growth was not observed, while logarithmic phase continued until the 5^{th} day before reaching a stationary phase.

This result of chitinase production of *Streptomyces* sp. P4, induced in a colloidal chitin-containing environment as previously reported [10, 24] and indicating growth-associated behaviour, is similar to that obtained from the study on *S. hygroscopicus* [25]. However chitinase production in *S. hygroscopicus* occurred 1-2 days before cell growth, while in our case chitinase production of *Streptomyces* sp. P4 was closely associated with cell growth, which should be because the pre-cultured and pre-induced bacteria were used in our experiment. Closely paralleling growth, the chitinolytic enzyme production by *Streptomyces* may be for the purpose of hydrolysing chitin into monosaccharides to be used as carbon and nitrogen sources [26]. However, the chitinase activity of 0.00093 U/mL in *Streptomyces* sp. P4, which corresponds to a specific activity of 0.050 U/mg protein, was 4 times lower than that in *S. viridificans* (0.0038 U/mL) [10]. In nature chitinase is produced by actinomycetes in order to degrade complex nutrients from the soil. As fungal cell walls and insect structures largely contain chitin, chitinase produced from endophytes can be deleterious to pathogens and pests [27-28].

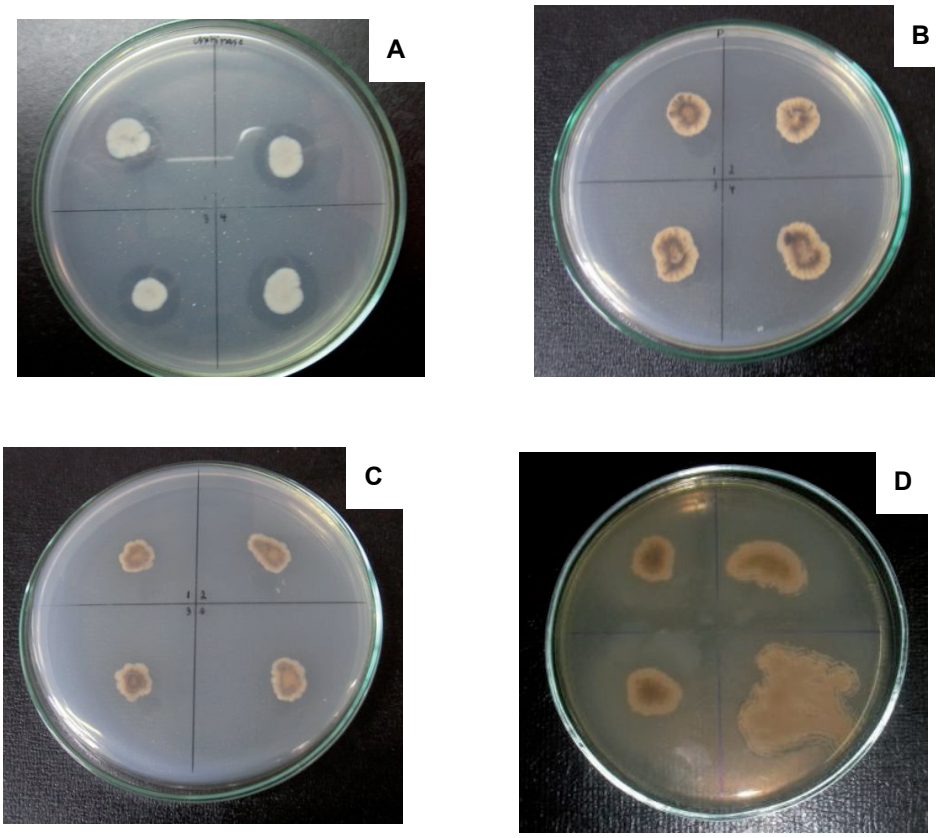

Figure 1. Plate screening tests for hydrolytic enzyme production of *Streptomyces* sp. P4. Agar plates contain the corresponding substrates for chitinase (A), protease (B), cellulase (C) and lipase (D). Each plate represents a duplicate experiment.

Antifungal Activity

The results in Figures 3-4 show that *Streptomyces* sp. P4 could effectively suppress the growth of *Fusarium oxysporum f.*sp. *lycopersici,* a fungus causing Fusarium wilt, a severe disease in tomato [29]. Maximal inhibition was observed on the 9th day with 12.50% inhibition (Figure 3). The radial growth diameter of *F. oxysporum* when grown on the same plate as *Streptomyces* sp. P4 (5.37±0.23 cm) was statistically smaller than that when cultured alone (6.13±0.38 cm). However, *Streptomyces* sp. P4 did not suppress the growth of the other two tested fungi, i.e. *Corynesopra cassiicola* (which causes leaf spot [30]) and *Rhizoctonia solani* (which causes root rot [31]) during the 14 days of observation (Figure 3). Anitha and Rabeeth [28] also reported the different responses of fungi to *S. griseus* chitinase. They suggested that the protein composition in the cell walls of different pathogenic fungi might make some fungal cell walls more resistant to chitinolytic degradation. Thus, only the co-culture containing *F. oxysporum* and *Streptomyces* sp. P4 was selected for SEM experiment.

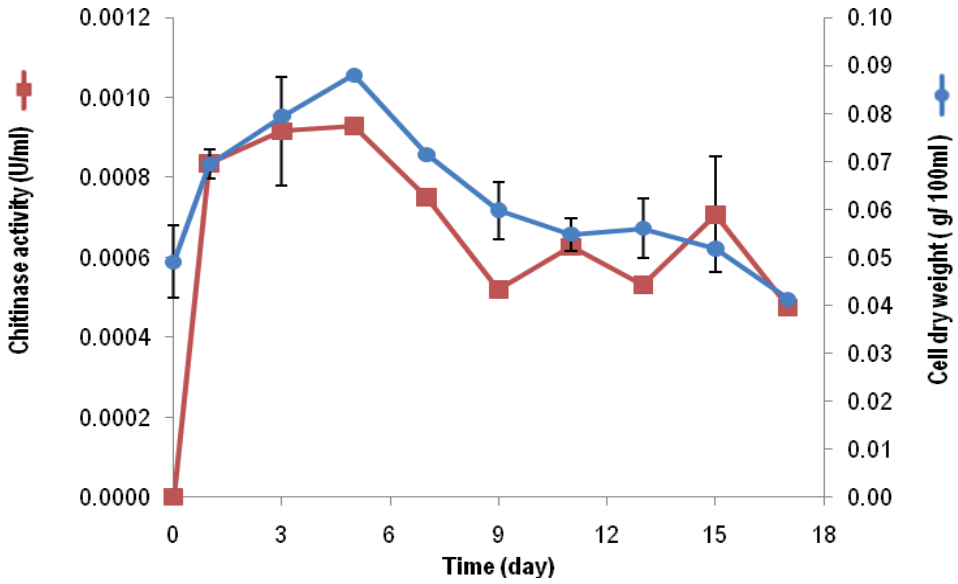

Figure 2. Chitinase activity and cell dry weight during the growth of *Streptomyces* sp. P4 . Error bars represent the standard deviation of 3 replicates.

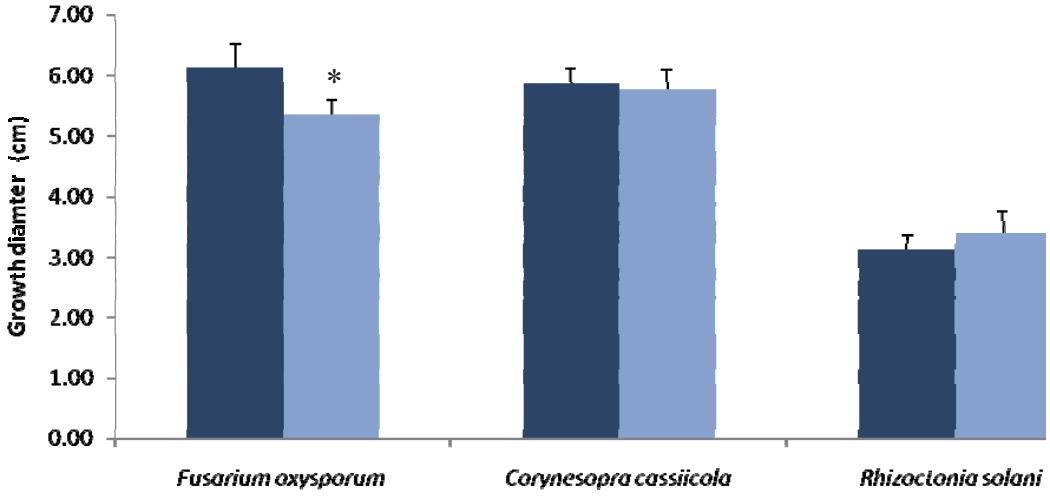

Figure 3. In vitro inhibitory activity of *Streptomyces* sp. P4 against three fungi: *Fusarium oxysporum f.*sp. *lycopersici*, *Corynesopra cassiicola* and *Rhizoctonia solani*. Dark blue and light blue bars correspond to radial growth diameters of the fungi cultured alone (control) and co-cultured with *Streptomyces* sp. P4 (dual culture) respectively on the 9th day of growth on PDA plates. Error bars represent standard deviation of 3 replicates. The asterisk indicates that the value differs significantly from control (p<0.05).

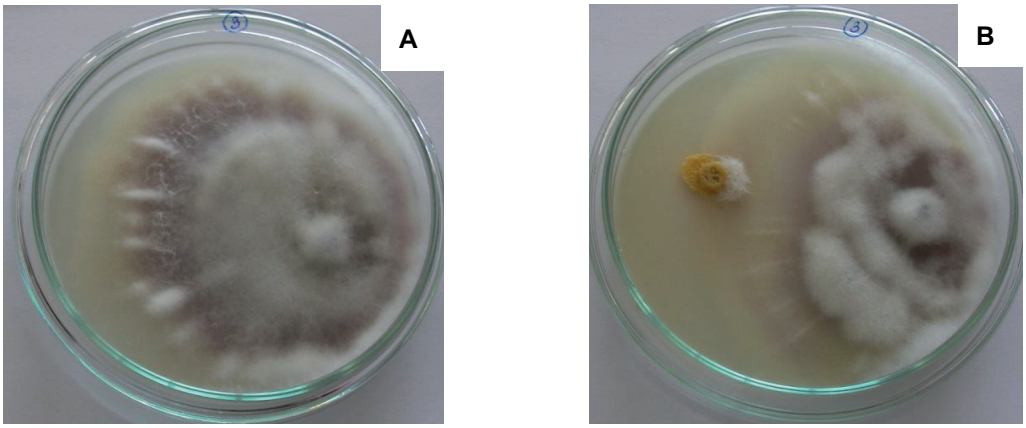

Figure 4. Growth of *Fusarium oxysporum f.*sp. *lycopersici* grown alone (A) and co-cultured with *Streptomyces* sp. P4 (B) on PDA for 14 days

Results obtained from SEM showed the breakage of the cell walls of *F. oxysporum* mycelia growing towards *Streptomyces* sp. P4 (Figure 5B) as compared to a control region (Figure 5A). The findings suggest that extracellular secondary metabolites and/or hydrolytic enzymes including chitinase play a crucial role in fungal growth inhibition. Prapagdee et al. [25] reported that the antifungal activity of *S. hygroscopicus* during exponential growth was mainly due to hydrolytic enzymes, while in the stationary phase it was due to secondary thermostable compound(s). In addition, there was a report on a positive correlation between chitinolytic and antagonistic activities of *Streptomyces* against the fungi *Collectotrichum sublineolum, Guignardia citricarpa, Rhizoctonia solani* and *Fusarium oxysporum*, but not in the oomycetes *Pythium* sp. and *Phytophthora parasitica*, which contain cellulose as a major cell wall component [16].

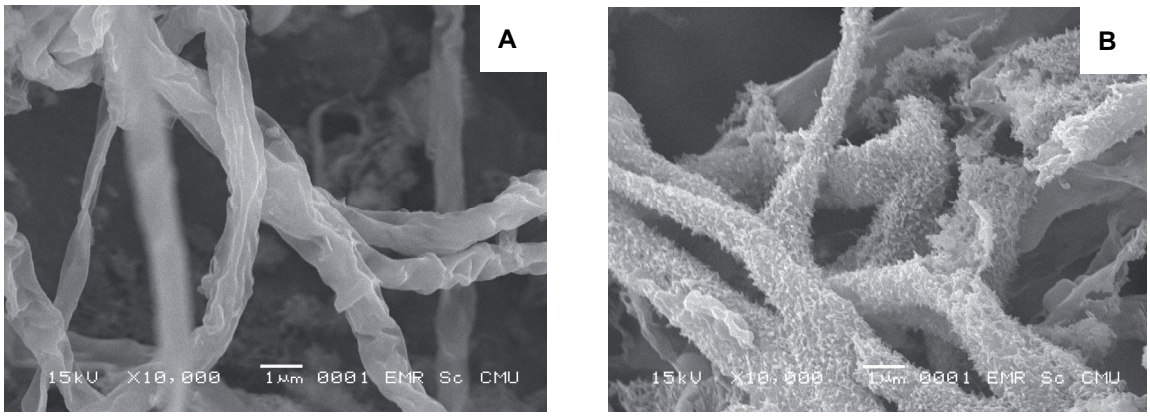

Figure 5. Scanning electron microscopic analysis of *Fusarium oxysporum f.*sp. *lycopersici* grown alone (A) and co-cultured with *Streptomyces* sp. P4 (B). Bars indicate 1 µm.

CONCLUSIONS

The present study provides background information for the potential use of the endophytic *Streptomyces* sp. P4 strain as a biocontrol agent antagonistic to specific fungi. The chitinase production and its association with the growth of *Streptomyces* sp. P4 were demonstrated. The fungal growth inhibition of *F. oxysporum f.*sp. *lycopersici* by *Streptomyces* sp. P4 was observed and demonstrated to result from the disruption of the fungal cell walls.

ACKNOWLEDGEMENTS

This work was financially supported by the Centre of Excellence for Innovation in Chemistry (PERCH-CIC), Lanna Products Company and the Graduate School of Chiang Mai University. We thank S. Chantal E. Stieber (Department of Chemistry and Chemical Biology, Cornell University) for critical reading of the manuscript.

REFERENCES

1. H. Willer and L. Kilcher (Eds.), "The world of organic agriculture–statistics and emerging trends 2011", IFOAM and FiBL, **2011**, http://www.organic-world.net/ (Accessed: 1 August 2011).
2. M. Shoda, "Bacterial control of plant diseases", *J. Biosci. Bioeng.*, **2000**, *89*, 515-521.
3. D. R. Fravel, "Commercialization and implementation of biocontrol", *Annu. Rev. Phytopathol.*, **2005**, *43*, 337-359.
4. S. Sabaratnam and J. A. Traquair, "Formulation of a *Streptomyces* biocontrol agent for the suppression of Rhizoctonia damping-off in tomato transplants", *Biol. Control*, **2002**, *23*, 245-253.
5. G. Sykes and F. A. Skinner, "Actinomycetales: Characteristics and Practical Importance", Academic Press, London, **1973**, pp.64-75.
6. M. S. Abdelfattah, "Screening of terrestrial *Streptomyces* leading to identification of new stereoisomeric anthracyclines", *World J. Microbiol. Biotechnol.,* **2008**, *24*, 2619-2625.
7. P. Dyson, "*Streptomyces*", in "Encyclopedia of Microbiology" (Ed. M. Schaechter), 3rd Edn., Academic press, London, **2009**, pp.318-332.
8. P. Thapanapongworakul, "Characterization of endophytic actinomycetes capable of controlling sweet pea root rot diseases and effect on root nodule bacteria", MS Thesis, **2003**, Chiang Mai University, Thailand.
9. M. Shimizu, Y. Nakagawa, Y. Sato, T. Furumai, Y. Igarashi, H. Onaka, R. Yoshida and H. Kunoh, "Studies on endophytic Actinomycetes (I) *Streptomyces* sp. isolated from rhododendron and its antifungal activity", *J. Gen. Plant Pathol.*, **2000**, *66*, 360-366.
10. R. Gupta, R. K. Saxena, P. Chaturvedi and J. S. Virdi, "Chitinase production by *Streptomyces viridificans*: Its potential in fungal cell wall lysis", *J. Appl. Bacteriol.*, **1995**, *78*, 378-383.
11. C. P. Souza, E. M. Burbano-Rosero, B. C. Almeida, G. G. Martins, L. S. Albertini and I. N. G. Rivera, "Culture medium for isolating chitinolytic bacteria from seawater and plankton", *World J. Microbiol. Biotechnol.*, **2009**, *25*, 2079-2082.
12. D. A. Benson. I. Karsch-Mizrachi, D. J. Lipman, J. Ostell and E.W. Sayers, "GenBank", *Nucleic Acids Res.*, **2011**, *39* (Database issue), D32-37.

13. T. Taechowisan, J. F. Peberdy and S. Lumyong, "Chitinase production by endophytic *Streptomyces aureofaciens* CMU Ac 130 and its antagonism against phytopathogenic fungi", *Ann. Microbiol.*, **2003**, *53*, 447-461.
14. G. L. Maria, K. R. Sridhar and N. S. Raviraja, "Antimicrobial and enzyme activity of mangrove endophytic fungi of southwest coast of India", *J. Agric. Technol.*, **2005**, *1*, 67-80.
15. F. Green, C. A. Clausen and T. L. Highley, "Adaptation of the Nelson-Somogyi reducing-sugar assay to a microassay using microtiter plates", *Anal. Biochem.,* **1989**, *182*, 197-199.
16. M. C. Quecine, W. L. Araujo, J. Marcon, C. S. Gai, J. L. Azevedo and A. A. Pizzirani-Kleiner, "Chitinolytic activity of endophytic *Streptomyces* and potential for biocontrol", *Lett. Appl. Microbiol.*, **2008**, *47*, 486-491.
17. B. Lanoot, M. Vancanneyt, B. Hoste, K. Vandemeulebroecke, M. C. Cnockaert, P. Dawyndt, Z. Liu, Y. Huang and J. Swings, "Grouping of *Streptomycetes* using 16S-ITS RFLP fingerprinting", *Res. Microbiol.*, **2005**, *156*, 755-762.
18. F. M. Atta and A. A. Zohri, "Transformation reactions of progesterone by different species of *Streptomyces*", *J. Basic Microbiol.,* **1995**, *35*, 3-7.
19. I. Höfer, M. Crüsemann, M. Radzom, B. Geers, D. Flachshaar, X. Cai, A. Zeeck and J. Piel, "Insights into the biosynthesis of hormaomycin, an exceptionally complex bacterial signaling metabolite", *Chem. Biol.*, **2011**, *18*, 381-391.
20. H. Imai, A. Nakagawa and S. Omura, "Biosynthesis of the antibiotic okilactomycin", *J. Antibiot.*, **1989**, *42*, 1321-1323.
21. K. Ochi, Y. Tsurumi, N. Shigematsu, M. Iwami, K. Umeharaand and M. Okuhara, "Physiological analysis of bicozamycin high-producing *Streptomyces griseoflavus* used at industrial level", *J. Antibiot.*, **1988**, *41*, 1106-1115.
22. R. Nazari, A. Akbarzadeh, D. Norouzian, B. Farahmand, J. Vaez, A. Sadegi, F. Hormozi, M. Kiani-Rad and B. Zarbaksh, "Applying intra-specific protoplast fusion in *Streptomyces griseoflavus* to increase the production of desferrioxamine B", *Curr. Sci.*, **2005**, *88*, 1815-1820.
23. A. Kuramoto, A. Lezhava, S. Taguchi, H. Momose and H. Kinashi, "The location and deletion of the genes which code for SSI-like protease inhibitors in *Streptomyces* species", *FEMS Microbiol. Lett.*, **1996**, *139*, 37-42.
24. B. Mahadevan and D. L. Crawford, "Properties of the chitinase of the antifungal biocontrol agent *Streptomyces lydicus* WYEC108", *Enzyme Microb. Technol.*, **1997**, *20*, 489-493.
25. B. Prapagdee, C. Kuekulvong and S. Mongkolsuk, "Antifungal potential of extracellular metabolites produced by *Streptomyces hygroscopicus* against phytopathogenic fungi", *Int. J. Biol. Sci.*, **2008**, *4*, 330-337.
26. M. Charpentier and F. Percheron, "The chitin-degrading enzyme system of a *Streptomyces* species", *Int. J. Biochem.,* **1983**, *15*, 289-292.
27. N. Dahiya, R. Tewari and G. S. Hoondal, "Biotechnological aspects of chitinolytic enzyme: A review", *Appl. Microbiol. Biotechnol.*, **2006**, *71*, 773-782.
28. A. Anitha and M. Rabeeth, "Degradation of fungal cell walls of phytopathogenic fungi by lytic enzyme of *Streptomyces griseus*", *Afr. J. Plant Sci.*, **2010**, *4,* 61-66.
29. A. Anitha and M. Rabeeth, "Control of fusarium wilt of tomato by bioformulation of *Streptomyces griseus* in green house condition", *Afr. J. Basic Appl. Sci.,* **2009**, *1,* 9-10.

30. S. Kurt, "Genetic variation in *Corynesopra cassiicola*, the target leaf spot pathogen", *Pakistan J. Biol. Sci.,* **2005**, *8,* 618-621.
31. K. L. Olmos, S. H. Delgado and N. M. Pérez, "AFLP fingerprinting for identification of anastomosis groups of *Rhizoctonia solani* Kühn from common bean (*Phaseolus vulgaris* L.) in Mexico", *Rev. Mexicana Fitopatol.*, **2005**, *23,* 147-151.

Maejo Int. J. Sci. Technol. **2012**, *6*(01), 105-118

Maejo International Journal of Science and Technology

ISSN 1905-7873
Available online at www.mijst.mju.ac.th

Full Paper

Water quality variation and algal succession in commercial hybrid catfish production ponds

Chatree Wirasith [1,2] and Siripen Traichaiyaporn [3,*]

[1] Program of Environmental Science, Department of Biology, Faculty of Science, Chiang Mai University, Chiang Mai 50200, Thailand
[2] Program of Fisheries, Faculty of Agricultural Technology and Agro-Industry, Rajamangala University of Technology, Suvarnabhumi, Ayutthaya 13000, Thailand
[3] Department of Biology, Faculty of Science, Chiang Mai University, Chiang Mai 50200, Thailand

* Corresponding author, e-mail: tsiripen@yahoo.com

Received: 8 October 2011 / Accepted: 23 March 2012 / Published: 30 March 2012

Abstract: This study on water quality variation and algal succession in commercial hybrid catfish production ponds was conducted in 2007 in Bang Pa-In district, Ayutthaya province, Thailand. The study covered two fish crops, May-August and September-December. The physico-chemical water quality in the catfish ponds changed dramatically over the study period due to the practices of water changing, lime application and the culture duration before harvesting. Samples of algae collected during the first crop period contained 83 species belonging to the following divisions: Chlorophyta (34 species), Cyanophyta (28 species), Euglenophyta (12 species), Bacillariophyta (6 species), Chrysophyta (1 species), Pyrrhophyta (1 species) and Cryptophyta (1 species). Samples collected during the second crop contained 60 species of the following divisions: Chlorophyta (28 species), Cyanophyta (16 species), Euglenophyta (10 species) and Bacillariophyta (6 species). Cyanophyta was the most abundant in both crops, followed by Chlorophyta, Euglenophyta, Bacillariophyta, Chrysophyta, Cryptophyta and Pyrrhophyta. The blue-green algae *Microcystis* increasingly dominated the algal population during the course of the culture period. *Pseudanabaena* spp. were succeeded by *Oscillatoria* spp. and then *Microcystis* spp. in the first crop. *Microcystis* spp. dominated during the first two months of the second crop, and then was succeeded by *Planktolyngbya* spp. and *Nitzschia* spp. in the third and fourth months. In summary, water quality may account for algal proliferation resulting in algal blooms and influence algal succession in commercial catfish production ponds.

Keywords: water quality, algal succession, commercial production pond, hybrid catfish

INTRODUCTION

Hybrid catfish, the offspring of *Clarias macrocephalus* crossed with *Clarias gariepinus*, is among the most popular freshwater fish cultured commercially in South-east Asia, especially in Thailand [1]. In 2006, the production of this hybrid catfish in Thailand was estimated at 149,000 tons and valued at about 4,998.9 million Baht [2]. Since they are air breathers, hybrid catfish can be pond-cultured at extremely high density, up to 100 fish/m^2, with production reaching up to 100 tons/ha [1]. However, the off-flavour in the flesh of cultured catfish can be a problem, leading to market value reduction and/or making the fish unmarketable for a certain period of time, from a few days to weeks [3]. The off-flavour problem in cultured catfish is caused by compounds produced by certain kinds of blue-green algae, which are absorbed by the catfish and impart a bad flavour to the flesh if the harvest is delayed [4]. These blue-green algae can be found growing in catfish production ponds where an excessive amount of waste nutrients are generated. High density of the fish stocks and intensive feed input can result in extreme quantities of waste nutrients entering the production pond, which may account for the algal proliferation and resulting algal blooms [5]. Catfish cultured entirely and intensively in production ponds are commonly fed with pellet feed, trash fish and ground chicken skeletons and offal. Although the water in the production pond is normally changed completely during each production cycle of about 120-150 days, such feeding nevertheless causes a general deterioration of water quality and a decrease in dissolved oxygen in the pond water [6]. Low water quality also influences fish growth. In addition, the wastewater effluent from hybrid catfish production ponds can contain concentrated algal compounds and nutrients with a high nitrogen content, making it unsuitable for other profitable uses such as the culturing of other aquatic animals [7–9].

The seasonal succession of nutrients and phytoplankton populations in temperate and tropical systems has been extensively documented [10,11]. In tropical shallow water systems the roles of wet/dry seasons and wind typically have a greater impact on phytoplankton biomass production than inter-seasonal variations [12]. However, many other different types of algae prevailing in other climates also exhibit these wide swings in population densities. Some possible causes of these fluctuations include changes in temperature, pH, carbon dioxide, light intensity, nutrient concentration and the release of toxins by other organisms including competing algae [3]. Inthamjit et al. [9] reported a significant change in water quality during intensive culturing of hybrid catfish, where the value ranges of the parameters contributing to water quality were: dissolved oxygen (DO), 4.8-30.8 mg/L; biochemical oxygen demand (BOD), 24-90 mg/L; chemical oxygen demand (COD), 62-330 mg/L; chlorophyll a, 218-1,908 µg/L; total suspended solids (TSS), 378-1,490 mg/L; ammonia-nitrogen (NH_3-N), 0.003-0.270 mg/L; nitrate-nitrogen (NO_3^--N), 0.00-0.06 mg/L; nitrite-nitrogen (NO_2^--N), 0.01-0.03 mg/L; total phosphorus (TP), 1.50-5.81 mg/L; orthophosphate phosphorus (PO_4^{3-}-P), 0.00-2.11 mg/L; alkalinity, 91-388 mg/L; hardness (as $CaCO_3$), 300-580 mg/L; electrical conductivity, 800-1,900 µS/cm; and pH, 6.7-7.8. Stephens and Farris [13] compared the water quality from two channel catfish farms near Paragould, Arkansas (USA) during the summer of 2001 and found the following values: DO, 8.3 and 9.6 mg/L; chlorophyll a, 62 and 143 mg/L; TSS, 102 and 81 mg/L; NH_3-N, 0.16 and 0.16 mg/L; NO_3^--N, <0.005 and <0.005 mg/L; NO2¯N, <0.81 and <0.001 mg/L; phosphorus (as soluble reactive

phosphorus (SRP)), 1.188 and 2.38 mg/L; alkalinity, 118 and 167 mg/L; hardness, 93 and 192 mg/L; conductivity, 303 and 354 µS/cm; pH, 9.0 and 8.9; water temperature, 23 and 29 ºC; and fecal coliform bacteria, 603 and 433 CFU/100 mL.

In Thailand, Ayutthaya province has many commercial hybrid catfish farms. Geographically, the province is mainly a lowland plain situated in the Chao Phraya River basin of central Thailand, where the soil is highly fertile and water is readily available year-round. Because of these natural advantages, the province is an important farming area for many other types of fish in addition to hybrid catfish. Based on Thailand's fisheries statistics in 2005 [2], Ayutthaya, with a total land area of 2,412.8 ha, has a total of 3,623 farms engaged in pisciculture with a total yield of 2,176 tons. In Bang Pa-In district of the province (Figure 1) where this study was conducted, various forms of fish culture are practiced, including extensive, semi-intensive, intensive and integrated fish culture. For commercial hybrid catfish farming in this area, most of the culture are intensive systems.

This study investigated the variations of water quality in terms of physical, chemical and biological aspects, as well as the succession of algae in commercial hybrid catfish production ponds.

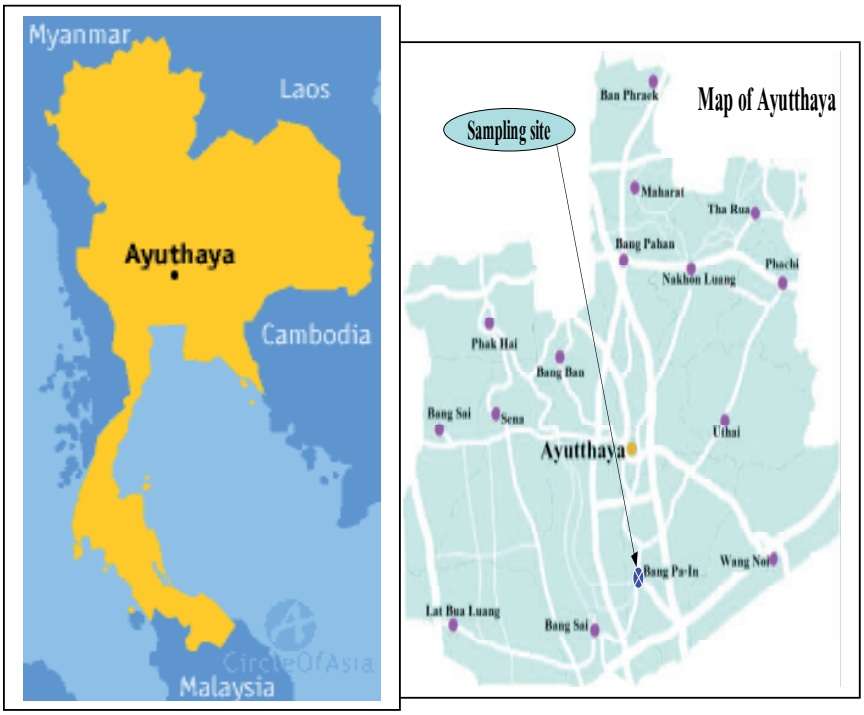

Figure 1. Map of Thailand and location of the study area in Phra Nakhon, Sri Ayutthaya province

MATERIALS AND METHODS

Study Area

The study area selected, Bang Pa-In district of Ayutthaya province (Figure 1), has a total land area of 488.8 ha, where 873 farmers were involved in fish culture [14]. Early in 2007, a field survey was conducted in the district. Three hybrid catfish farms, which were located near to one another and

which practiced similar fish culture systems, were selected as the sampling sites for this study. The study duration covered two fish crops in 2007, with the first crop from May to August and the second from September to December. Three replicates of water samples were collected monthly from the hybrid catfish production ponds at the three selected fish farms. In keeping with standard industrial practice for the culture of hybrid catfish, farmers released fingerlings into the production ponds (each 0.08 ha in size) at a density of 50 fingerlings/m2. The fingerlings were fed twice a day between 8-9 a.m. and 5-6 p.m. with pellet feed during the first and second months. Then during the third and fourth months they were fed chicken offal mixed with cassava chips in a ratio of 95:5. Water changing and lime application were carried out occasionally to manage water quality in the production ponds. The fish were cultured for 120-130 days before being harvested. The average fish yields were 59.38 tons/ha and 57.50 tons/ha for the first and second crops respectively, with the food conversion rate reaching 3.8-4.2.

Physico-Chemical Water Quality Analysis

Three replicates of water samples were collected monthly from the production ponds during both fish crops: May-August and September-December, 2007. All water samples were collected at a depth of 0.3-0.4 m and then preserved in an icebox until further processing. Water temperature, pH and DO were measured in situ using a portable hand-held meter (Multi 350i; WTW, Germany). Water transparency and water depth were measured using a Secchi disk and a measuring tape respectively. The analyses of chemical parameters were then carried out using suitable methods [15-16]: BOD by azide modification method; NH_3-N by Nesslerisation method; NO_3^--N by phenoldisulphonic acid method; total Kjeldahl nitrogen (TKN) by macro-Kjeldahl method; total phosphate by persulphate digestion/stannous chloride method; and orthophosphate phosphorus (PO_4^{3-}-P) by stannous chloride method.

Algal Analysis

For the algae count, the water sample (500 mL) from each production pond was transferred to a 500-mL cylinder and fixed with 5 mL of Lugol's solution (20 g glacial acetic acid, 20 g potassium iodide and 20 g iodine dissolved in 200 mL distilled water). The preserved sample was left to stand in the dark for 10 days to allow concentration by decantation. A 20-25 mL sample from the lower layer of the 500-mL cylinder, containing the sedimented algae, was obtained and transferred to a 50-mL cylinder. A second decantation was conducted after another 7 days in the dark; a 10-mL sample from the lower layer of the 50-mL cylinder, containing the sedimented algae, was put into a glass vial and stored in a dark cupboard [17]. This concentrated sample of algae was used for their identification [18-22] and counting under a compound light microscope [17].

Statistical Analysis

Collected data were statistically analysed using SPSS software program, version 14. Differences in means of water quality and algal population were established using analysis of variance (ANOVA), and relationships between algae and water quality parameters were tested using Pearson product-moment correlation. The level of significance was set at 0.05.

RESULTS AND DISCUSSION

Water Quality

Water quality based on physico-chemical and biological parameters from production ponds at all three sampling sites and for both fish crops is presented in Table 1. The temperature optimum for aquaculture in Thailand is between 25-33ºC, depending on the species of fish being cultured; at temperatures above or below the optimum, fish growth is reduced [23]. There was a significant difference in temperature between the two study crops and a marked decline during the 4th month (December) for the second crop. The optimal water transparency for aquaculture is 30 cm [24]. Water transparency in the study ponds ranged between 2.3-25.5 cm for the first fish crop and 1.1-10.3 cm for the second crop—a significant difference between the two crops. There was no significant difference in water depth between the two crops.

The optimal pH range for water used in aquaculture is between 6.5-8.5; however this will vary slightly depending on the cultured species [25]. Ingthamjit et al.[9] reported a pH range of 6.8-7.9 in hybrid catfish production ponds. The pH in the study ponds ranged between 6.6-7.1 for the first fish crop and 6.7-7.4 for the second crop. Generally, it is recommended that alkalinity be maintained within 50-300 mg/L to provide a sufficient buffering (stabilising) effect against pH swings that occur in ponds due to the respiration of the aquatic flora [25, 26]. Alkalinity in the study ponds ranged between 115.7-145.7 mg/L and 114.4-160.0 mg/L in the first and second fish crops respectively, thus displaying a significant difference.

DO is probably the most critical water quality variable in freshwater aquaculture ponds. To achieve optimal growth, a good rule of thumb is to maintain the DO level at saturation or at least 5 mg/L [25, 26]. The ranges of DO values in the study ponds were between 0.8-4.8 mg/L during the first fish crop and 1.5-4.3 mg/L during the second crop, with a significant difference in the 4th-month values of the two study crops. Also, in the 4th month, BOD reached 78.3 and 85.8 mg/L for the first and second fish crops respectively. These values were significantly different from the 1st- and 2nd-month values for both fish crops.

According to a study by Boyd [26] on unfertilised woodland ponds in Alabama, the average total NH_3-N (NH_4^+ plus NH_3 expressed in terms of N) was 0.052 mg/L and and that for NO_3^--N was 0.075 mg/L. In intensive fish culture ponds, much higher concentrations of inorganic N are common. Channel catfish culture ponds can contain up to 0.5 mg/L of total NH_3-N and 0.25 mg/L of NO_3^--N [26]. NH_3-N concentrations in the study ponds showed no significant difference between the first and second fish crops (0.06-1.77 mg/L). NO_3^--N concentrations varied between 0.01-0.24 mg/L and 0.02-0.03 mg/L for the first and second fish crops respectively, a significant difference being found between the 1st and 4th months of the first crop. Nitrogen is also present as soluble organic compounds and as constituents of living and dead particulate organic matter. Concentrations of organic nitrogen are usually well below 1 mg/L in unpolluted natural water [26]. In fish production ponds, phytoplankton blooms are normally heavy and the concentration of organic nitrogen may exceed 2-3 mg/L. In the study ponds, the TKN concentration reached a maximum level (5.6 mg/L) in the 4th month of the second fish crop.

Table 1. Monthly means and standard deviations (mean ± SD) of physico-chemical characteristics of water samples from commercial hybrid catfish production ponds, Ayutthaya province, Thailand, 2007

Parameter	Month							
	Crop 1 (mean ± SD)				Crop 2 (mean ± SD)			
	May	June	July	August	September	October	November	December
Water temperature (ºC)	$29.4^{a} \pm 0.1$	$31.8^{a} \pm 0.1$	$31.0^{a} \pm 0.1$	$30.8^{a} \pm 0.1$	$29.0^{b} \pm 0.1$	$28.8^{b} \pm 0.1$	$28.4^{b} \pm 0.1$	$27.5^{b} \pm 0.3$
Water transparency (cm)	$25.5^{a} \pm 0.1$	$10.4^{a} \pm 0.9$	$5.7^{a} \pm 0.8$	$2.3^{a} \pm 0.2$	$10.3^{b} \pm 0.3$	$5.5^{b} \pm 0.9$	$1.7^{b} \pm 0.2$	$1.1^{b} \pm 0.1$
Water depth (m)	1.25 ± 0.1	1.25 ± 0.1	1.25 ± 0.1	1.25 ± 0.1	1.25 ± 0.1	1.25 ± 0.1	1.25 ± 0.1	1.00 ± 0.2
pH	6.7 ± 0.1	$7.1^{a} \pm 0.2$	6.6 ± 0.1	$7.0^{b} \pm 0.1$	6.7 ± 0.1	$6.7^{b} \pm 0.1$	6.7 ± 0.1	$7.4^{a} \pm 0.2$
Alkalinity as $CaCO_3$ (mg/L)	$145.7^{a} \pm 5.1$	$140.0^{a} \pm 3.0$	$123.7^{b} \pm 3.5$	$115.7^{b} \pm 2.1$	$121.1^{b} \pm 3.9$	$114.4^{b} \pm 1.9$	$151.0^{a} \pm 3.6$	$160.0^{a} \pm 1.7$
DO (mg/L)	4.8 ± 0.6	3.2± 0.9	2.6 ± 0.4	$0.8^{b} \pm 0.2$	4.3 ± 0.4	3.5 ± 0.3	2.4 ± 0.5	$1.5^{a} \pm 0.3$
BOD (mg/L)	$24.2^{b} \pm 1.4$	$38.2^{b} \pm 2.8$	65.1 ± 6.8	78.3 ± 6.0	$49.7^{a} \pm 3.2$	$61.1^{a} \pm 4.6$	75.0 ± 2.5	85.8 ± 5.2
NH_3-N (mg/L)	0.2 ± 0.1	0.06 ± 0.02	0.7 ± 0.1	1.7 ± 0.1	0.06 ± 0.04	0.1 ± 0.05	0.6 ± 0.2	1.8 ± 0.3
NO_3^--N (mg/L)	$0.01^{b} \pm 0.01$	0.02 ± 0.01	0.03 ± 0.02	$0.2^{a} \pm 0.04$	$0.03^{a} \pm 0.01$	0.02 ± 0.01	0.03 ± 0.01	$0.03^{b} \pm 0.01$
TKN (mg/L)	1.2 ± 0.1	1.0 ± 0.1	2.4 ± 0.4	$2.9^{b} \pm 0.3$	1.3 ± 0.05	1.27 ± 0.2	2.0 ± 0.2	$5.6^{a} \pm 0.7$
Total P (µg/L)	4.1 ± 3.4	11.8 ± 2.9	11.9 ± 2.4	22.1 ± 4.3	6.0± 1.0	17.0 ± 3.8	12.7 ± 2.5	14.9 ± 3.5
PO_4^{3-}-P (µg/L)	$0.1^{b} \pm 0.1$	$0.8^{b} \pm 0.5$	9.5 ± 1.8	$16.6^{a} \pm 0.9$	$4.5^{a} \pm 1.2$	$8.6^{a} \pm 1.2$	8.6 ± 1.3	$10.6^{b} \pm 0.5$

Note: Values in the same row followed by different superscripts indicate significant difference ($p<0.05$).

The phosphorus concentration in water is usually quite low; dissolved orthophosphate concentration lies within 5-20 µg/L and seldom exceeds 100 µg/L even in highly eutrophic waters, while the concentration of total phosphorus seldom exceeds 1,000 µg/L [26]. Total phosphorus concentrations in the study ponds varied between 4.1-22.1 µg/L with no significant difference between the two crops, while PO_4^{3-}-P concentrations were significantly different between the two crops in the 1st, 2nd and 4th months.

The waste effluent from intensive fish culture as a source of pollution of natural bodies of water has been a major concern [27]. In the present study, water quality deteriorated as the farming season progressed, an occurrence shared by several other findings [9, 13, 28-30]. However, there was a difference in the amount of nutrients added to the water in the fish production ponds owing to difference in the feed applied. In this study, hybrid catfish were fed chicken offal mixed with cassava chips as fresh feed, which actually caused the water quality to deteriorate more rapidly. This was similar to the findings of Yi et al. [6], who showed that using trash fish and chicken offal as feed for fish culture could lead to a rapid deterioration of water quality.

Algal Succession

Algae found in the water samples of the first fish crop were categorised into 83 species of 7 divisions, namely Chlorophyta (34 species), Cyanophyta (28 species), Euglenophyta (12 species), Bacillariophyta (6 species), Chrysophyta (1 species), Pyrrhophyta (1 species) and Cryptophyta (1 species), whereas those of the second fish crop were categorised into 60 species of 4 divisions, namely Chlorophyta (28 species), Cyanophyta (16 species), Euglenophyta (10 species) and Bacillariophyta (6 species) (Table 2).

Abundance percentages of the algal divisions are shown in Table 3. There was no significant difference between the two fish crops in the number of algae of each division. Chlorophyta was most abundant in both fish crops, followed by Cyanophyta, Euglenophyta, Bacillariophyta, Chrysophyta, Cryptophyta and Pyrrhophyta. This confirmed the results obtained by Ingthamjit et al. [9] and Boyd [26] as well as several other reports [28-33]. Phytoplankton occurring in fish production ponds includes members of the following taxonomic divisions: green algae (Chlorophyta), blue-green algae (Cyanophyta), euglenophytes (Euglenophyta), yellow-green and golden-brown algae, diatoms (Chrysophyta) and dinoflagellates (Pyrrhophyta) [26, 28-33]. The dominant algae in the first fish crop were *Microcystis* spp., followed by *Pseudanabaena* spp., *Monoraphidium* spp., *Oscillatoria* spp., *Scenedesmus* spp., *Euglena* spp., *Merismopedia* spp., *Cyclotella* spp., *Coelastrum* spp., *Tetrastrum* sp. and *Spirulina* sp.(Table 4). The second fish crop was dominated by *Microcystis* spp., followed by *Planktolyngbya* sp., *Spirulina* sp., *Cyclotella* spp., *Pseudanabaena* spp., *Merismopedia* spp., *Nitzschia* spp., *Monoraphidium* spp., *Scenedesmus* spp., *Tetrastrum* sp. and *Phacus* spp. (Table 5). Algae of the division Cyanophyta (*Microcystis*) grew densely and were the dominant division in both fish crops. As reported by Welker et al. [34], *Microcystis* is commonly present in eutrophic temperate lakes during summer. These findings are supported by the results of the present study: *Microcystis* species demonstrated better growth in summer and under eutrophic conditions with high concentrations of nutrients in the fish production pond water. Lin [32] and Chowdhury and Mamun[33] also reported that Cyanophyta dominated nutrient-rich channel catfish ponds.

Table 2. Diversity and classification of algae occurring in commercial hybrid catfish production ponds, Ayutthaya province, Thailand, 2007

DIVISION CHLOROPHYTA
Actinastrum hantzschii, Ankistrodesmus sp., *Closteriopsis* sp., *Closterium* sp. 1, *Coelastrum astroideum, Coelastrum pseudomicroporum, Coelastrum* sp.1, *Cosmarium* sp.1, *Crucigenia crucifera, Crucigeniella rectangularis, Dictyosphaerium granulatum, Dictyosphaerium* sp., *Elakatothrix* sp., *Kirchneriella* sp, *Monoraphidium arcuatum, Monoraphidium caribeum, Monoraphidium contortum, Monoraphidium griffithii, Monoraphidium minutum, Oocystis* sp., *Pediastrum duplex, Pediastrum simplex, Scenedesmus bernardii, Scenedesmus disciformis, Scenedesmus microspina, Scenedesmus opoliensis, Scenedesmus pannonicus, Scenedesmus perforates, Scenedesmus velitaris, Scenedesmus* sp. 1, *Scenedesmus* sp. 2, *Staurastrum cingulum, Tetraedron caudatum, Tetrastrum heteracanthum*
DIVISION CYANOPHYTA
Anabaena catenula, Aphanothece sp., *Arthrospira* sp., *Chloroflexus* sp., *Chroococcus minutes, Chroococcus* sp, *Cylindrospermopsis curvispora, Cylindrospermopsis helicoidea, Cylindrospermopsis raciborskii, Gomphosphaeria* sp., *Komvophoron* sp., *Lyngbya* sp., *Merismopedia convulata, Merismopedia glauca, Merismopedia punctata, Microcystis aeruginosa, Microcystis wesenbergii, Microcystis* sp., *Oscillatoria agardhii, Oscillatoria limosa, Oscillatoria redekei, Planktolyngbya limnetica, Pseudanabaena catenata, Pseudanabaena* sp.1, *Pseudanabaena* sp.2, *Raphidiopsis* sp., *Romeria* sp., *Spirulina* sp.
DIVISION EUGLENOPHYTA
Euglena acus, Phacus orbicularis, Phacus triqueter, Phacus sp.1, *Phacus* sp.2, *Phacus* sp.3, *Strombomonas* sp., *Trachelomonas acanthostoma, Trachelomonas caudata, Trachelomonas cylindrical, Trachelomonas volvocina, Trachelomonas* sp.
DIVISION BACILLARIOPHYTA
Aulacoseira granulata, Cyclotella sp., *Fragilaria* sp., *Melosira* sp., *Nitzschia* sp.1, *Nitzschia* sp.2
DIVISION CHRYSOPHYTA
Isthmochloron sp.
DIVISION PYRRHOPHYTA
Peridinium sp.
DIVISION CRYPTOPHYTA
Cryptomonas sp.

Table 3. Means and standard deviations of the percentages of abundance of each algal division in hybrid catfish ponds by month

Division	Abundance (%)							
	Crop 1 (mean ± SD)				Crop 2 (mean ± SD)			
	May	June	July	August	September	October	November	December
Chlorophyta	16.26 ± 8.43	34.67 ± 2.61	19.42 ± 12.52	29.79 ± 10.30	12.29 ± 10.88	9.24 ± 7.15	10.56 ± 4.11	21.23 ± 7.18
Cyanophyta	68.40 ± 14.84	41.26 ± 8.59	73.23 ± 5.91	53.57 ± 1.9	74.77 ± 15.68	76.03 ± 12.46	69.02 ± 16.76	49.40 ± 12.98
Bacillariophyta	3.77 ± 0.52	9.51 ± 10.69	2.69 ± 1.29	15.59 ± 11.85	7.33 ± 4.96	9.51 ± 5.16	19.88 ± 14.21	28.36 ± 7.73
Euglenophyta	8.61 ± 4.83	12.10 ± 11.52	4.66 ± 0.65	0.75 ± 0.07	5.60 ± 0.38	5.19 ± 1.6	0.54 ± 0.21	1.02 ± 0.5
Chrysophyta	0.00 ± 0.00	0.00 ± 0.00	0.00 ± 0.00	0.31 ± 0.03	0.00 ± 0.00	0.00 ± 0.00	0.00 ± 0.00	0.00 ± 0.00
Pyrrhophyta	1.07 ± 0.38	2.47 ± 1.80	0.00 ± 0.00	0.00 ± 0.00	0.00 ± 0.00	0.00 ± 0.00	0.00 ± 0.00	0.00 ± 0.00
Cryptophyta	1.89 ± 1.63	0.00 ± 0.00	0.00 ± 0.00	0.00 ± 0.00	0.00 ± 0.00	0.00 ± 0.00	0.00 ± 0.00	0.00 ± 0.00

Table 4. Means and standard deviations of the percentages of abundance of each algal genus in hybrid catfish ponds by month (Crop 1)

Genus (Division)	Abundance (%)			
	May	June	July	August
Microcystis spp. (Cyanophyta)	0.00 ± 0.00	1.45 ± 0.37	74.66 ± 7.60	28.89 ± 3.27
Pseudanabaena spp. (Cyanophyta)	47.96 ± 21.62	4.14 ± 0.91	3.38 ± 1.01	4.39 ± 3.80
Monoraphidium spp. (Chlorophyta)	12.62 ± 8.20	27.43 ± 8.60	3.17 ± 0.34	11.50 ± 9.15
Oscillatoria spp. (Cyanophyta)	4.92 ± 0.76	37.37 ± 3.89	3.59 ± 1.37	1.30 ± 0.71
Scenedesmus spp. (Chlorophyta)	11.41 ± 0.24	6.86 ± 3.99	4.83 ± 1.63	9.10 ± 4.64
Euglena spp. (Euglenophyta)	12.58 ± 6.01	10.75 ± 9.08	1.53 ± 0.42	0.62 ± 0.04
Merismopedia spp. (Cyanophyta)	3.73 ± 6.46	0.68 ± 1.18	3.57 ± 6.18	13.18 ± 4.99
Cyclotella spp. (Bacillariophyta)	0.00 ± 0.00	3.47 ± 2.81	2.15 ± 2.33	14.35 ± 10.03
Coelastrum spp. (Chlorophyta)	6.79 ± 5.96	2.07 ± 0.46	1.48 ± 1.18	2.33 ± 1.99
Tetrastrum sp. (Chlorophyta)	0.00 ± 0.00	4.76 ± 5.02	1.29 ± 0.64	5.14 ± 4.06
Spirulina sp. (Cyanophyta)	0.00 ± 0.00	1.00 ± 0.57	0.67 ± 0.46	9.18 ± 9.54

Table 5. Means and standard deviations of the percentages of abundance of each algal genus in hybrid catfish ponds by month (Crop 2)

Genus (Division)	Abundance (%)			
	September	October	November	December
Microcystis spp. (Cyanophyta)	32.93 ± 4.57	30.03 ± 5.45	23.31 ± 11.12	16.22 ± 9.73
Planktolyngbya sp. (Cyanophyta)	14.21 ± 4.32	9.56 ± 6.30	28.90 ± 23.35	6.51 ± 4.89
Spirulina sp. (Cyanophyta)	17.68 ± 8.68	29.84 ± 11.36	3.37 ± 0.63	0.95 ± 0.63
Cyclotella spp. (Bacillariophyta)	3.80 ± 2.04	7.04 ± 7.20	19.21 ± 18.01	16.65 ± 3.49
Pseudanabaena spp. (Cyanophyta)	14.33 ± 7.13	10.83 ± 1.20	12.77 ± 20.85	6.51 ± 4.89
Merismopedia spp. (Cyanophyta)	3.91 ± 4.15	5.17 ± 0.68	5.50 ± 4.33	15.93 ± 6.86
Nitzschia spp. (Bacillariophyta)	1.20 ± 0.38	0.00 ± 0.00	0.52 ± 0.13	19.48 ± 2.33
Monoraphidium spp. (Chlorophyta)	3.91 ± 4.15	1.42 ± 1.11	1.87 ± 1.49	8.94 ± 6.15
Scenedesmus spp. (Chlorophyta)	3.09 ± 0.77	2.57 ± 3.28	2.14 ± 0.76	6.09 ± 5.99
Tetrastrum sp. (Chlorophyta)	2.34 ± 3.01	0.22 ± 0.38	1.85 ± 0.80	1.25 ± 1.92
Phacus spp. (Euglenophyta)	4.37 ± 4.42	1.91 ± 0.72	0.20 ± 0.20	0.18 ± 0.13

Figure 2 shows the dominant species among the algal populations during the different months of the study. *Pseudanabaena* spp. were the dominant species during the 1st month of the first fish crop, followed by *Oscillatoria* spp. and *Microcystis* spp. in the 2nd and 3rd months respectively. For the 2nd fish crop, *Microcystis* spp. dominated during the first two months, followed by *Planktolyngbya* sp. in the 3rd month and *Nitzschia* spp. in the 4th month. The succession of algae seemed to be associated with nutrient accumulation and water changing. This could be determined from the results of the correlation analysis of algal populations and water quality parameters. The prevalence of *Pseudanabaena* spp. was found to be significantly associated with water transparency, which was at the highest level in the first month when these species were the dominant algae. *Microcystis* spp. showed a high correlation with nitrate-nitrogen levels, which increased in the 3th and 4th months of the first fish crop and in the 1st and 2nd months of the second fish crop. The decrease in nitrate-nitrogen level also coincided with a decline in the population of *Microcystis* and an increase of *Planktolyngbya* and *Nitzschia* in the succeeding months. *Planktolyngbya* sp. showed no significant correlation with any of the studied water quality parameters, but tended to grow better in water with less transparency and lower temperature. *Nitzschia* spp. were found to significantly correspond to TKN level. An increase in TKN during the last month of the second fish crop might contribute to the succession of *Nitzschia* spp., as also indicated in studies by Ingthmjit et al.[9], Brunson et al. [35], and Zimba et al [36]. However, the succession of algae in the catfish production ponds differs from that occurring in natural lakes, owing to the dense stock of fish in the ponds and the daily feeding which provides abundant nutrients. As reported by Stephens and Farris [13], algal density in commercial channel catfish production ponds is limited more by nutrient availability than by light. Many other different types of algae also exhibit these wide swings in population density. Possible causes of these fluctuations include changes in temperature, pH, carbon dioxide concentration, light intensity and nutrient concentration, and the release of toxins by other organisms including competing algae [3].

CONCLUSIONS

The physico-chemical water quality in commercial hybrid catfish production ponds located in Ayutthaya changed dramatically over the culture period. Certain water quality parameters influenced algal dominance and succession. While *Microcystis* of the division Cyanophyta dominated throughout, *Pseudanabaena* was succeeded by *Oscillatoria*, followed by *Microcystis* in the first fish crop period, whereas *Microcystis* was succeeded by *Planktolyngbya* and *Nitzschia* in the second fish crop period.

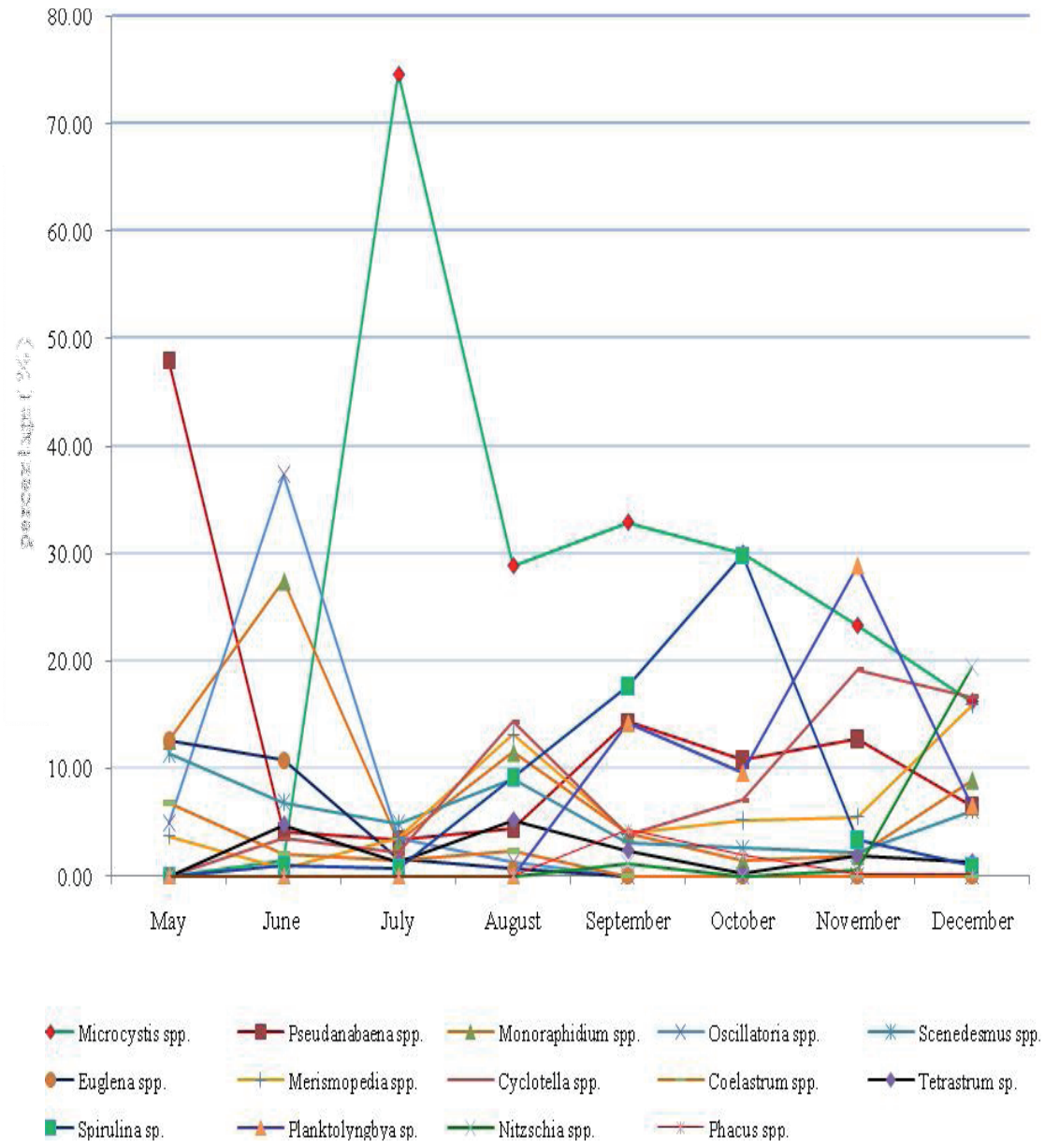

Figure 2. Percentages of abundance of algae in hybrid catfish ponds by month

ACKNOWLEDGEMENTS

Our sincere gratitude is extended to Rajamangala University of Technology Suvarnabhumi for financial support.

REFERENCES

1. S. Areerat, "*Clarias* culture in Thailand", *Aquaculture*, **1987**, *63*, 355-362.

2. Fisheries Information Technology Center, "Fisheries Statistics of Thailand 2005", Department of Fisheries, Ministry of Agriculture and Cooperatives, Bangkok, **2007.**
3. H. S. Killian, "Phytoplankton in catfish ponds", Cooperative Extension Program, University of Arkansas, http://www.uaex.edu/aquaculture2/FSA/FSA9070.htm (Accessed: **2011**).
4. P. V. Zimba, C. S. Tucker, C. C. Mischke and C. C. Grimm, "Short-term effects of diuron on catfish pond ecology", *N. Am. J. Aquaculture*, **2002**, *64*, 16-23.
5. P. V. Zimba, L. Khoo, P. S. Gaunt, S. Brittain and W. W. Carmichael, "Confirmation of catfish, *Ictalurus punctatus* (Rafinesque), mortality from *Microcystis* toxins", *J. Fish Diseas.*, **2001**, *24*, 41-47.
6. Y. Yi, C. K. Lin and J. S. Diana, "Hybrid catfish (*Clarias macrocephalus* x *C. gariepinus*) and Nile tilapia (*Oreochromis niloticus*) culture in an integrated pen-cum-pond system: Growth performance and nutrient budgets", *Aquaculture*, **2003**, *217*, 395-408.
7. P. R. Adler, F. Takeda, D. M. Glenn and S. T. Summerfelt, "Enhancing aquaculture sustainability through utilizing byproducts", *World Aquaculture*, **1996**, *27*, 24-26.
8. T. V. R. Pillay, "The challenges of sustainable aquaculture", *World Aquaculture*, **1996**, *27*, 7-9.
9. S. Ingthamjit, S. Areerat, P. Tientong and S. Wallie, "Variation of water quality, phytoplankton and bacteria in catfish ponds", Academic document No. 129, **1992**, Freshwater Fisheries Research Institute, Department of Fisheries, Ministry of Agriculture and Co-operatives, Bangkok.
10. G. E. Hutchinson, "A Treatise on Limnology", Vol. 1, Wiley, New York, **1957.**
11. W. S. Rast, V. H. Smith and J. A. Thornton, "Characteristics of eutrophication", in "The Control of Eutrophication in Lakes and Reservoirs" (Ed. S. O. Ryding and W. Rast (Eds.), UNESCO and Parthenon Publishers, London, **1989**, pp.37-64.
12. P. V. Zimba, "The use of nutrient enrichment bioassays to test for limiting factors affecting epiphytic growth in Lake Okeechobee, Florida: Confirmation of nitrogen and silica limitation", *Archiv. Hydrobiol.*, **1998**, *141*, 459-468.
13. W. W. Stephens and J. L. Farris, "Instream community assessment of aquaculture effluents", *Aquaculture*, **2004**, *231*, 149-162.
14. The Center for Fisheries Development of Phranakorn-Sri Ayutthaya, "Fisheries statistics of Phranakorn-Sri Ayutthaya 2007" (unpublished document), Department of Fisheries, Ministry of Agriculture and Co-operatives, Bangkok.
15. APHA, AWWA and WPCF, "Standard Methods for Examination of Water and Wastewater", 20th Edn., American Public Health Association, Washington, DC, **1998.**
16. S. Traichaiyaporn, "Water Quality Analysis", Department of Biology, Faculty of Science, Chiang Mai University, Chiang Mai, **2000** (Textbook in Thai).
17. S. Traichaiyaporn, "Applied Phycology", Department of Biology, Faculty of Science, Chiang Mai University, Chiang Mai, **2000** (Textbook in Thai).
18. L. Wongrat, "Phytoplankton", Department of Fishery Biology, Faculty of Fisheries, Kasetsart University, Bangkok, **1999** (Textbook in Thai).
19. G. W. Prescott, "How to Know the Freshwater Algae", 3rd Edn., W. C. Brown, Dubuque, **1978.**
20. C. B. Harrold and J. W. Michaell, "Introduction to the Algae", 2nd Edn., Prentice-Hall, Englewood Cliffs, **1985.**

21. A. Shirota, "The Plankton of South Vietnam: Fresh Water and Marine Plankton", Overseas Technical Cooperation Agency, Tokyo, **1966.**
22. X. N. Verlencar and S. R. Desai, "Phytoplankton Identification Manual", National Institute of Oceanography, Dona Panla, **2004.**
23. M. Duangsawasdi and J. Somsiri, "Water Quality and Analytical Methods for Fisheries Research", Department of Fisheries, Ministry of Agriculture and Cooperatives, Bangkok, **1986** (Textbook in Thai).
24. Y. Musit, "Water Quality for Aquaculture", Department of Aquaculture, Faculty of Fisheries, Kasetsart University, Bangkok, **1992** (Textbook in Thai).
25. J. K. Buttner, R. W. Soderberg and D. E. Terlizzi, "An introduction to water chemistry in freshwater aquaculture", Fact Sheet No.170, **1993**, Northeastern Regional Aquaculture Center, Dartmouth, Massachusetts, USA.
26. C. E. Boyd, "Water Quality in Ponds for Aquaculture", Department of Fisheries and Allied Aquacultures, Auburn University, Auburn (USA), **1990.**
27. H. S. Egna and C. E. Boyd, "Dynamics of Pond Aquaculture", CRC Press, Boca Raton, **1997.**
28. B. Sen and F. Sonmez, "A study on the algae in fish ponds and their seasonal variations", *Int. J. Sci. Technol.*, **2006**, *1*, 25-33.
29. M. A. Burford and D. C. Pearson, "Effect of different nitrogen sources on phytoplankton composition in aquaculture ponds", *Aquat. Microb. Ecol.*, **1998**, *15*, 277-284.
30. C. S. Tucker and M. van der Ploeg, "Seasonal changes in water quality in commercial channel catfish ponds in Mississippi", *J. World Aquaculture Soc.*, **1993**, *24*, 473-481.
31. M. M. Littler and J. H. Graffius, "The annual distribution of phytoplankton communities in a south-eastern Ohio pond", *Ohio J. Sci.*, **1974**, *74*, 313-324.
32. C. K. Lin, "Biological principles of pond culture: Phytoplankton and macrophytes", in "Principles and Practices of Pond Aquaculture" (Ed. J. E. Lamann, R. O. Smitherman and G. Tchobanoglous), Oregon State University, Corvallis, **1983.**
33. A. H. Chowdhury and A. A. Mamun, "Physio-chemical conditions and plankton population of two fishponds in Khulna", *Univ. J. Zool. Rajshahi Univ.*, **2006**, *25*, 41-44.
34. M. Welker, M. Brunke, K. Preussel, I. Lippert and H. von Döhren, "Diversity and distribution of *Microcystis* (Cyanobacteria) oligopeptide chemotypes from natural communities studied by single-colony mass spectrometry", *Microbiology*, **2004**, *150*, 1785-1796.
35. M. W. Brunson, C. G. Lutz and R. M. Durborow, "Algae blooms in commercial fish production ponds", Publication No. 466, **1994**, Southern Regional Aquaculture Center, Stoneville, Mississippi, USA.
36. P. V. Zimba, C. C. Mischke and S. S. Brashear, "Pond age-water column trophic relationships in channel catfish *Ictalurus punctatus* production ponds", *Aquaculture*, **2003**, *219*, 291-301.

Maejo Int. J. Sci. Technol. **2012**, *6*(01), 119-129

Maejo International Journal of Science and Technology

ISSN 1905-7873
Available online at www.mijst.mju.ac.th

Communication

Determination of production-shipment policy using a two-phase algebraic approach

Yuan-Shyi Peter Chiu [1], **Hong-Dar Lin** [1] **and Huei-Hsin Chang** [2,*]

[1] Department of Industrial Engineering and Management, Chaoyang University of Technology, Wufong, Taichung 413, Taiwan
[2] Department of Finance, Chaoyang University of Technology, Wufong, Taichung 413, Taiwan

*Corresponding author, e-mail: chs@cyut.edu.tw

Received: 31 March 2011 / Accepted: 31 March 2012 / Published: 7 April 2012

Abstract: The optimal production-shipment policy for end products using mathematical modeling and a two-phase algebraic approach is investigated. A manufacturing system with a random defective rate, a rework process, and multiple deliveries is studied with the purpose of deriving the optimal replenishment lot size and shipment policy that minimises total production-delivery costs. The conventional method uses differential calculus on the system cost function to determine the economic lot size and optimal number of shipments for such an integrated vendor-buyer system, whereas the proposed two-phase algebraic approach is a straightforward method that enables practitioners who may not have sufficient knowledge of calculus to manage real-world systems more effectively.

Keywords: manufacturing system, replenishment lot size, delivery, two-phase algebraic approach, random defective rate

INTRODUCTION

With the purpose of minimising total set-up and holding costs, inventory controllers in most companies need to address two basic issues for items they routinely stock: when to start replenishment and how much to refill. For items made in-house by manufacturing firms, production planners must, without exception, decide when to initiate a production run and how many items to produce in a run [1]. An inventory model that uses mathematical techniques to derive the most economical production lot was first proposed by Taft [2] several decades ago. This is also known as the economic production quantity (EPQ) model [3].

The classic EPQ model assumes a continuous inventory issuing policy to satisfy product demand. However, in real-world vendor-buyer systems, multiple or periodic deliveries of end items are commonly adopted. Hence, the determination of the optimal number of shipments for a finished lot becomes a critical issue to such a vendor-buyer system in terms of production-delivery cost minimisation. Schwarz [4] examined a one-warehouse N-retailer deterministic inventory system with the objective of determining the stock policy that minimises the long-run average system cost per unit time. He derived optimal solutions along with a few necessary properties for a one-retailer and N-identical-retailer problems. Heuristic solutions for the general problem were also suggested. Goyal [5] studied an integrated single-supplier-single-customer problem and presented a method that is typically applicable to those inventory problems where a product is procured by a single customer from a single supplier using examples to demonstrate the proposed model. Studies related to various aspects of supply chain optimisation have since been extensively carried out [e.g. 6-13]. The classic EPQ model also assumes that all items produced are of perfect quality. However, in a real-life manufacturing environment, the generation of nonconforming items is almost inevitable due to process deterioration or various other factors. In the past decades, many studies have attempted to address the issues of defective products and quality assurance in production systems [e.g. 14-24].

Shih [14] extended two inventory models to the case where the proportion of defective units in the accepted lot is a random variable with known probability distribution. Optimal solutions to the amended systems were developed and comparisons with the traditional models were also presented via numerical examples. Moinzadeh and Aggarwal [17] studied a production-inventory system that was subjected to random disruptions. They assumed that the time between breakdowns is exponential, the restoration times are constant, and excess demand is back-ordered. An (s, S) policy was proposed and the policy parameters that minimise the expected total cost per unit time were investigated. A procedure for finding the optimal values of the policy was also developed. Makis [18] investigated the optimal lot sizing and inspection policy for an economic manufacturing quantity (EMQ) model with imperfect inspections and assumed that the process could be monitored through inspections and that both the lot size and the inspection schedule were subjected to control. It was assumed that the in-control periods were generally distributed and the inspections imperfect. Using Lagrange's method and solving a non-linear equation, a two-dimensional search procedure was proposed for finding the optimal lot sizing and inspection policy. Rahim and Ben-Daya [19] studied the simultaneous effects of deteriorating product items and deteriorating production processes on the economic production quantity, inspection schedules, and economic design of control charts. Deterioration times for both product and process were assumed to follow an arbitrary distribution, and the product quality characteristic was assumed to be normally distributed. Numerical examples were provided to demonstrate the usage of their models. Chiu et al. [21] studied the optimal replenishment policy for the EMQ model with rework failure, backlogging and random breakdowns. Mathematical modelling and cost analysis were employed in their study, along with a renewal reward theorem for dealing with variable cycle length. They derived a long-run average cost function for their proposed model and proved that it was a convex function. Finally, they obtained an optimal replenishment policy for such an imperfect EMQ model.

Recently, an algebraic method of determining the economic order quantity (EOQ) model with backlogging was introduced by Grubbström and Erdem [25]. They used algebraic derivation to find the optimal order quantity without reference to the first- or second-order derivatives. Similar methodologies have been applied to solve various aspects of supply chain optimisation [26-28]. This paper extends such an approach in order to re-examine a manufacturing system with a random defective rate, a rework process, and multiple deliveries of its end product [13].

METHODS

We present a two-phase algebraic approach [13] in order to re-examine a manufacturing system with a random defective rate, a rework process, and multiple shipments of finished items. Such a specific model is described as follows. Assume a production system has an annual production rate P and randomly produces a proportion x of defective items during its uptime at a production rate d. All manufactured items are screened and the inspection cost is included in the unit production cost C. Non-conforming products fall into two groups: the scrap (a proportion of θ) and the repairable (1-θ). The rework process has a rate of P_1 units per year and commences immediately after regular production in each cycle. A proportion θ_1 of reworked items fails during rework and is treated as scrap. Under regular supply, the constant production rate P must be larger than the sum of the demand rate λ and the production rate of defective items d, i.e. $(P\text{-}d\text{-}\lambda) > 0$, where d can be expressed as $d = Px$. Let d_1 denote the production rate of scrap during rework; d_1 can then be expressed as $d_1 = P_1\theta_1$. Furthermore, the proposed system considers a multi-delivery policy for the end items with quality assurance. That is, the finished items can only be delivered to the customers if the whole lot is quality assured at the end of the reworking process. A fixed quantity of n installments of the finished batch is delivered to customers at fixed interval of time during production downtime t_3 (Figure 1). Other notations used in the proposed system are listed below.

t_1 = regular production time in the proposed model,
t_2 = time required to rework defective items,
t_3 = time required to deliver all perfect-quality end products,
t_n = fixed interval of time between each installment of finished end products delivered during production downtime t_3,
T = cycle length,
Q = manufacturing batch size—the decision variable,
n = number of fixed-quantity installments of finished batch to be delivered to customers—the decision variable,
H_1 = maximum level of on-hand inventory when regular production ends,
H = maximum level of on-hand inventory when the rework process finishes,
$I(t)$ = on-hand inventory of perfect quality end items at manufacturer's end at time t,
$TC(Q,n)$ = total production-inventory-delivery costs per cycle,
K = set-up cost per cycle,
C = unit production cost,
h = unit holding cost,
C_R = unit rework cost,
h_1 = holding cost for each reworked item,

C_S = disposal cost per scrap item,
K_1 = fixed delivery cost per shipment,
C_T = delivery cost per item shipped to customers,
φ = overall scrap rate per cycle (sum of scrap rates in periods t_1 and t_2),
h_2 = holding cost for each item kept by customer,
E[$TCU(Q,n)$] = long-run average cost per unit time.

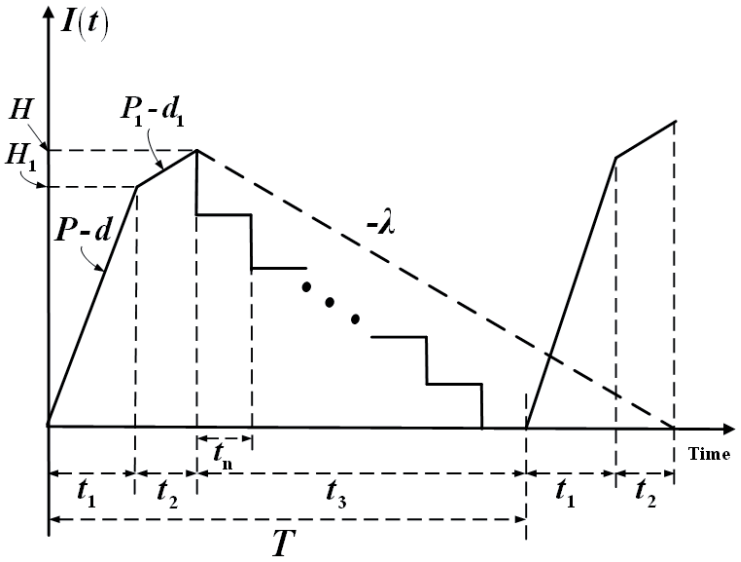

Figure 1. On-hand inventory of perfect end items in the proposed model with random defective rate, reworking and multi-delivery policy [13]

With reference to Figure 1, the total production-inventory-delivery cost per cycle, $TC(Q, n)$, consists of the following. (a) set-up cost and variable manufacturing costs per cycle; (b) total quality costs including variable repairing costs, holding costs for reworked items, and disposal costs for scrap items per cycle; (c) fixed and variable delivery costs per cycle; (d) total holding costs at the manufacturer's end for all items produced in the periods t_1, t_2 and t_3; and (e) total holding costs at the customer's end for all items stocked in t_3:

$$\begin{aligned} TC(Q,n) = {} & K + CQ + C_R\left[x(1-\theta)Q\right] + h_1 \cdot \frac{P_1 \cdot t_2}{2} \cdot (t_2) + C_S\left[x\varphi Q\right] + nK_1 \\ & + C_T\left[Q(1-\varphi x)\right] + h\left[\frac{H_1 + dt_1}{2}(t_1) + \frac{H_1 + H}{2}(t_2) + \left(\frac{n-1}{2n}\right)Ht_3\right] \\ & + \frac{h_2}{2}\left[\frac{H}{n}t_3 + T\left(H - \lambda t_3\right)\right] \end{aligned} \quad (1)$$

With further derivations, the long-run average cost per unit time E[$TCU(Q,n)$] for the proposed system can be written as follows (see mathematical modelling section in Chiu et al. [13]):

$$
\begin{aligned}
E\left[TCU\left(Q,n\right)\right] &= \frac{E\left[TC\left(Q,n\right)\right]}{E\left[T\right]} = \frac{C\lambda}{1-\varphi E\left[x\right]} + \frac{\left(K+nK_1\right)\lambda}{Q\left(1-\varphi E\left[x\right]\right)} + C_T\lambda \\
&+ \frac{C_R E\left[x\right]\left(1-\theta\right)\lambda}{\left(1-\varphi E\left[x\right]\right)} + \frac{h_1\left(E\left[x\right]\right)^2 Q\lambda\left(1-\theta\right)^2}{2P_1\left(1-\varphi E\left[x\right]\right)} + \frac{C_S E\left[x\right]\varphi\lambda}{\left(1-\varphi E\left[x\right]\right)} \\
&+ \frac{hQ\lambda}{2P\left(1-\varphi E\left[x\right]\right)} + \frac{hQ\lambda}{2P_1\left(1-\varphi E\left[x\right]\right)}\left[\left(2E\left[x\right]-\left(E\left[x\right]\right)^2-\varphi\left(E\left[x\right]\right)^2\right)\left(1-\theta\right)\right] \\
&+ \left(1-\frac{1}{n}\right)\left[\frac{hQ\left(1-\varphi E\left[x\right]\right)}{2} - \frac{hQ\lambda}{2P} - \frac{hQE\left[x\right]\left(1-\theta\right)\lambda}{2P_1}\right] \\
&+ \left(\frac{1}{n}\right)\frac{h_2 Q}{2}\left(1-\varphi E\left[x\right]\right) + \left(1-\frac{1}{n}\right)\frac{h_2 Q\lambda}{2P} + \frac{h_2 Q}{2}\left[\left(1-\frac{1}{n}\right)\frac{E\left[x\right]\lambda\left(1-\theta\right)}{P_1}\right]
\end{aligned}
\tag{2}
$$

Derivation of Optimal Policy using Two-phase Algebraic Approach

Unlike the conventional method, which uses differential calculus on the cost function E[*TCU*(*Q, n*)] to find the optimal point [13], a straightforward two-phase algebraic approach to determining the optimal production-shipment policy for the proposed model is adopted here.

*Phase 1: Derivation of n**

It can be seen that Eq.2 has two decision variables, namely Q and n. Moreover, there are several different forms of these decision variables in the right-hand side of Eq.2, e.g., Q, Q^{-1}, nQ^{-1} and Qn^{-1}. Therefore, Eq.2 can be rearranged as

$$
\begin{aligned}
E\left[TCU\left(Q,n\right)\right] &= \frac{C\lambda}{1-\varphi E\left[x\right]} + C_T\lambda + \frac{C_R E\left[x\right]\left(1-\theta\right)\lambda}{\left(1-\varphi E\left[x\right]\right)} + \frac{C_S E\left[x\right]\varphi\lambda}{\left(1-\varphi E\left[x\right]\right)} \\
&+ \left\{\frac{\lambda}{\left(1-\varphi E\left[x\right]\right)}\cdot\left[\frac{h_1\left(E\left[x\right]\right)^2\left(1-\theta\right)^2}{2P_1} + \frac{h}{2P} + \frac{h}{2P_1}\left[\left(2E\left[x\right]-\left(E\left[x\right]\right)^2-\varphi\left(E\left[x\right]\right)^2\right)\left(1-\theta\right)\right]\right]\right\}Q \\
&+ \left[\frac{h\left(1-\varphi E\left[x\right]\right)}{2} - \left(h-h_2\right)\left[\frac{\lambda}{2P} + \frac{E\left[x\right]\left(1-\theta\right)\lambda}{2P_1}\right]\right]Q + \frac{K\lambda}{\left(1-\varphi E\left[x\right]\right)}Q^{-1} \\
&+ \frac{K_1\lambda}{\left(1-\varphi E\left[x\right]\right)}\left(nQ^{-1}\right) \\
&+ \left[\left(h-h_2\right)\left[-\frac{\left(1-\varphi E\left[x\right]\right)}{2} + \frac{\lambda}{2P} + \frac{E\left[x\right]\left(1-\theta\right)\lambda}{2P_1}\right]\right]\left(n^{-1}Q\right)
\end{aligned}
\tag{3}
$$

or

$$
E\left[TCU\left(Q,n\right)\right] = \alpha_1 + \alpha_2\left(Q\right) + \alpha_3\left(Q^{-1}\right) + \alpha_4\left(nQ^{-1}\right) + \alpha_5\left(n^{-1}Q\right) \tag{4}
$$

where α_1, α_2, α_3, α_4 and α_5 denote:

$$
\alpha_1 = \frac{C\lambda}{1-\varphi E\left[x\right]} + C_T\lambda + \frac{C_R E\left[x\right]\left(1-\theta\right)\lambda}{\left(1-\varphi E\left[x\right]\right)} + \frac{C_S E\left[x\right]\varphi\lambda}{\left(1-\varphi E\left[x\right]\right)} \tag{5}
$$

$$\alpha_2 = \frac{\lambda}{\left(1-\varphi E[x]\right)} \cdot \left[\frac{h_1 \left(E[x]\right)^2 (1-\theta)^2}{2P_1} + \frac{h}{2P} + \frac{h}{2P_1}\left[\left(2E[x] - \left(E[x]\right)^2 - \varphi\left(E[x]\right)^2\right)(1-\theta) \right] \right] + \left[\frac{h\left(1-\varphi E[x]\right)}{2} - \left(h-h_2\right)\left[\frac{\lambda}{2P} + \frac{E[x](1-\theta)\lambda}{2P_1} \right] \right] \tag{6}$$

$$\alpha_3 = \frac{K\lambda}{\left(1-\varphi E[x]\right)} \tag{7}$$

$$\alpha_4 = \frac{K_1\lambda}{\left(1-\varphi E[x]\right)} \tag{8}$$

$$\alpha_5 = \left(h-h_2\right)\left[-\frac{\left(1-\varphi E[x]\right)}{2} + \frac{\lambda}{2P} + \frac{E[x](1-\theta)\lambda}{2P_1} \right] \tag{9}$$

With further rearrangements, Eq.4 becomes

$$E\left[TCU(Q,n)\right] = \alpha_1 + Q^{-1}\left[\alpha_2 \cdot Q^2 + \alpha_3\right] + \left(n^{-1}Q\right)\left[\alpha_4\left(nQ^{-1}\right)^2 + \alpha_5\right] \tag{10}$$

$$E\left[TCU(Q,n)\right] = \alpha_1 + Q^{-1}\left[\left(\sqrt{\alpha_2}\cdot Q\right) - \sqrt{\alpha_3}\right]^2 + \left(n^{-1}Q\right)\left[\left(nQ^{-1}\sqrt{\alpha_4}\right) - \sqrt{\alpha_5}\right]^2 + 2\sqrt{\alpha_2\cdot\alpha_3} + 2\sqrt{\alpha_4\cdot\alpha_5} \tag{11}$$

Eq.11 will be minimised if its second and third terms in it equal zero. That is:

$$Q = \sqrt{\frac{\alpha_3}{\alpha_2}} \tag{12}$$

$$n = \sqrt{\frac{\alpha_5}{\alpha_4}} \cdot Q \tag{13}$$

Substituting Eq.6 and 7 into Eq.12, and then substituting Eq.8, 9 and 12 into Eq.13, the optimal number of shipments n^* is

$$n = \sqrt{\frac{\alpha_5\cdot\alpha_3}{\alpha_4\cdot\alpha_2}} = \sqrt{\frac{\left(h-h_2\right)\left[-\left(1-\varphi E[x]\right) + \frac{\lambda}{P} + \frac{E[x](1-\theta)\lambda}{P_1}\right]\cdot\frac{K}{K_1}}{\frac{\lambda}{\left(1-\varphi E[x]\right)}\cdot\left[\frac{h_1\left(E[x]\right)^2(1-\theta)^2}{P_1} + \frac{h}{P} + \frac{h}{P_1}\left[\left(2E[x] - \left(E[x]\right)^2 - \varphi\left(E[x]\right)^2\right)(1-\theta)\right]\right] + \left[h\left(1-\varphi E[x]\right) - \left(h-h_2\right)\left[\frac{\lambda}{P} + \frac{E[x](1-\theta)\lambda}{P_1}\right]\right]}} \tag{14}$$

It is noted that Eq.14 is identical to that obtained using the conventional differential calculus method [13]. We can also see that although in real-world situation the number of deliveries takes integer values only, Eq. 14 results in a real number. In order to locate the integer value of n^* that minimises the long-run average cost for the proposed system, the two adjacent integers to n must be examined respectively for cost minimisation [11]. Let n^+ denote the smallest integer greater than or

equal to n (derived from Eq. 14) and n^- denote the largest integer less than or equal to n. Because n^* is either n^+ or n^-, we can first treat E[$TCU(Q,n)$] (Eq. 4) as a cost function with a single-decision variable Q, and perform the following rearrangements.

*Phase 2: Searching for Q**

First, the long-run cost function E[$TCU(Q, n)$] (i.e. Eq.4) can be rearranged as the following single-decision-variable function:

$$E\left[TCU\left(Q,n\right)\right]=\alpha_1+\alpha_6\left(Q\right)+\alpha_7\left(Q^{-1}\right) \tag{15}$$

where α_6 and α_7 denote:

$$\alpha_6=\alpha_2+n^{-1}\alpha_5 \tag{16}$$

$$\alpha_7=\alpha_3+n\alpha_4 \tag{17}$$

With further rearrangements, Eq.15 becomes

$$E\left[TCU\left(Q,n\right)\right]=\alpha_1+Q\left[\sqrt{\alpha_6}-\sqrt{\alpha_7}\cdot Q^{-1}\right]^2+2\sqrt{\alpha_6}\sqrt{\alpha_7} \tag{18}$$

Upon derivation of Eq.18, it can be noted that E[$TCU(Q,n)$] will be minimised if the second term in it equals zero. That is:

$$Q^*=\sqrt{\frac{\alpha_7}{\alpha_6}} \tag{19}$$

Substituting Eq.16 and 17 into Eq. 19, the optimal production lot size is

$$Q^*=\sqrt{\frac{2\left(K+nK_1\right)\lambda}{\left[\frac{\lambda h_1\left(E\left[x\right]\right)^2\left(1-\theta\right)^2}{P_1}+\frac{h\lambda}{P}+\frac{h\lambda}{P_1}\left[\left(2E\left[x\right]-\left(E\left[x\right]\right)^2-\varphi\left(E\left[x\right]\right)^2\right)\left(1-\theta\right)\right]\right]+\left(1-\frac{1}{n}\right)h\left(1-\varphi E\left[x\right]\right)^2-\left(1-\frac{1}{n}\right)\left(1-\varphi E\left[x\right]\right)\left(h-h_2\right)\left[\frac{\lambda}{P}+\frac{E\left[x\right]\left(1-\theta\right)\lambda}{P_1}\right]+h_2\left(1-\varphi E\left[x\right]\right)^2\frac{1}{n}}} \tag{20}$$

It is noted that Eq.20 is identical to that obtained using the conventional differential calculus method [13].

To find the optimal production-shipment (Q^*, n^*) policy, we substitute all related system parameters, along with n^+ and n^-, into Eq.20. Then, applying the resulting (Q, n^+) and (Q, n^-) respectively in Eq. 4, we choose the one that gives the minimum long-run average cost as the optimal production-shipment policy (Q^*, n^*). A numerical example to demonstrate the practical usage of this method is provided in the next section.

NUMERICAL EXAMPLE

The aforementioned two-phase algebraic approach and its resulting Eq.14, 20 and 4 are verified in this section using the same numerical example [13]. Suppose an end product can be produced at a rate of 60,000 units per year, its annual demand being estimated to be 3,400 units, and during the production process there is a random defective rate x that follows a uniform distribution over a range of [0, 0.3]. A proportion $\theta = 0.1$ of the imperfect items is considered to be scrap and the other portion is assumed to be repairable with a rework rate of $P_1 = 2{,}100$ units per year. It is further estimated that there is a proportion $\theta_1 = 0.1$ of reworked items that fail (become scrap) during the rework period. As a quality assurance policy, the finished items can only be delivered to customers if the whole lot is quality-assured after reworking. A fixed quantity of n installments of the perfect end items are shipped to customers at a fixed interval of time during delivery time t_3 (Figure 1). Other selected parameter values in this example are as follows:

C = \$100 per item,
C_R = \$60 for each reworked item,
C_S = \$20 for each scrap item,
K = \$20,000 per production run,
h = \$20 per item per year,
h_1 = \$40 per reworked item per unit time,
K_1 = \$2,400 per shipment,
C_T = \$0.1 per item delivered,
h_2 = \$80 per item kept at the customer's end per unit time.

Applying Eq.14, we obtain n=2.736. Because the number of deliveries has to be an integer, we have n^+=3 and n^-=2. Substituting all system parameters, along with n^+ and n^- respectively, into Eq.20, we find two possible policies, namely (Q, n^+)=(1735, 3) and (Q, n^-)=(1579, 2). We then apply (Q, n^+) and (Q, n^-) in Eq.4 to obtain E[TCU(1735,3)]=\$485,541 and E[TCU(1579,2)]=\$487,071.

Selecting that with the minimum cost, we find that the optimal policy (Q*, n*)=(1735, 3) and the long-run average cost E[TCU(Q*, n*)]=\$485,541. The results are noted to be identical to those obtained by Chiu et al. [13].

The effect of varying the lot-size Q on the long-run average cost function E[TCU(Q, n)] and on the components of E[TCU(Q, n)], for n* = 3, is depicted in Figure 2.

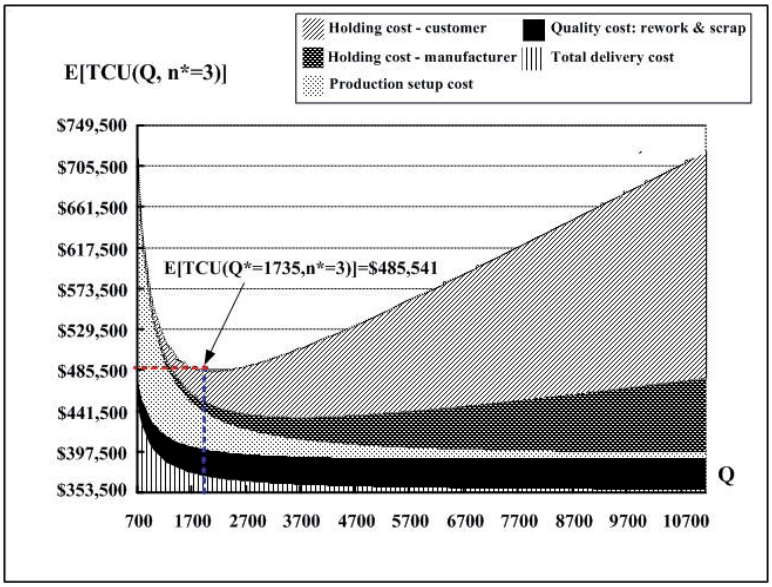

Figure 2. Effect of varying lot size Q on the long-run average cost function E[$TCU(Q, n)$] and on the components of E[$TCU(Q, n)$] for $n^* = 3$

CONCLUSIONS

This paper proposes a two-phase algebraic approach to determining the optimal production-shipment policy for an end product in an integrated supplier-customer system with quality assurance.

Unlike the conventional method, which uses differential calculus on the system cost function to find the economic lot size and optimal number of deliveries, the proposed two-phase algebraic approach is a straightforward method that may enable practitioners with little or no knowledge of differential calculus to understand and manage real-world systems more effectively. The research results were confirmed to be identical to those obtained by the traditional method

ACKNOWLEDGEMENTS

The authors would like to express their appreciation of the support of this research project by the National Science Council of Taiwan under grant number: NSC 99-2221-E-324-017.

REFERENCES

1. F. S. Hillier and G. J. Lieberman, "Introduction to Operations Research", McGraw Hill, New York, **2001**.
2. E. W. Taft, "The most economical production lot", *Iron Age*, **1918,** *101*, 1410-1412.
3. S. Nahmias, "Production and Operations Analysis", McGraw Hill, New York, **2005**, pp.183-205.
4. L. B. Schwarz, "A simple continuous review deterministic one-warehouse N-retailer inventory problem", *Manage. Sci.*, **1973,** *19*, 555-566.
5. S. K. Goyal, "An integrated inventory model for a single supplier-single customer problem", *Int. J. Prod. Res.*, **1977,** *15*, 107-111.

6. L. B. Schwarz, B. L. Deuermeyer and R. D. Badinelli, "Fill-rate optimization in a one-warehouse N-identical retailer distribution system", *Manage. Sci.,* **1985**, *31*, 488-498.
7. A. Banerjee and S. Banerjee, "Coordinated order-less inventory replenishment for a vendor and multiple buyers", *Int. J. Tech. Manage.*, **1992,** *7*, 328-336.
8. R. M. Hill, "The optimal production and shipment policy for the single-vendor singlebuyer integrated production-inventory problem", *Int. J. Prod. Res.*, **1999,** *37*, 2463-2475.
9. D. J. Thomas and S. T. Hackman, "A committed delivery strategy with fixed frequency and quantity", *Eur. J. Oper. Res.*, **2003,** *148*, 363-373.
10. K. Ertogral, M. Darwish and M. Ben-Daya, "Production and shipment lot sizing in a vendor-buyer supply chain with transportation cost", *Eur. J. Oper. Res.*, **2007,** *176*, 1592-1606.
11. Y-S. P. Chiu, F-T. Cheng and H-H. Chang, "Remarks on optimization process of manufacturing system with stochastic breakdown and rework", *Appl. Math. Lett.*, **2010**, *10*, 1152-1155.
12. C-C. Chern and I-C. Yang, "A heuristic master planning algorithm for supply chains that consider substitutions and commonalities", *Expert Syst. Appl.*, **2011**, *38*, 14918-14934.
13. S. W. Chiu, H-D. Lin, M-F. Wu and J-C. Yang, "Determining replenishment lot size and shipment policy for an extended EPQ model with delivery and quality assurance issues", *Sci. Iran.*, **2011,** *18*, 1537-1544.
14. W. Shih, "Optimal inventory policies when stockouts result from defective products", *Int. J. Prod. Res.*, **1980,** *18*, 677-686.
15. M. J. Rosenblatt and H. L. Lee, "Economic production cycles with imperfect production processes", *IIE Trans.*, **1986,** *18*, 48-55.
16. X. Zhang and Y. Gerchak, "Joint lot sizing and inspection policy in and EOQ model with random yield", *IIE Trans.*, **1990,** *22*, 41-47.
17. K. Moinzadeh and P. Aggarwal, "Analysis of a production/inventory system subject to random disruptions", *Manage. Sci.*, **1997,** *43*, 1577-1588.
18. V. Makis, "Optimal lot sizing and inspection policy for an EMQ model with imperfect inspections", *Naval Res. Log.*, **1998,** *45*, 165-186.
19. M. A. Rahim and M. Ben-Daya, "Joint determination of production quantity, inspection schedule, and quality control for an imperfect process with deteriorating products", *J. Oper. Res. Soc.*, **2001,** *52*, 1370-1378.
20. S. W. Chiu, D-C. Gong and H-M. Wee, "Effects of random defective rate and imperfect rework process on economic production quantity model", *Japan J. Ind. Appl. Math.*, **2004,** *21*, 375-389.
21. S. W. Chiu, K-K. Chen and J-C. Yang, "Optimal replenishment policy for manufacturing systems with failure in rework, backlogging and random breakdown", *Math. Comput. Model. Dyn. Sys.*, **2009,** *15*, 255-274.
22. A. Amirteimoori and A. Emrouznejad, "Input/output deterioration in production processes", *Expert Syst. Appl.*, **2011,** *38*, 5822-5825.
23. Y-S. P. Chiu, H-D. Lin and H-H. Chang, "Mathematical modeling for solving manufacturing run time problem with defective rate and random machine breakdown", *Comput. Ind. Eng.*, **2011,** *60*, 576-584.

24. B. Sarkar, S. S. Sana and K. Chaudhuri, "An imperfect production process for time varying demand with inflation and time value of money - An EMQ model", *Expert Syst. Appl.*, **2011,** *38*, 13543-13548.
25. R. W. Grubbström and A. Erdem, "The EOQ with backlogging derived without derivatives", *Int. J. Prod. Econ.*, **1999,** *59*, 529-530.
26. S. W. Chiu, "Production lot size problem with failure in repair and backlogging derived without derivatives", *Eur. J. Oper. Res.*, **2008,** *188*, 610-615.
27. H-D. Lin, Y-S. P. Chiu and C-K. Ting, "A note on optimal replenishment policy for imperfect quality EMQ model with rework and backlogging", *Comput. Math. Appl.*, **2008,** *56*, 2819-2824.
28. Y-Y. Xiao, R-Q. Zhang and I. Kaku, "A new approach of inventory classification based on loss profit", *Expert Syst. Appl.*, **2011,** *38*, 9382-9391.

Maejo Int. J. Sci. Technol. **2012**, *6*(01), 130-151

Maejo International Journal of Science and Technology

ISSN 1905-7873
Available online at www.mijst.mju.ac.th

Full Paper

IIS-Mine: A new efficient method for mining frequent itemsets

Supatra Sahaphong* and Veera Boonjing

Department of Mathematics and Computer Science, Faculty of Science, King Mongkut's Institute of Technology Ladkrabang, Bangkok 10520, Thailand

* Corresponding author, e-mail: supatra@ru.ac.th

Received: 11 September 2011 / Accepted: 4 March 2012 / Published: 23 April 2012

Abstract: A new approach to mine all frequent itemsets from a transaction database is proposed. The main features of this paper are as follows: (1) the proposed algorithm performs database scanning only once to construct a data structure called an inverted index structure (IIS); (2) the change in the minimum support threshold is not affected by this structure, and as a result, a rescan of the database is not required; and (3) the proposed mining algorithm, IIS-Mine, uses an efficient property of an extendable itemset, which reduces the recursiveness of mining steps without generating candidate itemsets, allowing frequent itemsets to be found quickly. We have provided definitions, examples, and a theorem, the completeness and correctness of which is shown by mathematical proof. We present experiments in which the run time, memory consumption and scalability are tested in comparison with a frequent-pattern (FP) growth algorithm when the minimum support threshold is varied. Both algorithms are evaluated by applying them to synthetics and real-world datasets. The experimental results demonstrate that IIS-Mine provides better performance than FP-growth in terms of run time and space consumption and is effective when used on dense datasets.

Keywords: association rule mining, data mining, frequent itemsets mining, frequent patterns mining, knowledge discovering

INTRODUCTION

The objective of frequent itemset mining is to identify all frequently occurring itemsets using a support threshold. Decision-makers are interested in all itemsets associated with high frequencies. Association rule mining algorithms can be broken down into two major phases. The first phase finds all of the itemsets that satisfy the minimum support threshold, which are the frequent itemsets. The

second phase is rule generation, in which all the high confidence rules from the frequent itemsets found in the previous phase are extracted [1]. Many previous investigations focused on the first phase. Early algorithms based on generated and tested candidate itemsets have two major defects. First, the database must be scanned multiple times to generate candidate itemsets, which increases the I/O load and is time-consuming. The search space of itemsets that must be explored grows exponentially. Second, enormous candidate itemsets are generated and calculated from their supports, which consumes a large amount of CPU time [2].

To overcome the above-mentioned problems, a next generation of algorithms using a compact tree structure was proposed, called a frequent-pattern (FP) tree [3], which finds frequent itemsets directly from the data structure. However, most of the FP-tree-based algorithms have the following weaknesses. First, the mining of frequent itemsets from the FP-tree to generate a huge conditional FP-tree requires a large amount of run time and space. The best case is when a database has the same set of transactions; an FP-tree then contains only a single branch of nodes. The worst case is when a database has a unique set of transactions [3]. Second, when the users change to a new minimum support threshold for their new decision, the algorithm restarts the whole operation and scans the database twice.

Many researchers have tried to solve the above problems using a vertical data layout. However, most of the algorithms have the drawback of increasing the run time and space consumption due to the following reasons. First, when the users change to a new minimum support threshold for their new decision, the algorithm restarts the whole operation more than one time to scan a database and construct their data structure. Rescanning the database for a new minimum support threshold wastes both run time and space. Second, all of the FP-tree-based algorithms generate a huge conditional FP-tree, which has a large number of recursive processing steps and requires a large amount of run time and space consumption.

In this paper we present a new, efficient method to solve the above-mentioned problems by proposing both a data structure and a mining algorithm for decreasing the consumption of run time and space. First, the proposed method performs database scanning to construct a data structure called an inverted index structure (IIS) only once. In addition, changing the minimum support threshold does not affect the IIS; therefore, database rescanning is not required. Second, IIS-Mine is a new algorithm that mines all of the frequent itemsets without generating candidate itemsets and uses a new tree structure called the IIS_{item}Tree. IIS-Mine employs an efficient property of the extendable itemset, which decreases the number of recursive processing steps when mining frequent itemsets. The completeness and correctness of the algorithm is proved using a mathematical proof. Last, the efficiency of IIS-Mine is compared with that of FP-growth in terms of run time and space consumption through simulation experiments. Our experiments show that IIS-Mine is more efficient than FP-growth in run time and space consumption for dense datasets.

RELATED WORK

The first algorithm to generate all frequent itemsets is the AIS algorithm, which was first introduced by Agrawal et al [4]. However, this algorithm constructs a list of all of the possible

itemsets at each level of traversal, so infrequent itemsets that are not needed are also generated. Later, the algorithm was improved upon and renamed the Apriori algorithm by Agrawal et al [5]. The Apriori algorithm uses a level-wise and breadth-first search approach for generating association rules. Many efficient association mining techniques have been developed based on the Apriori algorithm. Vu et al. [6] proposed a rule-based location prediction technique to predict the user's featured location, but this proposal generates more candidate itemsets than are required. These algorithms are also expensive in terms of I/O load and run time when the database must be scanned multiple times to generate candidate itemsets.

The above-mentioned problems can be improved upon by using a compact tree structure and finding frequent itemsets directly from the data structure. The algorithms scan a database twice. The first scan of the database is to discard infrequent itemsets; the second is to construct a tree. The FP-growth algorithm, developed by Han et al. [7], is the most popular method. It performs a depth-first search approach in a search space. It encodes a dataset using a compact data structure called an FP-tree or prefix tree and extracts frequent patterns directly from the FP-tree. Many approaches have been proposed to extend and improve upon this algorithm. Pei et al. [8] developed the H-mine algorithm using array- and tree-based data structures to improve the main memory cost. The PatriciaMine algorithm [9] compressed Patricia tries to store datasets, which is space efficient for both dense and sparse datasets. The FP-growth algorithm [10] reduces the FP-tree traversal time using an array technique. Zhu [11] proposed a new method to compress a large database into an FP-tree with a children table but not a header table, and applied a depth-first search with this tree for the mining step, which reduces both the run time and the space consumption. Sahaphong and Boonjing [12] proposed a new algorithm which constructs a pattern base using a new method that is different from the pattern base in the FP-growth and mined frequent itemsets using a new combination method without the recursive construction of a conditional FP-tree. An approach based on the FP-tree and co-occurrence frequent items (COFI) was proposed to find frequent items in multilevel concept hierarchy by using a non-recursive mining process [13]. A new data structure called improved FP tree was proposed, which can reduce space consumption and enhance the efficiency of an attribute reduction algorithm [14]. To maintain the anti-monotone property of approximate weighted frequent patterns, a robust concept was proposed to relax the requirement for exact equality between the weighted supports of patterns and a minimum threshold [15]. However, most of the FP-tree-based algorithms require a large amount of run time and space to generate the huge conditional FP-trees. Moreover, the algorithm restarts the whole operation and requires that a database be scanned twice when the minimum support threshold is changed.

As mentioned above, most of the algorithms that mine frequent itemsets use a horizontal data layout. However, many researchers use a vertical data layout. The Eclat algorithm was proposed [16] to generate all frequent itemsets in a breadth-first search using the joining step from the Apriori property when no candidate items can be found. The Eclat algorithm is very efficient for large itemsets but is less efficient for small ones. The diffset technique [17] was introduced to improve the memory requirement. Chai et al. [18] detailed a data structure called large-item bipartite graph to accommodate the data when a database is scanned. Similar to the FP-growth algorithm, this method

mines frequent patterns using the recursive conditional FP-tree. The BitTableFI algorithm [19] uses horizontal and vertical data layouts to compress a database. Yen [20] presented an algorithm based on an undirected itemset graph that finds frequent itemsets by searching undirected graphs. When the database and minimum support change, this algorithm requires that the graph structure be re-searched to generate new frequent itemsets. The Index-BitTableFI [21] was developed to reduce the cost of candidate generation and to support counting. Sahaphong and Boonjing [22] proposed a new algorithm that reduces the run time. The drawback of this algorithm is its large memory consumption from generation of many repeated nodes. The JoinFI-Mine algorithm [23] uses a sorted-list structure constructed from the vertical data layout and finds all frequent itemsets using a depth-first search for joining frequent itemsets. Therefore, this algorithm consumes time and space in its joining step.

METHODS

Frequent-Itemsets Mining Problem

We introduce the basic concepts of mining frequent itemsets. All terminologies in this section are proposed by Han et al [2].

Let $I = \{x_1, x_2, ..., x_m\}$ be a set of items and $DB = \{T_1, T_2, ..., T_n\}$ be a transaction database, where $T_1, T_2, ..., T_n$ are transactions that contain items in *I*. The support, or *supp* (occurrence frequency), of a pattern *A*, where *A* is a set of items, is the number of transactions containing *A* in DB. A pattern *A* is frequent if *A*'s support is no less than a predefined minimum support threshold, *minsup*.

Given a DB and a minimum support threshold *minsup*, the problem of finding a complete set of frequent itemsets is called the frequent-itemsets mining problem.

For a greater understanding, we provide an example to illustrate the above definitions.

Example 1. An example of the database by Han et al. [2] is used here. Table 1 is a DB. It consists of 5 transactions (T_1, T_2, T_3, T_4, and T_5) and 17 items (*a, b, c, d, e, f, g, h, i, j, k, l, m, n, o, p*, and *s*). For example, the first transaction is T_1, which contains *f, a, c, d, g, i, m*, and *p*.

Table 1. A transaction database

Transaction	Item
T_1	*f, a, c, d, g, i, m, p*
T_2	*a, b, c, f, l, m, o*
T_3	*b, f, h, j, o*
T_4	*b, c, k, s, p*
T_5	*a, f, c,* e, *l, p, m, n*

IIS: Design and Construction

We present a data structure that contains transaction data called an inverted index structure (IIS). The IIS is a structure that holds a relationship between items and the transactions included within. The IIS is constructed from one scan of the DB. This original IIS can support every *minsup*;

therefore, it does not need to rescan the DB when the *minsup* is changed. According to the definitions in the previous section, we present a new definition with an example and an algorithm to demonstrate how to construct this IIS.

Definition 1 (IIS). Let DB be a transaction database and I be a non-empty finite set of all items in each transaction in the DB, where each transaction is a set of items in I associated with an identifier, and let S be a set of all non-empty subsets of DB. An IIS is the function $f: I \rightarrow S$ defined by $f(a) = S_1$ if T contains a for each $T \in S_1$. This function can be identified as a table consisting of the attributes of the items in I and the corresponding transactions in the DB. That is, each row in the IIS contains an item in I as well as the transactions in the DB that contain that item. The set of transactions are written in the order of their ascending identification numbers.

With the above definition, the IIS represents the relationship between each item in I and its corresponding transactions; therefore, the IIS can apply to all minimum support thresholds, and a rescan of the database is not required. We demonstrate the steps to construct the IIS through the following example.

Example 2. We use the example of a DB in Table 1. The DB is scanned once to create the IIS. The scan of the first transaction is T_1, which consists of items *f, a, c, d, g, i, m* and *p*. The transaction T_1 will be inserted for each corresponding item sorted in ascending order (*a, c, d, f, g, i, m, p*). T_1 will be the first transaction inserted in the transactions of item *a*. The second examined item is *c*, so we insert T_1 in item *c*. Next, we examine item *d*; we then subsequently insert T_1 in item *d*. The remaining items (*f*, *g*, *i*, *m* and *p*) in T_1 can be similarly inserted. The remaining transactions (T_2, T_3, T_4 and T_5) in the DB are performed in a similar manner.

Algorithm 1 shows how to construct the IIS. Figure 1 shows all of the items of the IIS after scanning the DB once, and the bold items are all frequent items that have a support greater than or equal to the *minsup*, which is assumed to be 3.

```
Algorithm 1 (IIS construction)
Input: DB.
Output: IIS.
Method: The IIS is constructed as follows.
1 Begin
2   Create header that contains all items.
3   For each transaction T in DB do  // scanning DB once
4     Sort items in T                // ascending order
5     Create transaction to each corresponding item
6   End //For
7 End //Begin
```

Item	Transaction			
a	T_1	T_2	T_5	
b	T_2	T_3	T_4	
c	T_1	T_2	T_4	T_5
d	T_1			
e	T_5			
f	T_1	T_2	T_3	T_5
g	T_1			
h	T_3			
i	T_1			
j	T_3			
k	T_4			
l	T_2	T_5		
m	T_1	T_2	T_5	
n	T_5			
o	T_2	T_3		
p	T_1	T_4	T_5	
s	T_4			

Figure 1. An example of the IIS

IIS-Mine Algorithm

We present a new algorithm called IIS-Mine. This algorithm uses a new tree structure, called the IIS_{item}Tree, to mine frequent itemsets. The main features of this algorithm are as follows: (1) every frequent itemset is found without generating candidate itemsets; (2) the algorithm reduces the recursion of mining steps using the property of extendable itemset; and (3) the algorithm supports the mining of frequent itemsets with any value of the *minsup* without needing to rescan the database. From the above features, we can quickly find the frequent itemsets and completely and correctly obtain them. We now introduce the terminologies of the IIS_{item}Tree, its construct, the theorem, the examples and the algorithms to describe how to mine frequent itemsets.

Definition 2 (Itemset-tree structure). An itemset-tree structure is a tree structure constructed from the IIS. It is a finite set of one or more nodes with the following structure:

(i) It consists of the root which contains an item, a set of item subtrees as the children of the root, and a set of header tables.

(ii) Each node in this tree comprises five fields: *item-name*, which registers which item this node represents; *support,* which registers the number of transactions represented by the portion of the path reaching this node; *same-item,* which represents a pointer that points to the node in the itemset-tree structure that carries the same item-name; *parent*, which represents a pointer that points to the previous node in the same path; and *child*, which represents a pointer that points to the child node.

(iii) Each member of the *header table* consists of two fields, *item-name* and *head of node link*, where *head of node link* represents a pointer that points to the first node in the itemset-tree structure carrying the *item-name*.

Definition 3 (IIS_{item}tree). Let x_0 be an arbitrary frequent item in a given transaction database and IIS be the inverted index structure of the transaction database. A tree T constructed from the IIS is called an inverted index structure-x_0 tree, denoted by $IIS_{x_0}tree$, if it satisfies the following:

(i) Each node of T is of the form $(A:s)$, where A is a frequent itemset and s is its support. If $(A:s)$ is a node of T and $A=\{a\}$, where a is a frequent item, then $(A:s)$ is simply written by $(a:s)$.

(ii) Let $(x_0:s_0)$ be its root, where s_0 is the support of x_0.

(iii) Let $x_0, x_1, ..., x_k$ be frequent items in the IIS, and $s_i = supp\{x_0, x_1, ..., x_i\}$ for all $i = 0,1,...,k$. In this case, $P=((x_0:s_0),(x_1:s_1),...,(x_k:s_k))$ is a path from the root $(x_0:s_0)$ to a leaf $(x_k:s_k)$ of the tree T if and only if $s_0 \geq s_1 ... \geq s_k > 0$, $x_0 <_l x_1 <_l ... <_l x_k$, where $<_l$ is the lexicographic order. If a is a frequent item in the IIS and if $(a:s)$ is a node of T such that $x_k < a$ or $x_i <_l a <_l x_{i+1}$ for all $i = 0,1,...,k$, then $supp\{x_0, x_1, ..., x_i, a\} = 0$ and $(a:s)$ is not a node of P.

The header table of $IIS_{x_0}tree$ is a set of all frequent items a of a node $(a:s)$ of this tree.

Based on the above definition, we have the IIS_{item}Tree construction algorithm, as shown in Algorithm 2. It is evident that if *minsup*>0 is a minimum support threshold, then every frequent itemset can be derived from an IIS_{item}Tree.

Algorithm 2 (IIS_{item} Tree construction)
Input: IIS.
Output: IIS_{item} Tree.
Method: An IIS_{item} Tree is constructed as follows.
1Begin
2 Create *header table*
3 Read frequent item *x* in IIS
4 Create root *R* and initial *supp*(*R*) to 1
5 Link *R* to *header table*
6 For each transaction *T* of root *R* where $T = T_1$ to T_n do
7 While next frequent item≠(last frequent item)+1 do
8 Read next frequent item (*N*) that has same *T* with *R*
9 Call InsertTree (*N*,*R*)
10 End//While
11 End//For
12End //Begin
Procedure InsertTree (*N*,*R*)
1Begin
2 If $IIS_R Tree$ has a node *C* such that *C.item-name* = *N.item- name* then
3 Increment *supp*(*N*) by 1
4 Else
5 Create new node *N* and initial *supp*(*N*) to 1
6 Link *N* to *N*'s *parent*
7 Link *N* to *N*'s *header table*
8 Link *N* to *same-item*
9 End //If
10End //Begin

If no confusion arises, then $\{x_1, x_2, ..., x_n\}$ and $(\{x_1, x_2, ..., x_n\}:s)$ are replaced by $x_1x_2...x_n$, and $<x_1x_2...x_n:s>$ respectively, where $x_1, x_2, ..., x_n$ are items.

Example 3. In this example, we describe the steps to construct all of the IIS_{item}Trees except the last frequent item *p* using the IIS in Figure 1 and *minsup* = 3. The first frequent item in the IIS is

a; therefore, we first construct the *IIS$_a$Tree*, and item *a* is a root. We obtain two paths: (<*a*:2>, <*c*:2>, <*f*:2>, <*m*:2>, <*p*:2>) and (<*a*:1>, <*b*:1>, <*c*:1>, <*f*:1>, <*m*:1>). The first path consists of frequent items (*a*,*c*,*f*,*m*,*p*) that appear twice in the DB. Similarly, the second path indicates frequent items (*a*,*b*,*c*,*f*,*m*) that are contained in only one transaction in the DB. These two paths share the frequent item *a*; thus, *a* appears three times in the DB. Other IIS$_{\text{item}}$Trees, except the *IIS$_p$Tree*, can be similarly constructed. In Figure 2, all of the IIS$_{\text{item}}$Trees, except the last *IIS$_p$Tree*, are illustrated.

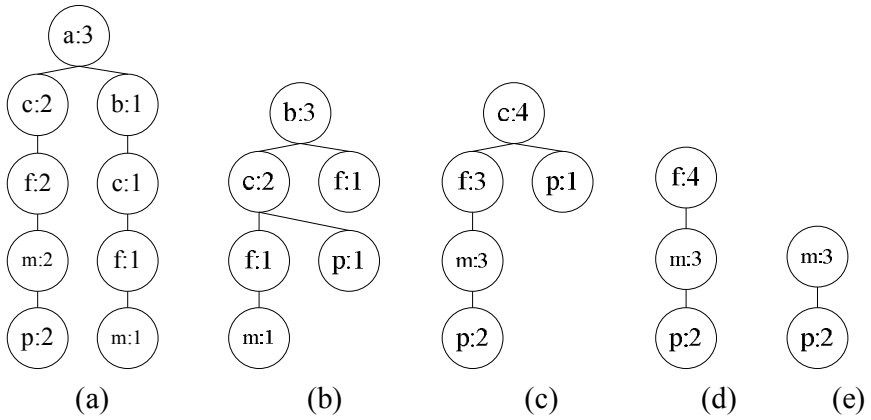

Figure 2. IIS$_{\text{item}}$Trees

Definition 4 (A$_1$-tree). Let DB be a transaction database; let *T* be a tree such that each node of the tree is of the form $(A:s)$, where *A* is a frequent itemset in DB and *s* is the support of *A*; and let A_1 be a frequent itemset in the DB. *T* is called an *A$_1$-tree* if, for any path *P* of *T*, *P* is of the form $P=((A_1:s_1),(A_2:s_2),...,(A_k:s_k))$, where *k* is a positive integer; A_i and A_j are pairwise disjoint frequent itemsets for all $i, j = 1,2,\ldots,k$ with $i \neq j$; s_i is the support of $\bigcup_{m=1}^{i} A_m$ for $i = 1,2,\ldots,k$; $(A_1{:}s_1)$ is the root of *T*; and $(A_k:s_k)$ is a leaf of *T*.

Example 4. According to Figure 2 (a), the *ac*-tree is shown in Figure 3.

Definition 5 (Prefix subpath). Let *T* be a tree, a_1 be the root of *T*, and $P=(a_1,...,a_m)$ be a path of *T*, where *m* is a positive integer. Every path $Q=(a_1,...,a_k)$ of *T* is then called a prefix subpath of *P*, where $1 \le k \le m$.

Example 5. According to Figure 2(a), the paths ((*a*:3),(*c*:2)) and ((*a*:3),(*c*:2),(*f*:2)) are prefix subpaths of ((*a*:3),(*c*:2),(*f*:2),(*m*:2)).

Definition 6 (Subheader). Let *T* be an *A-tree* and (*x*:*s*(*x*)) be a node of *T*, where *x* is a frequent item in a given transaction database and *s*(*x*) is the support of *x*. Suppose that all of the nodes (of *T*) containing *x* are only in the paths $P_1,\ldots,P_k$ of *T* from the root (*A*:*s*) to some leafs of *T*, and suppose that Q_i is a prefix subpath (of P_i) from the root $(A:s)$ to $(x:s(Q_i))$ for all $i=1,...,k$. The subheader of *T*, denoted by *SH*(*A*), is defined as the order set *SH(A)* = {*x*|*x* is a frequent item not contained in *A*, $(x:s(Q_i))$ is a node in Q_i for $i = 1,\ldots,k$ and $\sum_{i=1}^{k} s(Q_i) \ge minsup\}$.

Example 6. According to Figure 2(a), SH(*a*) = {*c*,*f*,*m*}, where SH(*a*) is the subheader of the tree in Figure 2 (a), *supp*(*c*) = 3, *supp*(*f*) = 3, and *supp*(*m*) = 3.

Definition 7 (Conditional itemset-tree). Let A_1 be a frequent itemset, T be an A_1-*tree*, x_2 be a frequent item with $x_2 \in SH(A_1) - A_1$, and $A_1x_2 := A_1 \cup \{x_2\}$ be a frequent itemset. A *conditional* A_1x_2-*tree*, denoted by $T(A_1x_2)$, is a tree that satisfies the following:

(i) $(A_1x_2 : s_2)$ is the root of $T(A_1x_2)$, where s_2 is the support of A_1x_2 and $s_2 \geq minsup$.

(ii) The number of items in $SH(A_1) > 1$.

(iii) All of the paths are derived from T in the following way: $Q = ((A_1x_2 : s_2),(x_3 : s_3),...,(x_k : s_k))$ is a path of $T(A_1x_2)$ if and only if a path $P = ((A_1 : s_1),(x_2 : s_2),...,(x_l : s_l))$ exists from the root $(A_1 : s_1)$ to the leaf $(x_l : s_l)$ of T, where $l \geq k$ and x_k is in $SH(A_1)$; and if there is a node $(x_r : s_r)$ of P such that $r > k$ and $((A_1 : s_1),(x_2 : s_2),...,(x_r : s_r))$ is a prefix subpath of P, then x_r must not be in $SH(A_1)$.

Example 7. According to Figure 2 (a), the conditional itemset-tree, or conditional *ac*-tree, is shown in Figure 4.

Notably, every non-empty subset of a frequent itemset is also frequent. This fact leads to the following definition.

Definition 8 (Frequent itemset* of length m derived from tree). Let A be a frequent itemset, x be a frequent item, and $x \notin A$. Suppose that T is a conditional Ax-tree, m is a positive integer greater than 1, and $Ax = A \cup \{x\}$ has m elements. Ax is called a frequent itemset* of length m derived from T, denoted by $FS^*_m(Ax)$, if T contains precisely two nodes and Ax is a frequent itemset, or if $SH(A) = \{x\}$.

Example 8. According to Figure 5, the frequent itemset* of length 4 derived from the conditional *acf*-tree is $FS^*_4(acfm) = acfm.$.

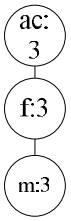

Figure 3. *ac*-tree

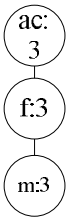

Figure 4. Conditional *ac*-tree

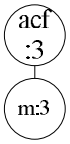

Figure 5. Conditional *acf*-tree

Definition 9 (Extendable frequent itemset*). Let m be a positive integer greater than 1, T be a $T(Ax)$ defined as in definition 7 with $A_1 = A$ and $x_1 = x$, and Ax be a frequent itemset* of length m derived from T. Each itemset in $FS^*_m(Ax)$ is said to be extendable if $m \geq 3$. For every k = 2, 3,…, m, we let $Ext^*_k(Ax)$ denote the set of all itemsets containing exactly k items of $FS^*_m(Ax)$, where $m \geq 3$. Each element of $Ext^*_k(Ax)$ is called an extendable frequent itemset* (derived from T) of length k for all $k \geq 2$. The set of all extendable frequent itemsets* of length k that is denoted by $Ext^*_k = \cup\{Ext^*_k(Ay) \mid Ay$ is a frequent itemset* of length at least k derived from a conditional Ay-*tree*$\}$ for all $k \geq 2$.

Example 9. According to the previous example, the length of $FS_4^*(acfm)$ is 4; we then find that $Ext_2^*(acfm)$ = {*ac*, *af*, *am*, *cf*, *cm*, *fm*} and $Ext_3^*(acfm)$ = {*acf*, *acm*, *afm*, *cfm*}. Therefore, Ext_2^* = {*ac*, *af*, *am*, *cf*, *cm*, *fm*, and all members of other $Ext_2^*(Ay)$ } and Ext_3^* = {*acf*, *acm*, *afm*, *cfm*, and all members of other $Ext_3^*(Ay)$ }.

Definition 10 (Frequent itemset* of length *m*). Let *k* be the maximum length of all frequent itemsets in a transaction database, $FS_m^*(Ax)$ and Ext_k^* be given as in definitions 8 and 9 respectively; let $A_m = \{FS_m^*(Ax) \mid Ax$ being a frequent itemset* of length *m* derived from *T*} for *m* = 2, 3,…, *k*; define $FS_2^* = A_2 \cup \{Ax \mid Ax$ being a frequent itemset of length 2}; and define $FS_m^* = A_m$ for *m* = 2, 3,…, *k*}. Let FI_m^* be defined by $FI_1^* = \{\{x\} \mid x$ being a frequent item} and $FI_m^* = FS_m^* \cup Ext_m^*$ for *m* = 2, 3,…, *k*}. Any element of FI_m^* is called the frequent itemset* of length *m*.

Example 10. According to the previous example, we find that FI_2^* = {*ac*, *af*, *am*, *cf*, *cm*, *fm*}, FI_3^* = {*acf*, *acm*, *afm*, *cfm*}, and FI_4^* = {*acfm*}.

Definition 11 (Frequent itemset*). Let FI_m^* be given as in definition 10, and let FI^* denote $\cup_{m=1}^{k} FI_m^*$, where *k* is the maximum length of all frequent itemsets in a transaction database. Any element of FI^* is called a frequent itemset*.

Example 11. According to the previous example, FI^* is {*ac*, *af*, *am*, *cf*, *cm*, *fm*, *acf*, *acm*, *afm*, *cfm*, *acfm*}.

On the basis of the above definitions and examples, Algorithm 3 presents the IIS-Mine algorithm to show how it can be used to mine all frequent itemsets.

```
Algorithm 3: (IIS-Mine: Mining frequent itemsets using IIS_itemTree)
Input: IIS, IIS_item Trees constructed according to Algorithm 2, and minsup
Output: FI*
Procedure AllFreqItemset (IIS, FI*)
1 Begin
2   For each frequent item x in the IIS do
3     FI_1^* = {{x | x ∈ I, supp(x) ≥ minsup}
4     Call IIS_xTree , which is constructed from Algorithm 2
5     If Tree ≠{}
6       Call IIS-Mine (Tree, x)
7     End //If
8   End //For
9   Find FI^* = ∪_{m=1}^{k} FI_m^*                    // FI* is given in definition 11
10 End //Begin
Procedure IIS-Mine(Tree, x)
1 Begin
2   Call SubHeader (A-tree, subheaderA)
3   Generate all Ax with its support
     //All Ax are the frequent itemsets where A is the root of A-tree and x ∈subheaderA
4   For each |λ|>1 do  // λ is Ax
5     Flag=1
6     While Flag = 1 do
7       Call SkipFreqItemset (subheaderA, λ , δ ,FlagRepeat, FlagTree)
8       If FlagRepeat=0 and FlagTree=0 then  // (δ ∉ FI_m^* )
9       Call CondItemsetTree (A-tree, δ , conditional δ -tree)
```

```
10    Else
11      Flag=0
12    End // If
13    If conditional Ax-tree contains greater than two nodes
14      Call IIS-Mine(conditional δ -tree, x)
15    Else Flag=0
16    End //If
17  End //While
18  If |FS*m(δ)|≥3 and FS*m(δ) ∉ FI*m then
19    Call ExtFreqItemset( FS*m(δ) , Ext*k )                    // FS*m is given in definition 8
20    Save FS*m(δ) and all Ext*k to FI*m                        // FI*m is given in definition 10
21  Else
22    If FS*m(δ) ∉ FI*m then
23      Save FS*m(δ) to FI*m
24    End //If
25  End //If
26  End //For
27 End //Begin
Procedure SubHeader (A-tree, subheaderA)
1 Begin
2  Each frequent item x of A-tree                              // SH(A) is given in definition 6
3  Find {(x:s(x))|x ∈SH(A), s(x) is the support of x in A-tree}
4 End // Begin
Procedure CondItemsetTree(Tree, δ , conditional δ -tree)
1 Begin
2  Scan tree once to collect the paths that have an association with root δ
3  For all paths are derived from tree do
4    Connect all paths to δ
5  End //For
6 End //Begin
Procedure SkipFreqItemset (SubheaderA, λ , δ , FlagRepeat, FlagTree)
1 Begin // To skip the construction of conditional item tree
2 // x is the frequent item in subheaderA  // λ is the root of tree; or a frequent itemset
3 // FlagRepeat=0 means δ ∉ FI*m          // FlagTree=0 means the conditional item-tree is constructed
4 // n is the maximum number of elements of itemsets in subheaderA
5  FlagRepeat =1, FlagTree=1
6  β = λ, α = β
7  While( FlagRepeat=1 and (order of x ≤n )) do
8   If β ∉ FI*m then
9     FlagRepeat=0, FlagTree=0
10      If x is the last item
11        If |δ|= 2 then FlagTree=1
12        End //If
13        δ = α
14      End //If
15    Else
16      If x is the last item then
17        Increment order of item x
18      Else
19        Increment order of item x
20        β = δ ∪x
21        α = δ
22      End// If
```

```
23        δ = β
24      End //If
25    End //while
26 End //Begin
Procedure ExtFreqItemset( FS*_m(δ) , Ext*_k )
1 Begin                                   // Ext*_k is given in definition 9
2   Generate all subsets of FS*_m(δ) and save to Ext*_k
3 End // Begin
```

Example 12. This example is given to demonstrate how the proposed IIS-Mine algorithm can be used to mine all frequent itemsets. Assume *minsup* = 3 for all of the definitions above, and for Examples 1-3, Figure 2 and Algorithm 3. For simplicity, this example is divided into five main steps ordered by five frequent items in the IIS. The proposed mining algorithm proceeds as follows.

Let step 1 be the first main step. According to Procedure AllFreqItemset, the frequent item *a* is the first frequent item in the IIS that is mined. The *IIS$_a$Tree* is constructed, as illustrated in Figure 2(a). The algorithm calls Procedure IIS-Mine, so Procedure Subheader is called in order. The SH(*a*) is (*c*,*f*,*m*), where *supp*(*c*) = 3, *supp*(*f*) = 3 and *supp*(*m*) = 3. After line 3 in the procedure, IIS-Mine generates all of the frequent itemsets with its support, i.e. *ac*, *af* and *am*; all of these frequent itemsets have support equal to three. Let steps 1.1, 1.2 and 1.3 represent each of the frequent itemsets.

The step 1.1, the first frequent itemset is *ac*, which has support equal to three. The algorithm checks |*ac*|>1 and then calls Procedure SkipFreqItem. At this procedure, *ac* is not in FI_2^*, so the algorithm rolls back to line 9 of Procedure IIS-Mine. The frequent itemset *ac* with its support is defined to be the root; then, the conditional *ac*-tree, which has root "<*ac*:3>", is constructed using the input *IIS$_a$Tree*. The conditional *ac*-tree is illustrated in Figure 4. The algorithm is iterated by calling Procedure IIS-Mine again because the conditional *ac*-tree contains more than two nodes; let this call be step 1.1.1.

In step 1.1.1, the Procedure IIS-Mine is called; SH(*ac*) = (*f*,*m*), where *supp*(*f*) and *supp*(*m*) are then equal to 3. At line 3, the algorithm generates frequent itemsets, which are *acf* and *acm*, where *supp*(*acf*) and *supp*(*acm*) are then equal to 3. The first frequent itemset in this step is *acf* and $|acf|>1$, so the procedure SkipFreqItem in line 7 is processed, and it finds that *acf* is not in FI_3^*. Next, the algorithm rolls back to line 9 to construct a conditional *acf*-tree that has a conditional *ac*-tree as an input tree, which is illustrated in Figure 5. The condition of line 13 is that the conditional *acf*-tree contains only two nodes, so the algorithm obtains $FS_4^*(acfm) = acfm$. At line 18, the size of $FS_4^*(acfm)$ is greater than three and $FS_4^*(acfm) \notin FI_4^*$. Thus, at line 19, Procedure ExtFreqItemset is called to find all of the subsets of $FS_4^*(acfm)$, which are $Ext_2^*(acfm)$ and $Ext_3^*(acfm)$: $Ext_2^*(acfm)$ = {*ac*, *af*, *am*, *cf*, *cm*, *fm*} and $Ext_3^*(acfm)$ = {*acf*, *acm*, *afm*, *cfm*}; hence, FI_2^* = {*ac*, *af*, *am*, *cf*, *cm*, *fm*}, FI_3^* = {*acf*, *acm*, *afm*, *cfm*}, and FI_4^* = {*acfm*}.

In step 1.1.2, the next frequent itemset generated together with step 1.1.1 is *acm*. At line 7 of Procedure IIS-Mine, the algorithm calls Procedure SkipFreqItem and obtains *acm*, which is already a

member of FI_3^*; *m* is the last frequent item in SH(*ac*), so we exit from this step without the construction of a conditional *acm*-tree.

In step 1.2, at line 4 of Procedure IIS-Mine, the next frequent itemset is *af*, and at line 7, Procedure SkipFreqItem is called and obtains *af*, which is contained in FI_2^*. In the loop in line 20 of Procedure SkipFreqItem, after *af* is combined with the next frequent item in SH(*a*), which is *m*, *afm* is obtained, which is contained in FI_3^*, and item *m* is the last item in SH(*a*). The algorithm rolls back to line 8 of Procedure IIS-Mine, so the conditional *af*-tree is not constructed.

In step 1.3, at line 4 of Procedure IIS-Mine, the next frequent itemset is *am*. At line 7, Procedure SkipFreqItem is called and obtains *am*, which is contained in FI_2^*, and there is no frequent item in SH(*a*). Therefore, the conditional *am*-tree is not constructed.

Let step 2 be the second main step. According to line 2 of Procedure AllFreqItemset, *b* is the second frequent item in the IIS that is mined. After line 4, the IIS_bTree is constructed, as illustrated in Figure 2(b). The algorithm calls Procedure IIS-Mine at line 6. At line 2 of Procedure IIS-Mine, Procedure Subheader is called and obtains an empty SH(*b*), so the size of the frequent itemset generated with *b* is one. The processing of this step is terminated, and we return to line 2 of Procedure AllFreqItemset.

Let the third main step be step 3. According to line 2 of Procedure AllFreqItemset, *c* is the third frequent item in IIS that is mined. Line 4 is called to construct the IIS_cTree, as illustrated in Figure 2(c). At line 6, the algorithm calls Procedure IIS-Mine to mine frequent itemsets. At line 2 of Procedure IIS-Mine, Procedure Subheader is called to obtain the SH(*c*) that is (*f*,*m*,*p*). Next, at line 3, the algorithm generates frequent itemsets, which are *cf*, *cm* and *cp*, where *supp*(*cf*), *supp*(*cm*) and *supp*(*cp*) = 3. Let steps 3.1, 3.2 and 3.3 represent each of the frequent itemsets.

In step 3.1, at line 4 of Procedure IIS-Mine, the first frequent itemset is *cf*, where $|cf| > 1$; line 7 then calls Procedure SkipFreqItemset. At Procedure SkipFreqItemset, *cf* combines with the next frequent item in SH(*c*), which is *m*, so *cfm* with a support of 3 is obtained after processing lines 19-23. Next, line 8 is checked, and as *cfm* is already obtained in FI_3^*, lines 19-23 are checked again, and *cfmp* is obtained. The frequent itemset *cfmp* is not a member in FI_4^*, and *p* is the last frequent item in SH(*c*), so *cfm* is set to be a root for a conditional *cfm*-tree. The algorithm goes back to line 8 of Procedure IIS-Mine to construct a conditional *cfm*-tree, where the IIS_cTree is an input tree, which is illustrated in Figure 6. *Supp*(*p*) is less than *minsup*, hence $FS_3^*(cfm) = cfm$. Procedure ExtFreqItemset in line 18 is not called because $FS_3^*(cfm)$ is contained in FI_3^*. In this step, the algorithm skips the construction of the conditional *cf*-tree.

In step 3.2, according to line 4 of Procedure IIS-Mine, the next frequent itemset is *cm*, and Procedure SkipFreqItemset in line 7 is called. Line 8 of Procedure SkipFreqItemset checks that *cm* is a member in FI_2^*. Next, lines 19-23 are checked, so *cm* combines with the next item in SH(*c*), which is *p*, and we obtain *cmp* with a support of 3. The frequent itemset *cmp* is not in FI_3^*, and *p* is the last frequent item in SH(*c*), so *cm* is set to be a root for a conditional *cm*-tree. The algorithm goes back to line 8 of Procedure IIS-Mine to construct a conditional *cm*-tree, where the IIS_cTree is an input tree, which is illustrated in Figure 7. *Supp*(*p*) is less than *minsup*, hence $FS_2^*(cm) = cm$ and $FS_2^*(cm)$ are already members in FI_2^*.

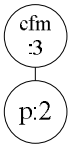

Figure 6. Conditional *cfm*-tree

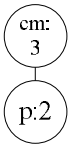

Figure 7. Conditional *cm*-tree

In step 3.3, according to line 4 of Procedure IIS-Mine, the next frequent itemset is *cp*. Next, at line 5, Procedure SkipFreqItemset is called, and *cp* is not a member in FI_2^*. There is no frequent item in SH(*c*), so this procedure is terminated, and we return to line 8 of Procedure IIS-Mine. After lines 22-23 are checked, the new answer is contained in FI_2^*, which is *cp*. This step skips the construction of a conditional *cp*-tree.

The remaining steps such as the fourth main step, which constructs the *IIS$_f$Tree* and is illustrated in Figure 2(d), and the fifth main step, which constructs the *IIS$_m$Tree* and is illustrated in Figure 2(e), are performed in the same way in sequence.

The complete frequent itemsets are shown by item in Table 2 and by length in Table 3.

Table 2. Complete frequent itemsets by item

Item	Frequent itemset
a	*a*, *acfm*, *ac*, *af*, *am*, *cf*, *cm*, *fm*, *acf*, *acm*, *amf*, *cfm*
b	*b*
c	*c*, *cp*
f	*f*
m	*m*
p	*p*

Table 3. Complete frequent itemsets by length

m-Length	Frequent itemset
1	*a*, *b*, *c*, *f*, *m*, *p*
2	*ac*, *af*, *am*, *cf*, *cm*, *cp*, *fm*
3	*acf*, *acm*, *afm*, *cfm*
4	*acfm*

The advantages of our algorithm are as follows. First, according to step 1.1.1 of Example 12, the frequent itemsets *acfm* are obtained, which are derived from a conditional *acf*-tree. This step shows the properties of an extendable frequent itemset*, which are given in Definition 9 and Procedure ExtFreqItemset in Algorithm 3. This step then finds all of the subsets of *acfm*, so we derive ten frequent itemsets, which are *ac*, *af*, *am*, *cf*, *cm*, *fm*, *acf*, *acm*, *amf* and *cfm*, without contributing more trees or using recursion to mine. Therefore, our algorithm can reduce many

subsequent steps in mining frequent itemsets. It can be noticed that if $|FS_m^*(Ax)|$ is large, then the property of an extendable frequent itemset* is frequently used. Second, the method is also good for reducing run time and space consumption, and its performance will be shown in the experimental section. Last, according to step 3.1 of Example 12, the conditional *cfm*-tree is obtained, which reduces one node in the tree because of the step that sets frequent itemsets as the root node in Procedure SkipFreqItemset in Algorithm 3. The algorithm reduces the number of nodes, levels and size of the tree, thus reducing space consumption. In general, users change many minimum support thresholds to make their decision. Our method, which uses an IIS and the restart algorithm shown in Algorithm 3, supports the ability to make these changes without rescanning the database.

Correctness

The following theorem and proof are given to demonstrate that the proposed IIS-Mine algorithm can mine frequent itemsets completely and correctly.

Theorem: The set of all frequent itemsets* derived from IIS-Mine is the complete set of all of the frequent itemsets.

Proof: Let *I* be the nonempty finite set of all items in a given transaction database, *FI* denote the set of all frequent itemsets in the transaction database, and $\alpha = minsup > 0$. It must be proved that $FI = FI^*$.

First, we prove that $FI \subseteq FI^*$. Let $F = \{a_1,...,a_k\} \in FI$ with $a_1 <_l ... <_l a_k$, and $s_i = supp\{a_1,...,a_i\}$ for all $i = 1,...,k$. Then, $s_1 \geq ... \geq s_k \geq \alpha$, and an item b exists such that $b \geq a_1$, and $IIS_b tree$ contains $a_1,...,a_k$. It can be assumed that b is the item in *I* having these properties because *I* is the nonempty finite set of all items. Because $s_i \geq ... \geq s_k \geq \alpha$ for all $i = 1,...,k$, there exists a path $((b_1 : s_1'),...(b_l : s_l'))$ of $IIS_b tree$ containing $(a_1 : s_1),...,(a_k : s_k)$; that is, for all $i = 1,...,k$, there exists $j = 1,...,l$ such that $(a_i : s_i) = (b_j : s_j)$. It is obvious from the IIS-Mine algorithm that $FI \subseteq FI^*$.

We also show that $FI^* \subseteq FI$. Let $F = \{a_1,...,a_k\} \in FI^*$ with $a_1 <_l ... <_l a_k$. Then, for some positive integer *m*, $F \in FI_m^*$. It is evident from definition 10 that if $m = 1$, $F \in FI_m^*$ implies $F \in FI$. Now, suppose $m \geq 2$; then, $F \in FI_m^*$ or $F \in Ext_m^*$. In the first case, $F \in FS_m^*$, and from Definition 8, $SH\{a_1,\ldots,a_{k-1}\}=(a_k)$ or the conditional $\{a_1,...,a_{k-1}\}a_k$ tree contains exactly two nodes, $(\{a_1,...,a_{k-1}\} : s_{k-1})$ and $(a_k : s_k)$, where $s_i = supp\{a_1,...,a_i\}$ for $i = k-1, k$. Then from definitions 7 and 8, we obtain $\{a_1,...,a_{k-1}\}a_k = \{a_1,...,a_k\} = F \in FI$. In the other case, suppose that $F \in Ext_m^*$ for $m \geq 2$. Then from definition 9, an Ax exists such that $F \in Ext_m^*(Ax)$, and Ax is a frequent itemset* of length at least *m* derived from the conditional *Ax*-tree. Again, from definition 9, a positive integer *k* greater than 2 exists such that *F* has itemsets containing precisely *m* items of $FS_k^*(Ax)$, and from definitions 6 and 8, $FS_k^*(Ax)$ is a frequent itemset, hence $F \in FI$. The proof is complete.

RESULTS AND DISCUSSION

We have presented the experiments in which the run time, memory consumption and scalability are tested for the IIS-Mine algorithm and FP-growth algorithm with different datasets and varying minimum support thresholds. The experiments were performed on a Microsoft Windows XP

Professional Version 2002 Service Pack 3 operating system on a personal computer with 1 GB of main memory and Pentium (R) CPU 3.00 GHz. All algorithms were coded using C language. Two groups of benchmark datasets, i.e. two synthetic datasets and two real datasets, were used.

For the first group of datasets, we also presented the experimental results for two synthetic datasets generated by the IBM Almaden Quest research group [24-25]. The datasets serve as the FIMI repository, which is a result of the workshops on frequent itemset mining implementations [26, 27]. The two original databases of synthetic datasets are T10I4D100K and T40I10D100K, which are sparse datasets. The notation *TxIyDzK* denotes a dataset where *K* is 1,000 transactions. Table 4 lists the parameters of the synthetic datasets, which vary in the number of transactions, i.e. 20%, 40%, 60% and 80% of the original database.

Table 4. Parameters of the synthetic datasets

$\|T\|$	Average number of items per transaction
$\|I\|$	Average length of a frequent itemset
$\|D\|$	Number of transactions

For the second group of datasets, the real datasets from the UCI machine learning repository [28] were used to test the proposed method. The real datasets used in the experiment were Chess [29] and Mushroom [30], which are dense datasets with a great number of long frequent itemsets. The characteristics of the real datasets are shown in Table 5.

Table 5. Characteristics of real datasets

Real dataset	Description
Chess	Average number of items per transaction = 37, number of transactions = 3,196, and number of items = 75
Mushroom	Average number of items per transaction = 23, number of transactions = 8,124, and number of items = 119

Run Time

Figures 8(a) and 8(b) show the performance of the algorithms on two synthetic datasets, T10I4D100K and T40I10D100K respectively. In Figure 8(a), IIS-Mine performs better than FP-growth in every support threshold. The gap in the graph becomes larger as the support threshold decreases. In Figure 8(b), when the minimum support is set at 20%, 17.5%, 15% or 12.5%, the run time between the two algorithms is not very different. However, when the minimum support is set at 10%, 7.5% or 5%, the run time of FP-growth increases significantly when compared to that of IIS-Mine, which confirms that IIS-Mine performs better than FP-growth. The results shown in Figures 8(a) and 8(b) can be explained as follows. With sparse datasets, when the minimum support is high, the number of frequent itemsets is low. However, when the minimum support is low, many frequent itemsets are obtained. IIS-Mine is always faster than FP-growth method, especially when the

minimum support is low, because FP-growth constructs bushy and wide FP-trees when the minimum support is low. So FP-growth is computationally expensive for tree traversing the FP-trees. IIS-Mine has the step of finding the root node from previous frequent itemsets, which can reduce the number of nodes and levels of the conditional itemset-tree. Therefore, traversing in the conditional itemset-tree is on a reduced tree, which can result in a low run time consumption. However, the run time of both algorithms relies on the length of the transaction (as observed in a comparison of the graphs in Figures 8(a) and 8(b) with a minimum support of 5%); when the transaction is long, so it the run time of both algorithms.

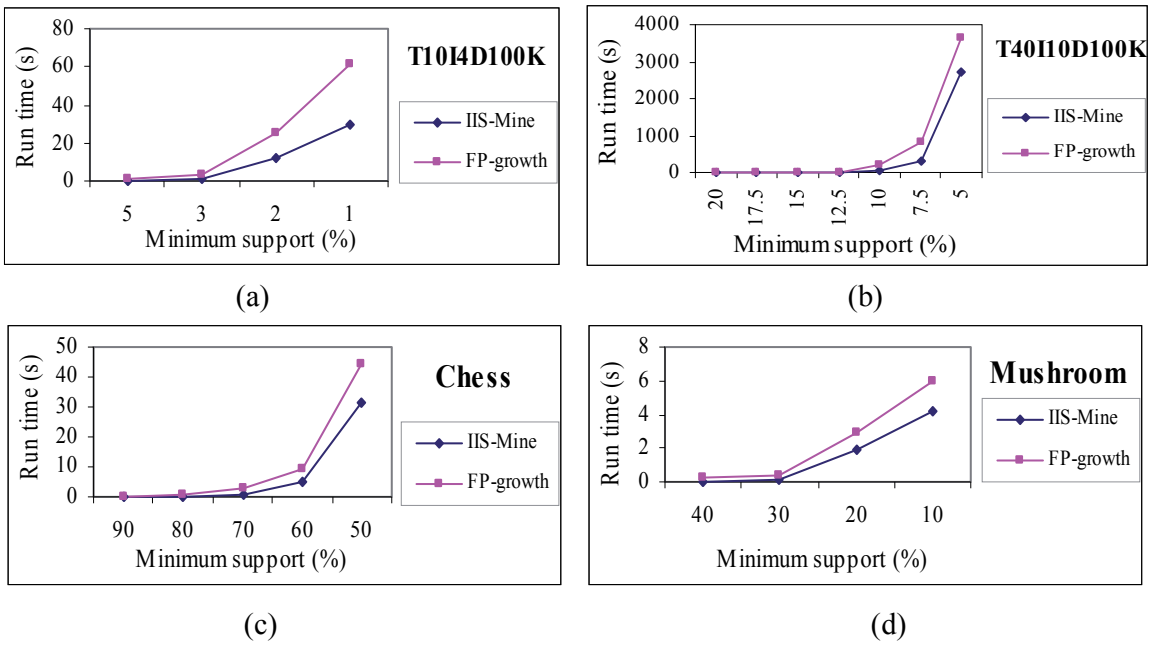

Figure 8. Run time of mining on: a) T10I4D100K; b) T10I4D100K; c) Chess; d) Mushroom

Figures 8(c) and 8(d) show the performance of algorithms on two dense datasets: chess and mushroom. Figure 8(c) shows that the run time of IIS-Mine is better than that of FP-growth in every support threshold. The run time of both algorithms increases when the minimum support threshold is reduced to 50%. In Figure 8(d), IIS-Mine again performs better than FP-growth in every minimum support. The run time of FP-growth increases significantly compared with IIS-Mine when the minimum support is less than 30%. The results shown in Figures 8(c) and 8(d) can be explained as follows. In the two Figures, IIS-Mine is faster than FP-growth for dense datasets. The main work in FP-growth is traversing FP-trees and constructing new conditional FP-trees after the first FP-tree is constructed from the original database. For dense datasets, we have found from numerous experiments that the time spent on traversing FP-trees is very long. IIS-Mine improves this problem using the property of extendable itemsets to reduce the number of recursive mining steps so that the size and number of constructing and traversing the trees are reduced. The run time of IIS-Mine is then less than that of FP-growth.

Memory Consumption

Figures 9(a) and 9(b) show the memory consumption of the algorithms on the synthetic datasets. In Figure 9(a), FP-growth consumes more memory than IIS-Mine. The graphs clearly separate out when the minimum support is less than 3%. In Figure 9(b), there is no difference in memory consumption until the minimum support is less than 15%. Thus, we can see that IIS-Mine consumes less memory than FP-growth on synthetic datasets. The large memory consumption of FP-growth when running on synthetic datasets can be explained by the fairly low minimum support and the presence of many single items in the datasets; therefore, FP-growth constructs wide and bushy trees to mine all frequent itemsets. However, IIS-Mine uses the property of extendable itemsets, which reduces the construction of conditional itemset-trees, and uses the step of finding the root node from previous frequent itemsets. Therefore, the node construction and tree sizes are reduced, resulting in a reduction in memory consumption.

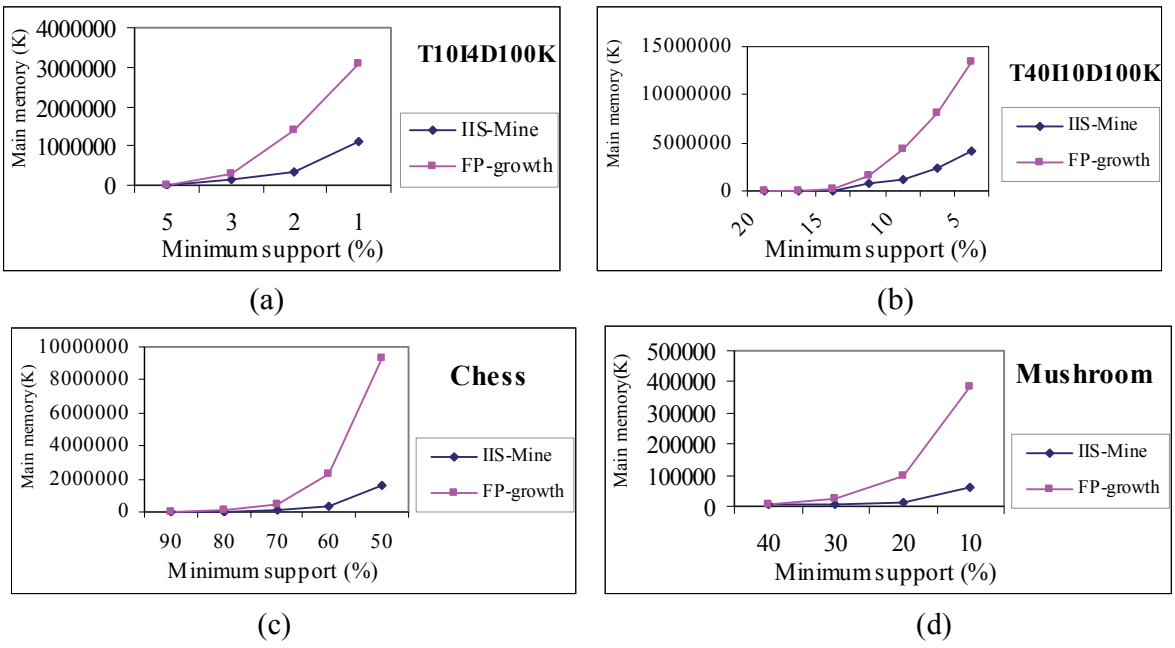

Figure 9. Memory consumption of mining on: a) T10I4D100K; b) T40I10D100K; c) Chess; d) Mushroom

Figures 9(c) and 9(d) show that the memory consumption of IIS-Mine is less than that of FP-growth on dense datasets. Figure 9(c) shows that when the minimum support is less than 80%, the memory consumption of FP-growth increases significantly compared with that of IIS-Mine. Figure 9(d) also shows that when the minimum support is less than 30%, the gap of the graphs clearly widens, which confirms that FP-growth consumes more memory than IIS-Mine. In both figures, FP-growth consumes a great deal more memory when the minimum support is low because FP-growth has constructed large FP-trees for mining all frequent itemsets, whereas IIS-Mine uses the property of extendable itemsets, which perform better for dense datasets. Consequently, the recursion of

mining frequent itemsets in the next loops is reduced. Therefore, the construction of nodes and the sizes of the conditional item-trees are reduced.

Scalability

The scalability of the algorithms was tested by running them on datasets generated from T10I4 and T40I10. The number of transactions in the datasets ranged from 20*K* to 100*K*, where *K* is 1000 transactions. In Figure 10(a) and Figure 11(a), the algorithms were run on all of the datasets generated from T10I4 at a minimum support of 1%. Both run time and memory consumption were recorded. Figure 10(a) shows the speed scalability, which means that the number of transactions increases as the run time increases. Figure 11(a) shows the memory scalability of the algorithms; the curve of FP-growth is over that of IIS-Mine, which means that FP-growth consumes more memory than IIS-Mine. The figure also shows that the memory consumption of the algorithms increases linearly with the size of the datasets.

In Figures 10(b) and 11(b), the algorithms were run on all of the datasets generated from T40I10 at a minimum support of 5%. Both run time and memory consumption were recorded. Figure 10(b) confirms that the run time of both algorithms relies on the length and number of transactions: if the length or number of transactions increases, so does the run time of both algorithms. However, the run time of IIS-Mine was better than that of FP-growth for every number of transactions. Figure 11(b) confirms that the memory consumption of the algorithms increases with the length and number of transactions. However, the memory consumption of IIS-Mine was better than that of FP-growth for every number of transactions.

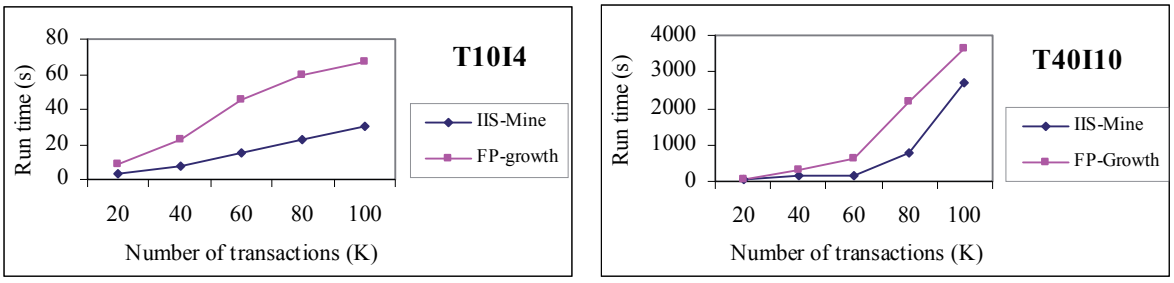

(a) (b)

Figure 10. Scalability of runtime on a) T10I4; b) T40I10

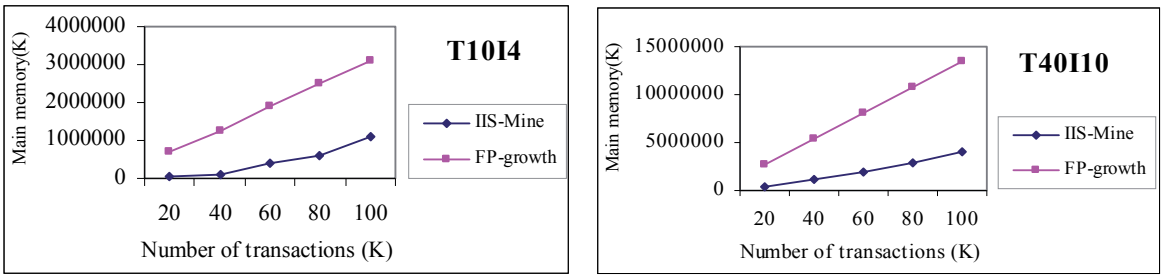

(a) (b)

Figure 11. Scalability of memory consumption on: a) T10I4; b) T40I10

CONCLUSIONS

A data structure called inverted index structure (IIS) can store transaction data by scanning a database only once. Changing the minimum support does not affect the IIS and rescanning of the database is not required. A new algorithm called IIS-Mine can find frequent itemsets without generating candidate itemsets. It employs a more efficient use of the extendable-itemset property to reduce the number of recursive steps of mining. The node construction and the size of trees are then reduced, thereby reducing the run time and memory consumption. Although the proposed method accesses the IIS structure multiple times, experimental results demonstrated that for dense datasets the IIS-Mine algorithm is better than FP-growth algorithm in run time and space consumption.

ACKNOWLEDGEMENTS

This work was supported by the National Centre of Excellence in Mathematics, PERDO, Office of the Higher Education Commission, Thailand.

REFERENCES

1. J. Han and M. Kamber, "Data Mining: Concepts and Techniques", Elsevier, Maryland Heights (MO), **2006**, pp.227-231.
2. J. Han, J. Pei, Y. Yin and R. Mao, "Mining frequent patterns without candidate generation: A frequent-pattern tree approach", *Data Mining Knowl. Discov.*, **2004**, *8*, 53-87.
3. G. Grahne and J. Zhu, "Fast algorithms for frequent itemset mining using FP-Trees", *IEEE Trans. Knowl. Data Eng.*, **2005**, *17*, 1347-1362.
4. R. Agrawal, T. Imielinski and A. Swami, "Mining association rules between sets of items in large databases", Proceedings of ACM SIGMOD International Conference on Management of Data, **1993**, Washington, DC, USA, pp.207-216.
5. R. Agrawal and R. Srikant, "Fast algorithms for mining association rules", Proceedings of 20th International Conference on Very Large Data Bases, **1994**, Santiago de Chile, Chile, pp.487-499.
6. T. H. N. Vu, J. W. Lee and K. H. Ryu, "Spatiotemporal pattern mining technique for location-based service system", *ETRI J.*, **2008**, *30*, 421-431.
7. J. Han, J. Pei and Y. Yin, "Mining frequent patterns without candidate generation", Proceedings of ACM SIGMOD International Conference on Management of Data, **2000**, Dallas (TX), USA, pp.1-12.
8. J. Pei, J. Han, H. Lu, S. Nishio, S. Tang and D. Yang, "H-mine: Hyper-structure mining of frequent patterns in large databases", Proceedings of IEEE International Conference on Data Mining, **2001**, San Jose (CA), USA, pp.441-448.
9. A. Pietracaprina and D. Zandolin, "Mining frequent itemsets using Patricia tries", Proceedings of 3rd IEEE International Conference on Data Mining, **2003**, Melbourne (FL), USA.
10. G. Grahne and J. Zhu, "Efficiently using Prefix-Trees in mining frequent itemsets", Proceedings of 3rd IEEE International Conference on Data Mining, **2003**, Melbourne (FL), USA.

11. Q. Zhu and X. Lin, "Depth first generation of frequent patterns without candidate generation", Proceedings of 11th Pacific-Asia Conference on Knowledge Discovery and Data Mining, **2007**, Nanjing, China, pp.378-388.
12. S. Sahaphong and V. Boonjing, "The combination approach to frequent itemsets mining", Proceedings of 3rd International Conference on Convergence and Hybrid Information Technology, **2008**, Busan, Korea, pp.565-570.
13. V. K. Shrivastava, P. Kumar and K. R. Padasani, "FP-tree and COFI based approach for mining of multiple level association rules in large database", *Int. J. Comp. Sci. Inf. Secur.*, **2010**, *7*, 273-279.
14. L. Huang, J. Z. Liang, Y. Pan and Y. Xian, "A complete attribute reduction algorithm based on improved FP tree", Proceedings of International Conference on Circuits, Communications and System, **2010**, Beijing, China, pp.1-4.
15. U. Yun and K. H. Ryu, "Approximate weighted frequent pattern mining with/without noisy environments", *Knowl.-Based Syst.*, **2011**, *24*, 73-82.
16. M. J. Zaki, "Scalable algorithms for association mining", *IEEE Trans. Knowl. Data Eng.*, **2000**, *12*, 372-390.
17. M. J. Zaki and K. Gouda, "Fast vertical mining using diffsets", Proceedings of 9th ACM SIGKDD International Conference on Knowledge Discovery and Data Mining, **2003**, Washington, DC, USA, pp.236-355.
18. D. J. Chai, L. Jin, B. Hwang and K. H. Ryu, "Frequent pattern mining using bipartite graph", Proceedings of 18th International Conference on Database and Expert Systems Applications, **2007**, Regensburg, Germany, pp.182-186.
19. J. Dong and M. Han, "BitTableFI: An efficient mining frequent itemsets algorithm", *Knowl.-Based Syst.*, **2007**, *20*, 329-335.
20. W. Yen, "A new mining algorithm based on frequent item sets", Proceedings of International Workshop on Knowledge Discovery and Data Mining, **2008**, Adelaide, Australia, pp.410-413.
21. W. Song, B. Yang and Z. Xu, "Index-BitTableFI: An improved algorithm for mining frequent itemsets", *Knowl.-Based Syst.*, **2008**, *21*, 507-513.
22. S. Sahaphong and V. Boonjing, "Mining of frequent itemsets by using the property of extendable-itemset", Proceedings of 7th International Joint Conference on Computer Science and Software Engineering, **2010**, Bangkok, Thailand, pp.168-173.
23. S. Sahaphong and G. Sritanratana, "Mining of frequent itemsets with JoinFI-Mine algorithm", Proceedings of 10th WSEAS International Conference on Artificial Intelligence, Knowledge Engineering and Database, **2011**, Cambridge, United Kingdom, pp.73-78.
24. Frequent Itemset Mining Dataset Repository, "T10I4D100K", http://fimi.cs.helsinki.fi/data/, **2003** (Accessed: January 11, 2010).
25. Frequent Itemset Mining Dataset Repository, "T40I10D100K", http://fimi.cs.helsinki.fi/data/, **2003** (Accessed: January 11, 2010).
26. Workshop on Frequent Itemset Mining Implementations, http://fimi.ua.ac.be/fimi03/, **2003** (Accessed: January 2, 2010).

27. Workshop on Frequent Itemset Mining Implementations, http://fimi.ua.ac.be/fimi04/, **2004** (Accessed: January 2, 2010).
28. UCI Machine Learning Repository, http://archive.ics.uci.edu/ml/, **2007** (Accessed: March 15, 2010).
29. UCI Machine Learning Repository, "Chess", http://archive.ics.uci.edu/ml/datasets.html, **1989** (Accessed: July 19, 2010).
30. UCI Machine Learning Repository, "Mushroom", http://archive.ics.uci.edu/ml/datasets.html, **1987** (Accessed: July 19, 2010).

Maejo Int. J. Sci. Technol. **2012**, *6*(01), 152-158

Maejo International Journal of Science and Technology

ISSN 1905-7873
Available online at www.mijst.mju.ac.th

Communication

Lipase-catalysed sequential kinetic resolution of *α*-lipoic acid

Hong De Yan [1], Yin Jun Zhang [1], Li Jing Shen [2] and Zhao Wang [1,*]

[1] College of Biological and Environmental Engineering, Zhejiang University of Technology, Hang Zhou 310014, People's Republic of China
[2] Jiaxing Vocational and Technical College, Jiaxing 314036, Zhejiang, People's Republic of China

* Corresponding author, e-mail: hzwangzhao@163.com

Received: 16 April 2011 / Accepted: 18 April 2012 / Published: 30 April 2012

Abstract: Lipase from *Aspergillus* sp. WZ002 was employed to kinetically resolve racemic *α*-lipoic acid by a sequential esterification process. Though the remoteness of this substrate's stereocentre from the reaction centre provided a significant challenge, the introduction of sequential kinetic resolution dramatically enhanced the lipase's enantioselectivity for esterification at the terminal carbonyl group, producing the desired (*R*)-enantiomer virtually enantiomerically pure. The enantiomeric excess of the (*R*)-enantiomer increased from 52% in the first step to 92% for in second step.

Keywords: esterification, lipase-catalysed reactions, *α*-lipoic acid, sequential kinetic resolution

INTRODUCTION

(*R*)-*α*-Lipoic acid is a naturally occurring cofactor of several *α*-keto acid dehydrogenases and a growth factor for a variety of microorganisms [1-3]. It has also been reported that *α*-lipoic acid and its derivatives are highly active as an anti-oxidant [4], anti-inflammatory agent [5], anti-HIV [6] and anti-tumour [7]. Generally, the (*R*)-enantiomer is much more active than the (*S*)-enantiomer [8], which has fostered significant interest in stereoselective synthesis of the pure enantiomers. Chemical synthesis of (*R*)- and (*S*)-*α*-lipoic acid has been achieved either from a 'chiral pool' starting material [9] or by asymmetric synthesis [10-11]. Alternative methods involving enzyme catalysis include Bakers' yeast reduction [12], mono-oxygenase catalysis [13] and lipase-catalysed kinetic resolution [14-15]. *α*-Lipoic acid provides a significant challenge due to the remoteness of stereocentre located four carbon atoms away from the reaction centre (carboxylic group). Lipases from *Aspergillus oryzae* WZ007 [14] and

Candida rugosa [15] show enantionselectivity towards the (*S*)-enantiomer, leaving the target (*R*)-α-lipoic acid in unreacted form. In this study, the tested lipases show opposite enantionselectivity towards the (*R*)-enantiomer (Table 1) although with a low enantiomeric excess. In order to improve the enantiomeric purity, a sequential kinetic resolution was undertaken (Scheme 1). Herein we report on a successful application of sequential biocatalytic resolution of (*R*)-α-lipoic acid with high enantiomeric purity.

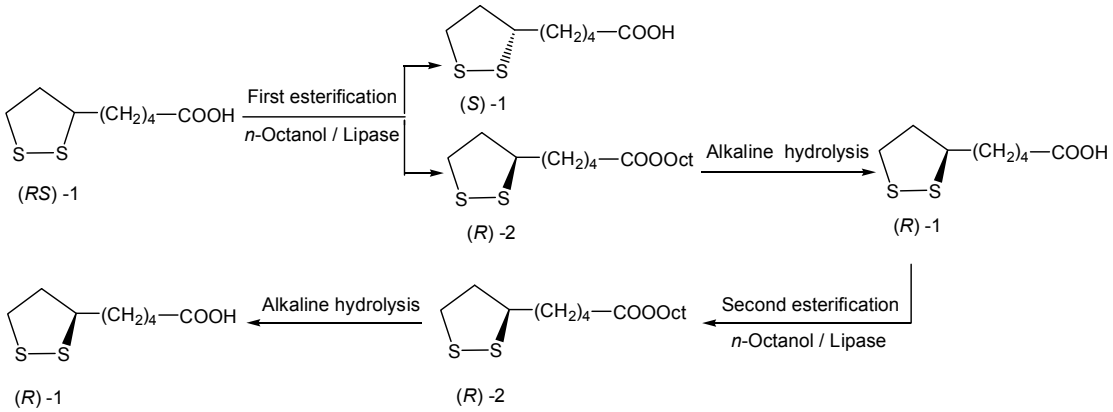

Scheme 1. Sequential kinetic resolution of α-lipoic acid ((*RS*)-1) with lipase

MATERIALS AND METHODS

Chemicals and Reagents

α-Lipoic acid (purity≥98.0%) was purchased from Fluka BioChemika (Switzerland). (*R*)-α-lipoic acid (purity≥98.0%) was purchased from Aladdin Reagent (China). Porcine pancreas lipase (Type II) was purchased from Sigma (USA). Nov 435 (an immobilised lipase from *Candida antartica*) and Lip□ TL (an immobilised lipase from *Thermomyces lanuginosus*) were purchased from Novozymes (Denmark). Lipase from *Penicillium expansum* was purchased from Shenzhen Leveking Bio-engineering (China). All other chemicals were obtained from commercial sources and were of analytical reagent grade.

Production of Lipase from *Aspergillus* sp. WZ002

The strain WZ002 of *Aspergillus* sp., isolated from carrion and conserved in our laboratory, was maintained on potato dextrose agar (PDA) medium. A sequence analysis revealed that the internal transcribed spacer (ITS) DNA sequence of the strain WZ002 (GenBank accession no. JQ670919) showed high similarity (100% homology) to 47 strains of *Aspergillus* sp. The strain WZ002 was therefore primarily identified as a strain of *Aspergillus* sp. The culture was grown aerobically at 30°C and 200 rpm for 48 hr in cell growth medium consisting of glucose (10 g/L), peptone (5 g/L), KH_2PO_4 (1 g/L), $MgSO_4 \cdot 7H_2O$ (0.5 g/L), $FeSO_4 \cdot 7H_2O$ (0.01 g/L), KCl (0.5 g/L) and olive oil (10 mL/L). After harvesting by filtration, cells were washed with 100 mM Tris-HCl buffer (pH 7.3) and then freeze-dried. The lyophilised microbial cells (intracellular lipase) were used to catalyse the esterification reaction.

Screening of Lipase

Lipase from *Aspergillus* sp. WZ002 (ASL), porcine pancreas lipase (PPL), lipase from *Penicillium expansum* (PEL), lipase from *Candida antartica* (Nov 435) and lipase from *Thermomyces lanuginosus* (Lip TL) were investigated in the catalysis of the esterification of α-lipoic acid with *n*-octanol [14]. The reaction mixture was made of α-lipoic acid (206 mg, 1 mmol), *n*-octanol (0.79 mL, 5 mmol), heptane (20 mL) and an appropriate amount of lipase. The reaction mixture was shaken at 200 rpm and after a specified time the reaction was quenched by removing enzyme particles through centrifugation. Unreacted α-lipoic acid was extracted with 0.5% $NaHCO_3$ and recovered with dichloromethane after acidification with 20% HCl. Dichloromethane was removed by vacuum distillation and the recovered α-lipoic acid was analysed by high performance liquid chromatography (HPLC).

Effect of Time on ASL-catalysed Esterifying Reaction

To investigate the effect of time on the conversion ratio and enantiomeric excess of (*R*)-1 at the first step of the esterification reaction (Scheme 1), the reaction mixture consisting of α-lipoic acid (206 mg, 1 mmol), *n*-octanol (0.79 mL, 5 mmol), heptane (20 mL) and ASL (400 mg) were shaken at 200 rpm and 40°C for 48, 60, 72 and 84 hr. Unreacted α-lipoic acid was extracted with 0.5% $NaHCO_3$, and the solvent of the resulting upper organic phase was removed by vacuum distillation to enrich ester (*R*)-2, which was hydrolysed to the corresponding (*R*)-1 by alkaline hydrolysis. The resulting enriched (*R*)-1 was subjected to HPLC analysis.

Sequential Kinetic Resolution

The esterification reaction was carried out at 200 rpm and 40°C on a shaker. The reaction mixture was made up of α-lipoic acid (206 mg, 1 mmol), *n*-octanol (0.79 mL, 5 mmol), heptane (20 mL) and ASL (400 mg). The reaction was quenched after 84 hr. Unreacted α-lipoic acid was extracted with 0.5% $NaHCO_3$ and the solvent of the resulting upper organic phase was removed by vacuum distillation to enrich ester (*R*)-2. The ester was dissolved in 20 mL of 95% ethanol and mixed with 150 mg of NaOH. The mixture was stirred for 6 hr at room temperature. The solvent was removed by vacuum distillation and the residue was partitioned with 10 mL of heptane and 20 mL of distilled water. The resulting aqueous phase was acidified by 20% HCl. The enriched (*R*)-1 was obtained by extraction with dichloromethane from the acidified solution.

(*R*)-1 was then subjected to a second enzymatic resolution by the same procedure.

Analysis

An Agilent 1100 HPLC with a Chiralpak AS-H column (250 mm×4.6 mm, 5 μm, Daicel) was used to analyse the conversion ratio and enantiomeric excess of α-lipoic acid. Hexane:2-propanol:trifluoroacetic acid (97:3:0.1) was used as eluent at a flow-rate of 0.8 mL/min. Absorbance of column effluent was monitored at 220 nm [14]. The two enantiomers of α-lipoic acid were identified in the HPLC chromatogram by their different retention times using optically pure (*R*)-α-lipoic acid as reference compound. The enantiomeric ratios (*E*) were calculated using the following equations [16]: $E = \ln[(1-c)(1-ee_S)]/\ln[(1-c)(1+ee_S)]$, $c = [(c_0-c_e)/c_0]\times100\%$, $ee_S = [([S]-[R])/([S]+[R])]\times100\%$, $ee_R =$

$[([R]-[S])/([S]+[R])]\times100\%$, where c is the conversion ratio of reaction, c_0 is the initial amount of racemic α-lipoic acid, c_e is the amount of residual α-lipoic acid at the end of reaction, ee_S is the enantiomeric excess of the residual α-lipoic acid, and $[R]$ and $[S]$ are the peak areas for (*R*)-α-lipoic acid and (*S*)-α-lipoic acid respectively.

RESULTS AND DISCUSSION

Screening of Lipase

The results were summarised in Table 1. All lipases tested showed (*R*)-stereopreference and considerable conversion ratio, but the enantiomeric ratios (*E*) of the transformations were very low. After 84 hr of transformation with ASL (59.2% conversion), the ester (*R*)-2 was separated from the unreacted substrate (*S*)-1; then the ester (*R*)-2 was hydrolysed under alkaline conditions to yield the corresponding (*R*)-1 enantiomer (ee_R 52.4%) (Scheme 1, Figure 1). PPL and PEL afforded 64.3% and 57% ee_S of the unreacted substrate ((*S*)-1) at 90.1% and 79.8% conversion respectively, and their *E*-values were close to 2.0. When immobilised Nov 435 and Lip TL were used, a high activity (>72% conversion after 1 hr) was observed, but the unreacted enantiomer ((*S*)-1) was obtained in poor enantiomeric excess, which was also shown in their *E*-values, suggesting that both enantiomers might easily enter into the catalytic active site of the enzymes, leading to little enantioselectivity by the enzymes [17]. Thus, ASL with the highest enantiomer selectivity (E = 3.4-3.6) was chosen as the biocatalyst in sequential esterification to resolve α-lipoic acid.

Table 1. Kinetic resolution of α-lipoic acid by different lipases

Enzyme	Temp. (°C)	Time (hr)	*c* (%)	ee_S (%)	Preferred enantiomer	*E*
ASL (400mg)	40	60	47.6	38.0	*R*	3.5
	40	72	52.7	43.6		3.4
	40	84	59.2	54.4		3.6
PPL (400 mg)	37	4	63.6	32.8	*R*	1.9
	37	5	71.0	43.9		2.1
	37	6	90.1	64.3		1.8
PEL (1000 mg)	37	3	39.6	17.0	*R*	2.0
	37	4	59.2	33.1		2.1
	37	5	79.8	57.0		2.1
Nov 435 (50 mg)	26	0.5	54.8	9.3	*R*	1.3
	26	1	77.6	20.0		1.3
Lip TL (50 mg)	26	0.5	46.7	8.7	*R*	1.3
	26	1	72.5	17.2		1.3

Effect of Time on ASL-catalysed Esterifying Reaction

Figure 1 plotted the time course for esterification of racemic α-lipoic acid ((*RS*)-1) by ASL. The conversion ratio increased significantly with increase in reaction time. On the contrary, enantiomeric excess of the hydrolysate of ester (*R*)-2 (ee_R), namely enriched (*R*)-1, decreased a little and ranged between 52.4-57%. So the reaction time of 84 hr, with 59.2% *c* and 52.4% ee_R, was selected in order to obtain a higher yield of the target (*R*)-enantiomer.

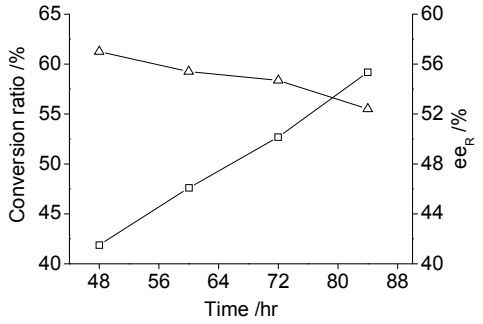

Figure 1. Time course for ASL-catalysed esterification of α-lipoic acid ((*RS*)-1) at the first resolution step: □ = conversion ratio; Δ = ee_R of (*R*)-1)

Sequential Kinetic Resolution of α-Lipoic Acid

As shown in Scheme 1, racemic α-lipoic acid ((*RS*)-1) was first subjected to enzymatic resolution to give ester (*R*)-2. After hydrolysis of the ester (*R*)-2, the resulting (*R*)-1 was then subjected to the second enzymatic resolution at about 65% conversion to furnish ester (*R*)-2. Subsequent hydrolysis of this ester (*R*)-2 furnished (*R*)-1 with an average ee of 92%, based on chiral chromatographic analysis (Table 2). Both the enantioselectivity of the lipase and the conversion ratio were clearly enhanced in the second resolution step, which could possibly be explained by the faster reacting (*R*)-enantiomer furnishing the major substrate in the second step.

Table 2. Second resolution of enriched (*R*)-1 by ASL

Reaction time (hr)	*c* (%)	ee_R (%)
48	59.3	92.8
60	65.6	91.6
72	66.7	93.2

Note: Reaction condition: a mixture of enriched (*R*)-1 (52% ee, 1 mmol), *n*-octanol (5 mmol), heptane (20 mL) and ASL (400 mg) was shaken at 200 rpm and 40°C.

CONCLUSIONS

A new and convenient way to prepare (*R*)-α-lipoic acid has been developed through a sequential kinetic resolution by *Aspergillus* sp. WZ002. Even though the substrate has a stereogenic centre four

carbon atoms away from the reaction site and a low *E*-value was exhibited in the first step, high enantiomeric purity (ee > 91%) of the target (*R*)-enantiomer was obtained at a high conversion ratio in the second step. The success of this method confirms the value of sequential kinetic resolution as an important approach in enzymatic resolution, especially in cases where a remote stereocentre is present.

REFERENCES

1. L. J. Reed, "Multienzyme complexes", *Acc. Chem. Res.*, **1974**, *7*, 40–46.
2. L. J. Reed, B. G. Debusk, I. C. Gunsalus and C. S. Jr. Hornberger, "Crystalline α-lipoic acid: A catalytic agent associated with pyruvate dehydrogenase", *Science*, **1951**, *114*, 93–94.
3. H. Sigel, "The hydrophobic and metal-ion coordinating properties of α-lipoic acid—an example of intramolecular equilibria in metal-ion complexes", *Angew. Chem. Int. Ed. Engl.*, **1982**, *21*, 389–400.
4. L. Packer, E. H. Witt and H. J. Tritschler, "Alpha-lipoic acid as a biological antioxidant", *Free Rad. Biol. Med.*, **1995**, *19*, 227–250.
5. Y. S. Cho, J. Lee, T-H. Lee, E. Y. Lee, K-U. Lee, J. Y. Park and H-B. Moon, "α-Lipoic acid inhibits airway inflammation and hyperresponsiveness in a mouse model of asthma", *J. Allergy Clin. Immunol.*, **2004**, *114*, 429–435.
6. A. Baur, T. Harrer, M. Peukert, G. Jahn, J. R. Kalden and B. Fleckenstein, "Alpha-lipoic acid is an effective inhibitor of human immuno-deficiency virus (HIV-1) replication", *Klin Wochenschr.*, **1991**, *69*, 722–724.
7. P. M. Bingham and Z. Zachar, "Lipoic acid derivatives and their use in treatment of disease", *Int. Patent*, WO/2000/024734 (**2000**).
8. I. C. Gunsalus, L. S. Barton and W. Gruber, "Biosynthesis and structure of lipoic acid derivatives", *J. Am. Chem. Soc.*, **1956**, *78*, 1763–1766.
9. S. P. Chavan, C. Praveen, G. Ramakrishna and U. R. Kalkote, "Enantioselective synthesis of *R*-(+)-α and *S*-(–)-α-lipoic acid", *Tetrahedron Lett.*, **2004**, *45*, 6027–6028.
10. T. T. Upadhya, M. D. Nikalje and A. Sudalai, "Asymmetric dihydroxylation and hydrogenation approaches to the enantioselective synthesis of *R*-(+)-α-lipoic acid", *Tetrahedron Lett.*, **2001**, *42*, 4891–4893.
11. S. Zhang, X. Chen, J. Zhang, W. Wang and W. Duan, "An enantioselective formal synthesis of (+)-(*R*)-α-lipoic acid by an *L*-proline-catalyzed aldol reaction", *Synthesis*, **2008**, *3*, 383–386.
12. A. S. Gopalan and H. K. Jacobs, "Bakers' yeast reduction of alkyl 6-chloro-3-oxohexanoates: Synthesis of (*R*)-(+)-α-lipoic acid", *J. Chem. Soc. Perkin. Trans.*, **1990**, *1*, 1897–1900.
13. B. Adger, M. T. Bes, G. Grogan, R. McCague, S. Pedragosa-Moreau, S. M. Roberts, R. Villa, P. W. H. Wan and A. J. Willetts, "The synthesis of (*R*)-(+)-lipoic acid using a monooxygenase-catalyzed biotransformation as the key step", *Bioorg. Med. Chem.*, **1997**, *5*, 253–261.
14. H. D. Yan, Z. Wang and L. J. Chen, "Kinetic resolution of α-lipoic acid via enzymatic differentiation of a remote stereocenter", *J. Ind. Microbiol. Biotechnol.*, **2009**, *36*, 643–648.
15. N. W. Fadnivas and K. Koteshwar, "Remote control of stereoselectivity: Lipase catalyzed enantioselective esterification of racemic α-lipoic acid", *Tetrahedron Asym.*, **1997**, *8*, 337–339.

16. C. S. Chen, Y. Fujimoto, G. Girdaukas and C. J. Sih, "Quantitative analyses of biochemical kinetic resolutions of enantiomers", *J. Am. Chem. Soc.*, **1982**, *104*, 7294–7299.
17. O. Jiménez, M. P. Bosch and A. Guerrero, "Lipase-catalyzed enantioselective synthesis of methyl (*R*)- and (*S*)-2-tetradecyloxiranecarboxylate through sequential kinetic resolution", *J. Org. Chem.*, **1997**, *62*, 3496-3499.